SYNTHESIS, CHARACTERIZATION AND PROPERTIES OF CONDUCTIVE ELASTOMERIC COMPOSITES BASED ON POLYPYRROLE AND SHORT NYLON-6 FIBER

Thesis submitted to the

Cochin University of Science and Technology

in partial fulfillment of the requirements

for the award of the degree of

Doctor of Philosophy

under the

Faculty of Technology

By

D. S. PRAMILA DEVI

Department of Polymer Science and Rubber Technology
Cochin University of Science and Technology
Kochi- 682 022, Kerala, India
http://psrt.cusat.ac.in

December **2012**

Synthesis, Characterization and Properties of Conductive Elastomeric Composites Based on Polypyrrole and Short Nylon-6 Fiber

Author

D.S. Pramila Devi
Associate Professor
Department of Chemistry
Sree Sankara College
Kalady- 683574, Kerala, India
E-mail: pramila5013@gmail.com

Guide:

Dr. Sunil K. Narayanan Kutty
Professor & Head
Department of Polymer Science and Rubber Technology
Cochin University of Science and Technology
Cochin- 682 022, Kerala, India
E-mail: sunil@cusat.ac.in

Department of Polymer Science and Rubber Technology
Cochin University of Science and Technology
Kochi - 682 022, Kerala, India
http://psrt.cusat.ac.in

Dr. Sunil K. Narayanan Kutty
Professor & Head

Mob: +91 9995300093
Email: sunil@cusat.ac.in

Certificate

Certified that, this thesis entitled **"Synthesis, Characterization and Properties of Conductive Elastomeric Composites Based on Polypyrrole and Short Nylon-6 Fiber",** is an authentic report of the original work carried out by Smt. D. S. Pramila Devi under my supervision and guidance in the Department of Polymer Science and Rubber Technology, Cochin University of Science and Technology, Kochi- 22. No part of the work reported in this thesis has been presented for any other degree from any other institution.

Dr. Sunil K Narayanankutty
(Supervising Guide)

Kochi- 22
12/12/12

Declaration

I hereby declare that the thesis entitled **"Synthesis, Characterization and Properties of Conductive Elastomeric Composites Based on Polypyrrole and Short Nylon-6 Fiber",** is the original work carried out by me under the supervision of **Dr. Sunil K. Narayanan kutty,** Professor & Head, Department of Polymer Science and Rubber Technology, Cochin University of Science and Technology, Kochi- 22 and that no part of the work reported in this thesis has been submitted for any other degree from any other institution.

Kochi-22 **D. S. Pramila Devi**

12-12-12

Dedicated to

My dear Achan & Amma....

Acknowledgement

At this moment of great satisfaction and relief I cherish and acknowledge the love and affection showered on me by many people without whose immense support this work would not have been materialised.

Words fail when I try to express my gratitude to Dr. Sunil K Narayanan Kutty. Having ventured to do Ph. D. at this stage of my career I could not have met a better "Guide" than him. More than a supervising teacher he was a friend and philosopher, always profusely spreading positive energy around. Whenever I was down with tension, which is the case more often than not, he lifted up my spirit with his own way of taking things in a lighter vein. Thank you Sir for all the support and valuable tips and suggestions.

The faculty members of PSRT have changed all my views of a research institution. Their simple and humble attitude has created a conducive working atmosphere. I would like to extend my sincere thanks to Dr. K. E. George, Dr. Rani Joseph, Dr. Eby Thomas Thachil, Dr. Thomas Kurian, Dr. Philip Kurian, and Smt. Jayalatha Gopalakrishnan for being so supportive. I am thankful to the adhoc teachers for their extreme co-operation and to the non teaching staff of the dept. for their promt service whenever I approached.

I wish to thank Dr. C. K, Anandan, Dept. of Electronics, Cochin University of Science and Technology for allowing me to carry out dielectric and microwave studies in their lab. Special thanks to Paulbert and Sreekala for assisting me to take the measurements.

I am grateful to University Grants Commission for granting me Teacher Fellowship under the Faculty Improvement Programme and to the Managing Director of Sree sankara College, Kalady for permitting me to do this Ph. D. work.

I am highly indebted to our CEO, Sri. P. S. Ramachandran and our Principal Dr. M. K. Ramachandran for the support and encouragement extended to me these years. I express my deep sense of gratitude to all the members of the Chemistry Dept., Sree sankara College for their whole hearted co-operation and constant encouragement: Our HOD, Smt. S.Bhagyalekshmi who always kept keen interest in the progress of my work; my dearest friend Jabin, without whose companionship I would never have thought of this venture; Sheela and Ajith for the genuine interest in my work; Lekha for her moral and spiritual support with sisterly affection; Rema, Shailaja, Sreekala and Manju for the wellwishes.

I am highly obliged to Dr. Saritha Chandran for rendering all possible assistance throughout this work. Now, my wonderful friends in PSRT, how can I formally thank you for all the love, care, affection and support. I can never forget the cheerful days we spent together. I wish to express my heart-felt thanks to one and all : Preetha, Dennymol, Zeena, Newly, Shobha and Jolly Antony for the nice friendship; Bipin for the selfless support in all areas connected with this work from the very beginning; Ajilesh for reaching me with a helping hand wherever I am, just on a missed call and for the affectionate companionship; Renju always ready to extend any help with that soft approach; Sona, Saisy and Nisha for familiarising me with the instruments; Aiswarya and Vidya Francis for providing me with many tips regarding computer; Abhilash and Janeesh for their "classes on polymer chemistry"; Sreejesh, Shadiya and Reshmi for their loving care; Anna, Asha, Sunitha,Vidya, and Teena for being so friendly; Manoj George for forwarding many reference papers; the new members of the dept., Neena, Bindu, Divya, Bhagyesh, Neethu, Remya, Soumya and Nishad for the affection shown to me.

Let me take this opportunity to thank Anu and Balu who rectified the problems of my system whenever required.

As always, I realize whatever little I have achieved in my life is because of the constant prayers of my dear parents. With his truthfulness, dedication and commitment to work my father inspires me a lot. Amma's timely advice gives me strength to overcome all the adversities in life.

I thank my in-laws and all other family members for their care and support. I remember with thanks Girija chechi and Kunjettan who took charge of my home whenever I was busy. My hearty thanks are also due to: Gopan chettan , Madhu chettan and Jee who were always eager to know the details of my work; Radha and Rema with whom I share all my feelings; Chandramohan, Sreekuttan, Chettathi and Ammu chechi for their loving enquiries .

I admit, personal debts are more difficult to express in formal terms. Still, I acknowledge my husband who motivated me to do Ph. D. and went through all the inconveniences with immense patience. I can only remember with tears, my daughter, Meera who persuaded me to go on with my work even at the time of her hospitalization. I don't know how far I did justice to Meera and my dear little Amal in the pressure of completing this work. Enormous support offered by Abhi and Kannan are highly appreciated at this moment.

Above all, I bow to God Almighty for blessing me with the strength to complete this work.

D.S. Pramila Devi

Preface

The search for new materials especially those possessing special properties continues at a great pace because of ever growing demands of the modern life. The focus on the use of intrinsically conductive polymers in organic electronic devices has led to the development of a totally new class of smart materials. Polypyrrole (PPy) is one of the most stable known conducting polymers and also one of the easiest to synthesize. In addition, its high conductivity, good redox reversibility and excellent microwave absorbing characteristics have led to the existence of wide and diversified applications for PPy. However, as any conjugated conducting polymer, PPy lacks processability, flexibility and strength which are essential for industrial requirements. Among various approaches to making tractable materials based on PPy, incorporating PPy within an electrically insulating polymer appears to be a promising method, and this has triggered the development of blends or composites. Conductive elastomeric composites of polypyrrole are important in that they are composite materials suitable for devices where flexibility is an important parameter. Moreover these composites can be moulded into complex shapes.

In this work an attempt has been made to prepare conducting elastomeric composites by the incorporation of PPy and PPy coated short Nylon-6 fiber with insulating elastomer matrices- natural rubber and acrylonitrile butadiene rubber. It is well established that mechanical properties of rubber composites can be greatly improved by adding short fibers. Generally short fiber reinforced rubber composites are popular in industrial fields because of their processing advantages, low cost, and their greatly improved technical properties such as strength, stiffness, modulus and damping. In the present work, PPy coated fiber is expected to improve the mechanical properties of the elastomer-PPy composites, at the same time increasing the conductivity. In addition to determination of DC conductivity and evaluation of mechanical

properties, the work aims to study the thermal stability, dielectric properties and electromagnetic interference shielding effectiveness of the composites.

The thesis consists of ten chapters.

Chapter 1 deals with an overview of the historical background of conducting polymers along with their structure, doping, charge transfer phenomena, methods of synthesis and applications. The importance of PPy amongst different conducting polymers is highlighted and its selection for the present work is justified. A review of literature in this field and the objectives of the work are also presented.

Chapter 2 describes the materials and reagents used for the synthesis of polypyrrole and polypyrrole coated short Nylon-6 fiber and for the development of blends and composites. A description of processing techniques and the analytical techniques used for the study is also included.

Chapter 3 explains the preparation and characterization of polypyrrole and polypyrrole coated short Nylon-6 fibers. Characterization includes infrared spectroscopy, scanning electron microscopy and X-ray diffraction. The thermal stability and glass transition temperature of polypyrrole, virgin Nylon fiber and polypyrrole coated fiber have also been studied.

Chapter 4 details the preparation of conducting elastomeric composites of natural rubber, polypyrrole and polypyrrole coated short Nylon fibers by mechanical mixing. The composites synthesized are characterized using scanning electron microscopic analysis. The cure pattern, cure kinetics and filler dispersion of the elastomeric composites are evaluated. The DC electrical conductivity and mechanical properties of the conducting elastomer composites are studied. The solvent swelling characteristics of the composites are investigated in toluene.

In **Chapter 5,** the preparation of natural rubber/ polypyrrole/ polypyrrole coated short Nylon fiber by *in situ* polymerization in latex is described. The

cure characteristics, cure kinetics, filler dispersion, morphology, DC electrical conductivity, mechanical properties and swelling characteristics of the elastomeric composites are evaluated.

The preparation and properties of conductive elastomeric composites of PPy and PPy coated short Nylon fiber with acrylonitrile butadiene rubber are discussed in **chapter 6.** The studies include cure characteristics, cure kinetics, filler dispersion, morphology, DC electrical conductivity, mechanical properties and swelling characteristics.

Chapter 7 investigates the thermal stability of conducting elastomer composites of polypyrrole and PPy coated Nylon fiber, compared to virgin matrices. Differential scanning calorimetric analysis of virgin matrices and the composites is also carried out.

In **chapter 8** a description of the dielectric properties of PPy and its elastomer composites measured in the frequency range 20 Hz to 2 MHz is included. The dependence of dielectric permittivity, dielectric loss and AC conductivity on frequency and filler loading is investigated.

Chapter 9 is divided into two parts. Part I gives an account of microwave properties of the composites studied in S band (2-4 GHz) frequency using cavity perturbation technique. In Part II, the evaluation of electromagnetic interference shielding effectiveness of the conducting elastomeric composites in the S band (2-4 GHz) and X band (7-13 GHz) frequencies is described.

Chapter 10 represents a summary of works presented in previous chapters and the major findings of the investigation.

A list of abbreviations and symbols used in the thesis and a list of publications and presentations are included at the end.

.....ooo.....

Contents

.....ꕥ.....

Chapter

1

INTRODUCTION

Contents

During the last decade, the focus on the use of intrinsically conducting polymers (ICPs) in organic electronic devices has led to the development of a totally new class of smart materials. This chapter summarizes a general account of conducting polymers, their synthesizing techniques, conducting mechanism and applications. As dielectric spectroscopy has been found to be a valuable experimental tool for understanding the phenomenon of charge transport in conducting polymers, an introduction to dielectric properties is also included. Two important applications of conducting polymers, electromagnetic interference shielding and radar absorption are based on the use of microwave properties Therefore a brief discussion on microwave characteristics is also given. Polypyrrole, one of the ICPs that has attracted the interest of researchers, is characterized by good electrical conductivity and relative ease of synthesis. To overcome polypyrrole's drawbacks of poor mechanical properties and processability, combining it with an electrically insulating polymer has been attempted and this triggered the development of blends and composites of polypyrrole. A survey of literature regarding the composites of polypyrrole with various insulating polymers including elastomers, fibers and fabrics is briefed here. The main objectives of the present work are summarized towards the end of this chapter.

During the past three decades, research on functional π-conjugated systems has rapidly grown as a broad multidisciplinary field inclusive of theoretical chemistry, organic chemistry, photophysics, electrochemistry, solid-state physics and device implementation [1].

The intrinsically conducting polymers, which are organic polymers that possess the electronic, magnetic, electrical and optical properties of a metal have been attracting the attention of countless of group of researchers all over the world because of their potential application in modern technology. These characteristics turn conducting polymers into the category of so-called 'synthetic metals'. Outstanding properties in one area alone, for example, conductivity, are not necessarily a guarantee of practical utility. The unique properties of conducting polymers stem from: (1) the possibility of fine tuning the conductivity by adjusting the amount of dopant incorporated within the polymer, ie., by proper doping, the conductivity of these materials can be varied from insulator to semi conducting and then to metallic range. (2) doping/dedoping reversibility, ie., if doping is achieved by an oxidant, treatment with a reducing agent gives back the neutral polymer, the insulator and vice versa. (3) the optical absorption characteristics in UV-visible and near IR spectra as well as its electromagnetic absorption characteristics. These unique properties have led to the existence of wide and diversified applications for conducting polymers, such as antistatic coating, conductive adhesives, electromagnetic shielding, printed circuit boards, artificial nerves, aircraft structures, molecular electronics, electrical displays, sensors, rechargeable batteries, electromechanical actuators, etc. [2-10]. Advantages of conducting polymer based devices compared to conventional semiconductor materials are: low weight, low cost, flexibility, colour change during oxidation/reduction and

ability to cover large surface areas. The main disadvantage of conducting polymers is its poor processability. Without processability, the appreciation for conducting polymer would be limited one. Incorporation of conducting polymer into a host polymer substrate, forming a blend, composite or interpenetrated bulk network has been used as an approach to combine electrical conductivities with desirable mechanical strength of polymers [11].

1.1 Historical background

Conducting polymer research dates back to the 1960s, when Pohl, Katon, and their coworkers, first synthesized and characterized semiconducting polymers [12]. Around that time, Natta polymerized acetylene gas using his newly developed Ziegler Natta catalyst. The polyacetylene he obtained was a black powder, with conductivity around 7×10^{-11}S/cm. The discovery of the high conductivity of polysulfur nitride (SN)x, a polymeric material containing interesting electrical properties, was a step forward for research in conducting polymers. Later in 1977, films of polyacetylene were found to exhibit profound increases in electrical conductivity when exposed to halogen vapor [13-16]. Heeger, Shirakawa and MacDiarmid produced conjugated conducting polyacetylene when monomer of acetylene was doped with bromine and iodine vapor; the resulting electrical conductivity was 10 times higher than the undoped monomers. After their discovery, research papers dealing with polyconjugated systems were very extensive and systematic. The trend was to understand the chemical and physical aspects,either in neutral (undoped) state or charged (doped) states. In 2000, these three brilliant scientists, founders of the conjugated conducting polymer science, were granted the Nobel Prize in chemistry.

1.2 The structure of conducting polymers

Conducting polymer is called a 'conjugated polymer' because of the alternating single and double bonds in the polymer chain. Due to the special conjugation in their chains, it enables the electrons to delocalize throughout the whole system and thus many atoms may share them. These localized electrons become the charge carriers to make them conductive. Structure of some π conjugated polymers are depicted in fig. 1. 1.

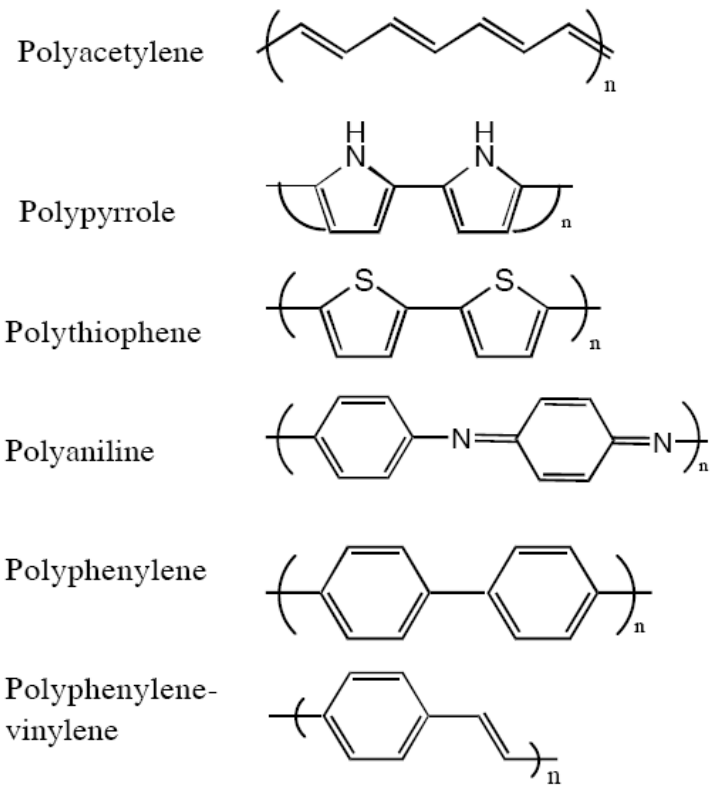

Fig. 1.1 Examples of conjugated polymers (adapted from *Resonance*. November, 1997, p54)

1.3 Charge storage

Even though conjugated polymers have a delocalized system of π electrons, and hence charge carrier mobility, the carrier concentration is low and therefore low conductivity. Doping is a process to increase carrier concentration and thus conductivity. In doping, a virgin polymer is treated with a strong oxidizing agent which abstracts electrons from the polymer, producing holes, or donates electrons to the polymer: In both cases increasing carrier concentration and thus conductivity.

Polymer + acceptor dopant(oxidant)→ polymer^{+} Dopant^{-} (P – doping)

Polymer + donor dopant(reductant)→ polymer^{-} Dopant $^{+}$ (N – doping)

Oxidative dopants- iodine, arsenic pentachloride, iron(III) chloride, etc. Reductive dopants- sodium naphthalide, molten lithium etc.

Doping in conjugated polymer is reversible. Now, depending upon whether the conjugated polymer has a degenerate or non-degenerate ground state, the charge carriers formed by doping may differ. The prototype conjugated polymers like *trans*-polyacetylene has a degenerate ground state in which there is no preferred sense of bond alternation. Oxidation of *trans*-polyacetylene generates a cation radical (positive polaron). This possesses both spin and charge. As there is no preferred sense of bond alternation, the positive charge and the unpaired electron of the cation radical can move independently along the polymer chain, forming domain walls between two phases of opposite orientation and identical energy. In solid state physics, a charge associated with a boundary or domain wall is called a 'soliton'.

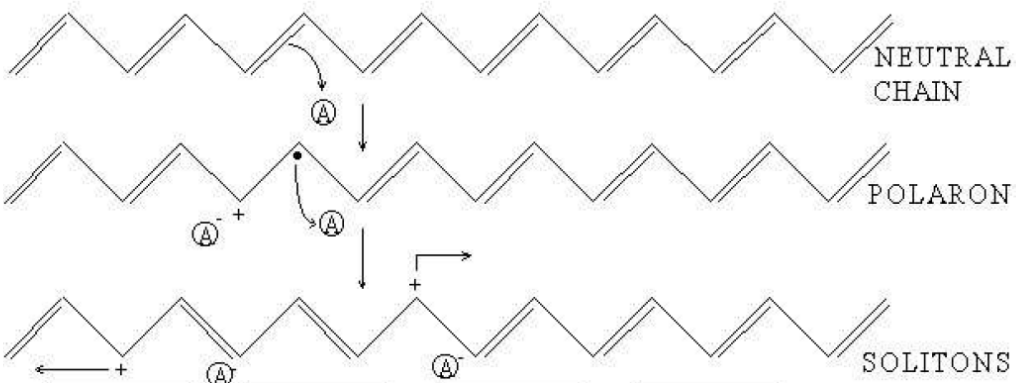

Fig. 1.2 Soliton in polyacetylene (adapted from *Conducting polymers* - ntlworld.com)

A positive soliton is depicted in fig. 1.2. A negative soliton results if the dopant is a reductant. Charged solitons (anions or cations) can explain the spinless transport since they carry charge but no spin. Solitons can sometimes be neutral when a free radical(unpaired electron) is present. Soliton has the properties of a solitary wave. That is it can move without deformation and dissipation [17].

Oxidation or reduction of non-degenerate ground state polymers such as polythiophene or polypyrrole have a different result. The initially formed cation radical possess both spin and charge. As there is preferred sense of bond alternation, the positive charge and unpaired electron of polaron cannot move independently. If the dopant is a reductant, a negatively charged electron site (radical anion or negative polaron) results. Polaron has a lattice relaxation (distortion) around the charge. Theoretical models demonstrates that two polarons on the same chain react exothermically to produce a dication or a dianion called 'bipolaron', which accounts for spinless conductivity in these polymers. Polaron and bipolaron formation are shown in fig. 1.3. An illustration of different charge carriers in chemical terms is shown in fig. 1.4.

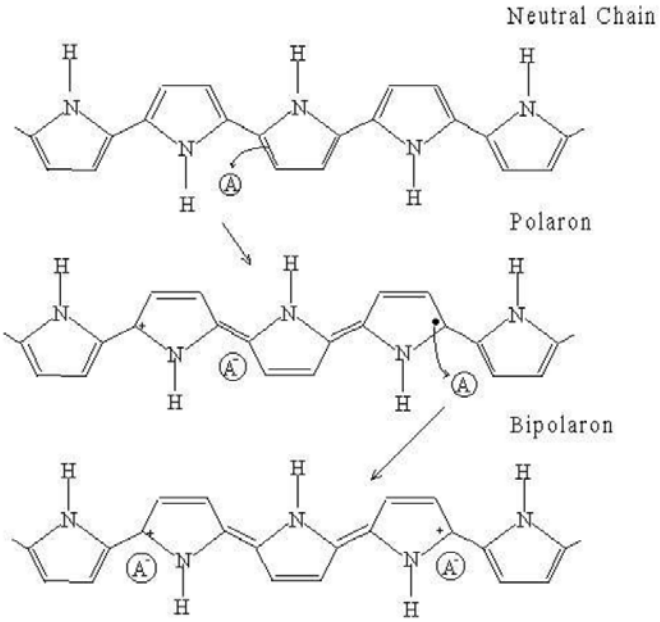

Fig. 1.3 Poloaron and bipolaron in polypyrrole (adapted from *Conducting polymers* - ntlworld.com)

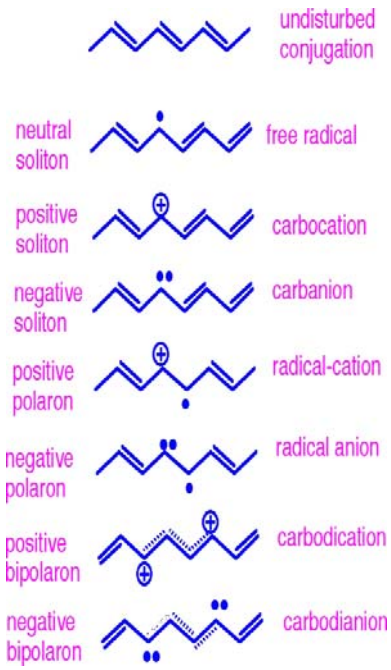

Fig. 1.4 Chemical representation of different charge carriers present in conducting polymers

1.4 Charge transport

The factors limiting the conductivity are the carrier mobility along with carrier concentration. Doping increases carrier concentration, but to enhance conductivity, they must be mobile. The conjugation length is an important parameter influencing the conductivity [18,19]. The carrier mobility and consequently the conductivity increases with increase in conjugation length. There are at least three elements contributing to carrier mobility- single chain or intramolecular transport, inter chain transport and inter particle contact. These three elements comprise a complicated resistive network, which determines the effective mobility of the carriers. Thus the mobility and therefore the conductivity are determined both on a microscopic (intra and inter chain) and macroscopic level [20].

Although solitons and bipolarons are known to be the main source of charge carriers, the precise mechanism is not yet fully understood. The problem lies in attempting to trace the path of the charge carriers through the polymer. All of these polymers are highly disordered, containing a mixture of crystalline and amorphous regions. It is necessary to consider the transport along and between the polymer chains and also the complex boundaries established by the multiple number of phases. This has been studied by examining the effects of doping, temperature, magnetism and the frequency of the current used. These tests show that a variety of conduction mechanisms exist such as tunneling conduction, impurity level conduction including hopping of charge carriers from one impurity level to another in the impurity band, space charge limited process due to the impediment of carriers at the interfaces under an external electric field and ionic conduction under high electric fields by the migration of cations and anions in opposite directions

[21-24]. However all the processes may not be present in all cases and even when present, one of these may be significant under certain conditions while the others may not be so.

Tunneling is a quantum mechanical phenomenon in which an electron passes through a potential energy barrier without acquiring enough energy to pass over the top of the barrier. The penetration probability of an electron from one electrode to the other through the insulator is much dependent on the applied electric field. Temperature, dielectric constant, shape of the potential barrier and effective mass of electron in the conduction band must be taken into account in determining the tunnel currents. If the barrier is thin enough, electrons can flow through the barrier between the conducting regions by quantum mechanical tunneling. Direct tunneling involves the transfer of electrons directly from one metallic island to the other through their Fermi surface levels.

When two molecules are separated by a potential barrier, a carrier on one side if moves to the other side by moving over the barrier via an activated state, the process is called hopping. The possibility for tunneling or hopping depends on the shape of the barrier and on the availability of thermal energy.

Carriers can be injected from the metal electrode into the conduction band of the polymer under an electric field. If the amount of injected carriers is more than that which can be transported across the film, a space charge will be built up at the interface. Electrons flowing through the system under an electric field will be impeded and controlled by the space charge collected at the interface and this gives rise to the phenomenon known as space charge limited conduction (SCLC).

1.5 Synthesizing techniques

Synthesized conjugated conducting polymers can be classified into two major categories: chemically polymerized materials and electrochemically polymerized. Via chemical polymerization, conjugated monomers react with an excess amount of an oxidant in a suitable solvent, such as acid. The polymerization takes place spontaneously and requires constant stirring. The second method is via electrochemical polymerization, which involves placing both counter and reference electrodes (such as platinum), into the solution containing diluted monomer and electrolyte (the dopant) in a solvent. After applying a suitable voltage, the polymer film immediately starts to form on the working electrolyte. A major advantage of chemical polymerization concerns the possibility of mass-production at a reasonable cost [25,26]. This is often difficult with electrochemical methods. On the other hand, an important feature of the electro-polymerization technique is the direct formation of conducting polymer films that are highly conductive, simple, and suitable for use, especially in electronic devices.

1.6 Applications

There are two main groups of applications for these polymers. The first group utilizes their conductivity as its main property. The second group utilizes their electro activity. The extended p systems of conjugated polymer are highly susceptible to chemical or electrochemical oxidation or reduction. These alter the electrical and optical properties of the polymer, and by controlling this oxidation and reduction, it is possible to precisely control these properties. Since these reactions are often reversible, it is possible to systematically control the electrical and optical properties with a great deal of precision. It is even possible to switch from a conducting state to an insulating state.

Group 1 - Conductivity:

a) Antistatic coating

By coating an insulator with a very thin layer of conducting polymer it is possible to prevent the build up of static electricity [2]. Such a discharge can be dangerous in an environment with flammable gases and liquids and also in the explosives industry. In the computer industry the sudden discharge of static electricity can damage microcircuits.

b) Conductive adhesives

By placing monomer between two conducting surfaces and allowing it to polymerize, it is possible to stick them together. This is a conductive adhesive and is used to stick conducting objects together and allow an electric current to pass through them.

c) Electromagnetic shielding

Many electrical devices, particularly computers, generate electromagnetic radiation, often radio and microwave frequencies. This can cause malfunctions in nearby electrical devices. The plastic casing used in many of these devices is transparent to such radiation. By coating the inside of the plastic casing with a conductive surface this radiation can be absorbed [3] .

d) Printed circuit boards

Many electrical appliances use printed circuit boards. These are copper coated epoxy-resins. The copper is selectively etched to produce conducting lines used to connect various devices. These devices are placed in holes cut into the resin. In order to get a good connection, the holes need to be lined with a conductor. Copper has been used, but the coating method, electroless copper plating, has several problems. It is an expensive multistage process,

the copper plating is not very selective and the adhesion is generally poor. This process is being replaced by the polymerization of a conducting plastic. If the board is etched with potassium permanganate solution a thin layer of manganese dioxide is produced only on the surface of the resin. This will then initiate polymerization of a suitable monomer to produce a layer of conducting polymer. This is much cheaper, easy and quick to do, is very selective and has good adhesion [4].

e) Artificial nerves

Due to the biocompatibility of some conducting polymers they may be used to transport small electrical signals through the body, i.e. act as artificial nerves [5].

f) Aircraft structures

Weight is at a premium for aircraft and spacecraft. A drop in magnitude of weight could give better performance to the internal combustion engine[5]. Modern planes are often made with light weight composites. This makes them vulnerable to damage from lightning bolts. By coating aircraft with a conducting polymer the electricity can be directed away from the vulnerable internals of the aircraft.

Group 2: Electro activity:

a) Molecular electronics

Molecular electronics are electronic structures assembled atom by atom. One proposal for this method involves conducting polymers. An example is a modified polyacetylene with an electron accepting group at one end and a withdrawing group at the other. A short section of the chain is saturated in order to decouple the functional groups. This section is known as a

'spacer' or a 'modulable barrier'. This can be used to create a logic device. There are two inputs, one light pulse which excites one end and another which excites the modulable barrier. There is one output, a light pulse to see if the other end has become excited. To use this there must be a great deal of redundancy to compensate for switching 'errors'[6].

b) Electrical displays

Depending on the conducting polymer chosen, the doped and undoped states can be either colourless or intensely coloured. However, the colour of the doped state is greatly redshifted from that of the undoped state. The colour of this state can be altered by using dopant ions that absorb in visible light. Unlike liquid crystal displays, the image formed by redox of a conducting polymer can have a high stability even in the absence of an applied field [7].

c) Sensors

This utilizes the ability of conducting materials to change their electrical properties during reaction with various redox agents (dopants). It has been shown that polypyrrole behaves as a quasi 'p' type material. Its resistance increases in the presence of a reducing gas such as ammonia, and decreases in the presence of an oxidizing gas such as nitrogen dioxide. Hence it can be used in a gas sensor. Conducting polymers also find application in biosensor, p^H sensor, chemical sensor, strain sensor, thermal sensor etc.

d) Rechargeable batteries

The polymer battery, such as a polypyrrole- lithium cell operates by the oxidation and reduction of the polymer backbone. During charging the

polymer oxidizes anions in the electrolyte which enter the porous polymer to balance the charge created. Simultaneously, lithium ions in electrolyte are electrodeposited at the lithium surface. During discharging electrons are removed from the lithium, causing lithium ions to re enter the electrolyte and to pass through the load and into the oxidized polymer. The positive sites on the polymer are reduced, releasing the charge-balancing anions back to the electrolyte. This process can be repeated about as often as a typical secondary battery cell [8].

e) Electromechanical actuators

Electromechanical actuators are based on the ability of many conducting polymers to undergo changes in dimension during doping and dedoping. This can be as large as 10%. Due to this property, conducting polymers can be used to directly convert electrical energy into mechanical energy. The method of doping and dedoping is very similar as that used in rechargeable batteries discussed above. What is required are the anodic strip and the cathodic strip changing size at different rates during charging and discharging. The applications of this include micro tweezers, micro valves, micro positioners for microscopic optical elements, and actuators for micromechanical sorting (such as the sorting of biological cells) [9].

f) 'Smart' structures

One of the most futuristic applications for conducting polymers are 'smart' structures. These are items which alter themselves to make themselves better. Applications of smart structures include active suspension systems on cars, trucks and train; traffic control in tunnels and on roads and bridges; damage assessment on boats; automatic damping of buildings and programmable floors for robotic [10].

1.7 Dielectric properties of conducting polymers

Dielectric spectroscopy is an informative technique to determine the molecular motions and structural relaxations present in polymeric materials possessing permanent dipole moments [27, 28]. Evaluation of AC electrical conductivity reveals a wealth of information regarding the usefulness of these materials for various applications. Moreover the study of AC electrical conductivity sheds light on the behavior of charge carriers under AC field, their mobility and the mechanism of conduction [29]. In dielectric measurements the material is exposed to an alternating electric field that is generated by applying a sinusoidal voltage; this process causes positive charges to move with the electric field and an equal number of negative charges to move against it resulting in no net charge anywhere and therefore no conduction within the polymer. In other words alignment of dipoles in the material occurs, which results in polarization. The charges cannot move and are bound in a dielectric. The amount of dipole alignment, both induced and permanent is represented by the dielectric permittivity, ε' and the energy required to align the dipoles is represented by the loss factor, ε". The ability of material to resist the passage of AC current or serve as a capacitor is determined by the dielectric constant (ε') and the dissipation factor (ε").

There are many polarization mechanisms that can occur within a dielectric material contributing to ε', such as electronic, ionic or atomic, dipolar or orientation and interfacial or space charge polarization. Electronic polarization occurs in neutral atoms when an electric field displaces the nucleus with respect to the electrons that surround it. Ionic polarization occurs when adjacent positive and negative ions stretch under an applied electric field. Dipolar polarization is

exhibited by molecules having permanent dipoles. Permanent dipoles are oriented in a random manner in the absence of an electric field. In the presence of an electric field, the dipole will rotate to align with the electric field causing orientation polarization to occur. Interfacial polarization occurs when the motion of migrating charges is impeded and become trapped within the interfaces of a heterogeneous system, where a relatively conductive component is mixed in an insulator. This localized accumulation of charge will induce its image charge on an electrode and gives rise to a dipole moment. This phenomenon has been first recognized by Maxwell in 1892. At very low frequency, all polarization mechanisms operate in a dielectric. As frequency increases, the material's net polarization drops as each polarization mechanism ceases to contribute, and hence its dielectric constant drops.

Dielectric spectroscopy has been found to be a valuable experimental tool for understanding the phenomenon of charge transport in conducting polymers. Low frequency conductivity and dielectric relaxation measurements especially have proven to be valuable in giving additional information on the conducting mechanism that DC conductivity measurement alone does not provide.

1.8 Microwave characteristics of conducting polymers

The microwave constitutes only a small portion of the electromagnetic spectrum (300 MHz to 300 GHz). Inherently conducting polymers are excellent microwave absorbers and make ideal materials for effecting welding of plastics [30]. Now a days it is very necessary to study the practical use of microwave properties of conductive polymers because of their wide areas of applications such as coating in reflector antennas, camouflage, satellite

communication links, micro strip antennas etc. Two important applications concerned with the use of microwave properties are electromagnetic interference (EMI) shielding and radar absorbing materials.

The proliferation of electronic devices, those at high frequencies, has brought about new emphasis on shielding of electromagnetic interference, caused by electric and magnetic fields. To provide shielding, a number of electrically conductive fillers such as copper, silver, nickel and alloys have been developed [31-33]. Later, shielding properties of conductive polymers have been studied as a consequence of their intrinsic conductivity [34].

The advancement of microwave technology during world war II has facilitated the use of RADAR for detecting and destroying military aircraft. The military aircraft industry has really taken into account the necessity of reducing the echo called Radar Cross Section (RCS) of their engines [35]. The absorption or dispersion of electromagnetic energy in the medium between the radar and a protected target by the use of a radar absorbing material (RAM) to cover the metallic surface of ships/ aircrafts is one method of reducing the radar signature of targets. The metallic aircraft surface is a reflector from the electromagnetic waves point of view, and therefore researches have been carried out to the conception of RAMs associated with optimized shape. A number of papers deal with the use of conducting polymers as RAMs due to their microwave absorbing capability and the chemical nature of macromolecular chains in which electronic conduction occurs at a long range. Among various types of RAMs, Salisbury screens [36], Dallenbach layers [37, 38] etc. are designed based on conducting polymers, especially polypyrrole.

1.9 Polypyrrole(PPy)

PPy is an inherently conducting polymer with interesting electrical properties, first discovered and reported in the early 1960s [39]. It is a non-degenerate ground state polymer with two different types of chain configurations containing repeating units of aromatic as well as quinoid scheme (fig.1.5) Polypyrroles are also called pyrrole blacks or polypyrrole blacks. Polypyrroles also occur naturally, especially as a part of a mixed copolymer with polyacetylene and polyaniline in some melanins. It is an opaque, brittle, amorphous material, although its specific properties are influenced by the dopant [40]. Amongst conducting polymers, PPy is one of the most studied one because of its high electrical conductivity, environmental stability and ease of synthesis [41-43].The heteroatomic and extended π-conjugated backbone structure of PPy provide it with chemical stability and electrical conductivity, respectively. Polypyrrole conducting polymers exhibit a wide range of surface conductivities (10^{-3} $Scm^{-1} < \sigma < 100$ Scm^{-1}) depending on the functionality and substitution pattern of the monomer and the nature of the counter ion or dopant [44].

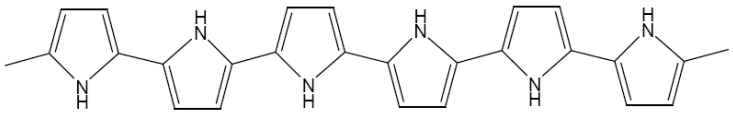

Aromatic

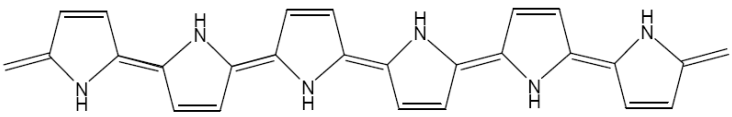

Quinoid

Fig. 1.5 Aromatic and Quinoid structures of polypyrrole (Adapted from *Defence Research and Development, Canada. January*, 2005, p.2)

It has also attracted a great deal of attention due to the wide potential applications, such as rechargeable batteries [45,46], electroplating [47-49], enzyme immobilization [50-52], gas separation membranes and sensors [53-57], biomedical [58], electromagnetic interference shielding materials [59-62], corrosion protection [63]electrochemical actuators [64-67], electrode for super capacitors [68,69] field effect transistor [70-72]etc.

1.9.1 Mechanism of conduction

The oxidative doping of polypyrrole proceeds in the following way. An electron is removed from the system of the backbone producing free radical and a spinless positive charge. The radical and cation are coupled to each other via local resonance of the charge and the radical. In this case, a sequence of quinoid-like rings is used. The distortion produced by this is of higher energy than the remaining portion of the chain. The creation and separation of these defects costs a considerable amount of energy. This limits the number of quinoid-like rings that can link these two bound species together. In the case of polypyrrole it is believed that the lattice distortion extends over four pyrrole rings. This combination of a charge site and a radical is called a polaron (fig. 1.6b). This could be either a radical cation or radical anion. This creates a new localized electronic state in the gap, with the lower energy state being occupied by a single unpaired electron. The polaron state of polypryyole are symmetrically located about 0.5 eV from the band edges (fig. 1.7). Upon further oxidation the free radical of the polaron is removed, creating a new spinless defect called a bipolaron. This is of lower energy than the creation of two distinct polarons. At higher doping levels it becomes possible that two polarons combine to form a bipolaron. Thus at higher doping levels the polarons are replaced with bipolarons (fig. 1.6c).

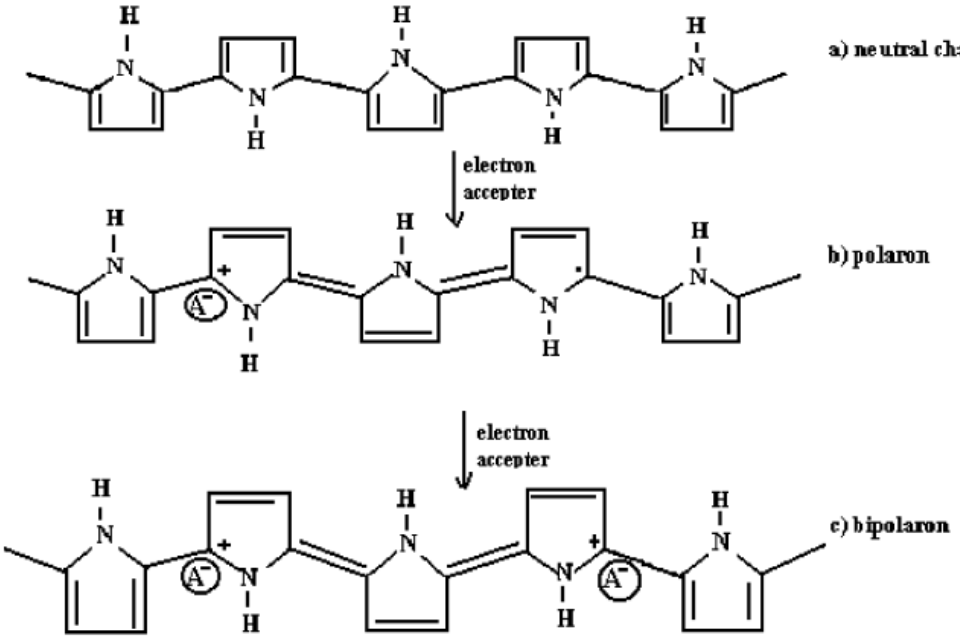

Fig. 1.6 Fomation of polarons and bipolarons (Adapted from *Polymer Bulletin*. **2006**, 57, p.537)

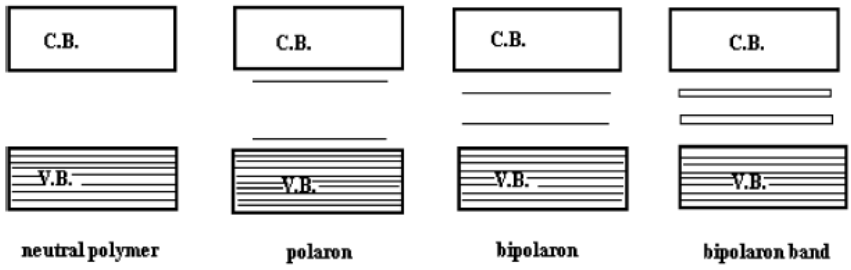

Fig. 1.7 Bands in conducting polymer (Adapted from *Polymer Bulletin*. **2006**, 57, p.537)

The bipolarons are located symmetrically with a band gap of 0.75 eV for polypyrrole (fig. 1.7). This eventually, with continued doping, forms into continuous bipolaron bands. Their band gap also increases as newly formed bipolarons are made at the expense of the band edges. For a very heavily

doped polymer it is conceivable that the upper and the lower bipolaron bands will merge with the conduction and the valence bands respectively to produce partially filled bands and metallic like conductivity.

1.9.2 Synthesis

Polypyrrole (PPy) and a wide range of its derivatives may be prepared by simple chemical or electrochemical methods [73-78]. Chemical polymerization is a simple and fast process with no need for special instruments. The polymerization takes place spontaneously and requires constant stirring. Bulk quantities of polypyrrole (PPy) can be obtained as fine powders using oxidative polymerization of the monomer by chemical oxidants like ferric chloride, ammonium per sulphate etc. in aqueous or non-aqueous solvents [75,76,79] or by chemical vapour deposition [77]. However, the use of chemical polymerization limits the range of conducting polymers that can be produced since only a limited number of counter ions can be incorporated. The chemical polymerization of pyrrole appears to be a general and useful tool for the preparation of conductive composites [80,81] and dispersed particles in aqueous media[82,83]. The second method is via electrochemical polymerization, which involves placing both counter and reference electrodes (such as platinum), into the solution containing diluted monomer and electrolyte (the dopant) in a solvent. After applying a suitable voltage, the polymer film immediately starts to form on the working electrolyte. A major advantage of chemical polymerization concerns the possibility of mass-production at a reasonable cost [25, 26]. This is often difficult with electrochemical methods. On the other hand, an important feature of the electro-polymerization technique is the direct formation of conducting polymer films that are highly conductive, simple, and suitable for use especially in electronic devices. During oxidative polymerization,

pyrrole typically polymerizes by linkage at α position, along with the loss of a proton at each of these positions [84] as shown in figs.1.8 and 1.9.

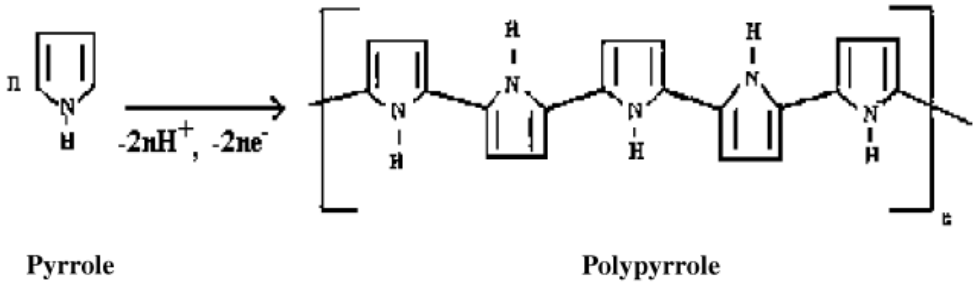

Pyrrole **Polypyrrole**

Fig. 1.8 Oxidative polymerization of pyrrole(Adapted from *Polymer Bulletin*. **2006**, 57, p.537)

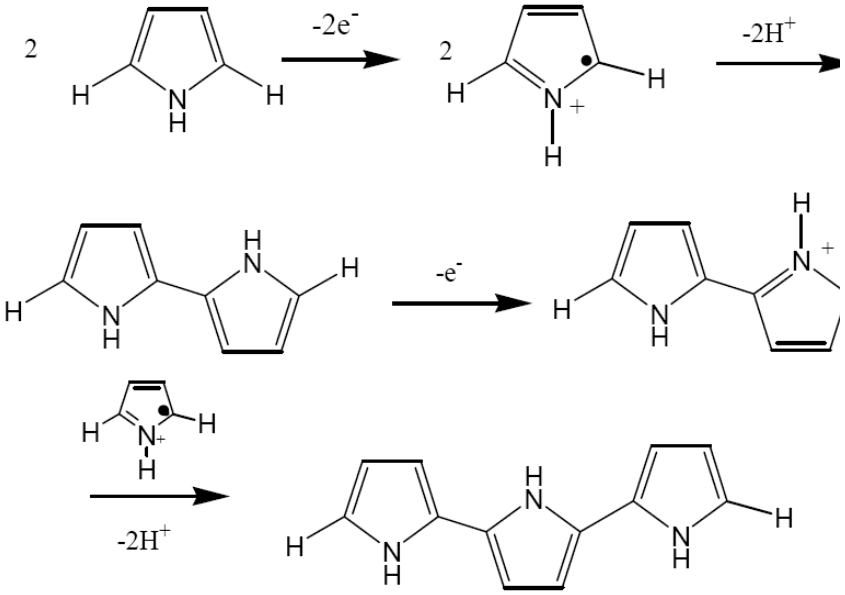

Fig. 1.9 Oxidative polymerization of pyrrole to polypyrrole proceeding via one electron oxidation of pyrrole to a radical cation, which subsequently couples with another radical cation to form 2,2'-bipyrrole. This process is repeated to form longer chains. (Adapted from *Defence Research and Development, Canada. January*, 2005, p.1)

1.9.3 Processability of polypyrrole

As already stated, polypyrrole is one of the most studied conducting polymer because of its high electrical conductivity, environmental stability and ease of synthesis [34-36]. However, the principal problems with the practical utilization of conducting polymers like polypyrrole include its poor mechanical properties like brittleness and low processability [85]. Much research will be needed before many of the above applications (section 1.6) will become a reality. The processability, stability and mechanical integrity need to be substantially improved if they are to be used in the market place. Research in the field of conducting polymers aims mainly at some suitable modifications of existing polymers so that their applicability can be improved. The incorporation of conductive particles (carbon black, metal, etc.) into a polymer matrix modifies considerably the electrical conductivity of the composite [86-88] but the presence of this type of load deteriorates considerably the mechanical characteristics of the composites compared with those of non-charged materials. The use of conducting polymers made it possible to obtain composites having at the same time a raised electric conductivity associated with good mechanical properties [89]. These materials have the effect of combining electric properties, of conducting polymers with the mechanical properties of the plastics [90].

1.9.4 Solutions

PPy prepared chemically or electrochemically was generally known to be insoluble and infusible [91]. One way to enhance processability of PPy is to synthesize soluble PPy. It has been proposed that the poor processability of PPy is caused not only by the strong inter-, intra-molecular interactions of the

PPy chains, or possible crosslinking of the PPy chain but by weak interaction of PPy with solvent molecule [92]. Pfluger and Street [93] reported the formation of about 30% of inter-chain links or branches through the 2, 3positions in a pyrrole ring during polymerization, while the rest of pyrrole units are linked at the 2, 5 positions to form straight chains. Recent progress in chemical synthesis using various dopants and organic solvents has led to the soluble PPy. Relatively large size dopants such as dodecylbenzene sulfonic acid (DBSA) or naphthalene sulfonic acid (NSA) reduce the interaction between PPy chains, giving rise to the PPy soluble in various organic solvents [94-96]. Oh [97] reports the synthesis and characterization of soluble polypyrrole with mixed dopants. However, mechanical properties of the soluble PPy synthesized with bulky dopants were relatively poor, which may be the disadvantage for various applications.

1.9.5 Copolymers and Graft Copolymers

Direct copolymerization of pyrrole with other monomers has produced soluble conducting product. Examples include the polymerization of pyrrole with various aniline derivatives [98-100], and methyl ethyl ketone formaldehyde resin [101]. Processable or soluble polypyrrole has also been formed by graft copolymerization of pyrrole. This has been accomplished by (i) coupling pyrrole to a reactive monomer, polymerizing the monomer and then polymerizing the pyrrole as was done for methylmethacrylate [102-104] or (ii) derivitization of a preformed polymer with pyrrole and then polymerizing the pyrrole as has been done for polystyrene-co-poly(chlorostyrene) [105]. A conducting graft copolymer of poly (vinyl carboxyethylether) (PVCEE) and polypyrrole was prepared by electrochemical polymerization of pyrrole using a precursor, poly (vinyl pyrrolylpropanone ether) by Shin *et al.* [106]. They

report that the copolymer showed higher conductivity and electrochemical activity compared to PVCEE/PPy composite. These materials were initially soluble with a tendency to become insoluble at high polypyrrole content.

1.9.6 Blends and Composites

To overcome PPy's drawbacks of poor mechanical properties and processability, incorporating PPy within an electrically insulating polymer is a promising method, and this has triggered the development of conducting polymer blends and composites. Blending conducting polymers with thermoplastic polymers is one attempt to increase their processability [107-109] Another way to enhance the processability is to synthesize a conducting polymer within an insulating polymer [110-114] either chemically or electrochemically. The principle advantage of the chemical method is the possibility of mass production at a low cost. Electrical polymerization, on the other hand, can be used to prepare conducting composite films with good mechanical properties and high conductivity. However, it is not suitable for large scale industrialization, because only thin films of pristine host polymers are used, which are only as large as the size of the electrode area of the products. Both techniques yield rather homogeneous products compared to blends. Polypyrrole composites can also be produced *in situ* by chemically oxidative polymerization. However, this is a diffusion-controlled process and needs a relatively long time to ensure the reactants efficiently diffuse into the matrix [115]. In a conducting polymer composite, in which a conducting polymer is incorporated into an insulating polymer, the conducting polymer supplies the conductivity, and the insulating component supplies the necessary mechanical properties. As for the host polymer several well known polymers have been used in the chemically prepared polypyrrole composite materials.

Natural and synthetic rubbers, polyolefins, polystyrene, polycaprolactone, polyethylene glycol, polyvinyl acetate etc. are some among the polymers forming composite materials with PPy.

Murugendrappa *et al*. [116] carried out *in situ* polymerization of pyrrole in the presence of fly ash to synthesize polypyrrole-fly ash composites by chemical oxidation method. The results of AC and DC conductivity studies showed a strong dependence on the weight percent of fly ash in polypyrrole. Studies on polypyrrole- yttrium oxide (Y_2O_3) composites by Vishnuvardhan et al. [117] also gave similar results. Three composite systems were prepared by polymerization of pyrrole in solution, in the gas phase and in supercritical CO_2 on porous polyethylene films [118]. The authors report that in the composites obtained, the conducting properties of polypyrrole were combined with the high mechanical characteristics of the porous support and the polymerization in solution yielded composite with higher conductivity compared to the other two systems.

Gang *et al*.[119] compared conductive PPy composites with polystyrene matrix prepared under supercritical carbondioxide(SC- CO_2) conditions with that prepared in aqueous solution. They claim that with regard to the morphology, conductivity and thermal stability, PPy composites prepared under SC- CO_2 conditions had unique advantages over those obtained by traditional method in aqueous solution. From their studies on morphology, conductivity and mechanical properties of polypyrrole/ polypropelene composites, Piontecka and co-workers [120] arrived at the conclusion that the processing route had a large influence on the morphology and properties of the composites. They found that the injection molded samples exhibited better mechanical properties, while compression molded samples showed better antistatic behavior and electrical conductivity.

Polypyrrole/ polycaprolactone composites were prepared [121] by emulsion polymerization to improve the mechanical and electrical properties and hence enhance electro-rheological response. The same authors carried out a similar study on polypyrrole/ SBS composites [122]. Thermal transitions of the semi-crystalline isotactic polypropylene, in polypropylene/ polypyrrole blends and polypropylene/ polypyrrole/montmorillonite composites, processed by two different ways, were investigated by differential scanning calorimetry by Kripotou et al. [123].

Karatas and co-workers [124] studied the electrical and mechanical properties of chemically and electrochemically prepared conducting composites of polypyrrole based on a flexible polymer produced from silane coupling agent and hydroxyl terminated polybutadiene rubber. They found that chemically prepared composite was highly flexible like rubber whereas electrochemically prepared composite possessed two orders of magnitude higher conductivity.

Zoppi *et al.* [125] obtained semi-interpenetrating polymer networks of PPy/ ethylene-propylene-diene rubber (EPDM) via oxidation polymerization of pyrrole using two methods. In the first method EPDM containing Copper chloride powder and dicumyl peroxide were obtained by mechanical mixing and crosslinking by heating and exposed to pyrrole vapors. In the second method crosslinked EPDM was swollen in an $FeCl_3$/ tetrahydrofuran solution and exposed to pyrrole vapors. Conductivity of the composites obtained by the second route(10^{-5}S/cm) was higher than for the first route.

Xie H *et al*. [126] dealt with two kinds of conducting PPy composites, namely, chlorinated polyethylene (CPE)/ PPy and natural rubber/ PPy composites,

prepared by *in-situ* oxidation polymerization of pyrrole in the presence of CPE suspension or natural rubber latex, using ferric chloride as oxidant. Preparation conditions, characterization and properties of the composites were studied. The evaluation of mechanical properties of the composites showed that maximum tensile strength obtained for CPE/PPy composite was of 7.3 MPa and the maximum value for natural rubber/PPy was 10 MPa. In both cases the tensile strength was found to be decreasing at higher loadings.

1.9.7 Polypyrrole coated fibers and textiles

The development of conducting polymer composites with natural and synthetic fibers with the polymer fully encapsulating the fiber, provides the opportunity to develop new composite materials that exhibit the inherent properties of both components. These properties include the tensile strength, flexibility and relatively high surface areas that are associated with fibers, and the electronic and chemical properties of conducting polymers [127]. The resulting fiber- conducting polymer hybrid materials can then be incorporated into other commodity/consumer type materials such as plastics, surface coatings and films to impart new or enhanced properties to them.

Milliken Research Corporation has developed an industrially feasible process for polymerizing pyrrole on the surface of fibers, yarns and fabrics, encasing individual fiber of textile assembly inside a smooth, coherent coating of electrically conductive polymer [128,129]. This can be achieved on any substrate, including fabrics, yarns, or fibers of quartz, glass, silicon, carbide, polyaramids, ultrahigh molecular weight polyethylene, polyacrylonitriles, polypropylene, polyester, nylon or cotton, without significantly affecting the strength or tensile properties of material [128-130]. The aging characteristics of these electrically conductive textile

composites are equal to or better than electrochemically produced free-standing films of the conductive polymers [128,129,131]. The performance of a polymer structure containing these polypyrrole treated textiles depends on the stress transfer between the fibers and the matrix, controlled by interfacial adhesion [132].

Main application areas of conducting polymer coated textiles are as EMI shielding materials and radar absorbing materials. Shielding from EMI using conducting polymer-coated textiles has some advantages including flexibility, access to a wide range of structures, reduced weight and lower cost. Conducting textiles provide an absorption dominant interaction with the microwave radiation. An example of a potential application of conducting polymers in EMI is control and modification of indoor wireless channel for minimization of interference by fabricating frequency selective absorbers and shields based on multilayer conducting polymer composites. These products could have specific absorption and reflection properties intended for radiation shields for electronic equipment. Subjecting a fabric substrate to metal vapour forms a thin layer of metal on the substrate, which inherently possesses a high shielding effectiveness. The disadvantage with this technique is that the metallic coating has poor abrasion resistance. Conducting polymer coatings generally have better abrasion resistance than metal coatings.

Kim *et al.*[133].investigated the effects of the chemical or the electrochemical polymerization conditions on the properties of the PET fabric/ polypyrrole composite such as surface morphology, electrical conductivity, environmental stability, and electromagnetic interference shielding effectiveness (EMI SE). They found that the composite shielded EMI by absorption as well as reflection and that EMI shielding through reflection increased with the electrical conductivity.

EMI SE of PPy coated PET fabric was also studied by Kim *et al.*[134]. They report that the PPy coated PET fabric was found to be exhibiting practically useful EMI SE and may be used in the application where EMI shielding by absorption rather than reflection is more important. They also claim that the elastic textile composite exhibited monotonic increase of electrical resistance with the elongation and can therefore be used as strain sensor for large deformation.

The EMI shielding properties of polypyrrole coated polyester composites in the 1-18 GHz frequency range were investigated by Hakansson. et al. [61]. Heat generation in PET fabrics coated with polypyrrole was investigated by Hakansson *et al*. [127]. The samples from the four different dopant systems showed an increase in temperature when a fixed voltage is applied to the fabric. The antraquinone-2-sulfonic acid (AQSA) sodium salt doped polypyrrole coating was the most effective in heat generation whereas the sodium perchlorate dopant system was the least effective.

Electro-conducting doped polypyrrole was deposited by *in situ* oxidative polymerization on PET fibers [135]. It was found that PPy gave good flame-proof property to PET because of its good chemical stability, and because it lowers the oxidative decomposition temperature of PET as revealed by TG analysis. Coating of cellulose and silk fibers with polypyrrole in vapour and liquid phases was carried out by Hosseini *et al*. [136]. From SEM analysis they concluded that vapour phase coating was more desirable. Polypyrrole was polymerized on the surface of cellulose fibers using a sequence of fiber impregnation in $FeCl_3$ solutions, thickening and redispersion in a pyrrole solution [137]. The authors observed a decrease in resistance of the fiber with

a high concentration of $FeCl_3$ in the impregnation solution associated with a not negligible degradation of cellulose fibers.

Kelly et al. [138] reported that the hybrid materials of individual cellulose fibers with polypyrrole or polyaniline coated on them exhibit the inherent properties of both the components. They include the electrical and chemical properties of polypyrrole and polyaniline and the strength, flexibility and available surface areas of the cellulose fiber. Electrically conductive fabrics were produced by deposition of a thin film of doped polypyrrole on the surface of cotton fibers [139]. The authors reported that: the PPy-coated fabrics exhibited good electrical properties: low electrical resistivity and heat generation performances suitable for heating devices, showed good antibacterial effect and PPy significantly increased tensile strength of cotton fabrics.

Kaynak and Beltran [140] examined the effects of reactant concentrations and synthesis parameters of PPy coatings on PET fabrics. Results showed that molar concentrations of the reactants, polymerization temperature and time had significant influence on the rate of polymerization, ratio of bulk to surface polymerization and electrical conductivity of the resulting fabric. The authors concluded that for applications such as electromagnetic interference (EMI) shielding and microwave absorption, where higher coating thickness is desired, and when exposure of the coating to abrasion was not an issue, room temperature synthesis was preferable. Where comparable conductivities, greater resistance to abrasion were required benefits were found in low temperature synthesis.

1.10 Scope and objectives of the present work

Conductive elastomer composites are important in that they are suitable for devices where strength and flexibility are important parameters. Moreover,

these composites can be moulded into complex shapes. Electrically conductive vulcanized rubber find application in fuel hoses, spark plug cables and high voltage cable insulations. Typical metals like copper and aluminium which have high conductivity and dielectric constant have been employed for fabricating such materials. While metals have good mechanical and conducting properties they have disadvantages such as heavy weight, easy corrosion and poor processability. In such a situation, conducting elastomer composites based on conducting polymers assume significance. A survey of literature reveals that the studies on PPy incorporated elastomer composites are rather scarce or seldom reported. In the works reported, it can be seen that eventhough the processability and mechanical properties of polypyrrole are enhanced, the composites never attain the strength of the host polymer matrix. Introduction of PPy into a composite, as a rule, decreases its strength and results in the loss of elasticity [118]. If PPy is adhered to a strong substrate and then used as a filler in polymer matrix, improvement in mechanical properties is expected [141]. The electrical and mechanical properties of polymer blends/ composites depend on the aspect ratio of the additive. Conducting polymers are usually spherical in shape, with small aspect ratio. But, fibers are characterized by high aspect ratios. It is well established that mechanical properties of rubber composites can be greatly improved by adding short fibers [142]. Generally short fiber reinforced rubber composites are popular in industrial fields because of their processing advantages, low cost, and their greately improved technical properties such as strength, stiffness, modulus and damping [143]. In the present work the incorporation of Nylon-6 fiber as filler for improving the mechanical properties of conducting elastomer composites based on PPy is explored. Since the introduction of Nylon fiber, an insulating material, tends to affect the conductivity of the composite, PPy coated Nylon

fiber is used. The use of PPy coated fiber is expected to improve the mechanical properties of the NR-PPy composite, at the same time increasing the DC conductivity and dielectric properties.

The specific objectives of the present work are:

- Synthesis and characterization of polypyrrole and polypyrrole coated short Nylon-6 fibers
- Exploration of the application of polypyrrole coated Nylon-6 fiber as strain sensor
- Fabrication of conducting elastomer composites of polypyrrole and polypyrrole coated short Nylon-6 fibers based on natural rubber and acrylonitrile butadiene rubber by dry rubber compounding
- Fabrication of conducting elastomer composites based on NR by *in situ* polymerization of pyrrole in natural rubber latex
- Evaluation of the DC conductivity, mechanical properties and swelling characteristics of the prepared composites
- Thermal analysis of the conducting elastomer composites
- Investigation of dielectric properties of pristine polypyrrole and that of the conducting elastomer composites in the frequency range 20 Hz to 2 MHz
- Study of microwave characteristics of the composites in the S band frequencies
- Determination of the electromagnetic shielding effectiveness of the composites in S and X band frequencies.

References

[1] Skotheim A, Elesenbaumer RL, Reynolds JR. *Handbook of Conducting Polymers*, *second ed. (Marcel Dekker Inc., New York)* **1998.**

[2] Margolis J. *Conductive Polymers and Plastics*, *Chapman and Hall*, **1989**, P. 121.

[3] Margolis J. *Conductive Polymers and Plastics*,*Chapman and Hall*, **1989**, P. 120

[4] Barlow A. *Entone-OMI representative*, **1997**.

[5] Alcacer L. *Conducting Polymers Special Applications*. *D. Reidel Publishing Company*,**1987**, p. 5.

[6] Alaneck WR, Clark DT, Samuelsen EJ. *Science and Application of Conducting Polymers*, *IOP Publishing*, **1991**, p. 135.

[7] Salaneck WR, Clark DT, Samuelsen EJ. *Science and Application of Conducting Polymers*, *IOP Publishing*, **1991**, p. 55.

[8] Margolis J, *Conductive Polymers and Plastics*, *Chapman and Hall*, **1989,** p. 33

[9] Salaneck WR, Clark DT, Samuelsen EJ. *Science and Application of Conducting Polymers*, *IOP Publishing*, **1991**, p .52 .

[10] Salaneck WR, Clark DT, Samuelsen EJ. *Science and Application of Conducting Polymers*, *IOP Publishing*, **1991**, p. 168 .

[11] Banarjee P, Mandal TK, Bhattacharya SN, Mandal BM. *Proceedings of the international symposium in macromolecules.* **1995,** p. 674.

[12] Stenger-Smith JD. *Prog Polym Sci*. **1998**, 23, 57.

[13] Bredas JL, Chance RR, Silbey R. *Phys Rev B.***1982**, 26, 5843.

[14] Clarke TC, Geiss RH, KwakJF, Street JB. *J Chem Soc Chem Commun*. **1978**, 338, 489.

[15] Pron A, Rannou P. *Prog Polym Sci*. **2002**, 27, 135.

[16] Shirakawa H, Louis EJ, MacDiarmidAG, Chiang CK, Heeger AJ. *J Chem Soc Chem Commun*.**1977**, 474, 578.

[17] Rebbi C. *Sci. Am*. **1979**, 71, 152.

[18] Garnier F, Harowitzer R, Hajlanui R. *Syn Met.* **1993**, 57, 4747.

[19] Fichon D, Harowitzer R, Garnier F. *Syn Met.* **1990**, 39, 125.

[20] Mark HF(editor). *Encyclopaedia of polymer Science and Engineering, second edition, Vol.5, John Wiley and sons Inc*. **1986**.

[21] Goswamy A. *Thin Film Fundamentals*, *Chapter 9, New age International, India*.**1996**.

[22] Simmons JG. *Handbook of Thin Film Technology*. *Chapter 14. (Edts.Maissel LI and Glang R, McGraw Hill, New York)* **1970**.

[23] Harrop PJ, Campbell DS.*Handbook of Thin Film Technology*.Chapter 16.(Edts.Maissel LI and GlangR, *McGraw Hill, New York)* **1970**.

[24] Anderson JC. *J Vac Sci Technol.* **1972**, 9, 1.

[25] Toshima N, Hara S. *Prog Polym Sci*. **1995**, 20, 155-183.

[26] Chao TH, March J. *J PolymSci: Part A: Polym Chem*. **1988**, 26, 743.

[27] Mc Crum NG, Read BE, Williams G. *Anelastic and dielectric effects in polymeric solids*. *Wiley, New York: Dover*, **1967**.

[28] Avakian P, Starkweather Jr. HW, Kampert WG. In: Cheng SZG, editor, *Dielectric analysis of polymers*, *Handbook of thermal analysis and calorimetry*, *Vol. 3, New York: Elsevier,* **2002**, p. 147.

[29] Koops, CG. *Phys Rev*. **1951**,83, 121

[30] Ellis JR. In: Skotheim TA, editor. *Handbook of conducting polymers. Vol. 1, New York; Marcel Dekker Inc,* **1986**, p.489.

[31] White DRJ. *Electromagnetic Shielding Materials and Perfomances*. *Don White consultants Inc., (2nd ed.)* **1980**.

[32] Paul CR. *Introduction to Electromagnetic Compatibility.* John *Wiley and Sons, New York*. **1992**.

[33] Ott HW. *Noise Reduction Techniques in Electronic Systems*. *John Wiley and Sons, New York*. **1987**.

[34] Unsworth J, Conn C, Jin Z, Kaynak A, Ediriweera R, Innis P. C, Booth N. *J Intell Mater Syst Struct*.**1994**, 5, 595.

[35] Richardson D, Steath. *Salamander Books Ltd.* **1989**.

[36] Salisbury WW, *US patent* 2599944, **1952**

[37] Truong VT, Riddel SZ, Muscat RF. *J Mat Sci Lett*. **1998**, 33, 4971.

[38] Truong VT, Turner BD, Muscat RF, Russo MS. *Proceedings of the SPIE The International Society for Optical Engineering.* **1997**, 3241, 98.

[39] Bolto BA, McNeill R, Weiss DE. *Aust J chem*. **1963**, `16, 1090.

[40] Wynne KJ, Street GB. *Macromolecules*.**1985**, 18, 2361.

[41] Tourillon G, Garnier F. *J Electroanal Chem*. **1982,**135,173.

[42] Gangopadhyay R, De A.*Chem Mater*. **2000**, 12, 608.

[43] Dutta K, De SK.*Solid State Commun*. **2006**,140, 167.

[44] da Cruz AGB, Wardell JL, Rocco AM. **2008**, *J Mater Sci,* 43, 5823.

[45] Bittihn R, Ely G, WoefflerF. *Makromol Chem, Makromol Symp*.**1987**, 8, 51.

[46] Mermillod N, Tanguy J, Petiot F. *J Electrochem Soc*. **1986**, 133, 1073.

[47] Gottesfeld S, Uribe FA. Armes SP. *J Electrochem Soc*. **1992**, 139, L14.

[48] Uribe FA, Valerio J, Gottesfeld AS. *Synth Met*. **1993**, 55, 3760.

[49] Deleeuw DM, Kraakman PA, Bongaerts PFG, Mutsaers CM J. *Synth Met.***1994**, 66, 263.

[50] Selampinar, Akbulut U, Ozden MY, Toppare L. *Biomaterials.***1997**, 18, 1163.

[51] Kizilyar N, Akbulut U, Toppare L, Ozden MY,Yagci Y. *Synth Met.* **1999,** 104, 45.

[52] Alkan S, Toppare L, Yagci Y, Hepuzer Y. *J Biomat Sci., Polym Ed.***1999**, 10, 1223.

[53] Martin CR, Liang W, Menon V, Parthasarathy R, Parthasarathy A.*Synth Met.***1993,** 57, 3766.

[54] MansouriJ, Burford RP. *J Membr Sci.***1994**, 87**,** 23.

[55] Anderson MM, Matter BR, Keiss H, Kaner RB. *Synth Met.***1991**, 41, 1151.

[56] Beelen E, Riga J, VerlistJJ. *Synth Met.* **1991**, 41, 449.

[57] Gulsen D, Hacarlioglu P, Toppare L, Yilmaz L. *J Membr Sci.* **2001**, 182, 29.

[58] Benabderrahmane SS, Bousalem C, Mangeney A, Azioune MJ, Vaulay, Chehimi MM,.*Polymer*. **2005**, 46, 1339.

[59] Hakansson E, Amiet A, Nahavandi S, Kaynak A. *Euro Polym J*. **2007**, 43, 205.

[60] Kuhn HH, Child AD, Kimbrell WC. *Synth Met.***1995**, 71, 2139.

[61] Hakansson E, Amiet A, Kaynak A. *Synth Met.* **2006**, 156, 917.

[62] Avloni J, Florio L, Henn AR, Lau R, Ouyang M, Sparavigna A. PACS numbers: 72.80.Le, 73.25.+i

[63] Narula AK, Singh R, ChandraS. *Indian Academy of Sciences.* **2000**, 23, 227.

[64] Baughman RH, *Synth Met.* **1996**, 78, 113.

[65] Hutchison AS, Lewis TW, Moulton SE, Spinks GM, Wallaceet GG. *Synth Met*, **2000**, 113, 121

[66] Madden JD, Cush RA, Kanigan TS, HunterIW.*Synth Met*.**2000**, 113, 185.

[67] Smela E, Gadegarrd N, *Adv Mater*. **1999**, 11, 953.

[68] Hughes M, Chen GZ, Shaffer MSP, Fray DJ, Windle AH.*Chem Mater*. **2002**, 14, 1610.

[69] Jurewicz K, Delpeux S, Bertagna V, Béguin F, Frackowiak E. *Chem Phys Lett*. **2001**, 347, 36.

[70] Lee MS, Lee SB, Lee JY, *Mol Cryst Liq Cryst*. **2003**, 405, 171.

[71] Kou CT, Liou TR. *Synth Met*. **1996**, 82, 167.

[72] Lee MS, Kang HS, Kang HS, Joo J, Epstein AJ, Lee JY.*Thin Solid Film*.**2005**, 477, 169.

[73] Diaz A, Bargon J.(Skotheim TA Ed) *Handbook of Conducting Polymers.* **1986**, 1, 82.

[74] Moss B K, Burford R P, Skyllas-Kazacos M, *Material Forum*, **1993**, 13, 35.

[75] Machida S, Miyata S, *Synth Met*. **1989**, 31, 311.

[76] Rapi S, Bocchi V, Gardini G P, *Synth Met*. **1988**, 24, 217.

[77] Mohhammadi A, Lundstrom I, Salaneck WR, Inganas O, *Synth Met*. **1987**, 21, 169.

[78] Warren LF, Anderson DP, *Electrochemical Society*. **1987**, 134, 101.

[79] Armes SP, *Synth Met*. **1987**, 20, 365.

[80] Bocchi V, Gardini G P, *J Chem Soc , Chem Commun*. **1986**, 2, 148.

[81] Armes SP, Vincent B. *J Chem Soc, Chem Commun*. **1987**, 4, 287.

[82] Eisazadeh H, Spinks G , Wallace GG, *Material Forum* . **1992**, **16**, 341.

[83] Bocchi V, Gardini G P, Rapi S. *J Mater Sci Lett*, **1987**, 6, 1283.

[84] Bunting RK, Swarat K, Yan D.*J Chem Edu*. **1997**, 74, 421.

[85] Migahed MD, Fahmy T, Ishra M, Barakat A. *Polymer Testing*. **2004**, 23, 360.

[86] Achour ME, BrosseauC. (ed) *Prospects in Filled Polymers Engineering: Mesostructure, Elasticity Network, and Macroscopic Properties, Transworld Research Network*. **2008**, p.129.

[87] Achour ME, Brosseau C, Carmona FJ. *Appl Phys.***2008**, 103, 9.

[88] Bryning MB, Islam MF, Kikkawa JM, Yodh AG. *Adv Mater.* **2005**, 17, 1186.

[89] Bohwon K, Koncar V, Devaux E, Dufour C, Viallier P. *Synth Met.* **2004**, 146, 167.

[90] Hansen TS, West K, Hassager O, Larsen NB. *Synth Met.* **2006**, 156 , 1203.

[91] Qian R, in: Salaneck WR, Lundstrom I, Ranby B. Eds.*Conjugated Polymers and Related Materials, Oxford Univ. Press, London*, **1993**, p. 161.

[92] Song KT, Lee JY, Kim HD, Kim DY, Kim SY, Kim CY. *Synth Met.* **2000**, 110, 57

[93] Pfluger P, Street GB. *J Chem Phys*. **1994**, 80, 544.

[94] Lee JY, Kim DY, Kim CY. *Synth Met*. **1995**, 74, 103.

[95] Kim IW, Lee JY, Lee H. *Synth Met*. **1996**, 78, 177.

[96] Kim DY, Lee JY, Kim CY, Kang ET, Tan KL, *Synth Met*. **1995**, 72, 243.

[97] Oh EU, Jang KS, Suh JS, Yo CH. *Mol Cryst Liq Cryst*. **1999**, 337, 101.

[98] Li XG, Huang MR, Wang LX, Zhu MF, Menner A, Springer J. *Synth Met.***2001**, 123, 435.

[99] Li XG, Wang LX, Jin Y, Zhu ZL, Yang YL. *JAppl Poly Sci.* **2001**, *82*,510.

[100] Li X-G, Wang L-X, Huang M-R, Lu Y-Q, Zhu M-F, Menner A, Springer J. *Polymer* **2001**, 42, 6095.

[101] Ustamehmetoglu B, Kizilcan N, Sarac AS, AkarA. *J Appl Poly Sci.* **2001**, 82,1098.

[102] Stanke D, Hallensleben ML, Toppare L. *Synth Met.***1995**, 72, 89.

[103] Stanke D, Hallensleben ML, Toppare L. *Synth Met.* **1995**, 72, 95.

[104] Ng S-C, Chan HSO, Xia J-F, Yu W. *J Mater Chem.* **1998**, 8, 2347.

[105] Nazzal, A. I.; Street, G. B. *J Chem Soc, Chem Commun.* **1985**, 1885, 375.

[106] Shin HW, Lee JY, Park YH. *Mol Cryst Liq Cryst*. **2008**, 492, 39/403-45/409.

[107] Stanke D, Hallensleben ML, Toppare L. *Synth Met.***1995**,73, 261.

[108] Balci N, Akbulut U, Toppare L, Stanke D, Hallensleben ML. *Mat Res Bull.* **1997**, 32, 1449.

[109] Aydinli B, ToppareL,Tincer T. *J Appl Polym Sci.* **1999**, 72, 1843.

[110] Hallensleben ML, Stanke D, Toppare L. *Macromol Chem Phys.***1995**,196 , 75.

[111] Wang HL,ToppareL, Fernandez JE. *Macromolecules.***1990**,23, 1053.

[112] Kalaycioglu E, Akbulut U, Toppare L. *J Appl Polym Sci.***1996**,61, 1067

[113] Selampinar F, Akbulut U, Yilmaz T, Gungor A,Toppare L. *J Polym Sci.* **1997**, 35, 3009.

[114] Stanke D, Hallensleben ML, Toppare L. *Synth Met.* **1995**, 72, 167.

[115] Li C J, Song Z G. *Synth Met*, **1991**, 40, 23.

[116] Murugendrappa MV, Myedkhasim, AmbikaPrasad MVN. *Bull Mater Sci.* **2005,** 28, 565.

[117] Vishnuvardhan TK, Kulkarni VR, BasavarajaC, RaghavendraSC. *Bull Mater Sci.* **2006**, 29, 77.

[118] Smirnov MA, Kuryndin IS, Nikitin LN, Sidorovich AV, Yu N, Sazanov OV, KudashevaV, Bukošek AR, Khokhlov, Elyashevich GK. *Russ J Appl Chem*. **2005**, 78, 1993.

[119] Gang L, Xia L, Xinghua S, Jian U, Jiasong H. *Front Chem China*. **2007**, 2, 118

[120] Piontecka J, Omastováb M, Pötschkea P, Simona F,Chodák I. *J Macromol Sci.-Phys*. **1999**, B38, 737.

[121] Kim YD, Kim JH. *Colloid Polym Sci*. **2008**, 286, 631.

[122] Kim YD, Kim JH. *Synth Met*. **2008**, 158, 479.

[123] Kripotou S, Apekis L, Rapti C, Nikaki KV, Pissis P, Mravcakova M, Omastova M. *Int J Polymer Mater*. **2007**, 56, 865.

[124] Karatas Y, Toppare L, Tincer T. *J Macromolecular Sci*, part A, **2003**, 40, 1081.

[125] Zoppi RA, DePaoli MA. *Polymer*. **1996,** 37, 1999.

[126] Xie H, Liu C, Guo J. *Polym Int*. 1999, 48, 1099.

[127] Hakansson E, Kaynak A,Lin T, Nahavandi S, Jones T, Hu E, *Synth Met.* **2004**, *144*, 21.

[128] Gregory RV, Kimbrell WC, Kuhn HH.*Synth Met.* **1989**,28, C823.

[129] Gregory RV, Kimbrell WC, Kuhn HH. *J Coat Fab.* 1991, 20, 167.

[130] Gregory RV, Kimbrell WC, Kuhn HH. *In Proc. 3rd Int*., *SAMPE Electronic Conf.* **1989**, 3, 570.

[131] Hosseini SH, Entezami AA, *Iran Polym J.* **1999**, 8, 205.

[132] Kuhn HH, Kimbrell WC, Worrell G, Chen CS. *In Proc. ANTEC.* **1991**, 91,760.

[133] Kim MS, Kim HK, Byun SW, Jeong SH, Hong YK, Joo JS, Song KT, Kim JK, Lee CJ, Lee JY. *Synth Met*. **2002**, 126 , 233.

[134] Kim HK, Kim MS, Chun SY. *Mol Cryst Liq Cryst*. **2003**, 405, 161.

[135] Varesano A, ToninC, FerreroF, StringhettaM. *J Therm Anal Calorim*. **2008**, 94 , 559.

[136] Hosseini SH, Pairovi A. *Ind Polym J*, **2005**, 14, 934.

[137] Beneventi D, Alila S, Boufi S, Chaussy D, Patrice N. *Cellulose*, **2006**, 13, 725.

[138] Kelly FM, Johnston HJ, Borrmann T, Richardson MJ. *Eur J Inog Chem*. **2007,** 5571.

[139] Varesano A, Aluigia A, Florio L, Fabris R. *Synth Met*. **2009**, 159 , 1082.

[140] Kaynak A, Beltran R. *Polym Int*. 2003, 52, 1021.

[141] Neoh KG, Tay BK, Kang ET. *Polymer*. **2000**, 41, 9.

[142] Goettler LA, Shen KS. *Rubber Chem Technol*. **1983**, 56, 619.

[143] Setue DK, De SK. *J Mater Sci*. **1984**, 19, 983.

Chapter

2

EXPERIMENTAL TECHNIQUES

Contents

This chapter deals with the materials and reagents used for the development of blends and composites, processing techniques and the analytical techniques used for the spectral, thermal and morphological characterization of the prepared samples. Methods adapted for the measurement of DC conductivity and determination of mechanical properties are also described. Lastly, the experimental set up for the evaluation of dielectric and microwave properties of the samples is also included.

2.1 Materials used

2.1.1 Natural rubber (NR)

Natural rubber used was solid block rubber ISNR-5 grade obtained from Rubber Research Institute of India, Kottayam, having the Mooney viscosity [ML (1+4)] at 100 ^{0}C = 85.3. The Bureau of Indian standard (BIS) specifications for this grade of rubber is given below.

Dirt content, % by mass, max	- 0.05
Volatile matter, % max	- 1.00
Nitrogen content, % max	- 0.70
Ash content (%)	- 0.60
Initial plasticity, P_0, min	- 30.00
Plasticity retention index, PRI, min	- 60.00

2.1.2 Natural rubber latex

Centrifuged NR latex concentrate with minimum 60% dry rubber content(DRC), preserved with high ammonia (HA) preservative system and conforming to the BIS 5430-1981 specifications was used in the study. BIS specification for the high ammonia latex is given below.

Dry rubber content , % by mass , min	- 60
Total solid content, % by mass , max	- 61
Coagulum content, % by mass , max	- 0.030
Sludge content, % by mass , max	- 0.007
Alkalinity as ammonia, % by mass	- 0.730
KOH number	- 0.496

2.1.3 Acrylonitrile butadiene rubber (NBR)

NBR was supplied by Kumho Petrochemicals, Korea. The sample used had following specifications:

Acrylonitrile content, %	- 33
Mooney viscosity [ML (1+4)] at 100 ^{0}C	- 45

2.1.4 Nylon- 6 fiber

Nylon-6 fiber was obtained from SRF Ltd. ,Chennai, India. Specifications are given below:

Twist	- S 392 – 374
Denier	- 3656 - 3886

2.1.5 Pyrrole

Pyrrole used for the synthesis was AR grade, having the following specifications and supplied by Spectrochem Pvt. Ltd. , Mumbai,India.

Assay	- 98%
Refractive index	- 1.507 – 1.508
Boiling point	- 129-131^{0}C

2.1.6 Ferric chloride

Anhydrous iron (III) chloride used was AR grade having molecular weight 162.2, obtained from Merck Specialties Pvt. Ltd., Mumbai,India.

2.1.7 *Para* toluenesulphonic acid

Para toluenesulphonic acid (98.5%) was obtained from Spectrochem Pvt. Ltd. , Mumbai, India.

2.1.8 Methanol

Methanol used was of AR grade and was supplied by S. D. Fine Chemicals Ltd., Mumbai, India.

It had a boiling point of 65 ^{0}C and density of 0.7866 g / cm^3.

2.1.9 Vulcastab VL

Vulcastab VL (polyethylene oxide condensate) used was supplied by ICI.

2.1.10 Zinc oxide

Zinc oxide obtained from Meta Zinc Ltd., Mumbai, India, had the following specifications:

Specific gravity	- 5.5
Zinc oxide content(%)	- 98
Heat loss (2 hours at 100^{0}C)(% max)	- 0.5

2.1.11 Stearic acid

Stearic acid used in this study, procured from Godrej Soaps Ltd., Mumbai, India, had the following specifications:

Melting point	- 50-69 ^{0}C
Acid number	- 185-210

2.1.12 Tetramethyl thiuram disulphide (TMTD)

TMTD was supplied by NOCIL, Mumbai, India. It had the following specifications:

Melting point	- 136 ^{0}C
Specific gravity	- 1.4

2.1.13 Dibenzthiazyl disulphide (MBTS)

MBTS having the following specifications was supplied by Bayer Chemicals, Mumbai, India.

Specific gravity	- 1.34
Melting point	- 165 ^{0}C

2.1.14 Sulphur (S)

Sulphur was supplied by Standard Chemical Company Pvt. Ltd., Chennai, India. Its specifications were:

Specific gravity	- 2.05
Acidity (% max)	- 0.01
Ash (% max)	- 0.01

2.1.15 Toluene

Toluene was supplied by Fine Chemicals Ltd., Mumbai. It has a boiling point of 95 ^{0}C

2.1.16 Methyl ethyl ketone(MEK)

Methyl ethyl ketone was supplied by Universal Laboratories Private Ltd., Mumbai. It has a boiling point of 80 ^{0}C.

2.2 Experimental methods

2.2.1 Pelletization of PPy powder

For electrical measurement, and for dielectric analysis, bulk sample of PPy is to be obtained in the form of pellets. Pellets of diameter 12mm and thickness of ≈ 2mm were prepared by compressing the fine powder of polypyrrole under a load of 6 tonnes in a pelletizer.

2.2.2 Compounding

Mixing and homogenization of elastomers and the compounding ingredients were done on a laboratory size (15 × 33 cm) two-roll mill at a friction ratio of 1:1. 25 as per ASTM D 3184 (1980). Once a smooth band is formed on the roll, the ingredients were added in the following order: filler (PPy, PPy coated fiber or both as required in the composites), activators, accelerators and finally sulphur. For NBR, sulphur was added first since solubility of sulphur in NBR is poor. After complete mixing the stock was passed six times through the tight nip and finally sheeted out at a fixed nip gap so as to orient the fibers preferentially in one direction. The sheets were kept for 24 hours for maturation.

2.2.3 Cure characteristics

The cure characteristics of the vulcanizates were determined (at 150 ^{0}C for 30 min in the case of NR and at 160 ^{0}C for 20 min in the case of NBR) as per ASTM D 2084-01 using a Rubber Process Analyzer (RPA 2000, Alpha Technologies) which is a computer controlled torsional dynamic rheometer with a unique test gap design, an advanced temperature control system and fully automated operation modes. A biconical die with a die gap of 0. 487 mm was used to achieve a constant shear gradient over the entire sample chamber. To determine the cure characteristics of the rubber compound, approximately 5 g of the sample was placed in the lower die, under pressurized conditions and submitted to harmonic torsional strain by the oscillation of the lower die through a small deformation angle of ± 0.2^0 at a frequency of 50 oscillations per minute. The torque transducer on the upper die senses the force being transmitted through the rubber.A typical cure curve is shown in fig. 2.1. The following data can be obtained from the torque-time curve.

1) Minimum torque, M_L: It is the lowest torque shown by the mix at the test temperature before the onset of cure

2) Maximum torque, M_H: It is the maximum torque recorded when curing of the mix is completed

3) Optimum cure time, T_{90}: This corresponds to the time to achieve 90% of the maximum torque which is calculated using the formula:

   Torque at optimum cure = $0.9 (M_H - M_L) + M_L$

4) Scorch time, T_{10}: It is time for attaining 10% of the maximum torque

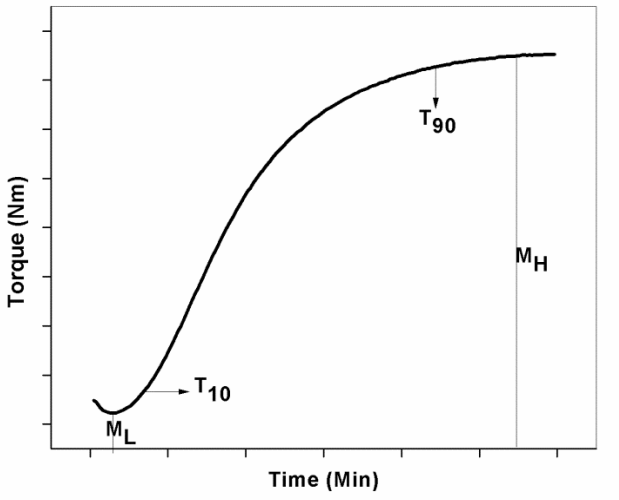

Fig. 2.1 A typical cure curve

2.2.4 Vulcanization

The test specimens marked with the mill grain direction were compression moulded in an electrically heated hydraulic press having 30cm× 30cm platens at a pressure of 200 kg/cm^2 into sheets using standard

mould (15cm× 15cm× 2cm). The rubber compounds were vulcanized to their respective optimum cure times at specified temperatures. After curing, the pressure was released and the sheets were stripped off from the mould and cooled suddenly by plunging into cold water. After a few seconds, the samples were taken from the cold water and stored in a cold dark place for 24 h and were used for the subsequent tests.

2.2.5 Measurement of DC conductivity

The DC electrical conductivity of the PPy sample (Pellets of diameter 12mm and thickness of ≈ 2mm) and the conducting elastomer composite samples(rectangular strips of dimensions 4mm× 2mm× 2mm) was measured by a standard two-probe electrode configuration using a Keithley 2400 source-measure unit which is a fully programmable instrument capable of sourcing and measuring voltage or current simultaneously with accuracy. A constant current source was used to pass a steady current through one of the probes and the voltage across the other was measured. The sample was placed between two electrodes through which current was passed and the resistance was measured directly from the instrument. The measurement was done at 25^0C and at RH of 65. The conductivity of the samples was calculated using the formula:

$$\sigma(S/cm) = (I / V) \times (l / A) \quad \text{----------} \quad (1)$$

where σ is the electrical conductivity, I is the current through the electrode in amperes, V is the voltage in volts, l is the thickness of the sample in centimeters and A is the area of contact of the electrodes with the sample in centimeter square.

In the case of fiber, resistance of one cm long yarn was measured with the same instrument using needle type electrodes with one mm foot diameter.

2.2.6 Determination of mechanical properties

The stress–strain behaviour of the composites was studied using a Shimadzu Universal Testing Machine (model AG-I) with a load cell of 10 KN capacity at a crosshead speed of 500 mm/min and at a gauge length of 14 mm. The measurements were carried out as per ASTM D 412. Dumbbell shaped samples punched out from the compression moulded sheets along the mill grain direction using a standard die (ISO type 4) were used for this. The tensile strength, elongation at break and modulus at different elongations were noted. Tear strength of the samples was measured as per ASTM D 624 using standard test specimens with 90^{o} angle on one side and tab ends (Type C die) which were punched out from the compression moulded sheets along the mill grain direction.

2.2.7 Infrared spectroscopy (IR)

Infrared spectroscopy is the absorption measurement of different IR frequencies (400-4000cm^{-1}) by a sample positioned in the path of an IR beam. IR spectroscopy exploits the fact that molecules have specific frequencies at which they rotate or vibrate corresponding to discrete energy levels. The IR spectrum of a sample is collected by passing a beam of infrared light through the sample. Examination of the transmitted light reveals how much energy was absorbed at each wave length. This can be done with a monochromatic beam, which changes in wave length over time, or by using a Fourier Transform Instrument to measure all wavelengths at once. From this, a transmittance or absorbance spectrum can be produced, showing at which IR wavelengths the

sample absorbs. Analysis of these absorption characteristics reveals details about the molecular structure of the sample. This technique works almost exclusively on samples with covalent bonds.

FTIR spectrum of the samples was taken using Thermo Nicolet Avatar 370 having spectral range of 4000 cm^{-1}- 400 cm^{-1} and a resolution of 0.9cm^{-1} and equipped with KBr beam splitter and DTGS Detector

2.2.8 Scanning electron microscopy (SEM)

Scanning electron microscopy is a very useful tool to gather information about topography, morphology, composition and micro structural information of materials. In a typical SEM, electrons are thermionically emitted from a tungsten or lanthanum hexaboride cathode and are accelerated towards an anode; alternatively, electrons can be emitted via field emission. The electron beam, which typically has an energy ranging from a few hundred eV to 100 keV, is focused by one or two condenser lenses into a beam. Characteristic X-rays are emitted when the primary beam causes the ejection of inner shell electrons from the sample and are used to tell the elemental composition of the sample. The back-scattered electrons emitted from the sample may be used alone to form an image or in conjugation with the characteristic X-rays. These signals are monitored by detectors (photo multiplier tubes) and magnified. An image of the investigated microscopic region of the specimen is thus observed in cathode ray tube and is photographed.

The SEM images of the samples were obtained using a scanning electron microscope, JEOL JSM-840 A. For obtaining SEM images of polypyrrole and the short fibers, the samples were mounted on a metallic stub and an ultra thin (< 10nm) coating of electrically conducting material (gold) was deposited by

low vacuum sputter coating. This was done to prevent the accumulation of static electric fields at the specimen due to the electron irradiation during imaging and to improve contact. In the case of composites, SEM images of tensile fracture surfaces of the composites were obtained. The fractured surfaces were sputtered with gold before they were observed in SEM.

2.2.9 X-ray diffraction (XRD)

X-rays are electromagnetic radiation of wavelength about 1 A^o, which is about the same size as an atom. X-ray diffraction has been in use in two main areas, for the fingerprint characterization of crystalline materials and the determination of their structure. Each crystalline solid has its unique characteristic X-ray powder pattern which may be used as "fingerprint" for its identification. Once the material has been identified, X-ray crystallography may be used to determine its structure, ie, how the atoms pack together in the crystalline state and what the interatomic distance and angle are, etc. X-ray diffraction is one of the most powerful characterization tools used in solid state chemistry and materials science. We can determine the size and the shape of the unit cell for any compound most easily using the diffraction of X-rays.

X- ray diffractograms of PPy, virgin fiber and PPy coated fiber were recorded using a Bruker AXS D8 Advance Diffractometer using CuKα radiation (λ = 1.54 A^o) at 35kV and 25 mA with a smallest addressable increment of 0.001 ^{o}. XRD results were obtained in the range $2\theta = 3^o$ to 80^o at a scan rate of 4^o/ min.

2.2.10 Thermogrvavimetric analysis (TGA)

Thermogravimetric analysis is a type of testing that is performed on samples to determine changes in weight in relation to change in temperature.

Such analysis relies on a high degree of precision in three measurements: weight, temperature and temperature change. TGA is commonly employed in research and testing to determine characteristics of polymers, to determine degradation temperatures, absorbed moisture content of materials, the level of inorganic and organic components in materials, composition of blends and composites etc. The analyzer usually consists of a high precision balance with a pan loaded with the sample. The sample is placed in a small electrically heated oven with a thermocouple to accurately measure the temperature. Analysis was carried out by raising the temperature gradually and plotting weight against temperature.

Thermogravimetric analysis of the samples was performed to determine changes in weight in relation to change in temperature. TGA studies were performed on a Q 50, TA Instruments Thermo Gravimetric Analyzer (TGA) with a programmed heating of 20^0C/min from room temperature to 800^0C. The chamber was continuously swept with nitrogen at a rate of 40-60 ml/min, to remove all corrosive gases formed during degradation and to avoid further thermo-oxidative degradation.

2.2.11 Differential scanning calorimetry (DSC)

Differential scanning calorimetry is a technique for measuring the energy necessary to establish a nearly zero temperature difference between a substance and an inert reference material, as the two specimens are subjected to identical temperature regimes in an environment heated or cooled at a controlled rate. Both the sample and the reference are maintained at nearly the same temperature throughout the experiment. The basic principle underlying this technique is that, when the sample undergoes a physical transformation such as phase transitions, more (or less) heat will need to flow to it than the

reference material to maintain both at the same temperature. Whether more or less heat must flow to the sample depends upon whether the sample is exothermic or endothermic. By observing the difference in heat flow between the sample and the reference, differential scanning calorimeters are able to measure the amount of heat absorbed or released during such transitions.

Differential scanning calorimetry was employed to determine the Tg of samples under study. The degree of crystallinity, heat of fusion, melting temperature and Tg of virgin fiber and PPy coated fiber were also evaluated. The measurements were conducted using a DSC Q-100, TA Instruments calorimeter, having a temperature accuracy of ± 0.1^{o}C.

2.2.12 Dielectric analysis

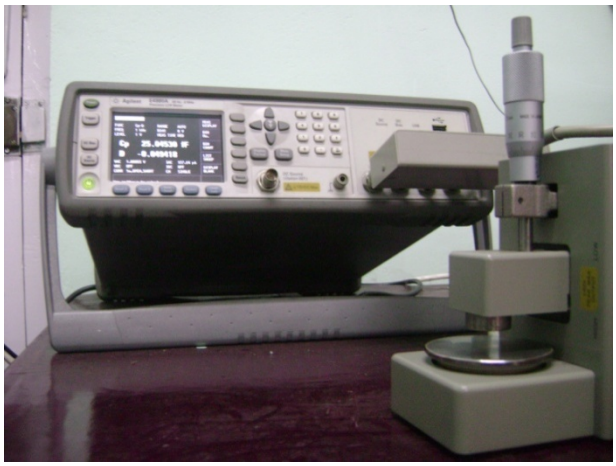

Fig. 2.2 Impedance analyzer

The dielectric measurements were carried out at frequencies ranging from 20Hz to 2MHz using an Impedance analyzer, Agilent E 4980 A Precision LCR Meter (fig. 2.2) Disc shaped samples having diameter 12mm and thickness ≈ 2mm were used for the measurements. The samples were mounted

in between the disc electrodes. Dielectric constant (ε_r), Dielectric loss (ε''**)** and the AC conductivity (σ_{AC}) were obtained from the instrument. The results were directly read on the monitor and recorded on a computer data sheet file.

2.2.13 Measurement of microwave properties

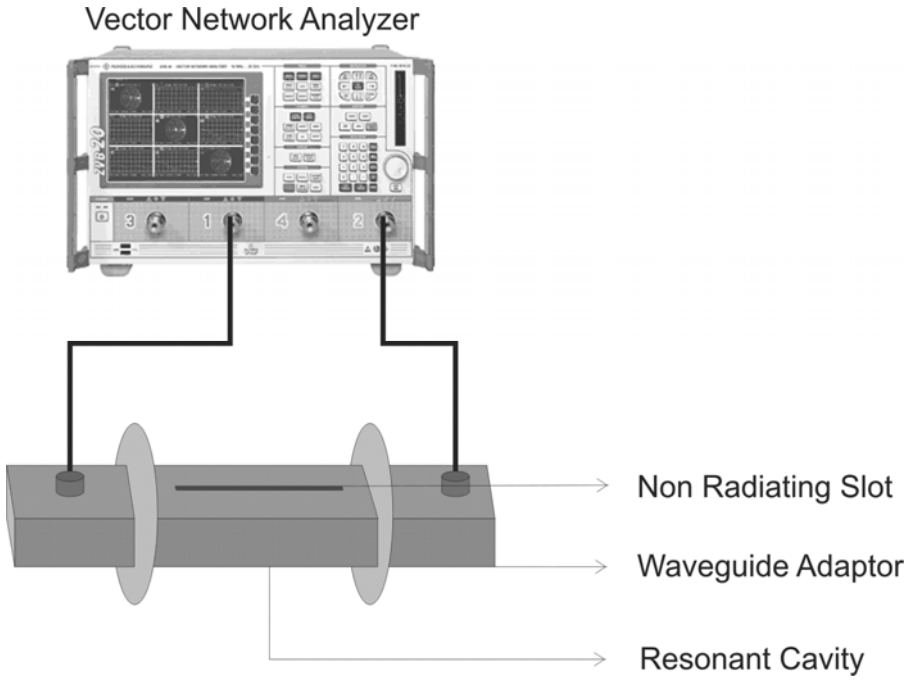

Fig. 2. 3 Network analyzer

The microwave characteristics of the prepared conducting elastomer composites (CECs) were studied using ZVB20 vector network analyzer. The measurements were done in S (2-4 GHz) band frequency at room temperature. The cavity resonators are constructed from brass or copper wave-guides. The inner walls of each cavity were silvered to reduce the wall losses. Both the resonators were of transmission type. The dimensions of the S band rectangular wave-guide resonator used in the measurements were 34.5 cm ×7.2 cm ×3.4cm. The schematic design of the network analyzer is shown in fig. 2.3.

2.2.14 Measurement of EMI shielding effectiveness

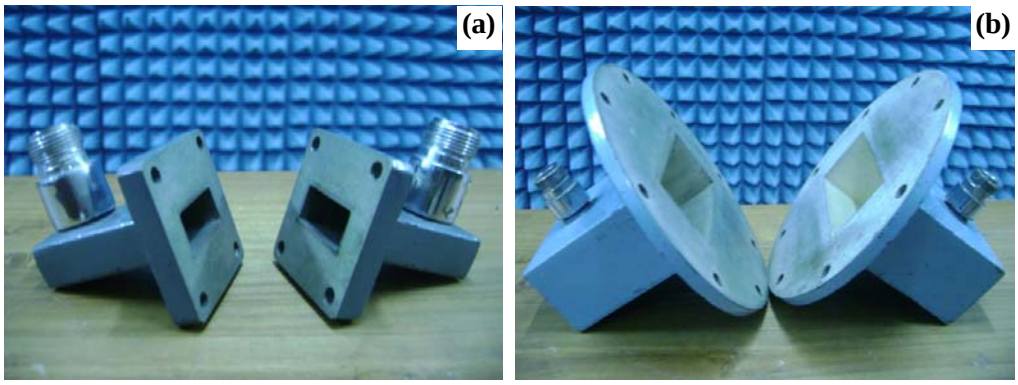

Fig. 2.4 (a) X band wave-guide (b) S band wave-guide

EMI shielding measurements were carried out in S (2-4 GHz) band and X(8-12 GHz) band frequencies using wave-guides coupled to a ZVB20 vector network analyzer. The wave-guides were of dimensions 2.3cm× 1cm× 13.5cm for X band and 7.2cm× 3.4cm× 35.2cm for S band. The two test port cables of the network analyzer were connected via two wave-guide to coaxial adapters. The photographs of the X and S band waveguides are shown in figs. 2.4 (a) and 2. 4(b), respectively. The network analyzer is shown in fig.2.3. The sample was placed between the two sections of the waveguide and the output recorded. The output from the vector network analyzer was in terms of scattering parameters, S_{xy}.The first number in the suffix refers to what port the output was measured at and the second number refers to where the signal originated from. Hence S_{11} is the reflected signal and S_{21} is the transmitted signal. Shielding efficiency of the sample can be calculated from S_{21}. Knowing reflectivity (R) and transmissivity (T), absorptivity (A) can be calculated using the relation A=1−T−R.

.....ꕥ.....

Chapter

3

SYNTHESIS AND CHARACTERIZATION OF POLYPYRROLE AND POLYPYRROLE COATED SHORT NYLON-6 FIBER

Contents

Pyrrole was polymerized in the presence of anhydrous ferric chloride as oxidant and p-toluene sulphonic acid as dopant. Polypyrrole coated short Nylon fibers were prepared by polymerizing pyrrole in the presence of short Nylon fibers. The reaction conditions were optimized to get a uniform coating of polypyrrole on Nylon. The resultant polypyrrole(PPy) and polypyrrole-coated Nylon fiber (F-PPy) were characterized using Infrared spectroscopy(IR), Scanning electron microscopy(SEM) and X-ray diffraction (XRD). DC conductivity of PPy and F-PPy was determined by a two probe method. The thermal stability of PPy, virgin Nylon fiber (F_v) and F-PPy was studied using thermogravimetric analysis (TGA). Differential scanning calorimetry (DSC) was used to determine the glass transition temperature (T_g) of PPy, Fv and F-PPy. The PPy coated fiber finds application as a strain sensor.

3.1 Introduction

Amongst the conducting polymers, polypyrrole (PPy) is one of the most studied one because of its high electrical conductivity, environmental stability and ease of synthesis [1]. However, as any other conjugated conducting polymer, PPy lacks processability, flexibility and strength. This can be improved either by forming copolymers of polypyrrole or by forming polypyrrole composites or blends with suitable, commercially available polymers. PPy-Polymer composites or blends can be classified as electrochemically prepared or chemically prepared. Chemically prepared polypyrrole has several distinct advantages over electrochemically prepared polypyrrole, especially concerning its potential use commercially. The chemically prepared polypyrrole is much more amenable to scale- up and commercial plant equipment. It also is considerably easier to apply to a substrate or structural material which would then be used in fabricating an end product [2].

Chemical polymerization is simple and fast process with no need for special instruments. Bulk quantities of PPy can be obtained as fine powders using oxidative polymerization of the monomer by chemical oxidants in aqueous or non aqueous solvents [3-6] or by chemical vapour deposition [7]. The chemical polymerization of pyrrole appears to be a general and useful tool for the preparation of conductive composites [8,9].

The most widely used oxidants for chemical oxidative polymerization of pyrrole are ammonium persulphate (APS) and ferric chloride ($FeCl_3$). Iron (III) chloride has been found to be the best chemical oxidant and water is the best solvent for chemical polymerization with respect to desirable conductivity

characteristics [3,8]. The overall stoichiometry resulting from chemical polymerization of PPy with ferric chloride oxidant is shown in Fig.3.1.

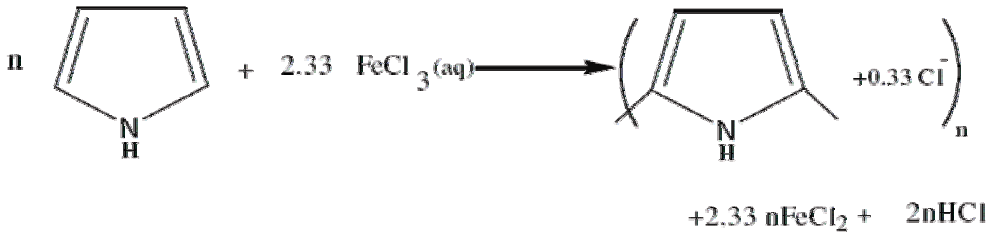

Fig. 3.1 Chemical polymerization of pyrrole (adapted from *E-Journal of Chemistry*, 2006, 3, 186)

The optimum initial mole ratio of Fe (III)/ Pyrrole for polymerization by aqueous iron(III) chloride solution has been found to be 2.25 or 2.33 [6,10]. During chemical polymerization of pyrrole, electro neutrality of the polymer matrix is maintained by incorporation of anions from the reaction solution. These counter ions are usually the anion of the chemical oxidant or reduced product of oxidant. For example, when $FeCl_3$ is used as oxidant, Cl^- ion is incorporated as counter ion. It has been found that factors such as solvent, reaction temperature, time, nature and concentration of the oxidising agent affect the oxidation potential of the solution. These in turn influence the final conductivity of the chemically synthesized polypyrrole [3,4]. Elemental analysis data has shown [10] that the composition of polypyrrole prepared chemically is almost identical with that electrochemically prepared.

Composites of PPy with many polymers such as poly(methyl methacrylate), poly(vinyl carboxyethylether),poly(ethylene terephthalate) (PET) fabrics, natural and synthetic rubbers, chlorinated polyethylene etc. have been reported [11-15]. Even though all these composites exhibit excellent conducting and shielding properties, the main concern with most of them is the lack of good mechanical

properties. Inorder to couple these two properties, special materials have to be developed. If PPy is adhered to a strong substrate and then used as a filler in polymer matrix, improvement in mechanical properties is expected [16]. The electrical and mechanical properties of polymer blends/composites depend on the aspect ratio of the additive. Conducting polymers are usually spherical in shape, with small aspect ratio. But, fibers are characterized by high aspect ratios. It is well established that mechanical properties of rubber composites can be greatly improved by adding short fibers [17]. Generally short fiber reinforced rubber composites are popular in industrial fields because of their processing advantages, low cost and their greatly improved technical properties such as strength, stiffness, modulus and damping [18]. Hence, conducting fibers used as additives can impart good mechanical properties along with desirable electrical properties.

The development of conducting polymer composites with natural and synthetic fibers with the polymer fully encapsulating the fiber, provide the opportunity to develop new hybrid materials that exhibit the inherent properties of both components. These properties include the tensile strength, flexibility and relatively high surface areas that are associated with fibers, and the electronic and chemical properties of conducting polymers. The resulting fiber-conducting polymer hybrid materials can then be incorporated into other commodity/ consumer type materials such as plastics, surface coatings and films to impart new or enhanced properties to them [19]

The surface resistance of the conductive textiles and fibers can be varied by controlling the thickness of the conductive polymer film through the adjustment of the concentration of chemicals and synthesis parameters such as time and temperature [20]. Effects of reactants and polymerization conditions on the conductivity of PPy coated textiles have been reported [21].To prepare the

conductive composite fabrics, many scientists have focused on *in situ* oxidative polymerization because this method does not require the destruction of the substrate and provides reasonably good conductivity [22-24]. Furthermore, *in situ* polymerization is expected to be one of the most convenient methods, because it is a relatively simple and easy method to control the conductivity by maintaining the high strength of the substrate fabric [16, 25, 26]

Electro-conducting doped polypyrrole was deposited by *in situ* oxidative polymerization on PET nonwovens and their thermal and flame resistance properties were studied by Varesano *et al.* [27]. Conducting fibers were prepared from cellulose and cotton by PPy coating in gas and liquid phase and the penetration of conductive polymer into fibers was studied by scanning electron microscope [28]. Pyrrole was polymerized on the surface of cellulose fibers after a sequence of fiber impregnations in $FeCl_3$ solutions [29]. Preparation and properties of bio based conductive composites of polypyrrole coated on silk fabrics, which find application in biomedical field was reported by Cucchi *et al.* [30]. PPy was coated on PET fabrics by chemical synthesis using four different oxidizing agent-dopant combinations and the heat generation of resultant PPy coated fabrics was studied by Hakansson *et al.* [31]. Electrically conductive fabrics which find potential applications as technical textiles with antistatic, antibacterial and high temperature resistance properties were produced by deposition of thin film of doped polypyrrole on surface of cotton fibers by Varesano *et al.* [32].

Kayanak and Beltran [21] investigated the effect of synthesis parameters on electrical conductivity of polypyrrole coated PET fabrics. PET fabric/ polypyrrole composite with high electrical conductivity was prepared and the effects of the chemical or the electrochemical polymerization conditions on the

properties such as surface morphology, electrical conductivity, environmental stability and EMI shielding effectiveness was investigated by Kim *et al.*[33]. Kelly, Johnston, Borrmann, and Richardson [34] introduced new functionalized hybrid materials of cellulose fibers with polypyrrole having antimicrobial properties that can be used in plastics and packaging industry.

This part of the work describes the preparation and characterization of PPy and PPy coated Nylon-6 fibers (F-PPy) to be used for preparing conductive elastomeric composites. Optimization of coating conditions are also discussed. Infrared spectroscopy (IR), Scanning electron microscopy (SEM) and X-ray diffraction (XRD) analysis are used to characterize the PPy and F-PPy. DC conductivity of PPy and F-PPy is determined by a two probe method.The thermogravimetric and differntial scanning calorimetric analysis of PPy, virgin Nylon fiber and PPy coated Nylon fiber are also presented. The Possibility of application of PPy coated fiber as a strain sensor is also explored.

3.2 Experimental

3.2.1 Materials

The details of pyrrole, anhydrous ferric chloride, *p*-toluene sulphonic acid, methanol and Nylon- 6 fibers used in this study are given in section 2.1. Pyrrole monomer was purified by distillation and stored at 4 ^{0}C in the absence of light.

3.2.2 Preparation of PPy

PPy was prepared by chemical oxidative polymerization of pyrrole using anhydrous ferric chloride as oxidant and *p*-toluene sulphonic acid as dopant in aqueous medium. The optimum concentration of pyrrole in the polymerization solution was determined to be approximately 0.045 mol/l [4]. The optimum molar ratio of Fe (III) /Pyrrole for polymerization has been found to be 2.25 or

2.33 [6,10] and the ratio of dopant/Pyrrole has been found to be 0.4 [35]. Using these findings the concentrations used were $C_{pyrrole}$ = 0.045mol/l, C_{dopant} = 0.02 mol/l and $C_{oxidant}$= 0.1 mol/l. The reaction was carried out at 4 ^{0}C with continued stirring for 4 hours. Precipitated PPy was filtered, washed with water till the filtrate became colorless, followed by a wash with methanol to remove unreacted pyrrole and then dried in air oven at 55 ^{0}C for 24 hours. PPy is obtained as a black flimsy powder.

3.2.3 Preparation of PPy coated short Nylon- 6 fiber

Nylon-6 fibers, chopped to 6mm length, were subjected to *in situ* polymerization of pyrrole using anhydrous ferric chloride as oxidant and *p*-toluene sulphonic acid as dopant in aqueous medium to get PPy coated short Nylon fibers(F-PPy). The coated fibers were then filtered, washed with water till the filtrate became colorless, followed by a wash with methanol to remove unreacted pyrrole and then dried in air oven at 55 ^{0}C for 24 hours.

Before *in-situ* polymerization, the coating conditions are to be optimized in order to have uniform coating, maximum conductivity and appreciable mechanical strength. For this, the virgin fiber was soaked in pyrrole or oxidant prior to polymerization.

3.2.4 Infrared spectroscopy

The IR spectrum of the PPy sample, virgin Nylon fiber and PPy coated fiber were obtained as described under section 2.2.7.

3.2.5 Scanning electron microscopy

The scanning electron micrographs of PPy, virgin Nylon fiber and PPy coated fiber were obtained as described under section 2.2.8.

3.2.6 DC conductivity

For electrical measurement of PPy bulk sample in the form of pellets were prepared (section 2.2.1). DC conductivity of the pellet was measured by a two probe method as described in section 2.2.5. At least five different measurements were used to calculate conductivity values.

In the case of fiber the surface resistance was measured using a two probe method (section 2.2.5). Here also at least five different measurements were taken for the fiber sample and the average value was taken as the surface resistance.

3.2.7 Thermogravimetric analysis

Thermogravimetric analysis of PPy, virgin Nylon fiber and PPy coated Nylon fiber was performed to determine changes in weight in relation to change in temperature. TGA studies were carried out as per section 2.2.10.

3.2.8 Differential scanning calorimetric analysis

Differential scanning calorimetry was employed to determine the Tg of PPy. The degree of crystallinity, heat of fusion, melting temperature and Tg of virgin fiber and PPy coated fiber were also evaluated. The measurements were conducted as described under section 2.2.11.

3.2.9 X-ray diffraction analysis

X- ray diffractograms of PPy, virgin fiber and PPy coated fiber were recorded. The details of XRD analysis is given in section 2.2.9.

3.2.10 Mechanical properties of fiber

The mechanical properties of the fiber was studied using a Shimadzu Universal Testing Machine (model AG-I) with a load cell capacity of 10kN.

The gauge length between the grips at the start of each test was adjusted to 50mm. The fibers were held between the two grips and a crosshead speed of 50mm/ min was applied. The strength was evaluated after each measurement automatically by the microprocessor and presented on a visual display. Average of at least six sample measurements was taken to represent each data point.

3.3 Results and discussion

3.3.1 Optimization of reaction conditions - PPy coating on Nylon fiber

Impregnation of fiber with pyrrole monomer prior to polymerization gave more uniform coating compared to oxidant ($FeCl_3$) impregnation as is evident from fig. 3.2.

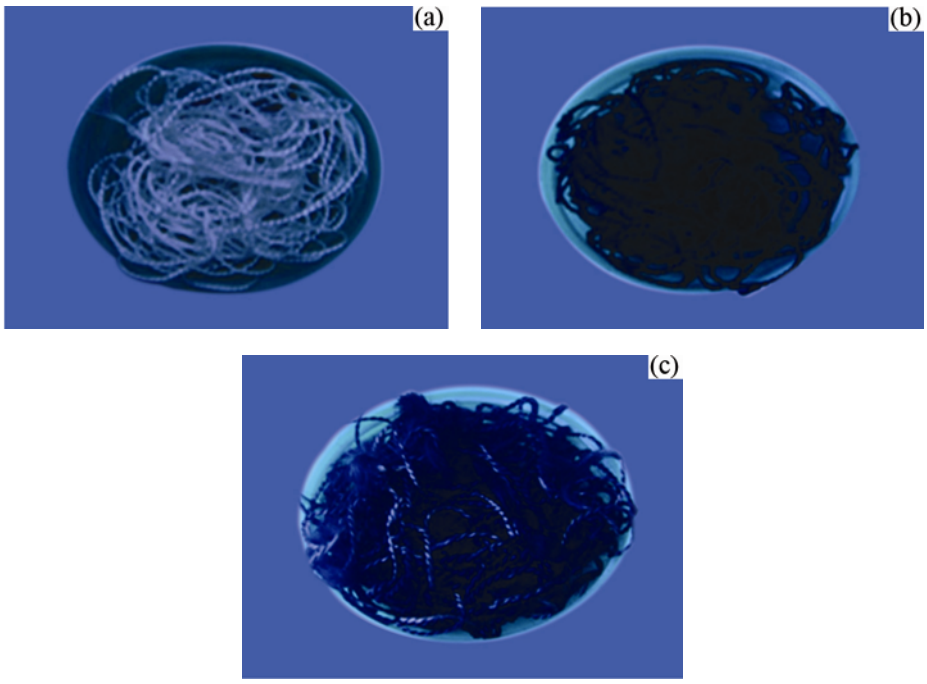

Fig. 3.2 (a) Virgin Nylon fiber (b) PPy coated Nylon fiber – monomer impregnated prior to polymerization (c) PPy coated Nylon fiber – oxidant impregnated prior to polymerization

The effect of dipping time on the surface resistance and strength of PPy coated fiber was evaluated by soaking the fiber to different time durations in monomer prior to polymerization. The surface resistance and strength of resulting fibers were determined as described under sections 2.2.5 and 3.2.10 respectively. The variations of surface resistance and strength of PPy coated fiber as a function of dipping time are shown in fig. 3.3 and fig. 3.4, respectively. It is found that as the time for which the fiber is dipped in monomer increases, resistance of fiber decreases. This is because more and more PPy gets coated on fiber with increased time of monomer dipping. Introduction of PPy into a composite, as a rule, decreases its strength and results in the loss of elasticity [36]. This accounts for the decrease in strength of PPy coated fiber with time of dipping. It is understood that as the extent of monomer dipping increases, resistance of PPy coated fiber decreases and therefore conductivity increases, while there occurs a substantial fall in strength of fiber. Since there occurs a drastic decrease in strength of fiber beyond 1 h, and a reasonable conductivity is obtained at 1 h, the optimum time of monomer dipping is fixed as 1 h.

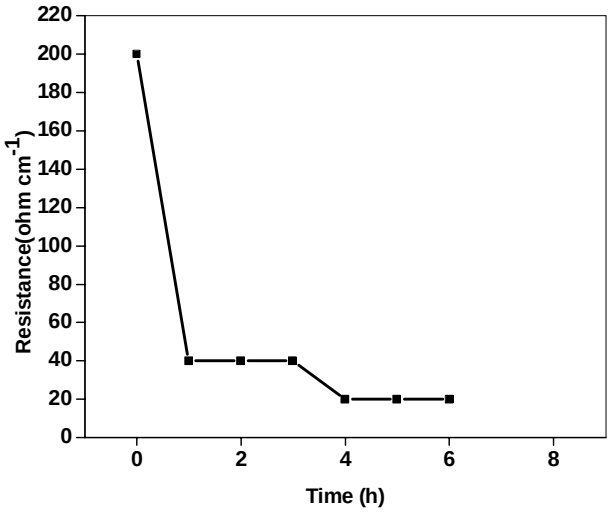

Fig. 3.3 Variation of resistance of PPy coated fiber with time of dipping in monomer

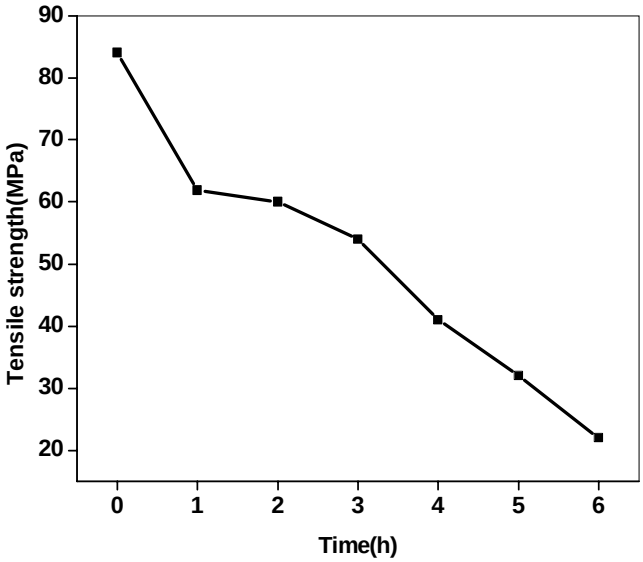

Fig. 3.4 Variation of tensile strength of PPy coated fiber with time of dipping in monomer

3.3.2 Infrared spectroscopy

Figure 3.5 shows the IR spectrum of PPy. The IR peak obtained at 3444 cm^{-1} is due to N-H stretching [37]. The band at 1534 cm^{-1} corresponds to C=C stretching and that at 1440 cm^{-1} to C-C and C-N stretching: ie, typical PPy ring vibrations. The peak at 1293 cm^{-1} may be assigned to mixed bending and stretching vibrations associated with C-N links [38,39]. C=N stretching gives a band at 1151 cm^{-1}. In-plane deformation vibrations of C-H bond and N-H bond of pyrrole ring give rise to a peak at 1032 cm^{-1}.[40] IR peak at 853 cm^{-1} is due to C=H out of plane vibration indicating polymerization of pyrrole [41]. The band at 777 cm^{-1} may be assigned to N-H out of plane vibration [32]. The band at 617 cm^{-1} may be assigned to C-Cl vibrations [42]. Thus PPy obtained by the chemical polymerization method using $FeCl_3$ as oxidant is Cl^- doped.

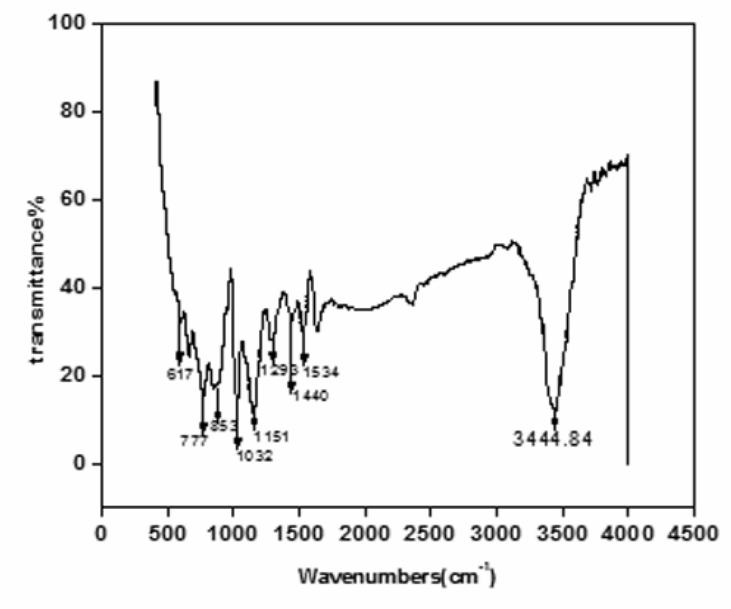

Fig. 3.5 IR spectrum of PPy

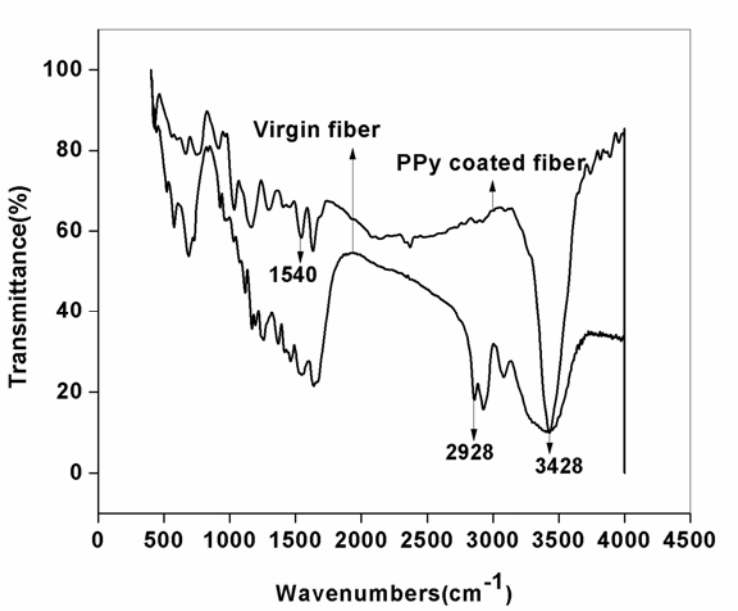

Fig. 3.6 IR spectrum of virgin Nylon fiber and PPy coated fiber

Comparison of IR spectrum of virgin Nylon fiber with PPy coated fiber(fig. 3.6) shows that the peak at 3428 cm^{-1} due to NH stretching in virgin fiber becomes more intense in PPy coated fiber as in the case of pristine PPy. Again, the peak at 2928cm^{-1} attributed to C-H stretching in virgin fiber disappears in PPy coated fiber. These two observations support the presence of a uniform coating of PPy on Nylon fiber. Peak at around 1534 cm^{-1} corresponds to C=C stretching in PPy. In the IR spectrum of coated fiber, there is an intense peak around 1540 cm^{-1} which is found to be less intense in virgin fiber. Such an observation has been reported in the case of PPy coated cellulose fibers [29] and was used to detect the presence of PPy on cellulose fibers.

3.3.3 Scanning electron microscopy

The granular morphology of PPy powder is visible in figure 3.7.The powder is composed of quasi spherical particles with diameter of about 250nm bonded to each other in irregular agglomerates. The agglomerates exhibit the typical three dimensional and dendritic structure of PPy obtained by chemical polymerization in water. Similar morphology for chemically polymerized PPy has been reported [32,43,44]. The size, regularity and roughness of the particles seem to depend upon the nature of oxidant, presence of surfactant, nature of dopant etc.

Varesano *et al*. [32] examined the SEM images PPy obtained by three methods: (1) ferric chloride oxidant (b) ammonium per sulphate oxidant (c) ferric chloride oxidant and additional doping agent, naphthalene di sulphonic acid (NDS). It was found that the particles are more regular and smaller when APS was used as oxidant. The roughness seems to be increased by the presence of NDS in the polymerization bath. The amorphous nature of polypyrrole seen in SEM picture is reflected in XRD spectra also (section 3.3.7).

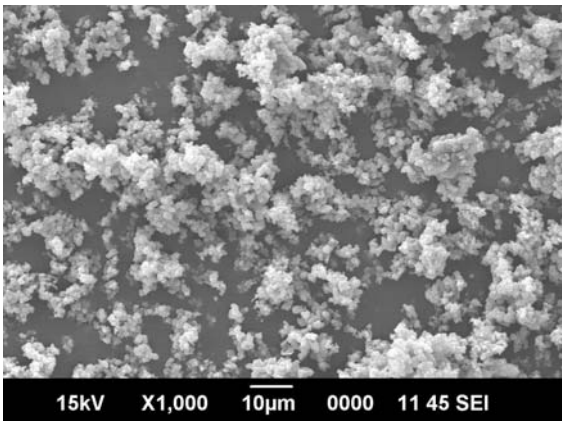

Fig. 3.7 Scanning electron micrograph of PPy

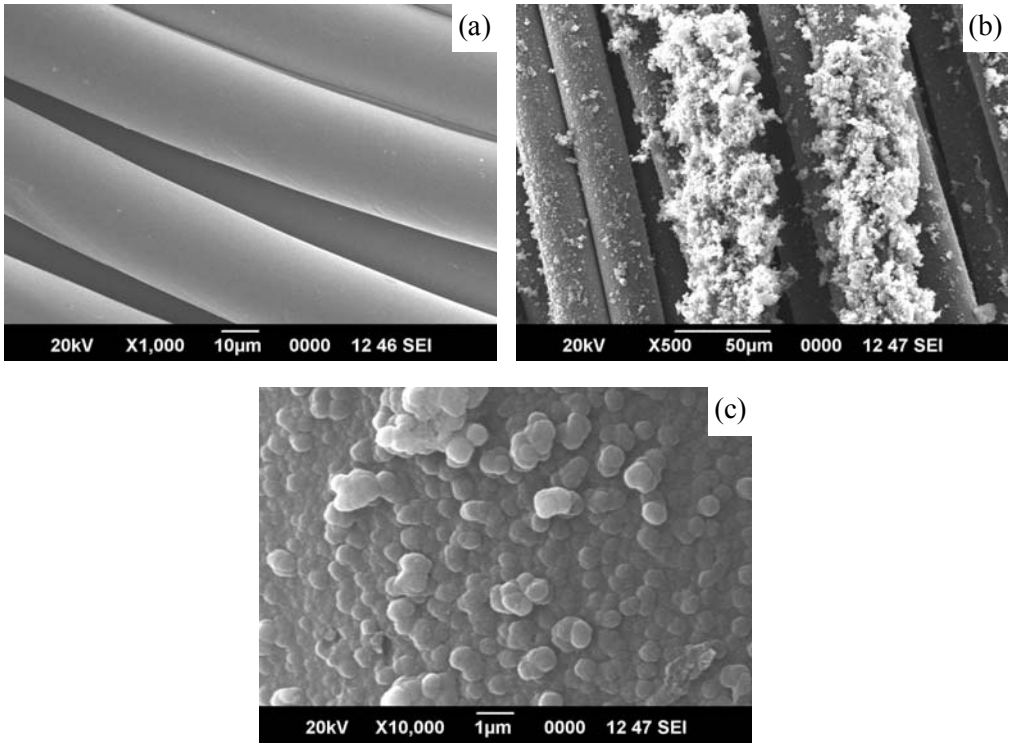

Fig. 3.8 Scanning electron micrographs of (a)virgin Nylon fiber, (b) PPy coated Nylon fiber and (c) PPy coated Nylon fiber at higher magnification

Figure 3.8(a) shows the smooth surface of uncoated Nylon-6 fiber. Fig. 3.8 (b) and (c) show that PPy forms a dense coating of fused small hemi spheres on Nylon fiber, fully encapsulating the fiber surface. During *in situ* polymerization, the individual fibers are coated with an even adherent polymer layer, directly grown on the fiber surface [27]. PPy coated PET fibers [27,21] exhibit similar morphology with each individual fiber covered with thin coherent film of PPy. Conductive polymer coating on textiles through chemical polymerization enables smooth coherent film to encase individual fibers [21]. Some aggregates of spherical particles are also formed. PPy coated cotton and cellulose with similar morphologies have also been reported [32,34]. This coherent coating of PPy on Nylon fiber results from the possible formation of chemical bonds between Nylon surface and the PPy molecules [45]. The adsorption of pyrrole at the substrate during the polymerization process therefore dictates the resulting structure of PPy coating [46]. The carbonyl groups on the Nylon backbones can provide a template for pyrrole monomers *via* hydrogen bonds, yielding a higher ordered and coherent PPy [47]. Individual fibers do not stick to each other but remain well separated. The presence of a continuous PPy layer covering each fiber surface indicates that pyrrole could penetrate into the interstices between fibers and polymerization occurred inside the threads, not only at the surface of the fiber. The feature is expected to have positive consequences on the electrical properties of PPy coated fiber. Such a phenomenon has been observed in the case of PPy coated silk fabrics [30].

3.3.4 DC conductivity

DC conductivity of 1.527×10^{-1} S cm^{-1} at room temperature is shown by the PPy sample prepared. PPy coated fiber obtained by dipping the fiber in monomer for 1h prior to *in situ* polymerization gives a surface resistance of 40Ω/cm.

3.3.5 Thermogravimetric analysis

Thermogravimetric analysis of pristine PPy is depicted in fig. 3.9. A first weight loss of 6.5% is due to loss of moisture. The second degradation, with a peak degradation occurring at 448 ^{0}C corresponds to degradation of PPy chain. Less than 30% weight loss occurs during this degradation. At 800 ^{0}C the residue weight is 55%. This indicates the high thermal stability of PPy which is in good agreement with the report of Cataldo and Omastova [48] that PPy produced with $FeCl_3$ as oxidant has a quite good thermal stability. Similar thermograms for PPy have been reported by others [49,50].

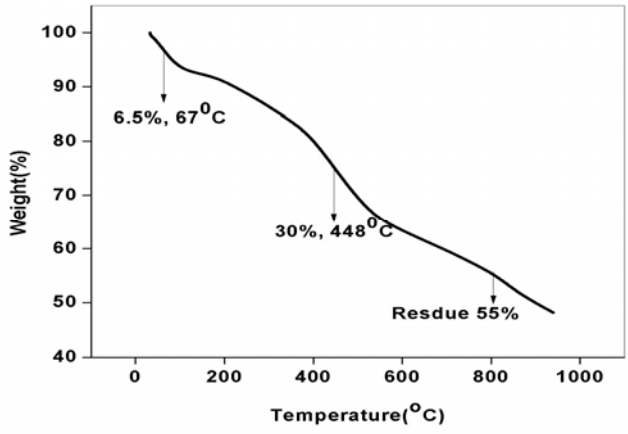

Fig. 3.9 TG curve of PPy

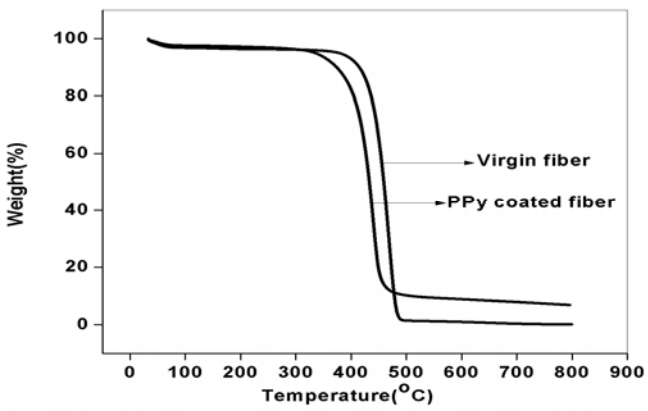

Fig. 3.10 TG curves of virgin fiber and PPy coated fiber

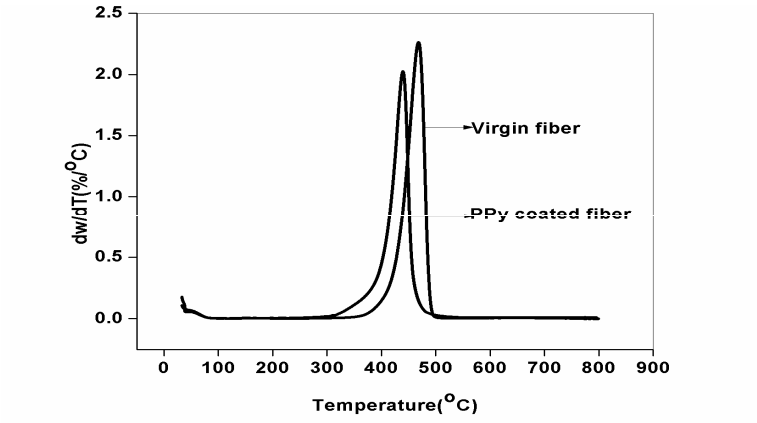

Fig. 3.11 DTG curves of virgin fiber and PPy coated fiber

Table 3.1 Thermal characteristics of the fiber

Thermal degradation parameters	**Virgin fiber**	**PPy coated fiber**
Onset degradation temperature (^{0}C)	376	338
Peak degradation temperature (^{0}C)	468	448
Peak degradation rate (%/^{0}C)	2.26	2.01
Weight loss at peak degradation temperature (%)	94.3	86
Temperature at 50% weight loss (^{0}C)	459	437
Weight remaining at 300^{0}C (%)	96.2	96.4
Weight remaining at 600^{0}C (%)	1	8.8
Residue at 800^{0}C(%)	0.2	6.7

The thermal mass loss traces obtained with the TG analysis from virgin Nylon fiber and PPy coated Nylon fiber are reported in fig. 3.10. Fig.3.11 represents the derivative thermograms. The thermal characteristics of the virgin and PPy coated fiber are presented in Table 3.1. The onset of thermal degradation of Nylon fiber occurs at about 376^{0}C whereas PPy coated fiber starts degrading at a lower temperature, at about 338^{0}C. PPy coated PET fibers [27] also show a decrease in onset of degradation from 370^{0}C of PET to 340^{0}C

of PET/PPy. It was pointed out by Wu *et al.* [51] that PPy coated fibers are less stable to heating than uncoatd fibers because of the breakdown of the PPy backbone. The peak degradation temperature is 448^0C for F-PPy which is also lower than that of virgin fiber. However, weight loss and rate of degradation at this temperature are lower for F-PPy. Residue weight is higher for F-PPy which may be due to the undegraded PPy. This is in good agreement with literature on PPy coated PET fibers where mass of residual char at 500^0C is higher in the coated fiber,16.1% compared to 12.6% for PET [27].

3.3.6 Differential scanning calorimetric analysis

DSC of PPy (fig. 3.12) shows a broad endothermic dip at about 108^oC which is the glass transition temperature of PPy overlapping the moisture release. A second endotherm starting at about 200^oC may be due to PPy backbone degradation.

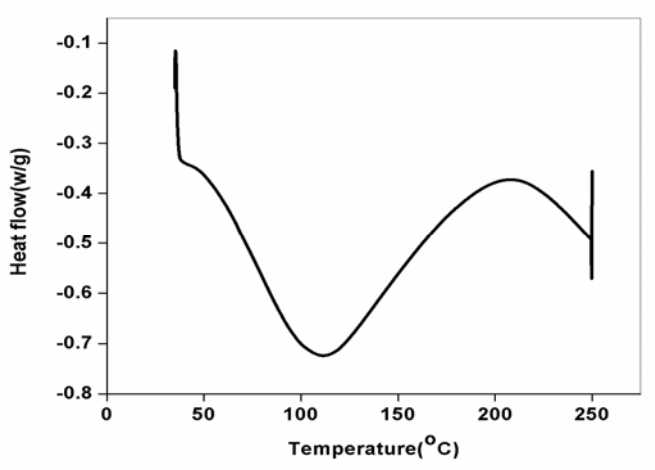

Fig. 3.12 DSC curve of PPy

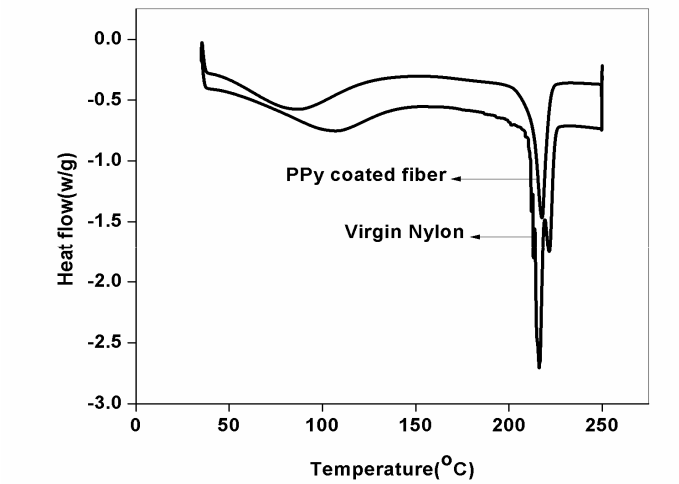

Fig. 3.13 DSC curves of virgin fiber and PPy coated fiber (F-PPy)

Table 3.2 DSC analysis of virgin fiber and PPy coated fiber

Fiber	Melting temp. T_m(°C)	Heat of fusion ΔH(J/g)	Degree of crystallinity (%)	Glass transition T_g(°C)
Virgin	216.2	77.15	35.6	105
PPy coated	217.7	46.51	30.7	88

Fig. 3.13 shows DSC curves of the virgin and PPy coated fiber. The melting temperature, heat of fusion, degree of crystallinity and glass transition temperature of virgin fiber and PPy coated fiber are presented in table 3.2. The melting temperature shifts to a slightly higher value on PPy coating. PPy coating reduces the heat of fusion and degree of crystallinity of Nylon fiber. The observations agree with the findings of Varesano *et al.* on PPy coated PET fibers [27]. This may be due to the destruction of crystalline regions by the formation of PPy on the fiber surface. Similar observations in the case of polyaniline coated Nylon fibers have been reported [52]. It is mentioned that diffusion of aniline into the Nylon fiber presumably disturbs the crystalline regions and decreases its thermal properties. A decrease in Tg of Nylon fiber on PPy coating may be attributed to an increase of segmental motion.

3.3.7 X-ray diffraction analysis

X-ray diffraction patterns of PPy, virgin fiber and PPy coated fiber are depicted in fig. 3.14 and the XRD data of virgin fiber and PPy coated fiber are given in table 3.3.

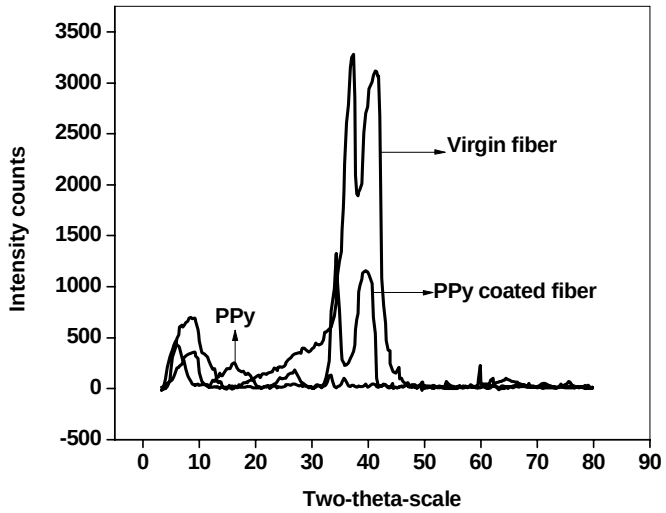

Fig. 3.14 X-ray diffraction patterns of PPy, virgin fiber and PPy coated fiber

Table 3.3 XRD data of virgin fiber and PPy coated fiber

Fiber	2θ (α_1)	2θ (α_2)
Virgin	20.1	23.1
PPy coated	18.8	22.2

Broad peak of PPy at about $2\theta=27^{o}$ is characteristic peak of amorphous PPy [53] and are due to the scattering from PPy chains at the interplanar spacing [54]. Previous X-ray scattering studies of polypyrrole films have been reported to be highly disordered and non-crystalline [55]. Intensity of α_1 and α_2 peaks of the uncoated Nylon fibers reduces upon PPy coating due to decrease in the percentage of crystallinity of the fiber.

3.4 Polypyrrole coated fiber as strain sensor

The mechanical properties of the virgin Nylon fiber and PPy coated fiber were studied as described under section 3.2.10. The mechanical properties of virgin fiber and PPy coated fiber are given in table 3.4.

Table 3.4 Mechanical properties of virgin fiber and PPy coated fiber

Fiber	Tensile strength(MPa)	Elongation at break (%)
Virgin	85.6	135.6
PPy coated	61.87	120

It is found that the Nylon fiber becomes stiffer on PPy coating due to less flexibility of PPy coating and decrease of free space for stretching. Tensile strength and elongation at break decrease significantly. Decrease of tensile strength may be due to the hydrolysis of the fiber surface by the strong oxidant solution during *in situ* polymerization. However, the mechanical properties of the prepared PPy coated fiber are found to be satisfactory for normal service conditions.

Recently, it has been reported that conductivity of PPy-coated fabrics is also sensitive to strain, thus the conductive fabrics can be used to measure and control the movement of human body and construct wearable devices [56]. In comparison with most of the commercially available sensors, based usually on metal oxides and operated at high temperatures, the sensors based on conducting polymers have many improved characteristics. They have high sensitivities and short response time; especially these features are ensured at room temperature. Conducting polymers are easy to be synthesized through chemical or electrochemical processes, and their molecular chain structure can be modified conveniently by copolymerization or structural deviations.

Furthermore, conducting polymers have good mechanical properties, which allow a facile fabrication of sensors [57].

Rossi *et al.* developed a sensorized glove based on the PPy coated Lyrca/ cotton [56]. Oh *et al.* have reported that the PPy coated Nylon-spandex was sensitive to strain change until a deformation of 50% [58]. Kim *et al* .also proposed the elastic composite, PPy /PET/Spandex can be used as a strain sensor for large deformation up to 50% [13].

The possibility of the prepared PPy coated Nylon fiber possessing practically applicable mechanoelectrical property was also explored. As shown in fig. 3.15 F-PPy is found to exhibit monotonic increase in surface resistance with the elongation upto break point. Therefore it is proposed that PPy coated Nylon fiber can be used as a strain sensor for large deformation.

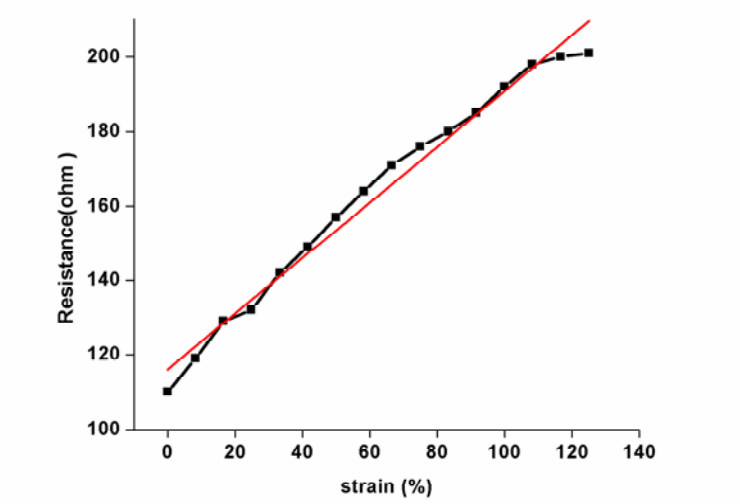

Fig. 3.15 Electrical resistance changes of PPy coated Nylon fiber with elongation

3.5 Conclusions

Polypyrrole having DC electrical conductivity 1.527×10^{-1}S $cm^{-1}$was prepared by chemical oxidative polymerization. It was characterized by infrared spectroscopy, scanning electron microscopy and X-ray diffraction. It was found from thermogravimetric analysis that PPy is highly stable: maximum degradation occurring at 448 ^{0}C with a residue weight of 55% at 800 ^{0}C. Electrically conducting PPy coated Nylon fibers were prepared by *in situ* polymerization of pyrrole on Nylon fibers. Dipping the fiber in monomer for 1 h prior to polymerization results in conducting fibers having higher conductivity compared to oxidant dipping. Comparison of IR spectrum of virgin Nylon fiber with PPy coated fiber indicated the presence of a uniform coating of PPy on Nylon fiber. SEM studies also revealed a dense uniform coating of PPy on Nylon fiber. The prepared PPy coated fiber finds application as a strain sensor.

References

[1] Gangopadhyay R, De A. *Chem Mater*. **2000**, 12, 608.

[2] Walker JA, Witucki EF, Warren F. *U.S. Patent No. 4697001*, **1987**.

[3] Machida S, Miyata S. *Synth Met*. **1989**, 31, 311.

[4] Rapi S, Bocchi V, Gardini G P. *Synth Met*. **1988**, 24, 217.

[5] Chao T H, March J. *J PolymSci*: *Part A: Polymchem.* **1988**, 26, 743.

[6] Armes SP. *Synth Met*. **1987**, 20, 365.

[7] Mohhammadi A, Lundstrom I, Salaneck W R. Inganas O. *Synth Met*. **1987**, 21, 169.

[8] Bocchi V, Gardini G P. *J Chem Soc Chem commun.***1986**, 148.

[9] Armes S P, Vincent B. *J Chem Soc Chem commun.***1987**, 287.

[10] Dhawan S K, Trivedi D C. *J Bull Mater Sci.***1993**, 16, 371.

[11] Achour ME, Droussi A, Zoulef S, Gmati F, Fattoum A, Mohamed BA, ZangarH. *Spectrosc Lett*. **2008**, 41, 299.

[12] Shin HW, Lee JY, HeumY. *Mol Cryst Liq Cryst*.**2008**, 492, 403.

[13] Kim HK, Kim MS, Chun SY, Park YH, Jeon BS, Lee JY. *Mol Cryst Liq Crys*. **2003**, 405, 161.

[14] Jamadade S, Jadhav S, Puri V. *Arch Phys Res*.**2010**, 1, 205.

[15] Xie H, Liu C, Guo J. *Polym Int*. **1999**, 48, 1099.

[16] Neoh KG, Tay BK, Kang ET. *Polymer*. **2000**, 41, 9.

[17] Goettler LA, Shen KS. *Rubber Chem Technol*. **1983**, 56, 619.

[18] Setue DK, De SK. *J Mater Sci.* **1984**, 19, 983.

[19] Johnston HJ, Kelly FM, Moraes J, Borrmann T, Flynn D. *Curr Appl Phys*. **2006**, 6, 587.

[20] Lin T,Wang L,Wang X, Kaynak A. *Thin solid films*. **2005**, 479, 77.

[21] Kaynak A, Beltran R. *Polym. Int*. **2003**, 52,1021.

[22] Kuhn HH, Kimbrell WC, Worrell G, Chen CS. *Tech Pap Soc Plast Eng*. **1991**, 37, 760.

[23] Gregory RV, Kimbrell WC, Kuhn HH. *J Coated Fabrics*. **1991**, 20, 167.

[24] Sengupta LC, Spurgeon WA. *Critical Mater. Processes; Int. SAMPE Electron 6th Conf.* **1992**, p. 146.

[25] MacDiarmid AG, Chiang JC, Richter AF. *Synth Met*.**1987**, 18, 285.

[26] Hsu CH, Segonds PV, Epstein AJ. *Synth Met*. **1991**, 1005, 41.

[27] Varesano A, Tonin C, Ferrero F, Stringhetta M . *J Therm Anal Calorim*.**2008**, 94 , 559.

[28] Hosseini SH, Pairovi A. *Ind Polym J*, **2005**, 14, 934.

[29] Beniventi D, Alila S, Boufi S, Chaussy D, Nortier P. *Cellulose*. **2006**, 13, 725.

[30] Cucchi I, Boschi A, Arosio C, Bertini F, Freddi G, CatellaniM. *Synth Met*. **2009**, 159, 246.

[31] Hakansson E, Kaynak A, Lin T, Nahavandi S, Jones T, Hu E. *Synth Met*. **2004**, 144, 21.

[32] Varesano A, Aluigia A, Florio L, Fabris R. *Synth Met*. **2009**, 159 , 1082.

[33] Kim MS, Kim HK, Byun SW, Jeong SH, Hong YK, Joo JS, Song KT, Kim JK, Lee CJ, Lee JY. *Synth Met*. **2002**, 126 , 233.

[34] Kelly FM, Johnston HJ, Borrmann T, Richardson MJ. *Eur J Inog Chem*. **2007,** 5571**.**

[35] Gregory RV, Kimbrell WC, Kuhn H. *Synth Met*. **1989**. 28, C823.

[36] Smirnov MA, Kuryndin IS, Nikitin LN, Sidorovich AV, Yu N, Sazanov OV, Kudasheva V, Bukosek AR, Khokhlov, Elyashevich GK. *Russ J Appl Chem*. **2005**, 78, 1993.

[37] Kassim A, Mahmud HNM, Yee LM, Hanipah N. *Pac J Sci Technol*. **2006**, 7, 103.

[38] Dias RHV, Fianchini M, Rajapakse GRM. *Polymer*, **2006**, 47, 7349.

[39] Shiigi H, Kishimoto M, Yakabe H, Deore B, Nagaoka. *JAnal Sci*. **2002**, 18, 41.

[40] Davidson RG, Turner TG. *Synth Met*. **1996**, 79, 165.

[41] Chen W, Xingwei L, Gi X, Zhaoquang W, Wenquing Z. *Appl Surf Sci*. **2003**, 218, 216.

[42] Adhikari A. *Ph. D. Thesis, University of Pune, India*, **2004**, p 86.

[43] Kim DK, Oh KW, Ahn HJ, Hun SK. *J ApplPolym Sci*. **2008**, 107, 3925.

[44] Taunk M, AtulKapil A, Chan S. *Solid State Commun*.**2010**, 150 , 1766.

[45] Myers RE. *J Electron Mater*. **1986**. 15, 61.

[46] Martin CR. *Science*, **1994**, 266, 1961.

[47] Zhang X, Bai R. *J Mater Chem*. **2002**, 12, 2733.

[48] Cataldo F, Omastova M. *PolymDegrad Stab*. **2003**, 82, 487.

[49] Gu Z, Zhang L, Li C. *J Macromol Sci, Part B*. **2009**, 48, 1093 .

[50] Zoppi RA, De Paoli MA. *Polymer*. **1996**, 37, 1999.

[51] Wu J, Zhou D, Too CO, Wallace GG. *Synth Met*. **2005**, 155, 698.

[52] Chandran AS. *Ph. D. Thesis, Cochin University of Science and Technology, India*, **2008**.

[53] Partch RE, Gangoli SG, Matijevic E, Cai W, Arajs S. *J Colloid Interface sci*. **1991**,144, 27.

[54] Ouyang JY, Li YF. *Polymer*. **1997**, 38, 3997.

[55] Kassim A, Davis FJ, Mitchell GR. *Synth Met*. **1994**, 62,41.

[56] Scilingo EP, Lorussi F, Massoldi A, Rossi DD. *IEEE Sensors J*. **2003**, 3, 460.

[57] Bai H, Shi G. *Sensors*, **2007**, 7, 267.

[58] Oh KW, Park HJ, Kim SH. *J Appl Polym Sci*. **2003**, 88, 1225.

.....ooo.....

Chapter

4

CONDUCTING ELASTOMER COMPOSITES: NR/PPy/PPy COATED SHORT NYLON FIBER

Contents

Polypyrrole(PPy) and Polypyrrole coated short Nylon fiber(F-PPy) were used to prepare rubber composites based on natural rubber(NR) by proper compounding on a two roll mill followed by moulding. The cure pattern, cure kinetics and filler dispersion of the elastomeric composites were evaluated. Compared to PPy, PPy coated fiber was effective in increasing the cure rate. Results of cure kinetic studies agreed with these observations. First order kinetics was observed for cure reactions. The composites prepared were characterized using scanning electron microscopic (SEM) analysis. The DC electrical conductivity and mechanical properties of the composites were studied. The solvent swelling characteristics of the composites were investigated in toluene. The DC conductivity of the composites was better for the F-PPy system compared to PPy- filled elastomeric composites. The highest conductivity obtained was 3.6×10^{-5} S/cm. The mechanical properties of NR were declined by PPy loading which was compensated by the addition of PPy coated fiber. The percentage swelling index and swelling coefficient of the composites decreased with increase in PPy loading and F-PPy loading. The solvent sorption mechanism in the conducting composites exhibits deviation from Fickian mode.

4.1 Introduction

Reports of a large number blends/ composites of PPy with many polymers including plastics, elastomers, fibers and fabrics have been described in chapter1. Elastomers are a class of polymers comprising of rubbers and latexes. The presence of unsaturated C=C bonds in elastomers promote crosslinking reactions with sulphur and they are used in polymer industry in the form of rubber compounds containing reinforcing fillers, curing agents, accelerators, pigments and other additives. Incorporation of conductive additives into elastomer matrix constitutes an excellent approach for the development of special materials, which combine electronic conductivity with elasticity and other important mechanical properties imparted by the insulating rubber matrix [1]. Even though incorporation of conductive particles like carbon black, metal, etc. modifies considerably the electrical conductivity of the composite, they deteriorate the mechanical characteristics of the composites compared with those of non-charged materials. The use of conducting polymers makes it possible to obtain composites having at the same time a raised electric conductivity associated with good mechanical properties[2]. The processability and properties of CECs depend on the nature and type of the elastomer *viz.*,polar/ non-polar and natural/ synthetic and the properties of conducting polymer incorporated into it.

Natural rubber(NR) is an addition polymer that is obtained as a milky white fluid known as latex from a tropical rubber tree. Natural rubber is from the monomer isoprene (2-methyl-1,3-butadiene). Since isoprene has two double bonds, it still retains one of them after the polymerization reaction. Natural rubber has the cis configuration (fig. 4.1)

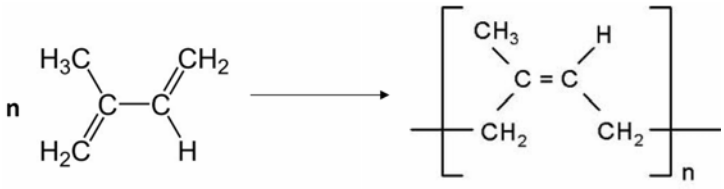

Fig. 4.1 Structure of natural rubber

The uniqueness of NR lies in its highly specific characteristics in addition to the general features of other rubbers. Due to biological origin, it is renewable, inexpensive and creates no health hazard problems. No synthetic substitute has comparable combination of elasticity, resilience, resistance to high temperature, extensibility and toughness. It possesses high tensile strength due to strain induced crystallization, superior building tack and good crack propagation resistance. These features make NR suitable for a variety of industrial applications in which it cannot be replaced by synthetic alternatives. However for practical purposes NR is further reinforced by particulate fillers [3,4] and fibrous fillers [5-8].

Even though the processability and mechanical properties of polypyrrole is highly enhanced by the fabrication of the conducting composites, the composites never attain the strength of the host polymer matrix as there is deterioration of properties of polymer by the incorporation of PPy. If it is adhered to a strong substrate and then used as a filler in polymer matrix, improvement in mechanical properties is expected [9]. The electrical and mechanical properties of the elastomer composites depend on the aspect ratio of the filler. Fibers are characterized by high aspect ratios. It is well established that mechanical properties of rubber composites can be greatly improved by adding short fibers [5-8, 10-13]. These composites combine the elastic behavior of rubber with the strength and stiffness of fiber.

This part of the work describes the synthesis of conducting elastomer composites (CECs) of PPy based on NR. Nylon-6 fiber is added as filler for improving the mechanical properties. Since the introduction of Nylon fiber; an insulating material, tends to affect the conductivity of the composite, PPy coated Nylon fiber is used. The use of PPy coated fiber is expected to improve the mechanical properties of the CECs, at the same time increasing the conductivity. The cure parameters, cure kinetics, filler dispersion and morphology of the prepared composites are studied. DC electrical conductivity, mechanical properties and swelling characteristics of the composites are also evaluated.

4.2 Experimental

4.2.1 Materials

The details of natural rubber (NR), zinc oxide, stearicacid, tetramethylthiuram disulphide (TMTD), mercaptobenzothiazyl disulphide(MBTS), sulphur and toluene used in this study are given in section 2.1.

4.2.2 Preparation of conductive elastomeric composites(CECs)

Polypyrrole (PPy) and PPy coated short Nylon fiber (F-PPy) were prepared as per sections 3.2.2 and 3.2.3, respectively. The formulation for the preparation of composites is given in Table 4.1. Three series of CECs were prepared. NP series represent the vulcanizates of natural rubber with varying amounts of PPy. NPFp series contain 50phr PPy and varying amounts of F-PPy. The third series, NFp represents NR/ F-PPy composites; ie, NR with varying amounts of F-PPy. These composites were prepared in a two-roll mill as described under section 2.2.2. The optimum cure time at 150^0C was determined using a Rubber Process Analyzer (section 2.2.3). The compounds were then compression moulded at 150^0C in an electrically heated hydraulic

press (section 2.2.4). The vulcanized sheets were kept in a cold dark place for 24 h and were used for the subsequent tests

Table 4.1 Formulation for the preparation of NR based CECs

Sample	PPy(phr)[a]	F-PPy(phr)[a]
NP0	0	0
NP1	30	0
NP2	50	0
NP3	75	0
NP4	100	0
NP5	120	0
NPFp1	50	5
NPFp2	50	10
NPFp3	50	25
NPFp4	50	50
NPFp5	50	75
NFp1	0	3
NFp2	0	5
NFp3	0	15
NFp4	0	25
NFp5	0	50

All mixes contain NR-100g, zinc oxide- 5phr, stearic acid- 2phr, tetramethylthiuram disulphide- 0.2phr, mercaptobenzothiazyl disulphide- 0.6phr, sulphur- 2.5phr

a - parts per hundred rubber

4.2.3 Cure characteristics and cure kinetics

The cure time T_{90}, scorch time T_{10}, maximum torque M_H, and minimum torque M_L values of the vulcanizates were determined at 150 ^{0}C using a Rubber Process Analyzer (section 2.2.3). The cure rate index (CRI) [14,15] which is a direct measure of the quickness of the curing reaction and the kinetic rate constant of cure reaction, were determined from the rheometric data:

$$CRI = 100/(T_{90} - T_{10}) \text{ ---------- (4.1)}$$

The vulcanization kinetics was studied by the method[16,17,18] given below. The general equation for the kinetics of a first-order chemical reaction is

$$\ln(a - x) = -kt + \ln a \text{ ---------- (4.2)}$$

where 'a' is the initial reactant concentration, 'x' is the reacted quantity of reactant at time 't' and 'k' is the first-order rate constant. For the vulcanization of rubber, measuring the torque developed during vulcanization monitors the rate of crosslink formation. The torque obtained is proportional to the modulus of rubber. Thus, the following substitutions can be made.

$$(a - x) = M_H - M_t \text{ ---------- (4.3)}$$

$$a = M_H - M_L \text{ ---------- (4.4)}$$

where 'M_t' is the torque at time t. Therefore, the equation can be written as

$$\ln (M_H - M_t) = -kt + \ln(M_H - M_L) \text{ ---------- (4.5)}$$

Therefore, if a plot of ln ($M_H - M_t$) against time t is a straight line, then the cure reaction follows first-order kinetics. The cure reaction rate constant(k) can be obtained from the slope of the corresponding straight lines [19].

4.2.4 Filler dispersion

The dispersion of filler within the matrix and formation of filler agglomerates were studied in detail by Lee and Costa [20,21]. According to Lee, even well dispersed filler–rubber systems show differences in the degree of filler agglomeration in the cured and uncured state. Lee assumed that $\eta_r > Er$ where η_r and Er are the relative viscosity (ratio of the viscosities due to loaded and unloaded elastomer) and the relative moduli (ratio of the modulus for

loaded and unloaded elastomer), respectively. Lee further proposed that η_r and Er could be determined from rheometric data by using the expressions

$$\eta_r = M^f_L/M^0_L \quad \text{and} \quad Er = M^f_H/M^0_H \quad \text{---------- (4.6)}$$

where 'M' denotes the torque and the superscripts f and 0 are related to the loaded and unloaded polymer, respectively. Lee introduced a new parameter 'L' defined as

$$L = \eta_r - Er \quad \text{---------- (4.7)}$$

For ideal dispersions, η_r = Er. This happens when the individual particles are well dispersed in the matrix. In the case of non-ideal dispersions, the value of L changes slowly at low filler loadings, but above certain limit, it increases very sharply. The abrupt rise of the index L at high filler loadings may be ascribed to the predominance of agglomerates remaining relatively undispersed in the rubber. In such a situation, it is assumed that the filler concentration has reached the point where there is not enough rubber to fill all available voids in the filler. Another mathematical expression has been proposed by Wolff [22] in terms of rheometric data to characterize filler structure present in rubber vulcanizates. When afiller is incorporated into a compound, the maximum torque variation, $\Delta M^f = M^f_H - M^f_L$ observed during vulcanization increases. The ratio between ΔM^f and ΔM^0, i.e., the torque variations for the loaded and unloaded compounds is directly proportional to filler loading. By plotting the relative torque as a function of filler loading, a straight line is obtained whose slope was defined by Wolf as α_f [23-25].

$$\Delta M^f/\Delta M^0 - 1 = \alpha_f (m_f/m_p) \quad \text{---------- (4.8)}$$

Where 'm_p' is the mass of polymer in the compound and 'm_f' is the mass of filler in the compound and 'α_f'is specific constant for the filler, which is

independent of the cure system and closely related to the morphology of the filler. The parameter α_f represents the final structure of the filler as it exists in the vulcanizates after all possible structure breakdowns that occurred during mixing and vulcanization. The reinforcement build-up and crosslinking reaction both take place during curing and without affecting each other. The application of Eq. (4.8) allows the definition of a filler specific constant, related to the filler structure, and also predicts whether or not crosslink density is unaffected by the presence of the filler, in which case, a straight line is obtained. The equation also shows that based on a single test, α_f can be calculated from the changes in the torque which occur during vulcanization of two compounds, the unloaded and loaded ones.

4.2.5 Scanning electron microscopy (SEM)

Scanning electron microscopic images of tensile fracture surface of the composites were obtained using a scanning electron microscope (section2.2.8).

4.2.6 DC electrical conductivity

The DC electrical conductivity of the composites was measured by the two-probe method as described in section 2.2.5.

4.2.7 Mechanical properties

The mechanical properties of the composites like tensile strength, elongation at break, modulus at 50% elongation and tear strength were determined using a Shimadzu Universal Testing Machine as described in section 2.2.6.

4.2.8 Swelling characteristics

Solvent swelling characteristics of the gum compound and the composites based on NR were studied in toluene. Circular specimens of diameter, 20 mm,

were punched out from the vulcanized sheets. Thickness and diameter of the specimens were measured by means of a thickness gauge and vernier calipers, respectively. Specimens of known weight were immersed in about 20 ml toluene in diffusion bottles, which were kept at constant temperature. Samples were removed from the bottles at periodic intervals and the wet surfaces were quickly dried using tissue paper and weights of the specimen after swelling were determined at regular intervals until no further increase in solvent uptake was detected. Thickness and diameter of the specimen after equilibrium swelling were also measured.

The results of diffusion experiments were expressed as diffusion curves, where mol% or wt% uptake is plotted against the square root of time in minutes. The mol % uptake of the solvent, Q_t, for the composite samples was determined using the equation:

$$Q_t = [(W_2 - W_1 / M_s)] / W_1 \times 100 \quad \text{---------- (4.9)}$$

where 'W_1' and 'W_2' are the weights of the specimen before and after swelling, and 'Ms' the molar mass of the solvent.

In order to assess the extent of swelling behaviour of the composites, the swelling parameters like swelling index and swelling coefficient were evaluated.

$$\text{Swelling index (\%)} = (W2 - W1) / W1 \times 100 \quad \text{----------(4.10)}$$

Swelling coefficient is an index of the ability with which the sample swells and is determined by the equation:

$$\text{Swelling coefficient, } \alpha = \{A_s/m\} \times [1/d] \quad \text{----------(4.11)}$$

Where 'A_s' is the weight of the solvent sorbed at equilibrium swelling, 'm' the mass of the sample before swelling and 'd' the density of the solvent used.

The transport of liquids through composite follows different mechanisms depending upon many factors, such as chemical nature of polymer matrix and that of filler, matrix–filler compatibility and interfacial adhesion. Diffusion behaviour is classified into three categories depending upon the relative rates of penetrant mobility and polymer segmental relaxation. They include: (1) Fickian behaviour: penetrant mobility is much less than the polymer segmental relaxation rates; (2) Anomalous behaviour: penetrant mobility and polymer segmental relaxation rates are comparable; (3) Non-Fickian behaviour: penetrant mobility is much greater than polymer segmental relaxation rates. In the present study, the mechanism of transport was analyzed using the empirical relation

$$\text{Log } Q_t / Q_\alpha = \log k + n \log t \quad \text{----------} \quad (4.12)$$

Where Q_t and Q_α are the number of moles of liquid absorbed by 100 g of sample at time *t* and at equilibrium swelling respectively. The constants 'n' and 'k' vary with the nature of materials and interfacial adhesion. The values of n and k were found out from the slope and y-intercept of the plots of log Q_t / Q_α *vs.* log t. The value of n determines the type of transport mechanism. For Fickian behavior, the value of n= 0.5; if n= 1, this indicates Non-Fickian behaviour, i.e. relaxation controlled transport. If its value is in between 0.5 and 1, the transport behaviour is termed as anomalous. The factor k is a constant that varies with the structure of composite and provides an idea about the interaction between the composite and solvent. Lower values of k indicate that there is less interaction between composite and solvent and also there is less absorption of solvent. If the composite and solvent both are either polar or non-polar, the

solubility increases; this is explained on the basis of the principle that 'like dissolves like' and hence the value of k is also high. If both composite and solvent are of different types, solubility decreases and hence the value of k also decreases.

4.3 Results and discussion

4.3.1 Cure characteristics

Figures 4.2 (a), (b) and (c) represent the rheograms of NP, NPFp and NFp series. The nature of the cure curves is different for the series, which indicates that in the matrix, PPy and F-PPy interact differently.

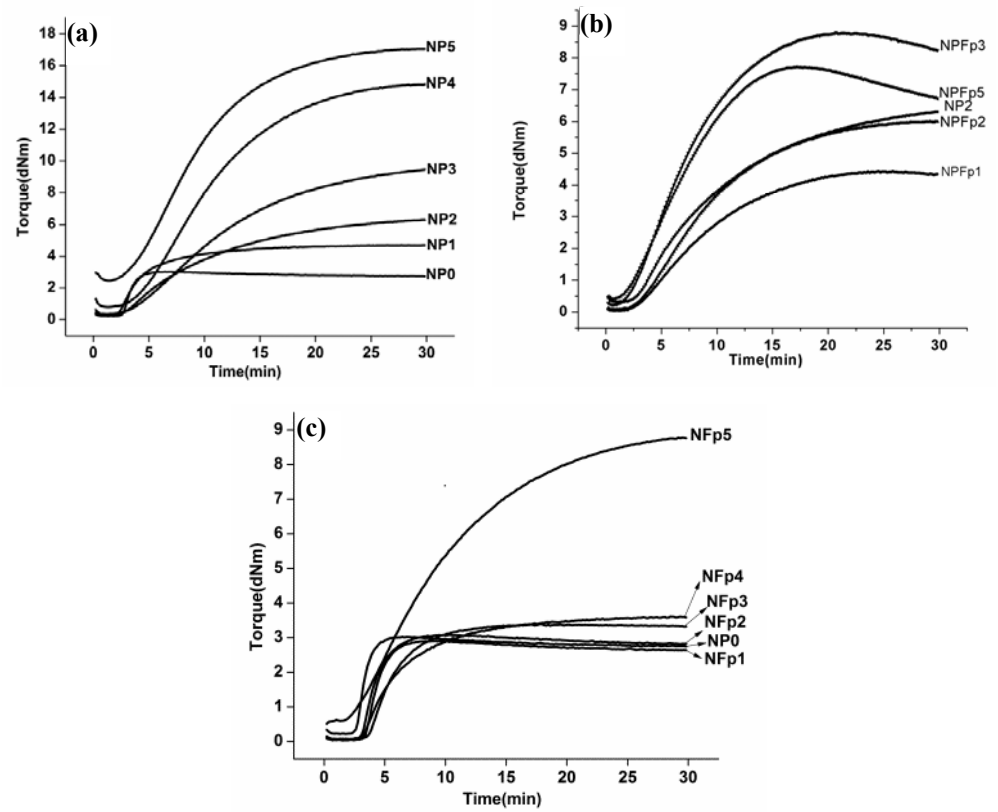

Fig. 4.2 Cure curves of (a)NP series (b) NPFp series (c) NFp series.

Table 4.2 Cure parameters of NR based CECs

Sample	T_{90}(min)	T_{10}(min)	M_H(dNm)	M_L(dNm)
NP0	4.9	2.9	3.0	0.22
NP1	11.1	2.5	4.7	0.29
NP2	20.5	3.6	6.3	0.31
NP3	21.7	4.6	9.4	0.36
NP4	19.3	4.8	14.8	0.79
NP5	17.5	4.1	17.0	2.44
NPFp1	16.9	3.6	4.4	0.03
NPFp2	18.1	3.7	6.0	0.07
NPFp3	16.4	3.2	7.2	0.11
NPFp4	14.0	2.9	8.8	0.23
NPFp5	12.2	2.7	7.7	0.41
NFp1	5.8	3.5	2.9	0.04
NFp2	6.2	3.1	3.1	0.08
NFp3	9.5	3.9	3.4	0.07
NFp4	13.7	3.5	3.6	0.03
NFp5	20.2	2.9	6.5	0.27

The cure parameters of the composites are presented in Tables 4.2. Cure time, $T_{90,}$ represents the time corresponding to the development of 90% of the maximum torque. Cure time is found to increase with the incorporation of PPy, reaches a maximum and then decreases at higher loading. The increase in cure time with PPy concentration is attributed to the presence of acidic dopant in PPy. Compared to PPy loaded samples, composites containing F-PPy exhibit lower cure values. This may be due to possible degradation of Nylon fiber at the curing temperature. The effect of PPy is not manifested here as the PPy content (coated on fiber) is very low in this case. The amine functionality

of the degradation products may accelerate the cure reaction. Similar results have been reported earlier in the case of NR/short Nylon fiber composites [8] and NR/ polyaniline/ polyaniline coated short Nylon fiber composites [26]. These observations are supported by the cure kinetic studies and cure rate index values, which will be discussed in the following sections.

Scorch time T_{10} is the time required for the torque value to reach 10% of maximum torque. It is a measure of the scorch safety of the rubber compound. For NP series scorch time increases with filler loading indicating a better processing safety. However, a decrease is observed at very high loading. For the NPFp series, scorch time decreases at higher fiber loadings. Such a decrease is attributable to the heat of mixing of highly fiber loaded samples, resulting in the premature curing of the compounds. For NFp series also such a decrease is observed at higher fiber loadings.

The maximum torque, M_H is an index of the extent of crosslinking reactions and represents the shear modulus of the fully vulcanized rubber at the vulcanization temperature. It is also a measure of the filler–polymer interactions. The value is found to increase for all the three series of CECs. The minimum torque, M_L which is a measure of the viscosity of the compound, also increases with filler loading for all the series. M_L can be considered as a measure of the stiffness of the unvulcanized compound. The increase in viscosity with the addition of filler suggests a reduced mobility of the rubber chains in the presence of these fillers.

4.3.2 Cure kinetics

Plots of $\ln(M_H–M_t)$ against time t of the NP series, NPFp series and NFp series at 150^0C are presented in figures 4.3 (a), (b) and (c), respectively. The

plots are found to be linear which proves that the cure reactions proceed according to first-order kinetics. CRI was determined by equation (4.1) for all the series. The variation of CRI with filler loading of CECs is presented in Fig. 4.4. For the NP series , CRI decreases with PPy incorporation initially and then levels off. Similar trend is also seen in the variation of cure time (Table 4.2). The CRI values increase with fiber loading for the NPFp series , again, in agreement with the trend seen in the variation of cure time. In the case of NFp series there is a gradual decrease in CRI with filler loading. This agrees with the increasing trend of cure time of NFp series.

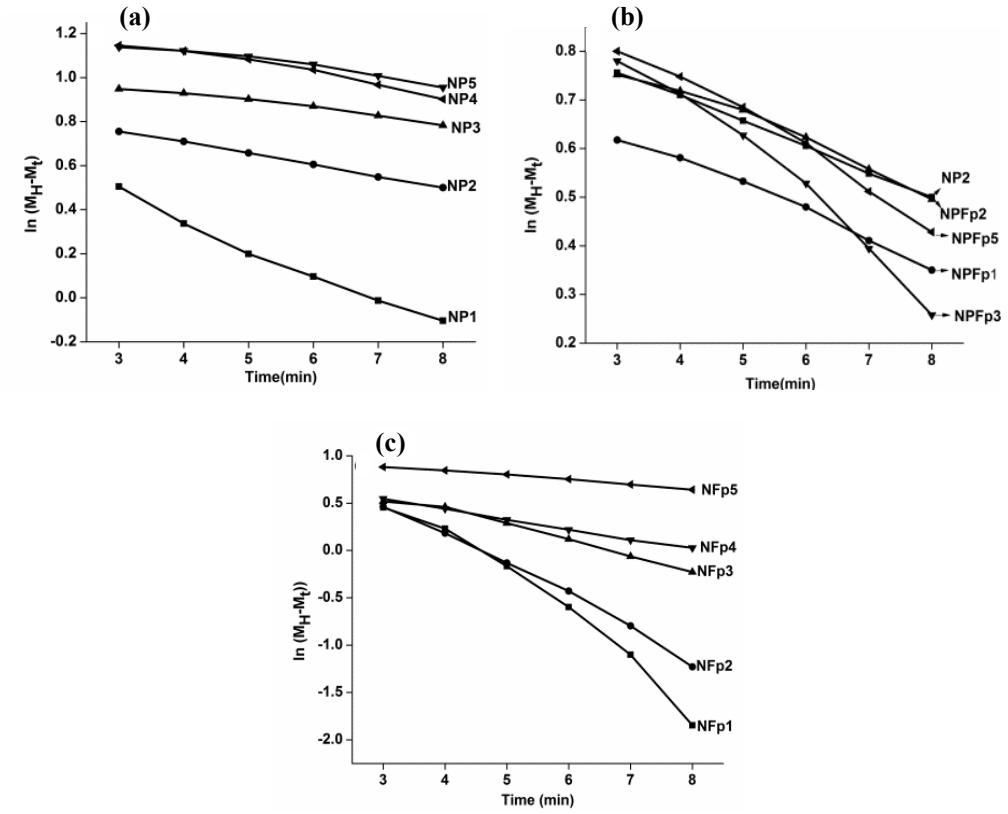

Fig. 4.3 Plots of ln(M_H-M_t) vs time for(a) NP series (b) NPFp series (c)NFp series.

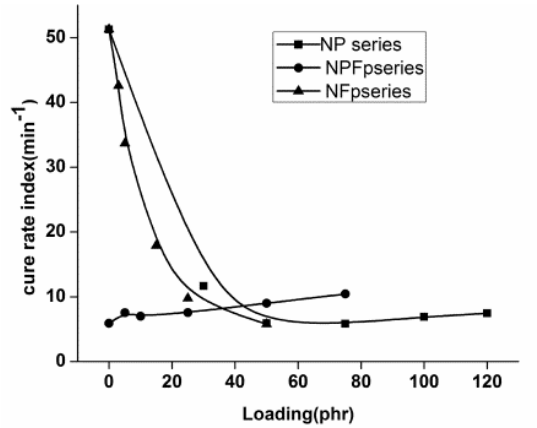

Fig. 4.4 Plots of CRI vs loadingof NR based CECs

4.3.3 Filler dispersion

The η_r and Er values of the three series were computed and are shown in Table 4.3. For the vulcanizates with PPy, i.e., for NP series, it is observed that there is not much difference between η_r and Er values initially which means that the filler is well dispersed in the matrix. Figure 4.5 shows the variation of the index L with filler loading. For NP series, L value is almost constant up to 100 phr loading after which it shows a sharp increase, indicating predominance of agglomerates in the matrix. The uniform dispersion of PPy in NR matrix is supported by SEM micrograph, to be discussed shortly. In the case of NPFp series also an increase in L is found only at very high filler loading. For NFp series, index L remains almost constant for the compositions under study which points to a well dispersed system.

Table 4.3 η_r and E_r values of NR based CECs

Sample	Relative viscosity η_r	Relative moduli E_r
NP1	1.28	1.55
NP2	1.37	2.09
NP3	1.57	3.14
NP4	3.49	4.91
NP5	10.80	5.55
NPFp1	0.08	0.70
NPFp2	0.22	0.95
NPFp3	0.35	1.15
NPFp4	0.73	1.39
NPFp5	1.33	1.22
NFp1	0.17	0.97
NFp2	0.33	1.02
NFp3	0.29	1.12
NFp4	0.13	1.19
NFp5	1.12	2.16

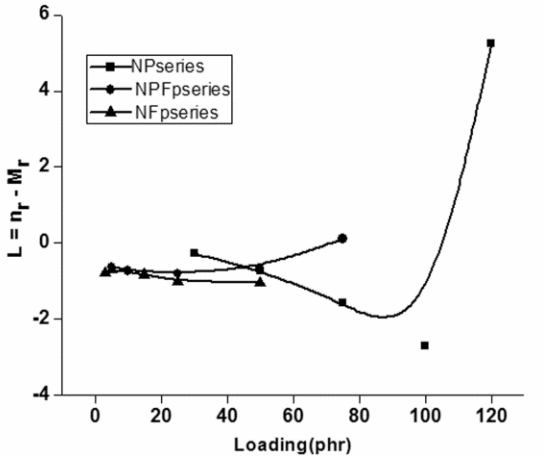

Fig.4.5 Variation of index L with loadingof NR based CECs

In Figure 4.6 Wolf equation is applied to NP, NPFp and NFp series. Slopes of the plots give filler specific constant, α_f. Since α_f is a measure of the structure

of the fillers in the matrix, the highest α_f value found for the PPy loaded compounds (α_f= 5. 3) would be an evidence for this filler to be more prone to agglomeration in the vulcanizates when compared to the fiber loaded compounds (α_f = 1.3 and 2.1). The absolute value of α_f for each composite was calculated using equation 4.8 and is plotted against filler loading in Figure 4.7. The value of α_f increases with filler loading for NP and NFp series indicating agglomeration at higher loadings. α_f does not vary much in the case of NPFp series. The observations are in agreement with those obtained from Lee's approach.

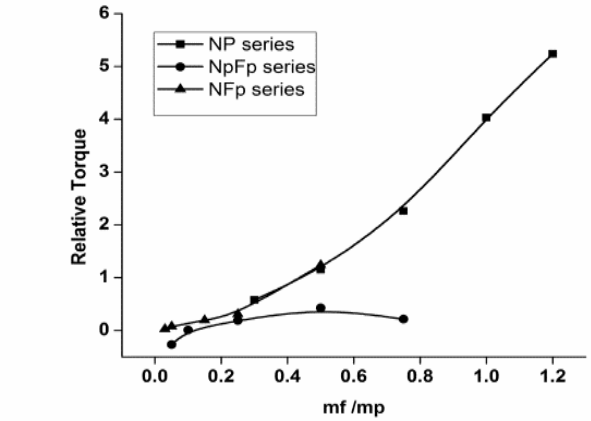

Fig. 4.6 Plots of Relative torque as a function of filler loading of NR based CECs

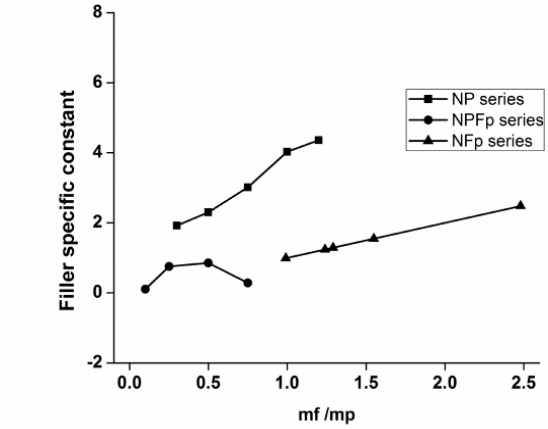

Fig. 4.7 Variation of filler specific constant, α_f with filler loading of NR based CECs

4.3.4 Morphology

The SEM micrographs of failed tensile surfaces of the CECs based on NR are shown in figure 4.8. The lamellar structure of NR gum vulcanizate is visible in figures 4.8(a). SEM image of PPy/ elastomer composites NP3 (fig. 4.8b) reveals a homogenous dispersion of PPy in the rubber matrix. The cluster and granular structure of PPy are maintained even in the composite. NR particles are covered by spherical PPy to form particle aggregates and these aggregates link with each other to form conductive chains or network in the matrix. Hence conductivity is expected to increase with filler loading. Murugendrappa *et al.*[27] have reported such a morphology for PPy/Fly ash composites. SEM studies on PPy/ Y_2O_3 composites by Vishnuvardhan *et al* [28] have reported similar observations. The SEM images of F-PPy loaded CECs, NPFp4 (figure 4.8 c) and NFp5(fig. 4.8 d) show good orientation of fiber in one direction and better adhesion between fiber and matrix resulting in improved mechanical properties as will be discussed shortly. Fig. 4.8(e) represents the Nylon 6 fibrils left in the unvulcanized compound NFp5 after dissolving out the NR matrix in toluene. The surface of the fibrils (at higher magnifications) are depicted in figures 4.8 (f)and 4.8(g). It reveals the firmness of PPy coating on fiber. There are also visible small clusters of PPy spheres on the surface of the encapsulated fiber. As intense mixing process does not dislodge these surface clusters, it is concluded that they are bonded through polymerization linkages to the PPy encapsulating the Nylon fiber. The polymer coating adheres closely to the fibrils and micro fibrils present on the surface of the larger parent fiber, as well as to the parent fiber itself. Such phenomenon has been observed in PPy coated cellulose fibers [29]. This explains the enhanced DC conductivity of the elastomer in presence of PPy coated fiber compared to PPy, which will be discussed in the following section.

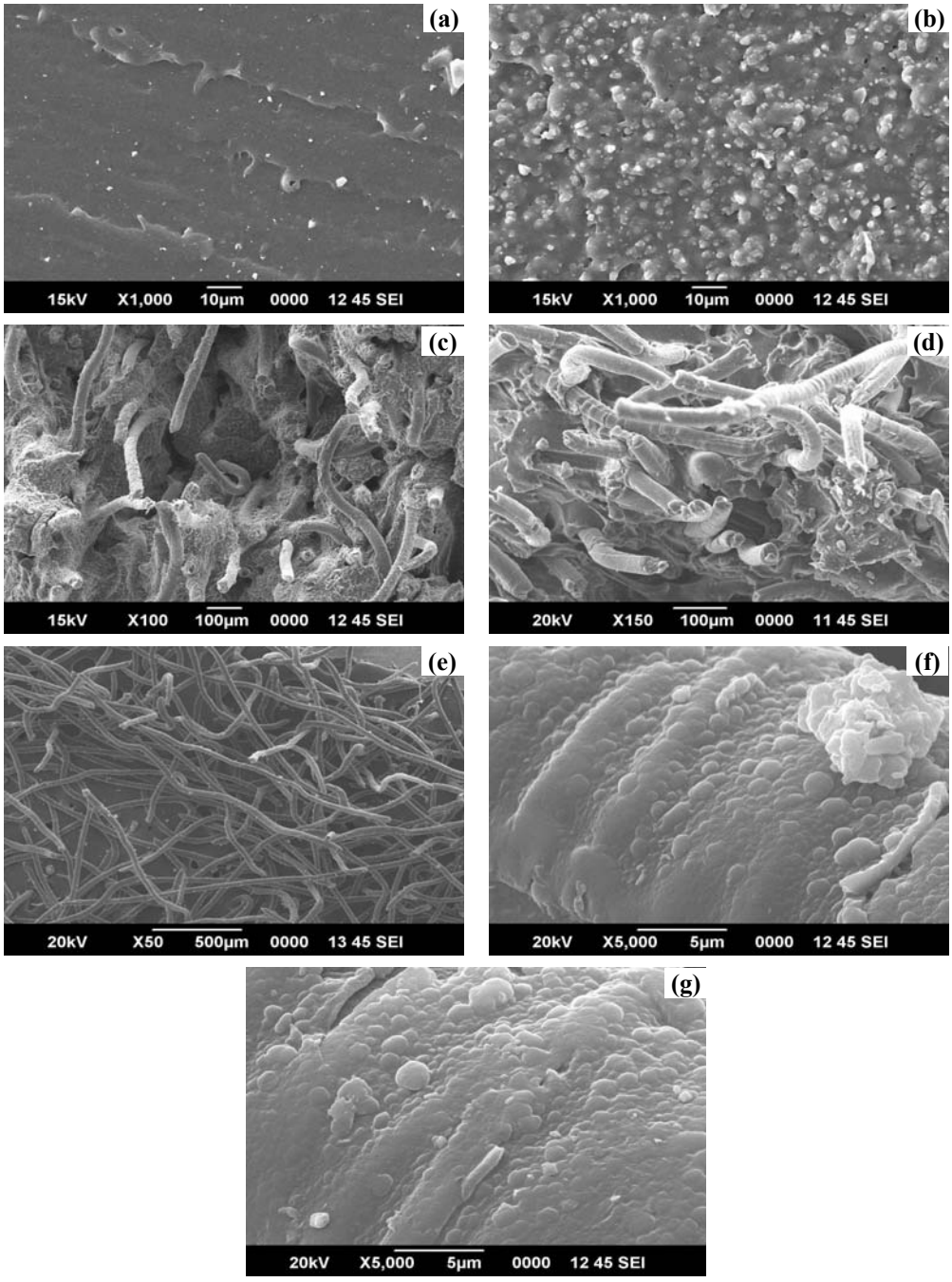

Fig. 4.8 SEM micrographs of (a)NP0, (b)NP3, (c)NPFp4, (d)NFp5 (e)Nylon fibrils in unvulcanized composite, NFp4 after dissolving out NR in toluene (f,g) surface of Nylon fibril from NFp4, with PPy coated on it.

4.3.5 DC electrical conductivity

The DC electrical conductivities of the composites are presented in Figure 4.9.

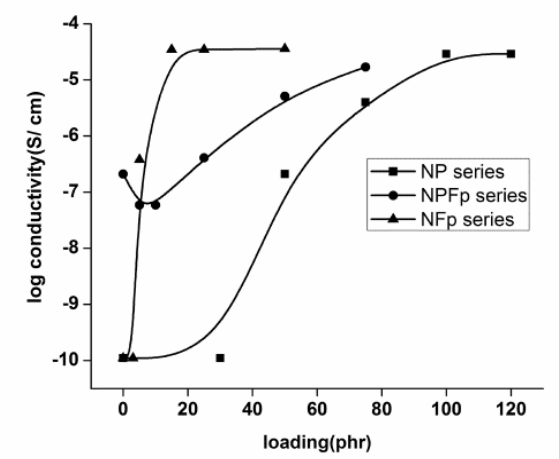

Fig. 4.9 Variation of log conductivity with loading of NR based CECs

For the NP series there is not much increase in conductivity up to 30 phr loading. After that, a sharp increase in conductivity is observed indicating that the percolation limit is at 50 phr loading. It is reasonable to assume that in NR/ PPy mixtures, conducting PPy rich regions are inter connected by insulating NR rich ones. By adding PPy, an increase in conductivity occurs due to electronic tunneling between well dispersed conductive units in the non - conducting NR matrix. For blends loaded with a small amount of PPy the conductivity values are small but not negligible. But as more PPy is added the conductivity increases appreciably due to reinforcement of an existing conductive network [30]. Conductivity increases substantially and tends to level off at higher loading. Maximum conductivity 2.9×10^{-5} is attained at 100 phr loading. In the case of NPFp series addition of F-PPy to NR/ PPy system decreases the conductivity initially which then shows a steady increase. For

NFp series percolation occurs comparatively at very low filler loading, 4phr and the system has a maximum conductivity of 3.6×10^{-5} on loading with 15phr F-PPy, after which it levels off.

Morphology, including the formation of microcells and the dispersion of conducting material in the composite become important factors that determine conductivity [31]. In spite of better dispersion of PPy in NR matrix as is evident from SEM images discussed earlier, one possible reason for the lower percolation threshold in the case of NFp series compared to NP series is the increasing fiber–fiber contact forming a conductive pathway in the matrix. This closed network of conducting species is absent in NP series and NPFp series at lower loading. The conductivity of a sample has two aspects: microscopic conductivity, which depends upon the doping level, conjugation length, chain length, etc. and macroscopic conductivity, which is determined by external factors such as the compactness of the samples. The microscopic conductivity did not vary a lot in our samples because the composites were prepared in an identical manner. However, the macroscopic properties, such as compactness, significantly changed depending on the type of filler in the composite- PPy or F-PPy. Pure PPy is a polymer with poor compactness; PPy particles were very randomly oriented and the linking between the polymer particles through the boundaries is very poor, which results in relatively high percolation threshold of PPy loaded composites. In the NR/ F-PPy composites, the filler is PPy coated fibers. So the compactness of PPy in the composite is much tighter than pure PPy. Moreover, because of the large aspect ratio and surface area of the fibers and due to the longitudinal orientation of PPy coated fibers they may serve as effective percolative conducting bridges that increase the conductivity of the composite. Such a

phenomenon has been observed by Gu Z. *et al.* [32] in composites of PPy with graphite oxide. In NPFp series even though F-PPy is added, higher loading is required to achieve good conductivity, since formation of continuous conducting bridges is impossible at lower loading due the interference of loosely bound PPy particles in between the fibers. Increased loading helps in forming a closed network of PPy and PPy coated fiber leading to better conduction. Such an increase in DC conductivity with polyaniline coated Nylon fiber loading in NR/PANI/PANI coated fiber composites[26] and in choroprene rubber/PANI/PANI coated fiber composites [33] have been reported.

4.3.6 Mechanical properties

Fig. 4.10 represents the stress - strain curves of NP and NPFp series. The variation of tensile strength of PPy loaded(NP series) and F-PPy loaded(NPFp and NFp series) samples are shown in fig. 4.11. The tensile strength of elastomer decreases sharply with PPy loading, the effect being less significant at higher loadings. Such a trend has been reported in an earlier work with PPy/polypropylene composites [34]. This reveals the non-reinforcing nature of PPy in NR matrix. Introduction of PPy into a composite, as a rule, decreases its strength and results in loss of elasticity [35]. The poor adhesion between polypyrrole (hydrophilic nature) to the natural rubber matrix (hydrophobic nature) is the main factor for the deterioration of tensile strength. It is found that tensile strength decreases by 70% by the incorporation of 50 phr PPy(NP2). NPFp series were prepared by adding varying amounts of F-PPy to NP2. Tensile strength of NPFp series increases sharply on loading with F-PPY, and the composite regains the strength of NR at 75% fiber loading. Thus the decrease in strength caused by PPy is compensated by the incorporation of

PPy coated fibers. PPy coated fibers is very effective in improving conductivity and mechanical properties simultaneously.

In the case of NFp series, there is an initial decrease in tensile strength and then substantial increase is observed. At about 50 phr F-PPy loading, maximum tensile strength is obtained. Initial decrease can be attributed to dilution effect. The critical fiber volume above which fiber can reinforce a matrix varies with nature of fiber, matrix, aspect ratio of fiber, fiber/ matrix adhesion etc. Generally 30-40 phr can reinforce the matrix. Here substantial increase in tensile strength is observed only at higher concentration of F-PPy due to poor adhesion between PPy coating and rubber matrix especially in the absence of any bonding agent to enhance adhesion. Among the three series, maximum tensile strength is observed for NPFp series

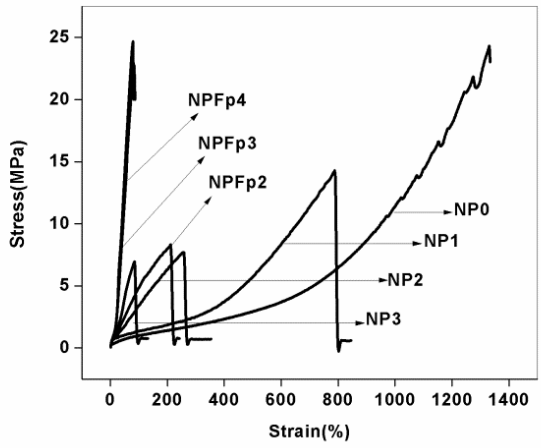

Fig. 4.10 Stress-strain curves of NP and NPFp series

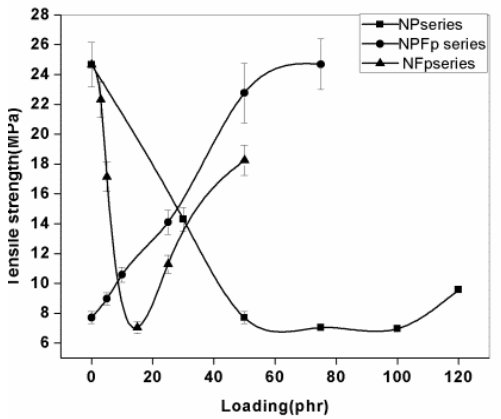

Fig.4.11. Variation of tensile strength with loading NR based CECs

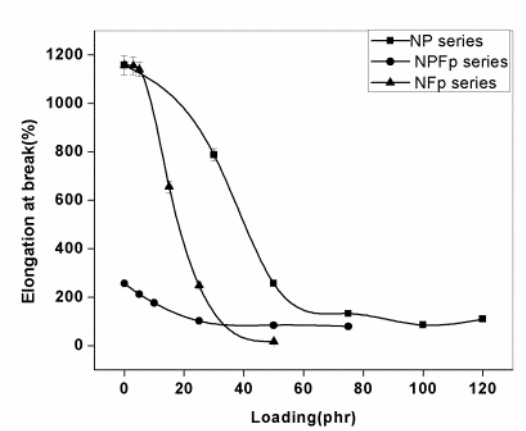

Fig. 4.12. Variation of elongation at break with loading NR based CECs

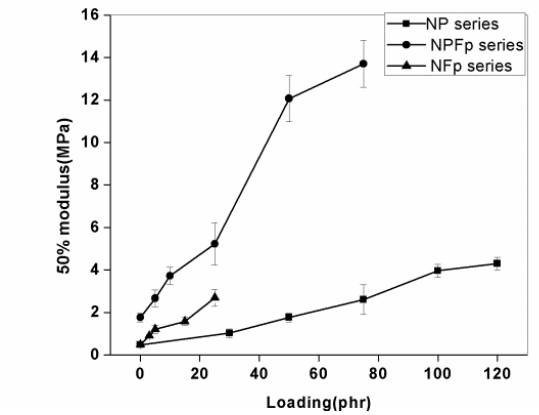

Fig. 4.13. Variation of modulus with loading NR based CECs

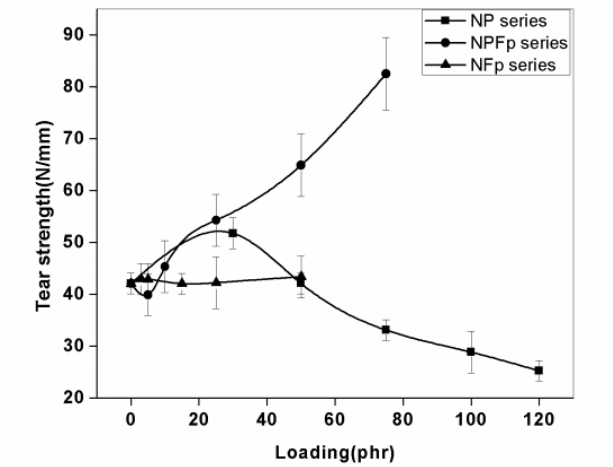

Fig. 4.14. Variation of tear strength with loading NR based CECs

Elongation at break decreases with filler loading and then levels off (fig. 4.12). The composites become stiffer and stiffer by the addition of PPy and F-PPy and there is decrease in stress bearing capacity of the filler-matrix interface.

Modulus at 50% elongation increases for all the three series (Fig. 4.13). Compared to NP series and NFp series, modulus values are higher for NPFp series. Modulus of NP4 (NR+100phr PPy) is comparable to that of NPFp2 (NR+50phrPPy+10phrF-PPy).

Variation of tear strength with filler loading for NP series, NPFp series and NFp series is shown in fig. 4.14. Tear strength increases initially and then decreases sharply for NP series due to the non-reinforcing effect of PPy. For the NPFp series the tear strength increases and the decrease occurred due to PPy is counterbalanced. The tear failure occurs by the propagation of tear front across the matrix. In the presence of fibers distributed in the bulk, these tear lines are either arrested or deviated. The energy of the propagating crack front is dissipated

at the fiber- matrix interface by way of its pull-out or breakage. This results in improved tear resistance. Tear resistance remains unchanged in the case of NFp series.

4.3.7 Swelling characteristics

Variation of mol% uptake of toluene with PPy loading and F-PPy loading in NR are shown in fig.4.15. and 4.17 respectively. It can be seen that sorption by CECs is much lower compared to gum vulcanizate, and both PPy loading and F-PPy loading decrease the solvent sorption. A fast rate of absorption is observed in the gum compound and the rate decreases with loading. The sorption becomes slower after a certain time and equilibrium is attained almost at the same time by all the composites.

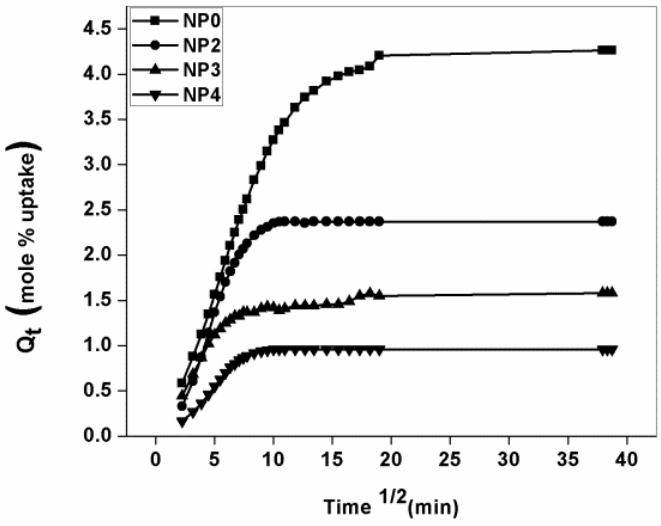

Fig. 4.15 Q_t vs $T^{1/2}$ of NP series

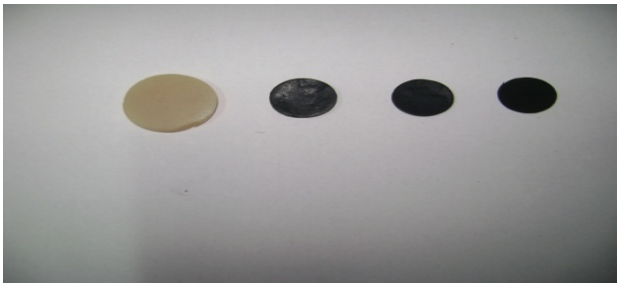

Fig. 4.16 Photographs showing the swelling of different samples of NP series (NP0, NP2, NP3, NP4)

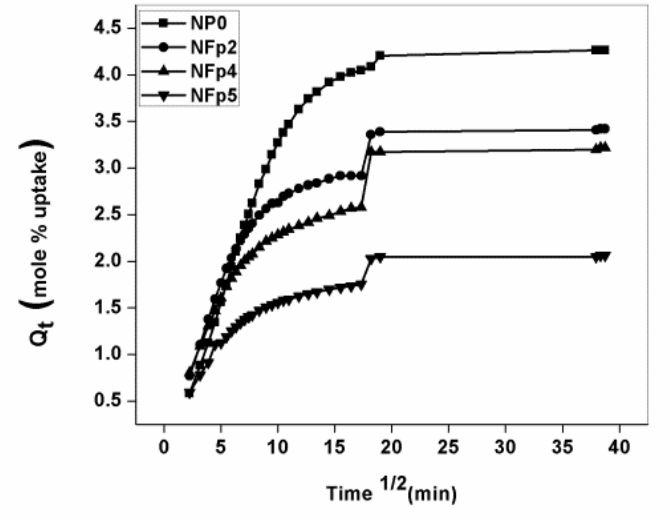

Fig. 4.17Q_t vs T ^{½} of NFp series

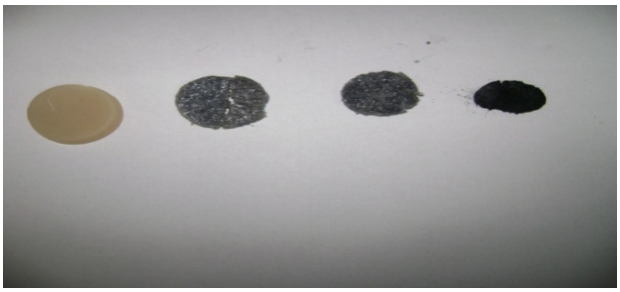

Fig. 4.18 Photographs showing the swelling of different samples of NFp series (NP0, NFp2, NFp4, NFp5)

Table 4. 4 Swelling parameters of NR based CECs

Sample	Before toluene sorption		After toluene sorption		Swelling index (%)	Swelling coefficient	n	k
	Thickness (mm)	Diameter (mm)	Thickness (mm)	Diameter (mm)				
NP0	1.90	12	3.55	22	393	4.50	0.58	1.27
NP2	1.22	12	1.46	21	218	2.52	0.75	1.33
NP3	1.15	12	1.78	15	146	1.68	0.51	0.88
NP4	1.35	12	1.68	15	88	1.02	0.60	1.12
NFp2	1.20	12	2.63	20	315	3.63	0.41	0.88
NFp4	1.20	12	4.10	15	296	3.40	0.36	0.81
NFp5	1.17	12	3.50	14	190	2.19	0.32	0.71

Decrease in solvent sorption of the CECs compared to the gum compound is also evident from the decreasing percentage swelling index and swelling coefficient values with increased loading (table 4.4). This may be due to the increased hindrance exerted by the filler.The reason for the decreased sorption at higher PPy and F-PPy loading may be the polarity of PPy. Toluene being a non polar solvent, its sorption decreases with increase in loading of polar filler and a decrease in NR content in the composites.

The photographs of the swollen samples of NP series and NFp series are shown in fig. 4.16 and 4.18. Dimensions of the composites before and after swelling in toluene were measured and reported in table 4.4. There is an increase in both thickness and diameter after equilibrium swelling. The values of kinetic parameters like n and k for toluene sorption by the conducting elastomer composites are given in table 4.4. The composites exhibit deviation from the Fickian mode of transport in toluene. Here the value of n varies from 0.3– 0.7. Deviation from the Fickian behaviour may be attributed to processes such as surface crazing, osmotic cracking, microcrack formation etc. [36]. k

values of the composites are lower than gum vulcanizate. Lower values of k indicate that there is less interaction between composite and solvent and also there is less absorption of solvent.

4.4 Conclusions

Natural rubber/ polypyrrole (NR/PPy), natural rubber/ polypyrrole/ polypyrrole- coated short nylon fiber (NR/PPy/F-PPy) and natural rubber/ polypyrrole-coated short nylon fiber (NR/F-PPy) composites were prepared by mechanical mixing. The cure characteristics, cure kinetics, filler dispersion, morphology, DC conductivity, mechanical properties and swelling characteristics of the composites prepared were evaluated. In NR/PPy composites PPy retards the cure reaction upto 75phr loading, after which the reaction rate is increased while in NR/PPy/F-PPy composites, addition of F-PPy accelerates the cure reaction substantially. Addiion of PPy coated fibers to NR, increases the cure time in NFp series. Results of cure kinetics studies agree with these observations. First order kinetics is observed for cure reactions. Filler dispersion studies indicate that PPy coated fibers form a well dispersed system with NR at lower loadings. In NR/PPy composites also considerable agglomerate formation occurs only at 100 phr loading. At lower loading PPy is uniformly dispersed in NR matrix which is further supported by SEM analysis. DC conductivity of NR/PPy composites is enhanced only at very high PPy loading and the percolation limit is about 50phr PPy. In NR/F-PPy composites, percolation occurs at about 5phr F-PPy loading and maximum conductivity of 3.6×10^{-5}S/cm is attained on loading with 15phr F-PPy. The mechanical properties of NR are reduced by PPy loading which is compensated by the addition of PPy coated fiber. Addition of 75phr PPy coated fibers to NR/PPy system causes 70% increase in tensile strength. The

NR/PPy/F-PPy composites show increased tensile strength, modulus and tear resistance. In NR/F-PPy composites maximum conductivity along with reasonable mechanical properties are observed at 50phr filler loading. The percentage swelling index and swelling coefficient of the composites decrease with increase in PPy loading and F-PPy loading. The solvent sorption mechanism in the conducting composites is found to deviate from Fickian mode.

References

[1] Anand J, Palaniappan S, Sathyanarayanan D N, *Prog Polym sci*, **1998,** 23, 993.

[2] Bohwon K, Koncar V, Devaux E, Dufour C, Viallier P. *Synth Met* .**2004**,146, 167.

[3] Choi S , Nah C, Jo BW, *Polym Int.***2003**, 52, 1382.

[4] Chae YK, Kang WY, Jang JH, Choi SS. *Polym Test*. **2010**, 29, 953

[5] George J, Joseph K, Bhagavan SS, Thomas S. *Mater Lett*. **1993,** 18, 163.

[6] Vargese S, Kuriakose B, Thomas S. *Plast Rubb Comp Proc Appl*. **1993,** 20, 930.

[7] Vargese S, Kuriakose B. *Polym Degrad stab*, **1994,** 44, 5561.

[8] Sreeja TD, Kutty SKN. *Polym Plast Technol Eng.* **2003**, 42, 239

[9] Neoh KG, Tay BK, Kang ET. *Polymer*. **2000**, 41, 9.

[10] Goettler LA, Shen KS. *Rubber Chem Technol*. **1983**, 56, 620.

[11] Sreeja TD, Kutty SKN. *J Elastomers Plast*. **2002**, 34, 157.

[12] Seema A, Kutty SKN. *J Appl Polym Sci*. **2006**, 99, 532.

[13] Rajeev RS, De SK, Bhowmic AK, Baby J. *Polym Degrad stab*. **2003**, 79, 449.

[14] Blow CM, Hepburn C(eds). *Rubber technology and manufacture*. *London, Butterworth*. **1982.**

[15] Wazzan AA. *Int J Polym Mater***. 2005**, 54, 783.

[16] Mathew G, Nah C, Rhee JM, Singh RP. *J Elastomers Plast*. **2006**, 38, 43.

[17] Fujimoto K, Nishi T, Okamoto T. *Int PolmSci Technol.* **1981**, 8, T/30

[18] Mathew G, Singh RP, Nair NR, Thomas S. *J Mater Sci*. **2003**, 38, 2469.

[19] Gonzalez L, Rodriguez A, Marcos A, Chamorro C. *Rubber Chem technol*. **1996**, 69, 203.

[20] Lee BL. *Rubber Chem Technol*. **1979**, 52, 1019.

[21] Costa HM, Visconte LLY, Nunes RCR, Furtado CRG. *Int J PolymMater* .**2004**, 53, 475.

[22] Wolff S. *Rubber Chem Technol*. **1996**, 69, 325.

[23] Kraus G. *Rubber ChemTechnol*. **1978**, 51, 297.

[24] Sobhy MS, El-Nashar DE, Maziad NA. *Egypt J Sol*. **2003**, 26, 241.

[25] Wolf S, Wang MJ. *Rubber Chem Technol***. 1992**, 65, 329.

[26] Chandran AS. *Ph. D Thesis, Cochin University of Science and Technology, India.* **2008**

[27] Murugendrappa MV, khasim M, Ambika Prasad MVN. *Bull. Mater.Sci.* **2005,** 28, 565.

[28] Vishnuvardhan TK, Kulkarni VR, Basavaraja, C, Raghavendra SC.*Bull Mate rSci.* **2006**, 29, 77.

[29] Johnston JH, Kelly FM, Moraes J, Borrmann T, Flynn D. *Current appl Phys*. **2006**, 6, 587.

[30] Shakoor A, Foot PJS, Rizvi TZ. *J Mater Sci: Mater Electron*. **2010**, 21, 1270

[31] Gang L, Xia L, Xinghua S, Jian U, Jiasong H. *Front Chem China*. **2007**, 2, 118

[32] Gu Z, Zhang L, Li C. *J Macromol Sci, Part B*. **2009,** 48, 1093.

[33] Chandran AS, Kutty SKN. *Eur Polym J*. **2008**, 44, 2418.

[34] Piontecka J, Omastovab M, Potschkea P, Simona F, Chodak I. *J Macromo l Sci- Phys*. **1999**, B38, 737.

[35] Smirnov MA, Kuryndin IS, Nikitin LN, Sidorovich AV, Yu N, Sazanov OV, Kudasheva V, Bukosek AR, Khokhlov, Elyashevich GK.*Russ J Appl Chem*. **2005**,78, 1993

[36] Sreekala MS, Goda K, Devi PV. *Compos Interfaces*. **2008**, 15, 281.

.....ꕥ.....

Chapter

5

CONDUCTING ELASTOMER COMPOSITES: NR/PPy/PPy COATED SHORT NYLON FIBER PREPARED BY IN SITU POLYMERIZATION IN LATEX

Contents

Polypyrrole/natural rubber (PPy/NR) composites were prepared by in situ polymerization of pyrrole in NR latex using anhydrous ferric chloride as oxidising agent, p- toluenesulphonic acid as dopant and vulcastab VL as stabilizer. Polypyrrole/ Polypyrrole coated short Nylon fiber/ natural rubber (PPy/ F-PPy/ NR) composites were prepared as above in NR latex containing short Nylon fibers of 6mm length. The products were coagulated out, dried, compounded on a two roll mill and moulded. The cure characteristics, cure kinetics, filler dispersion, morphology, DC electrical conductivity, mechanical properties and swelling characteristics of the elastomeric composites were investigated. Incorporation of PPy to elastomer retarded the cure reaction whereas addition of fiber accelerates the cure reaction. First order kinetics was observed for cure reactions. Scanning electron microscopic (SEM) images revealed a uniform dispersion of PPy and F-PPy in the matrix. DC conductivity upto 6.25×10^{-2}S/cm was attained for NR/PPy/F-PPy system. The composites containing F-PPy exhibited better mechanical properties compared to NR/PPy systems. The percentage swelling index and swelling coefficient of the composites were found to decrease with increase in PPy loading and F-PPy loading. The solvent sorption mechanism in the conducting composites was found to exhibit slight deviation from Fickian mode.

5.1 Introduction

Conducting composites of polypyrrole can be prepared directly by mechanical mixing of polypyrrole with host polymer. However, due to thermal aging of PPy during processing at elevated temperatures, the resultant composites usually have very low conductivity [1,2]. Electrical polymerization, on the other hand, can be used to prepare conducting composite films with good mechanical properties and high conductivity. However, it is not suitable for large scale industrialization, because only thin films of pristine host polymers are used, which are only as large as the size of the electrode area of the products. Polypyrrole composites can also be produced *in situ* by chemically oxidative polymerization. There are two *in situ* polymerization methods to obtain PPy composites. One is to form a substrate film mixed with oxidant first, followed by adding the monomer to the film. This method is adopted for obtaining PPy coated conducting fibers and fabrics. The second method is to polymerize pyrrole by means of an oxidant in the presence of an insulating polymer matrix, followed by precipitation, drying and moulding into various shapes.

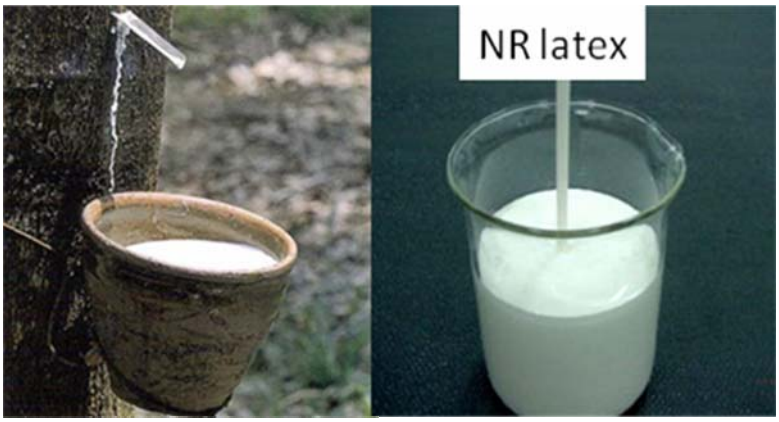

Conducting composites of polypyrrole can be prepared directly by mechanical mixing of polypyrrole with host polymer. However, due to thermal aging of PPy during processing at elevated temperatures, the resultant composites usually have very low conductivity[1,2]. Electrical polymerization, on the other hand, can be used to prepare conducting composite films with good mechanical properties and high conductivity. However, it is not suitable for large scale industrialization, because only thin films of pristine host polymers are used, which are only as large as the size of the electrode area of the products. Polypyrrole composites can also be produced *in situ* by chemically oxidative polymerization. There are two *in situ* polymerization methods to obtain PPy composites. One is to form a substrate film mixed with oxidant first, followed by adding the monomer to the film. This method is adopted for obtaining PPy coated conducting fibers and fabrics. The second method is to polymerize pyrrole by means of an oxidant in the presence of an insulating polymer matrix, followed by precipitation, drying and moulding into various shapes.

Electrically conductive composites were prepared via *in situ* chemical oxidative polymerization of the pyrrole monomer in polystyrene(PS) and zinc neutralized sulfonated polystyrene (Zn-SPS) films under super critical carbon dioxide(SC-CO_2) conditions by Gang *et al.* [3]. Due to the strong swelling effect of SC-CO_2, the pyrrole monomer was efficiently incorporated into and well dispersed in the matrix, thus leading to relatively higher conductivity after the polymerization. Zoppi *et al.*[4] obtained semi-interpenetrating polymer networks of PPy/ethylene-propylene-diene rubber (EPDM) via oxidation polymerization of pyrrole using two methods. In the frst method EPDM containing Copper chloride powder and dicumyl peroxide were obtained by

mechanical mixing and crosslinking by heating and exposed to pyrrole vapors. In the second method crosslinked EPDM was swollen in an $FeCl_3$/ tetrahydrofuran solution and exposed to pyrrole vapors. Conductivity of the composites obtained by the second route (10^{-5}S/cm) was higher than for the frst route. Omastova *et al.*[5] prepared PPy composites with polyethylene, polypropylene or poly (methyl methacrylate) (PMMA) by a chemical modification method, resulting in a network-like structure of PPy embedded in the insulating polymer matrix. Ruckerstein *et al.*[6] synthesized a stable conductive PPy/ PMMA latex composite through first preparing PMMA emulsion using sodium dodecyl sulfate as a stabilizer, followed by *in situ* polymerization of pyrrole. Xie *et al*. [7] dealt with two kinds of conducting PPy composites, namely, chlorinated polyethylene (CPE)/ PPy and natural rubber/ PPy composites, prepared by *in situ* oxidation polymerization of pyrrole in the presence of CPE suspension or natural rubber latex, using ferric chloride as oxidant. Preparation conditions, characterization and properties of the composites were studied.

This chapter describes the preparation of conducting elastomer composites (CECs) of PPy and PPy coated short Nylon 6 fibers based on natural rubber, prepared by *in situ* polymerization in NR latex. Latex stage polymerization is expected to enhance the DC conductivity compared to dry rubber compounding of PPy and PPy coated fiber. The cure parameters, cure kinetics, filler dispersion and morphology of the prepared composites are studied. DC electrical conductivity, mechanical properties and swelling characteristics of the composites are also evaluated.

5.2 Experimental

5.2.1 Materials

Details of fresh natural rubber latex, vulcastab VL, acetic acid, zinc oxide, stearic acid, tetramethylthiuram disulphide (TMTD), mercaptobenzothiazyl disulphide (MBTS), sulphur and toluene used in this study are given in section 2.1.

5.2.2 Preparation of conductive elastomeric composites (CECs)

The formulation for the preparation of composites by *in situ* polymerization method is given in Table 5.1. LNP series represent the vulcanizates of NR with PPy and LNPFp series contains PPy and F-PPy. These two series were prepared by a two-step process. In the first step NR/PPy and NR/PPy/F-PPy mixes were prepared by *in situ* polymerization as follows: To weighed amount of latex(corresponding to dry rubber content) diluted to 20% solid content, 2% vulcastab VL based on dry rubber content was added, followed by pyrrole. A solution of anhydrous ferric chloride (oxidant) and *p*-toluene sulphonic acid (dopant) were added to the mixture during stirring. The molar ratio of oxidant to monomer was 2.3 and dopant to monomer 0.4. The reaction was carried out at 4 ^{0}C with continued stirring for 4 hours. The product, NR/PPy, was precipitated out with the addition of 2% acetic acid, washed with water thoroughly and then with methanol and dried in air oven at 55^{0}C for 24 hours. For the preparation of NR/PPy/F-PPy, polymerization was carried out as above in latex containing short Nylon fiber of 6mm length, impregnated with monomer.

In the second step these mixes were compounded on a two-roll mill (section 2.2.2) and the sheets were kept for maturation for 24 hours. The

optimum cure time at at 150 ^{0}C for the compounds were determined using a Rubber Process Analyzer (section 2.2.3). The compounds were compression moulded at 150 ^{0}C in an electrically heated hydraulic press (section 2.2.4). The sheets obtained were kept in a cold dark place for 24 h and were used for the subsequent tests.

Table 5.1 Formulation for the preparation of NR based CECs prepared by *in situ* method

Sample	PPy(phr)[a]	F-PPy(phr)[a]
LNP0	0	0
LNP1	25	0
LNP2	50	0
LNP3	75	0
LNP4	100	0
LNPFp1	50	10
LNPFp2	50	25
LNPFp3	50	50
LNPFp4	50	75

All mixes contain NR-100g, zinc oxide-5phr, stearic acid-2phr, tetramethylthiuram disulphide- 0.2phr, mercaptobenzothiazyl disulphide-0.6 phr, sulphur- 2.5phr

a- parts per hundred rubber

5.2.3 Characterization

The cure characteristics of the vulcanizates were monitored using a Rubber Process Analyzer as explained in section 2.2.3. The cure time T_{90}, scorch time T_{10}, maximum torque M_H, and minimum torque M_L values were determined at 150 ^{0}C. The cure rate index (CRI) and the kinetic rate constant

of cure reaction, were determined from the rheometric data. The vulcanization kinetics was studied by the method described in section 4.2.3. The filler dispersion and the formation of filler agglomerates in polymer matrices were studied by the methods as described in section 4.2.4. Scanning electron microscopic images of tensile fracture surface of the composites were obtained using a scanning electron microscope (section2.2.8). The DC electrical conductivity of the composites was measured by the two-probe method as described in section 2.2.5. The mechanical properties of the composites like tensile strength, elongation at break, modulus at 50% elongation and tear strength were determined using a Shimadzu Universal Testing Machine as described in section 2.2.6. The swelling characteristics of the composites were studied in toluene as described in section 4.2.8 of this thesis.

5.3 Results and discussion

5.3.1 Cure characteristics

Fig 5.1 represents the rheogram of LNP and LNPFp series. The cure parameters of the composites are presented in Table 5.2.

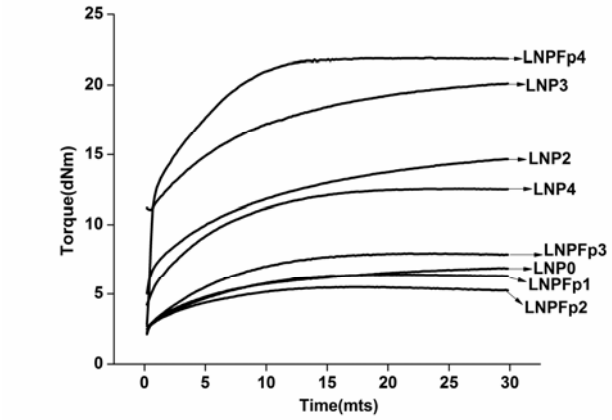

Fig. 5.1 Cure curves of LNP and LNPFp series

Table 5.2 Cure parameters of NR based CECs prepared by *in situ* method

Sample	Cure time T_{90}(min.)	Scorch time T_{10}(min.)	Maximum torque M_H(dNm)	Minimum torque M_L(dNm)
LNP0	4.0	2.2	3.1	0.1
LNP1	10.9	1.6	3.7	0.6
LNP2	18.2	0.4	6.9	2.1
LNP3	19.7	0.3	14.7	4.8
LNP4	19.5	1.1	20.1	8.5
LNPFP1	11.6	0.6	6.4	2.4
LNPFp2	10.6	0.6	5.5	2.6
LNPFp3	12.2	0.6	7.9	2.2
LNPFp4	11.3	0.4	14.5	2.2

Cure time, $T_{90,}$ represents the time corresponding to the development of 90% of the maximum torque. Cure time is found to increase with the incorporation of PPy. The increase in cure time with PPy concentration is attributed to the presence of acidic dopant in PPy. Compared to PPy loaded samples, composites containing F-PPy exhibit lower cure values. This may be due to possible degradation of Nylon fiber at the curing temperature as explained in section 4.3.1 of this thesis.

Scorch time, T_{10} is the time required for the torque value to reach 10% of maximum torque. It is a measure of the scorch safety of the rubber compound. For LNP and LNPFp series, scorch time is low compared to NP and NPFp series (section 4.3.1) and the value decreases with filler loading. This is due to higher heat generation during mixing and the resultant early start of cure reaction.

The maximum torque, M_H is an index of the extent of crosslinking reactions and represents the shear modulus of the fully vulcanized rubber at

the vulcanization temperature. It is also a measure of the filler–polymer interactions. The value is found to increase for the two series of CECs. The minimum torque, M_L which is a measure of the viscosity of the compound, also increases with filler loading.

5.3.2 Cure kinetics

Plots of ln (M_H–M_t) against time t of the LNP and LNPFp series at 150^0C are presented in fig. 5.2. The plots are found to be linear which proves that the cure reactions proceed according to first-order kinetics. CRI was determined by Eq. (4.1) for the composites.

As depicted in figure 5.3 in the case of the LNP series, CRI decreases with PPy incorporation initially and then levels off. Similar trend was seen in the variation of cure time (Table 5.2). The CRI values increase slightly and levels off with fiber loading for the LNPFp series, again, in agreement with the trend seen in the variation of cure time.

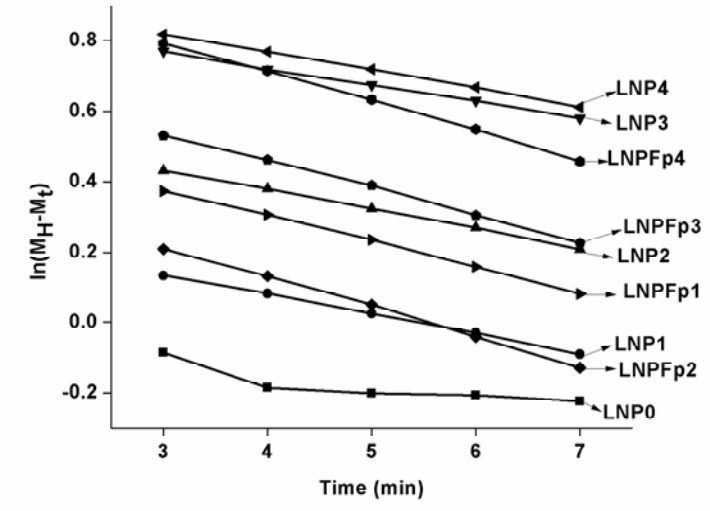

Fig. 5.2 Plots of ln(M_H-M_t) vs time for LNP series and LNPFp series

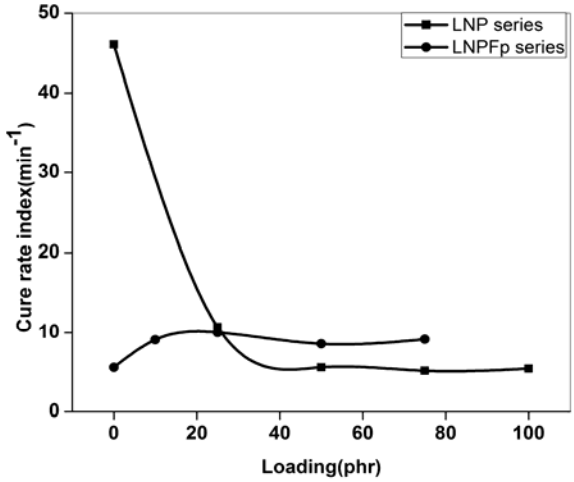

Fig. 5.3 Plots of CRI vs loading of NR based CECs prepared by *in situ* method

5.3.3 Filler dispersion

The η_r and Er values of the two series were computed and are shown in Table 5.3. For the vulcanizates with PPy, i. e., for LNP series, it is observed that as loading increases, there is much difference between η_r and Er values which means that the filler is not well dispersed in the matrix. In the case of LNPFp series, this difference is much low indicating a well dispersed system. Figure 5.4 showing the variation of the index L with filler loading also confirms this.

Table 5.3 η_r and E_r values of NR based CECs prepared by *in situ* method

Sample	Relative viscosity η_r	Relative moduli E_r
LNP1	5.89	1.19
LNP2	19.43	2.23
LNP3	44.51	4.76
LNP4	78.56	6.53
LNPFp1	1.15	0.93
LNPFp2	1.25	0.80
LNPFp3	1.06	1.15
LNPFp4	1.04	2.10

Variation of relative torque as a function of filler loading for composites is depicted in figure 5.5. α_f which is a measure of the structure of the fillers in the matrix is deduced from slopes of these plots. The highest α_f value found for the PPy loaded compounds (α_f= 5. 3) is an indication for this filler to be more liable to agglomeration in the vulcanizates when compared to the fiber loaded compounds (α_f = 2. 7). The absolute value of α_f for each composite was calculated using equation (4.8) and is plotted in Figure 5.6. Earlier results from Lee's approach also show that fiber loaded samples produce better dispersion with the matrix.

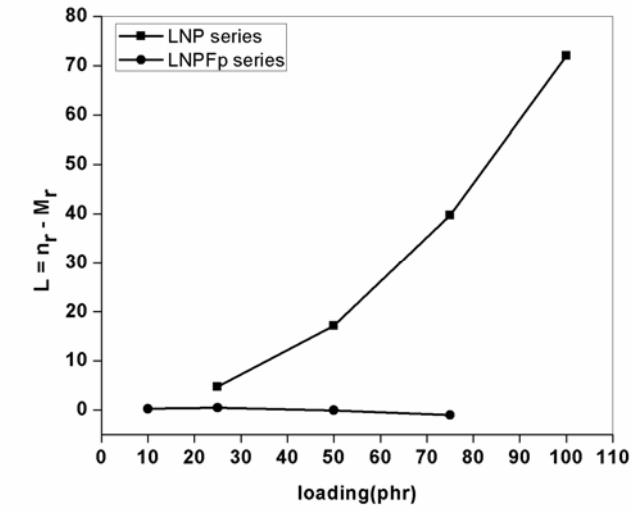

Fig.5.4 Variation of index L with loading of NR based CECs prepared by *in situ* method

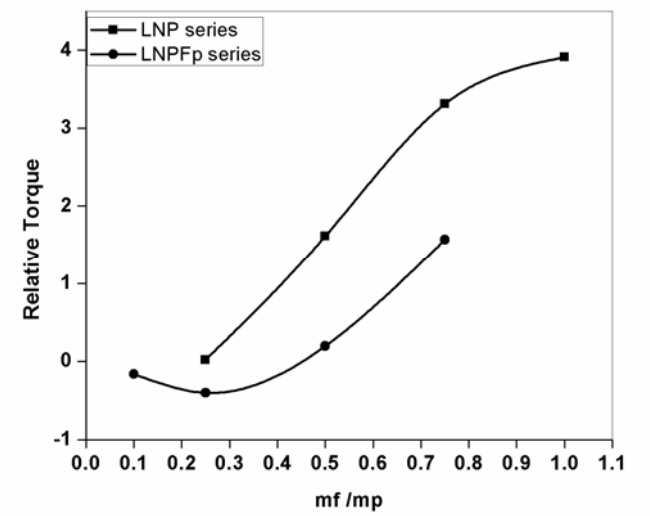

Fig. 5.5 Plots of relative torque as a function of filler loading of NR based CECs prepared by *in situ* method

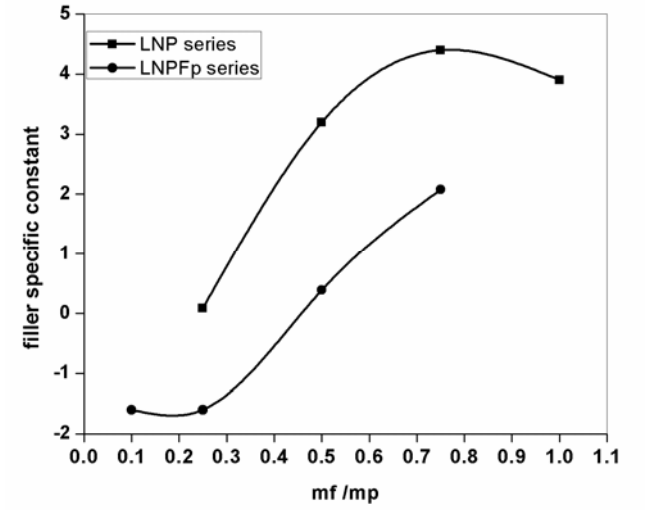

Fig. 5.6 Variation of filler specific constant, α_f with filler loading of NR based CECs prepared by *in situ* method

5.3.4 Morphology

The SEM micrographs of tensile fractured surfaces of the NR gum vulcanizate (coagulated from latex, dried, compounded and vulcanized) and the CECs are shown in fig. 5.7.

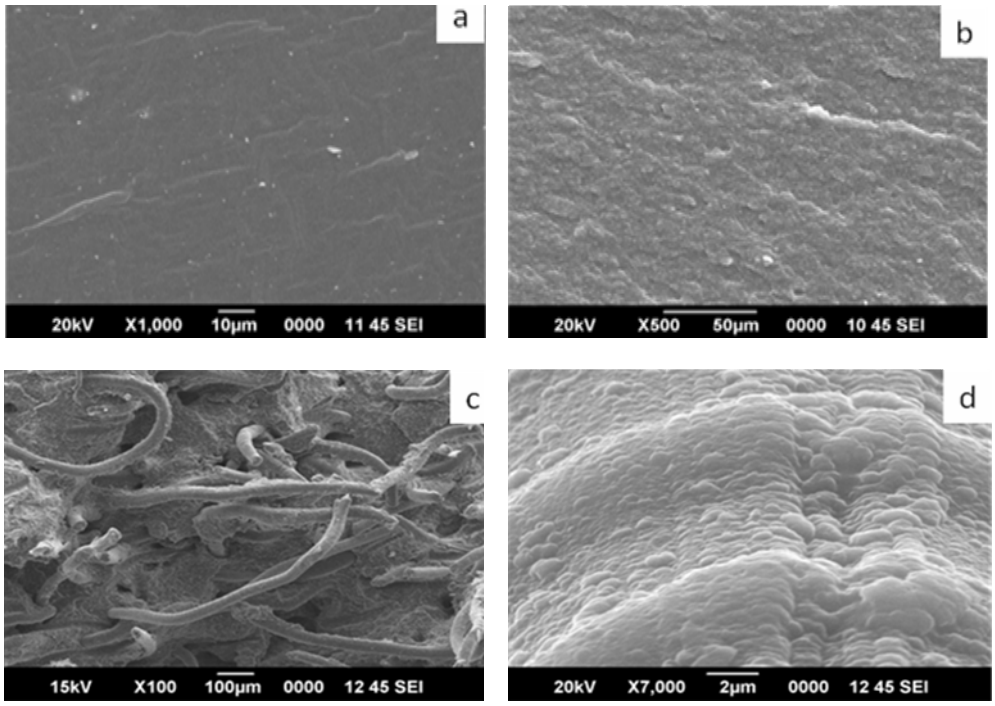

Fig. 5.7 SEM micrographs of (a)LNP0, (b)LNP2, (c)LNPFp2, (d)PPy coated fiber surface of LNPFp2

The lamellar structure of NR gum vulcanizate is visible in fig. 5.7 (a). SEM images of PPy/elastomer composites, LNP2 (fig. 5.7(b)) reveal agglomerate formation of PPy in the rubber matrix. PPy primary particles link with each other to form conductive chains or network in the matrix. Hence conductivity is expected to increase with filler loading. The SEM image of F-PPy loaded CEC, LNPFp2 (fig. 5.7(c)) shows good orientation of fiber in one direction and better adhesion between fiber and matrix resulting in improved mechanical properties as will be discussed shortly. Fig. 5.7 (d) shows that PPy particles are firmly attached to Nylon fiber contributing to improved DC conductivity.

5.3.5 DC electrical conductivity

The DC electrical conductivities of the composites are presented in Fig. 5.8.

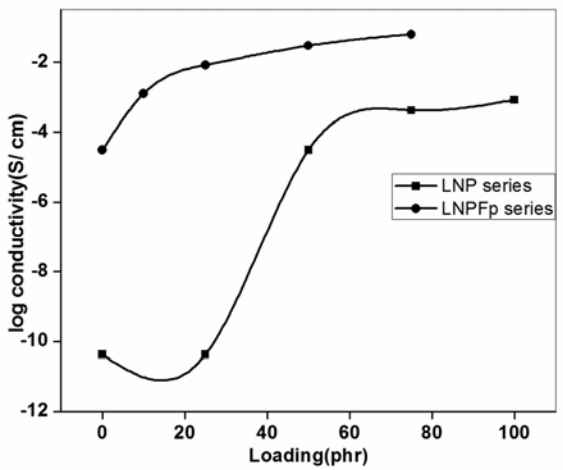

Fig. 5. 8 Variation of log conductivity with loading of NR based CECs Prepared by *in situ* method

For the LNP series there is not much increase in conductivity up to 25 phr loading. After that, a sharp increase in conductivity is observed, indicating that the percolation limit is at 50 phr loading. Conductivity increases substantially and tends to level off at higher loading. Maximum conductivity $8.3x10^{-4}$ S/cm is attained at 100 phr loading. In the case of LNPFp series, presence of PPy coated fibers in the NR/PPy system increases the conductivity substantially and a maximum of $6.25x10^{-2}$ S/cm is attained at a concentration of 75 phr F-PPy in the LNP2 system. It is interesting to note that for the same composition, dry rubber mixing gave a conductivity 1.7×10^{-5} S/cm (section 4.3.5). Latex stage polymerization gives higher conductivity than dry rubber compounding. This is due to better adhesion of PPy and PPy coated fiber to rubber particles since polymerization of pyrrole and coating of Nylon fiber are carried out in NR latex.

5.3.6 Mechanical properties

Fig. 5.9 represents the stress- strain curves of LNP and LNPFp series. The variation of tensile strength of PPy loaded (LNP series) and F-PPy loaded (LNPFp series) samples are shown in fig. 5.10. The tensile strength of elastomer decreases sharply with PPy loading, the effect being less significant at higher loadings. Such a trend has been reported in an earlier work with PPy/ polypropylene composites by Piontecka *et a.l* [8]. This reveals the non reinforcing nature of PPy in NR matrix. Introduction of PPy into a composite, as a rule, decreases its strength and results in the loss of elasticity [9]. The poor adhesion between polypyrrole (hydrophilic nature) to the natural rubber matrix (hydrophobic nature) is the main factor for the deterioration of tensile strength. It is found that a 57% decrease occurs by the incorporation of 25 phr PPy (LNP1). No further decrease is observed at higher loadings. Tensile strength of LNPFp series decreases first and then increases sharply on loading with F-PPY, and the composite regains 70% strength with the incorporation of 75 phr F-PPy to LNP2 system. Thus, the decrease in strength caused by PPy is counterbalanced by the incorporation of PPy coated fibers. PPy coated fibers is very effective in improving conductivity and mechanical properties simultaneously.

Elongation at break decreases with filler loading and then levels off (fig. 5.11). The composites become stiffer and stiffer by the addition of PPy and F-PPy and there is decrease in its extensability. Modulus at 50% elongation increases for the two series (Fig. 5.12). Variation of tear strength with filler loading for LNP series and LNPFp series is shown in fig. 5.13. Tear strength decreases for LNP series due to the non reinforcing effect of PPy. For the LNPFp series tear strength shows a decrease first and then increases sharply to

reach a value higher than that of NR. The tear failure occurs by the propagation of tear front across the matrix. In the presence of fibers distributed in the bulk, these tear lines are either arrested or deviated. The energy of the propagating crack front is dissipated at the fiber- matrix interface by way of its pull - out or breakage.

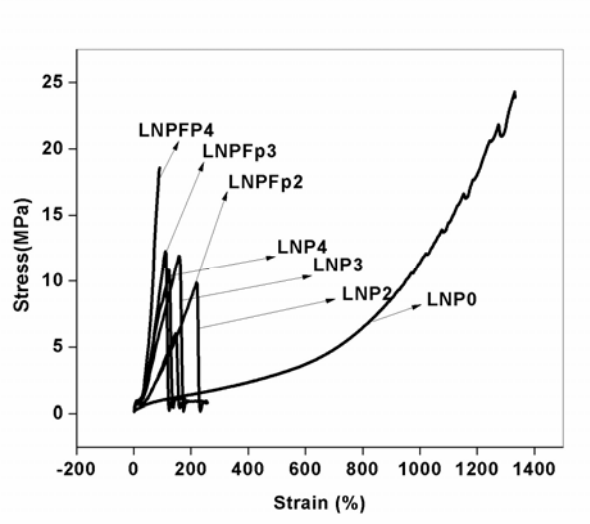

Fig. 5.9 Stress-strain curves of LNP and LNPFp series

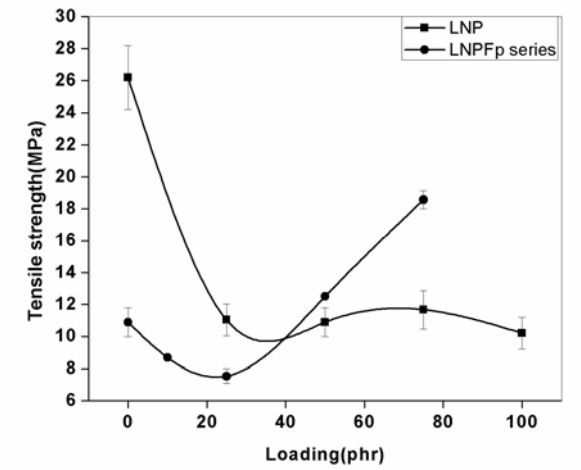

Fig. 5.10 Variation of tensile strength with loading NR based CECs prepared by *in situ* method

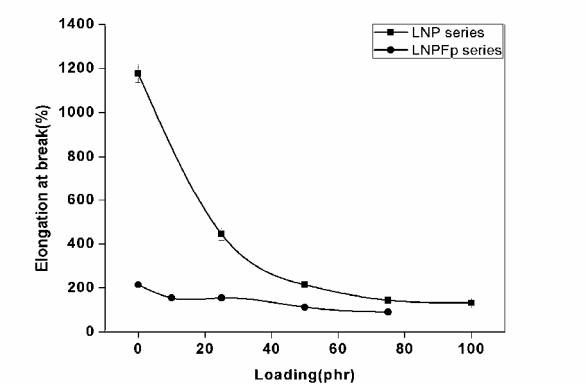

Fig. 5.11 Variation of elongation at break with loading of NR based CECs prepared by *in situ* method

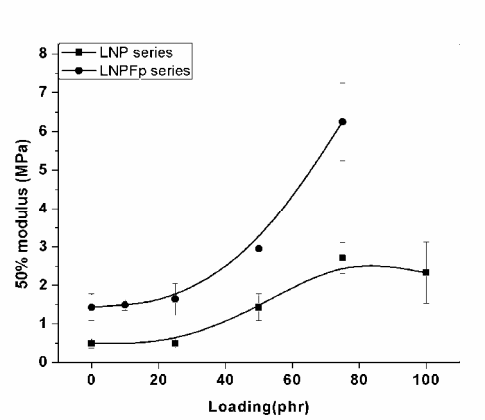

Fig. 5.12 Variation of modulus with loading of NR based CECs prepared by *in situ* method

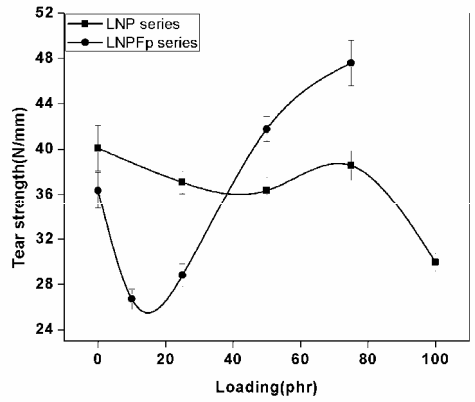

Fig. 5.13 Variation of tear strength with loading of NR based CECs prepared by *in situ* method

5.3.7 Swelling characteristics

Variation of mol percentage uptake of toluene with PPy loading and F-PPy loading in the composites are shown in figs. 5.14. and 5.16 respectively. The photographs showing the swelling of different samples of LNP and LNFp series are shown in figs. 5.15 and 5.17. It can be seen that PPy loading and F-PPy loading do not enhance the solvent sorption of the elastomer. The percentage swelling index and swelling coefficient values also decrease with increased loading (table 5.4). This may be due to the increased hindrance exerted by the filler. The polarity of filler also causes a decrease in solvent sorption. Toluene being a non-polar solvent its sorption is decreased when the matrix is loaded more and more with polar filler, PPy and PPy coated Nylon fiber. From table 5.4 it is evident that swelling takes place both in the thickness direction and diameter. The composites exhibit slight deviation from the Fickian mode of transport (section 4.2.8). Here the value of n varies from 0.3–0.5 (table 5.4).

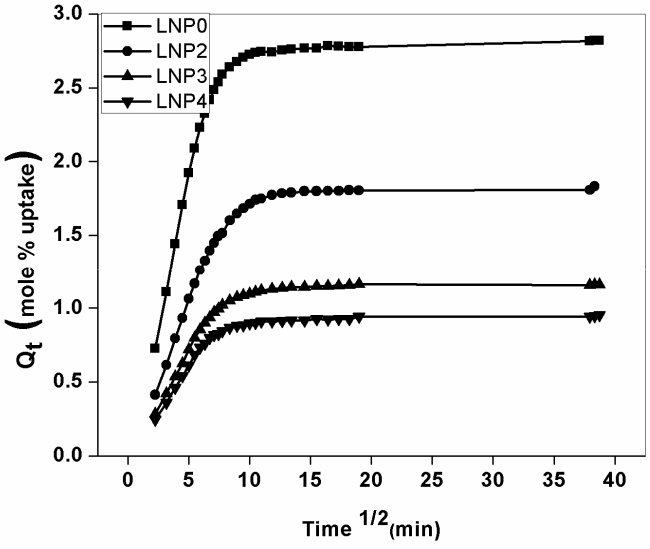

Fig. 5.14 Q_t vs $T^{1/2}$ of LNP series

Deviation from the Fickian behaviour may be attributed to processes such as surface crazing, osmotic cracking, micro crack formation, etc. [10]. The k values of the composites (table 5.4) are lower than gum vulcanizate. Lower values of k indicate that there is less interaction between composite and solvent and also there is less absorption of solvent.

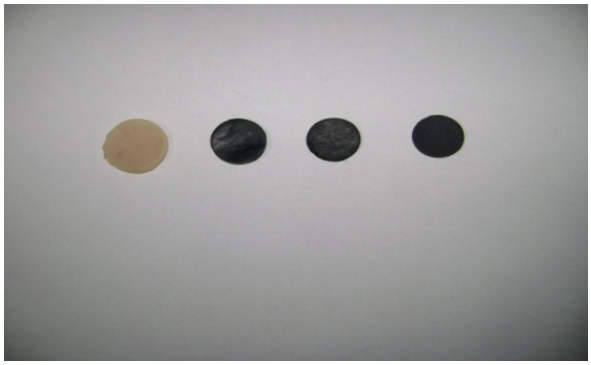

Fig. 5.15 Photographs showing the swelling of different samples of LNP series (LNP0, LNP2, LNP3, LNP4)

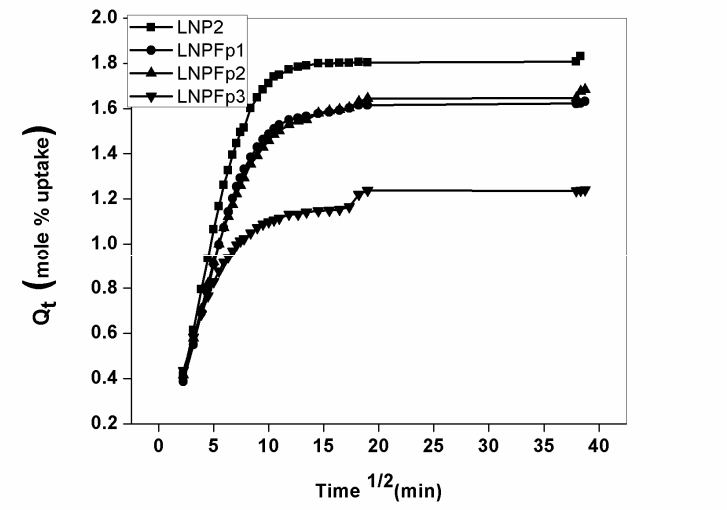

Fig. 5.16 Q_t vs $T^{1/2}$ of LNPFp series

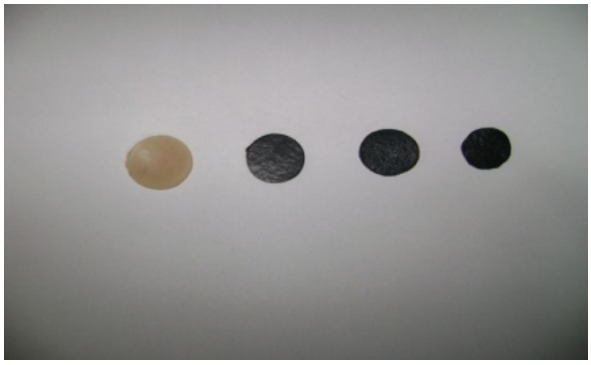

Fig.5.17 Photographs showing the swelling of different samples of LNPFp series(LNP2, LNPFp1, LNPFp2, LNPFp3)

Table 5.4 Swelling parameters of NR based CECs prepared by *in situ* method

Sample	Before toluene sorption		After toluene sorption		Swelling index(%)	Swelling coefficient	n	k
	Thickness (mm)	Diameter (mm)	Thickness (mm)	Diameter (mm)				
LNP0	1.22	12	1.95	19	260	2.99	0.34	0.99
LNP2	1.35	12	2.24	15	169	1.94	0.48	0.50
LNP3	1.31	12	3.02	14	106	1.23	0.54	0.97
LNP4	1.33	12	3.20	13	88	1.01	0.53	0.92
LNPFp1	1.12	12	2.20	15	150	1.73	0.46	0.70
LNPFp2	1.11	12	2.19	15	155	1.78	0.44	0.86
LNPFp3	1.28	12	2.04	13	114	1.32	0.32	0.63

5.4 Conclusions

Conductive elastomeric composites were prepared by *in situ* polymerization of PPy and PPy coated short Nylon fiber in NR latex, followed by coagulation and mechanical mixing. The cure characteristics, cure kinetics, filler dispersion, morphology, DC electrical conductivity, mechanical properties and swelling characteristics of the composites

prepared were evaluated. Compared to PPy, PPy coated fiber is effective in increasing the cure rate. This is supported by cure kinetic studies. The cure reaction follows first order kinetics. Filler dispersion studies show that PPy gets well dispersed in NR matrix at lower loadings while agglomeration occurs at higher loadings. Compared to NR/PPy system, NR/PPy/F-PPy exhibits better dispersion even at higher loading. Morphology of fracture surfaces of fiber loaded samples exhibit better adhesion between filler and matrix which may result in improved mechanical properties and enhanced conductivity. SEM image also shows that PPy forms a very uniform dense coating on Nylon fiber. DC conductivity of NR/PPy composites is enhanced only at very high PPy loading and the maximum conductivity $8.3x10^{-4}$ S/cm is attained at 100 phr loading. Presence of PPy coated fibers in the NR/PPy system increases the conductivity substantially and the maximum conductivity attained is $6.25x10^{-2}$ S/cm. The mechanical properties of NR are declined by PPy loading which is compensated by the addition of PPy coated fiber. Addition of 75phr PPy coated fibers to NR/PPy system causes 70% increase in tensile strength. The NR/PPy/ PPy coated fiber composites show increased tensile strength, modulus and tear resistance. The swelling studies reveal that both PPy and F-PPy loading decrease the solvent sorption of NR. This is further supported by percentage swelling index and swelling coefficient values which decrease with loading. The solvent sorption mechanism in the conducting composites exhibits slight deviation from Fickian mode.

References

[1] Omastova M, Chodak I, Pionteck J. *Synth Met*. **1999**, 102, 1251.

[2] Omastova M, Pionteck J, Kosina S. *Eur Polym J* . **1996**, 32, 681.

[3] Gang L, Xia L, Xinghua S, Jian U, Jiasong H. *Front Chem China*. **2007**, 2, 118.

[4] Zoppi RA, DePaoli MA. *Polymer*. **1996,** 37,1999.

[5] Omastova M, Kosina S, Pionteck J, Jenke A, Pavlinec J. *Syn Met*. **1996**, 81,49.

[6] Ruckerstein E , Yang S. *Polymer*. **1993**, 34, 4655.

[7] Xie H, Liu C, Guo J. *Polym Int*. **1999**, 48, 1099.

[8] Piontecka J, Omastova M, Potschkea P, Simona F, Chodak I. *J Macromol Sci-Phys*. **1999**, B38, 737.

[9] Smirnov MA, Kuryndin IS, Nikitin LN, Sidorovich AV, Yu N, Sazanov OV, Kudasheva V, Bukosek AR, Khokhlov, Elyashevich GK. *Russ J Appl Chem*. **2005**, 78, 1993

[10] Sreekala MS, Goda K, Devi PV. *Compos Interfaces*. **2008,**15, 281.

Chapter

6

CONDUCTING ELASTOMER COMPOSITES: NBR/PPy/PPy COATED SHORT NYLON FIBER

Contents

Conducting elastomer composites of polypyrrole (PPy) and polypyrrole coated Nylon fiber (F-PPy) based on acrylonitrile butadiene rubber (NBR) were prepared by proper compounding on a two roll mill followed by moulding. The cure pattern, cure kinetics and filler dispersion of the elastomeric composites were evaluated. Compared to NBR/PPy systems, NBR/F-PPy composites exhibited lower cure values. Results of cure kinetic studies agreed with these observations. First order kinetics was observed for cure reactions. The composites synthesized were characterized using scanning electron microscopic (SEM) analysis. The DC electrical conductivity of the conducting elastomer composites was measured. The mechanical properties of the composites were studied using a Shimadzu Universal Testing Machine. The solvent swelling characteristics of the composites were investigated in methyl ethyl ketone. The DC conductivity of the composites was found to be better for the F-PPy system compared to PPy-filled elastomer composite. The highest conductivity obtained was 5×10^{-5} S/cm. Both PPy and PPy coated fiber were very effective in improving the mechanical properties of NBR. The % swelling index and swelling coefficient of the composites were found to decrease with increase in PPy loading and F-PPy loading. The solvent sorption mechanism in the conducting composites exhibited minor deviation from Fickian mode.

6.1 Introduction

Acrylonitrile butadiene rubber (NBR) is a copolymer of acrylonitrile and butadiene and is polar in nature (structure-fig. 6.1). NBR has good resistance to a wide variety of oils and solvents and hence is widely used for products like oil seals, pipe protectors, blow out preventors etc. [1]. Major properties of NBR depend on the acrylonitrile content which varies from 20-50% by weight. Commercially available nitrile rubbers differ from one another in three respects: acrylonitrile content, polymerization temperature and Mooney viscosity. NBR has high viscosity that can be reduced by mastication. Vulcanization of NBR is usually accomplished with sulphur. The solubility of sulphur is considerably less and therefore sulphur is added early in the mixing sequence. Since nitrile rubber does not crystallize, reinforcing fillers are necessary to obtain good tensile, tear and abrasion properties. NBR reinforced with particulate fillers [2,3] and fibrous fillers have been studied [4-6].

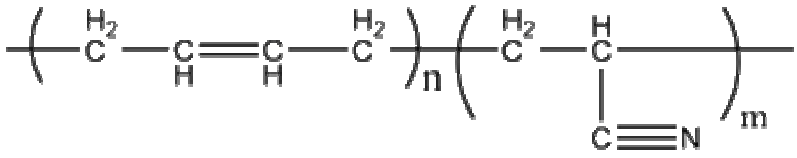

Fig.6.1 Structure of NBR

Electrical conductivity is important in many rubber and plastic goods for antistatic applications, wire and cable sheathing, shielding against electromagnetic interference etc. Elastomers and plastics are insulators to which conductivity is imparted by the addition of finely divided fillers of high intrinsic conductivity. Incorporation of a conducting polymer modifies the properties of the elastomer enhancing its potential for many applications. An appropriate selection of the

conducting polymer and the matrix can result in conducting elastomer composites with desired properties for different applications. The processability and properties of conducting elastomer composites depend on the nature of elastomer *viz*., polar/non polar and the type of elastomer *viz*., natural/ synthetic. It also depends on the properties of the conducting polymer incorporated into it. In this chapter the preparation, characterization and properties of NBR based PPy/PPy coated short Nylon fiber conducting elastomeric composites (CECs) are discussed. The cure characteristics and cure kinetics, filler dispersion, morphological characterization, DC conductivity, mechanical properties and swelling characteristics of the composites are also described.

6.2 Experimental

6.2.1 Materials

Details of acrylonitrile butadiene rubber (NBR), zinc oxide, stearic acid, tetramethylthiuram disulphide (TMTD), mercaptobenzothiazyl disulphide (MBTS), sulphur and methyl ethyl ketone (MEK) used in the present study are given in section 2.1

6.2.2 Preparation of conductive elastomeric composites (CECs)

The prepared polypyrrole (PPy) and PPy coated short Nylon fiber (F-PPy) (sections 3.2.2 and 3.2.3) were used to prepare conducting elastomer composites (CECs) based on NBR. The formulation for the preparation of composites is given in Table 6.1. BP series represent the vulcanizates of NBR with PPy, and BFp represents NBR/F-PPy composites. These composites were prepared in a laboratory size two-roll mill as described under section 2.2.2. The optimum cure time at 160^0C was determined using a Rubber Process

Analyzer (section 2.2.3). The compounds were then compression moulded at 160^0C in an electrically heated hydraulic press (section 2.2.4). The vulcanized sheets were kept in a cold dark place for 24 h and were used for the subsequent tests

Table 6.1 Formulation for the preparation of NBR based CECs

Sample	PPy(phr)[a]	F-PPy(phr)[a]
BP0	0	0
BP1	20	0
BP2	50	0
BP3	75	0
BP4	100	0
BFp1	0	10
BFp2	0	25
BFp3	0	50
BFp4	0	75

All mixes contain NR-100g, zinc oxide- 4.5phr, stearic acid-2phr, tetramethylthiuram disulphide- 0.25phr, mercaptobenzothiazyl disulphide-1 phr, sulphur-1.5phr

a- parts per hundred rubber

6.2.3 Characterization

The cure characteristics of the vulcanizates were monitored using a Rubber Process Analyzer as explained in section 2.2.3. The cure time T_{90}, scorch time T_{10}, maximum torque M_H, and minimum torque M_L values were determined at 160 ^{0}C. The cure rate index (CRI) and the kinetic rate constant of cure reaction, were determined from the rheometric data. The vulcanization kinetics was studied by the method described in section 4.2.3. The filler

dispersion and the formation of filler agglomerates in polymer matrices were studied by the methods described in section 4.2.4. SEM images of tensile fracture surface of the composites were obtained using a scanning electron microscope (section2.2.8). The DC electrical conductivity of the composites was measured by the two-probe method as described in section 2.2.5. The mechanical properties of the composites like tensile strength, elongation at break, modulus at 50% elongation and tear strength were determined using a Shimadzu Universal Testing Machine as described in section 2.2.6.The solvent swelling characteristics of the composites were investigated in methyl ethyl ketone (MEK) as described in section 4.2.8 of this thesis.

6.3 Results and discussion

6.3.1 Cure characteristics

Figure 6.2 represents the rheogramsof BP and BFp series. The nature of the cure curves is different for the series, which indicates that in the matrix, PPy and F-PPy interact differently.

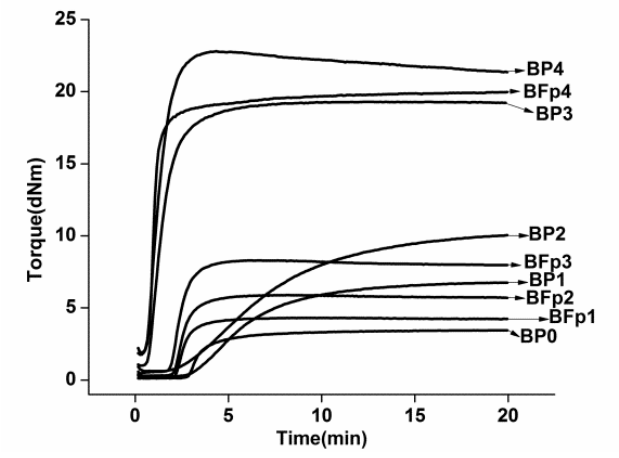

Fig.6. 2 Cure curves of BP seriesand BFp series

Table 6.2 Cure parameters of NBR based CECs

Sample	Cure time T_{90}(min.)	Scorch time T_{10}(min.)	Maximum torque M_H(dNm)	Minimum torque M_L(dNm)
BP0	6.5	2.9	3.5	0.1
BP1	10.9	3.5	6.8	0.2
BP2	13.2	3.2	10.0	0.6
BP3	3.0	0.8	19.3	1.0
BP4	2.2	0.7	22.8	1.9
BFp1	3.8	2.2	4.3	0.1
BFp2	3.8	2.2	5.9	0.3
BFp3	3.4	1.9	8.3	0.4
BFp4	1.9	0.7	19.9	1.7

The cure parameters of the composites are presented in Table 6.2. Cure time, $T_{90,}$ represents the time corresponding to the development of 90% of the maximum torque. Cure time is found to increase with the incorporation of PPy, reaches a maximum and then decreases at higher loading. The increase in cure time with PPy concentration may be attributed to the presence of acidic dopant in PPy. Compared to PPy loaded samples, composites containing F-PPy exhibit lower cure values. This may be due to possible degradation of Nylon fiber at the curing temperature. The effect of PPy is not manifested here as the PPy content (coated on fiber) is very low in this case. The amine functionality of the degradation products may accelerate the cure reaction. Similar results have been reported earlier in the case of NBR/short Nylon fiber composites [5]. These observations are supported by the cure kinetic studies and cure rate index values, which will be discussed in the following sections. Scorch time$T_{10}$is the time required for the torque value to reach 10% of maximum torque. It is a measure of the scorch safety of the rubber compound.

For BP series scorch time increases with filler loading indicating a better processing safety. With increased loading, the value decreases. For BFp series also a decrease is observed at higher fiber loadings. Such a decrease is attributed to the heat of mixing resulting in the premature curing of the compounds.

The maximum torque, M_H is an index of the extent of crosslinking reactions and represents the shear modulus of the fully vulcanized rubber at the vulcanization temperature. It also has a contribution from filler- polymer interactions. The value is found to increase for both BP and BFp series. This means that with the addition of PPy and F-PPy some sort of interaction between them and the matrix develops. The minimum torque, M_L which is a measure of the viscosity of the compound, also increases with filler loading for both the series.

6.3.2 Cure kinetics

Figure 6.3 represents plots of ln (M_H–M_t) against time t at 160^0C of the CECs based on NBR. The plots are found to be linear which proves that the cure reactions proceed according to first-order kinetics. CRI was determined by equation (4.1) for the two series. The variation of CRI with filler loading of CECs is presented in Fig. 6.4. For BP series, CRI decreases first, and then increases substantially, whereas the CRI values of BFp series increases with loading. These two observations are in full agreement with the variation of cure time of these series (Table 6.2).

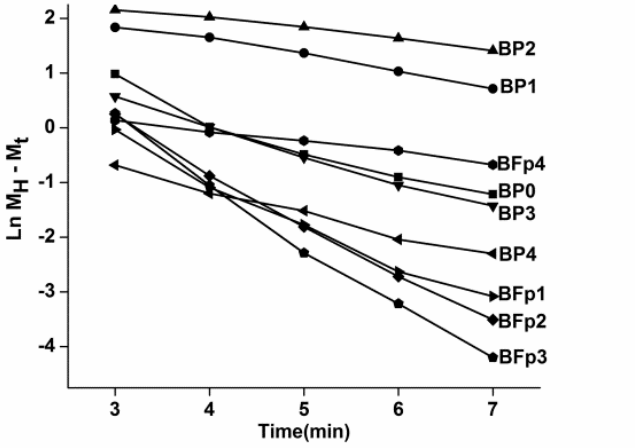

Fig. 6.3 Plots of ln(M_H-M_t) vs time for BP series and BFp series

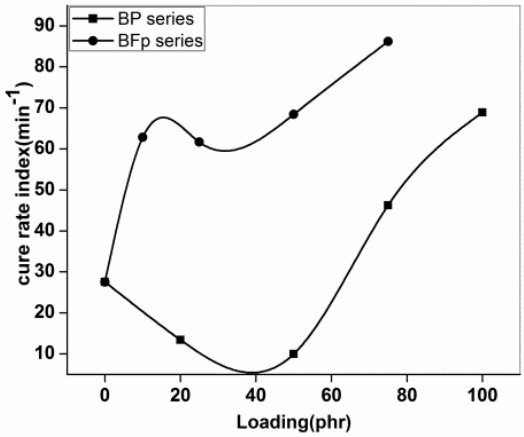

Fig. 6.4 Plots of CRI vs loading of NBR based CECs

6. 3. 3 Filler dispersion

The η_r and Er values of the two series were computed and are shown in Table 6.3. For BP and BFp series, it is observed that there is not much difference between η_r and Er values initially which means that the filler is well dispersed in the matrix.

Table 6.3 η_r and E_r values of NBR based CECs

Sample	Relative viscosity η_r	Relative moduli E_r
BP1	2.32	1.96
BP2	5.56	2.90
BP3	9.22	5.58
BP4	17.5	6.59
BFp1	1.29	1.24
BFp2	2.45	1.70
BFp3	4.26	2.40
BFp4	16.2	5.77

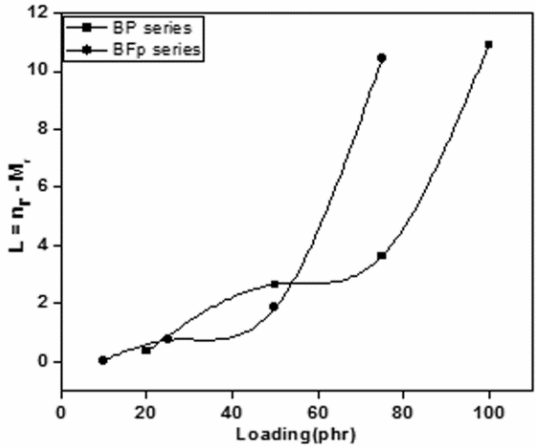

Fig. 6.5 Variation of index L with loading of NBR based CECs

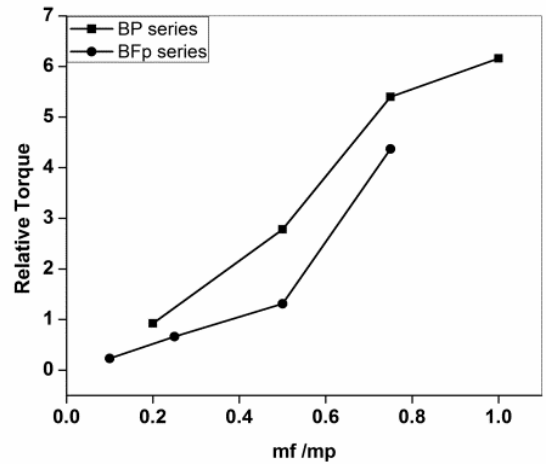

Fig.6.6 Plots of Relative torque as afunction of filler loading of NBR based CECs

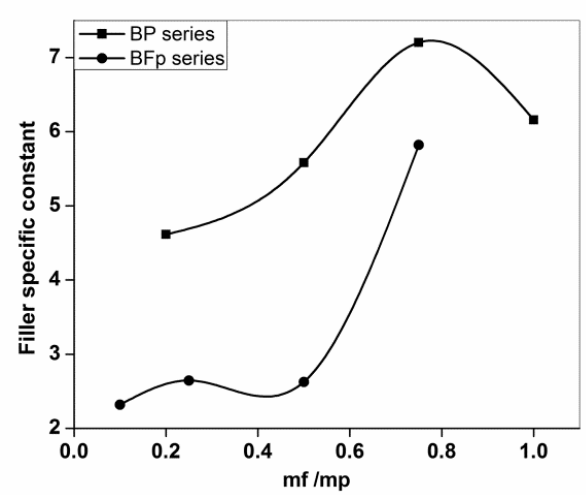

Fig. 6.7 Variation of filler specific constant, α_f with filler loading of NBR based CECs

From figure 6.5 it is clear that in the case of NBR composites, a sharp increase in index L occurs only at very high PPy and F-PPy loading, which points to well dispersed NBR/PPy and NBR/F-PPy systems at lower loadings. In Figure 6.6 Wolf equation is applied to BP and BFp series. Slopes of the plots give filler specific constant, α_f, the value of which is found to be high for BP series (α_f= 6. 9) compared to BFp series (α_f = 2. 6). This means tendency to agglomeration is less for fiber loaded samples. The absolute value of α_f for each composite was calculated using equation (4.8) and is plotted against filler loading in Fig. 6.7.The observations are in agreement with those obtained from Lee's approach.

6.3.4 Morphology

The SEM micrographs of failed tensile surfaces of the CECs based on NBR are shown in fig. 6.8

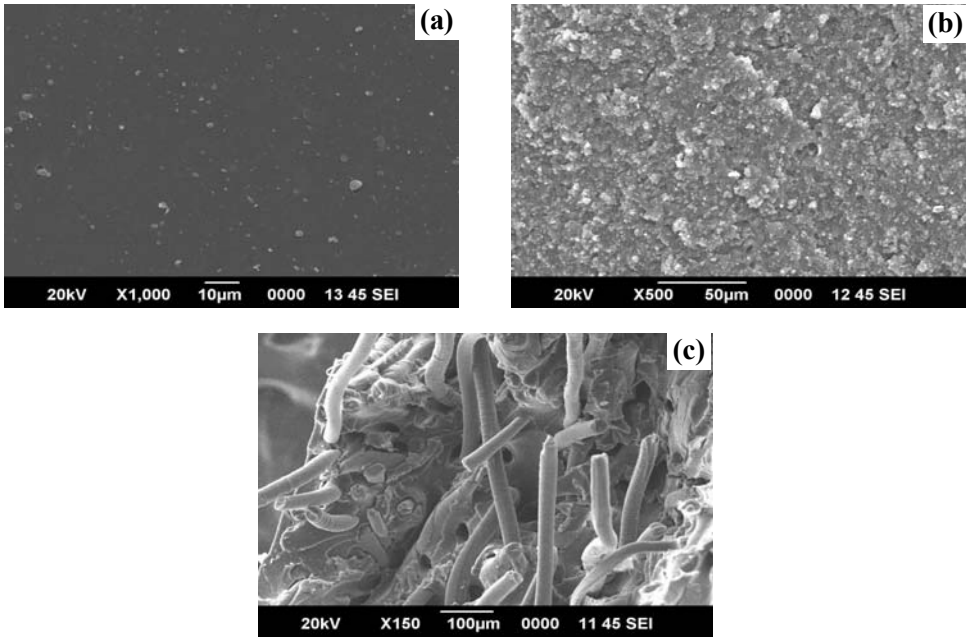

Fig. 6.8 SEM micrographs of (a)BP0, (b)BP2, (c)BFp2

Figure 6.8 (a) shows the scanning electron microscopy photograph of the tensile fracture surface of the NBR gum vulcanizate. The fracture surface is smooth and has no crack propagation lines. This pattern is typical of weak matrices. SEM images of PPy/elastomer composites, BP2 ,6.8 (b) reveals a homogenous dispersion of PPy in the rubber matrix. The globular PPy particles are loosely aggregated in the matrix. PPy primary particles link with each other to form conductive chains or network in the NBR matrix. Hence conductivity is expected to increase with filler loading. The SEM image of F-PPy loaded CEC, BFp2 (figures 6.8(c)) shows good orientation of fiber in one direction and better adhesion between fiber and matrix resulting in improved mechanical properties as will be discussed shortly.

6.3.5 DC electrical conductivity

The DC electrical conductivities of the NBR based composites are presented in Fig. 6.9. For the BP series there is not much increase in conductivity up to 50 phr loading. After that, a sharp increase in conductivity is observed with a maximum of 5×10^{-5} S/cm, attained at 100 phr loading.

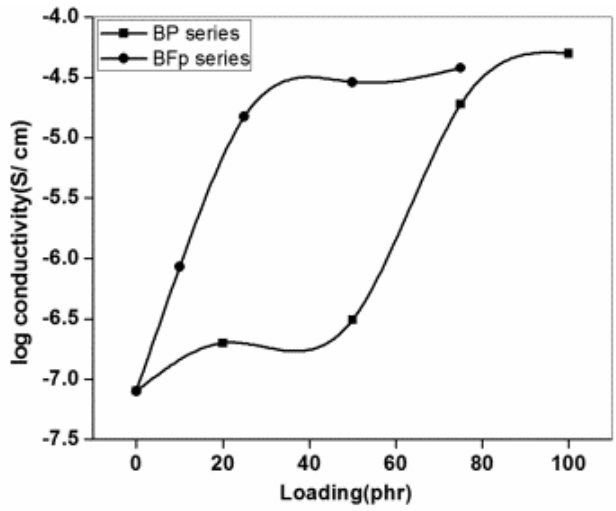

Fig. 6.9 Variation of log conductivity with loading of NBR based CECs

For BFp series the percolation occurs at about 25 phr F-PPy loading. The reason for lower percolation in the case of fiber loaded samples, compared to PPy loaded samples is as explained earlier in the case of NR based CECs. (section 4.3.5). Increasing fiber fiber contact with increased loading helps in forming a closed network of conducting species leading to better conduction.

6.3.6 Mechanical properties

Fig. 6.10 represents Stress- strain curves of NBR based CECs. The variation of tensile strength of PPy loaded (BP series) and F-PPy loaded (BFp series) samples is shown in fig. 6.11. The tensile strength of elastomer increases

gradually with PPy loading and an increase of 125% is observed at 75phr loading after which it levels off. This reveals the reinforcing nature of PPy in NBR matrix. Introduction of PPy into a composite, as a rule, decreases its strength and results in the loss of elasticity [7]. Here the better interaction between polypyrrole and the nitrile rubber matrix is the main factor for the increase of tensile strength.

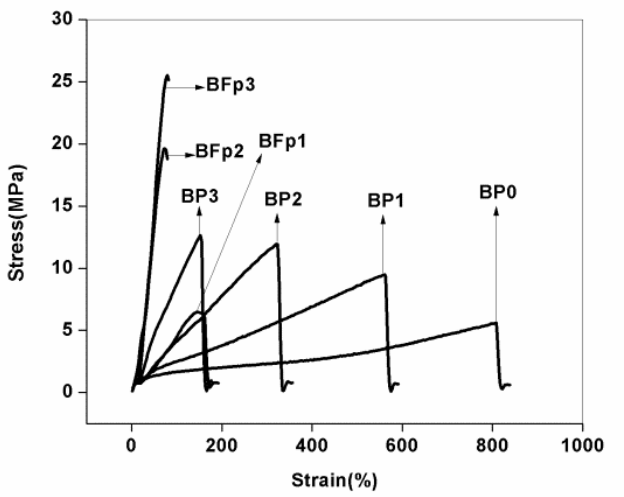

Fig. 6.10 Stress-strain curves of NBR based CECs

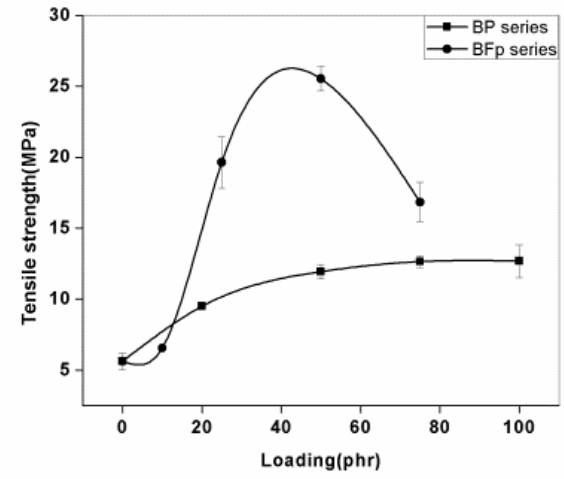

Fig.6.11. Variation of tensile strength with loading of NBR based CECs

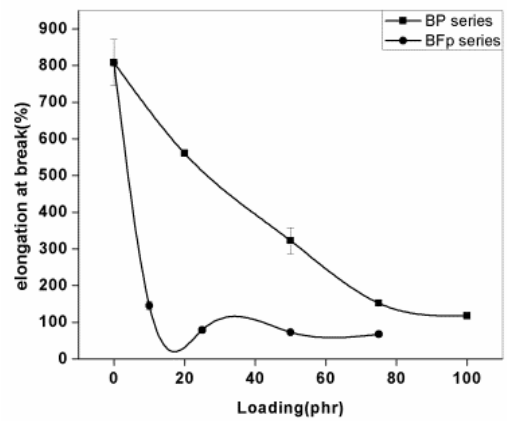

Fig. 6.12. Variation of elongation at break with loading of NBR based CECs

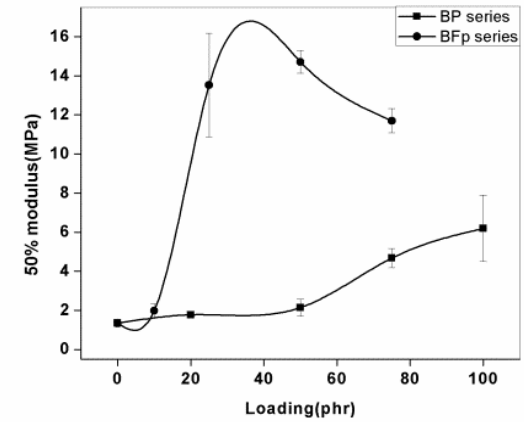

Fig. 6.13. Variation of modulus with loading of NBR based CECs

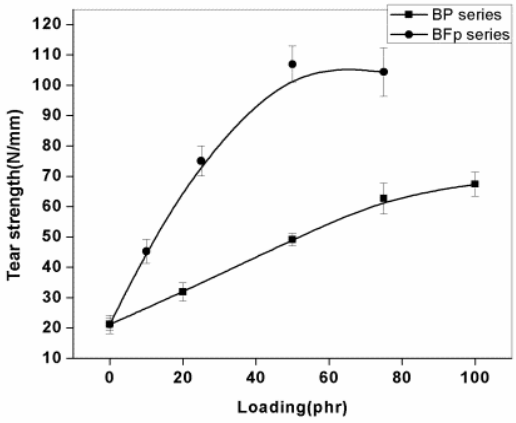

Fig. 6.14. Variation of tear strength with loading of NBR based CECs

Tensile strength of BFp series increases sharply on loading with F-PPy, reaches maximum at 50 phr loading after which it decreases. PPy coated fibers is very effective in improving conductivity and mechanical properties simultaneously. Elongation at break decreases with filler loading and then levels off (fig. 6.12). The composites become increasingly stiffer in the presence of PPy and F-PPy. Modulus at 50% elongation increases for the two series (Fig. 6.13). Variation of tear strength with filler loading for BP series and BFp series is shown in fig. 6.14. Tear strength is found to increase sharply with PPy and F-PPy loading.

6.3.7 Swelling characteristics

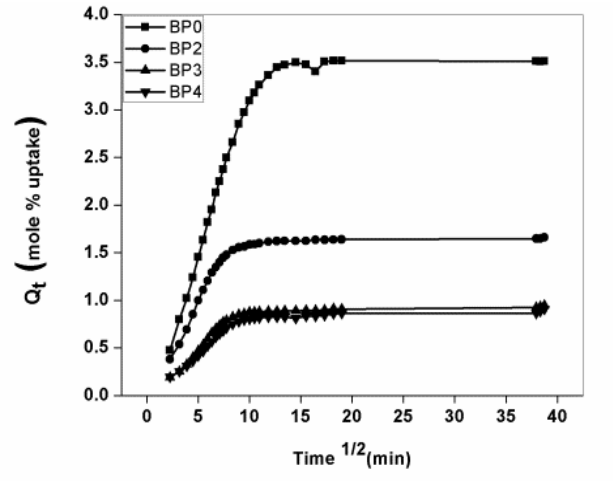

Fig. 6.15 Q_t vs $T^{1/2}$ of BP series

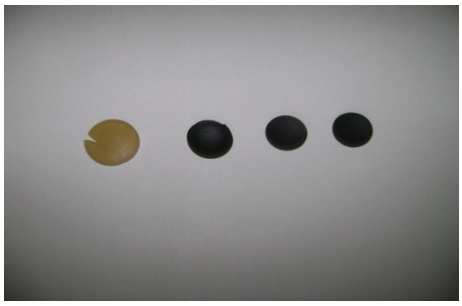

Fig. 6.16 Photographs showing the swelling of different samples of BP series (BP0, BP2, BP3, BP4)

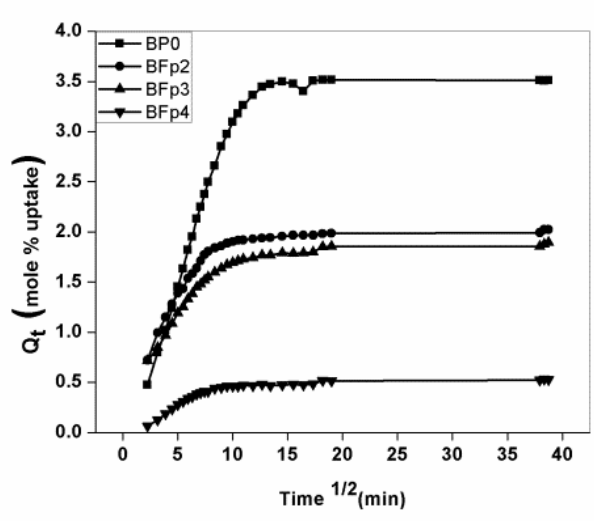

Fig. 6.17 Q_t vs $T^{1/2}$ of BFp series

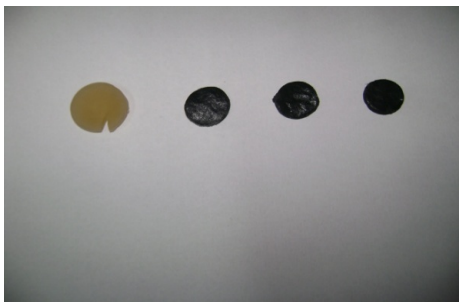

Fig.6.18 Photographs showing the swelling of different samples of BFp series(BP0, BFp2, BFp3, BFp4)

Table 6.4 Swelling parameters of NBR based CECs

Sample	Before MEK sorption		After MEK sorption		Swelling index(%)	Swelling coefficient	n	k
	Thickness (mm)	Diameter (mm)	Thickness (mm)	Diameter (mm)				
BP0	1.7	12	2.74	18	253	3.14	0.63	1.28
BP2	1.33	12	1.87	15	119	1.48	0.51	0.97
BP3	1.41	12	1.79	14	68.2	0.84	0.57	1.11
BP4	1.55	12	1.91	14	65.2	0.81	0.53	1.06
BFp2	1.16	12	2.69	13	145.8	1.81	0.33	0.63
BFp3	1.19	12	3.13	13	136.6	1.68	0.30	0.61
BFp4	1.21	12	2.09	12	37.8	0.47	0.66	0.66

Variation of mol percentage uptake of methyl ethyl ketone with PPy loading and F-PPy loading in NBR are shown in figs.6.15. and 6.17, respectively. It is seen that both PPy loading and F-PPy loading decrease the solvent sorption. The highest loaded sample attains equilibrium at an early stage. Decrease in solvent sorption of the CECs compared to the gum compound is also evident from the decreasing percentage swelling index and swelling coefficient values with increased loading (table 6.4). The filler–matrix interactions also affect the sorption behaviour considerably. The decreased sorption of CECs with loading may be due to increased interaction between filler and matrix.

The photographs of the swollen samples of BP series and BFp series are shown in figs. 6.16 and 6.18. Dimensions of the composites before and after swelling in MEK were measured and reported in table 6.4. There is an increase in both thickness and diameter after equilibrium swelling. The composites exhibit deviation from the Fickian mode of transport as is evident from the values of n which varies from 0.3–0.6(table 6.4). Deviation from the Fickian behaviour may be attributed to processes such as surface crazing, osmotic cracking, micro crack formation, etc. [8]. k values of the composites are lower than gum vulcanizate which indicates that there is less interaction between composite and solvent and also there is less absorption of solvent.

6.4 Conclusions

Conductive elastomeric composites of polypyrrole and polypyrrole coated short Nylon 6 fiber were prepared with acrylonitrile butadiene rubber by mechanical mixing. The cure characteristics, cure kinetics, filler dispersion, morphology, DC electrical conductivity, mechanical properties and swelling characteristics of nitrile rubber/ polypyrrole (NBR/PPy) and nitrile rubber/

polypyrrole coated short Nylon fiber (NBR/F-PPy) composites were investigated. Cure time increases with the incorporation of PPy, reaches a maximum and then decreases at higher loading, while fiber loading decreases the cure time significantly. This is supported by cure kinetic studies. The cure reaction follows first order kinetics. PPy and PPy coated fiber get well dispersed in NBR matrix at lower loadings as is evident from filler dispersion studies. At higher loadings, however, agglomeration occurs. The scanning electron microscopic images of the tensile fracture surfaces of the CECs also point to a well dispersed elastomer/ PPy system which may result in increased conductivity. Morphology of fracture surfaces of fiber loaded samples exhibit better adhesion between filler and matrix which results in improved mechanical properties and enhanced conductivity. Compared to PPy, PPy coated fiber is found to be very effective in enhancing the DC conductivity of NBR. Conductivity of 75 phr PPy loaded sample is attained by the addition of only 25 phr PPy coated fiber. Both PPy and PPy coated fiber are very effective in improving the mechanical properties of NBR. The swelling studies reveal that both PPy and F-PPy loading decrease the solvent sorption of NBR. The solvent sorption mechanism in the conducting composites exhibits slight deviation from Fickian mode.

References

[1] Hofman W. *Rubber Technology Handbook-Ed. Werner Hofmann, Hanser Publishers, Munich*. **1989,** Chapter 4, 284.

[2] Park SJ, Cho KS, Ryu SK. *Carbon*, **2003,** 41, 1437.

[3] Wang MJ, Wolff S, Donnet JB. *Rubber Chem Technol*. **1991,** 64, 559.

[4] Sreeja TD, Kutty SKN. *J Elastomers Plast*. **2002**, 34, 157.

[5] Seema A, Kutty SKN. *J Appl Polym Sci*. **2006**, 99, 532

[6] Rajeev RS, De S K, Bhowmic AK, Baby J. *Polym Degrad stab*. **2003**, 79, 449.

[7] Smirnov MA, Kuryndin IS, Nikitin LN, Sidorovich AV, Yu N, Sazanov OV, Kudasheva V, Bukosek AR, Khokhlov, Elyashevich GK. *Russ J Appl Chem*. **2005**, 78, 1993.

[8] Sreekala MS, Goda K, Devi PV. *Compos Interfaces*. **2008**,15, 281.

.....ꕥ.....

Chapter

7

THERMAL CHARACTERISTICS OF CONDUCTING ELASTOMER COMPOSITES

Contents

Thermal stabilities of the conducting elastomer composites based on NR and NBR prepared by conventional mixing and by insitu polymerization in NR latex were studied using thermogravimetric analysis. It is found that PPy and PPy coated fiber (F-PPy) do not alter the onset of degradation of NR and CECs based on NR at lower filler loadings. In the case of NR/PPy systems prepared by in situ polymerization in latex, the degradation starts at higher temperature. Considering NBR based composites, with PPy the onset of degradation is delayed while no such change is observed with F-PPy. The peak degradation rate, i.e., the maximum rate of degradation decrease with filler loading for all the series of composites prepared. The thermal degradation kinetics was studied by Coats and Redfern method. It is seen that the degradation reactions follow first order kinetics. The activation energies of thermal degradation reaction were estimated. Tg of the gum vulcanizates and the CECs were determined by DSC analysis.

7.1 Introduction

Thermal analysis is considered as an important analytical method in understanding the structure-property relationship and mastering the technology for the industrial production of different polymeric materials. TGA is widely used because of its relative simplicity. In TGA, the mass as a function of time and temperature is used to assess the thermal stability and degradation of polymers, which include the generation of kinetic data such as activation energies. It is employed to measure the weight loss and the derivative weight loss of the samples by heat. It is generally accepted that reliable degradation temperature and kinetic parameters, such as the onset of degradation temperature, the temperature of maximum degradation, activation energy for the decomposition can be used to assess a material's lifetime [1-7]. It is well known that thermal stability of a polymeric material can be improved by adding short fibers [2-5]. Strong interaction between the polymer and the filler particles is essential for achieving good mechanical properties and thermal stability [6-10].

Zoppi *et al.* [11] prepared semi- interpenetrating networks (SIPN) of PPy and EPDM rubber by chemical oxidative polymerization. Thermal analysis of the prepared samples showed that it was possible to improve the thermal stability of the elastomeric phase of the SIPN by incorporating stabilizing agents into the matrices. Thermal stability of PPy/ polyethylene composites and their components was studied by TGA [12]. The TGA curves showed that the degradation patterns of the PPy/ polyethylene composites were intermediate between those of pure components and differ from each other significantly. Gu *et al*. [13] found that PPy/ graphite oxide composites prepared by them showed improved thermal stability compared to the pure

PPy especially in the temperature range 430 ^{0}C - 700 ^{0}C. They suggested that these high conductivity polymer/ inorganic composites might be candidates for developing new applications in high-temperature electronics and other fields. TGA studies of PPy/PVC SIPN [14] showed that initial weight loss of 12% at 260 ^{0}C, of PPy alone was increased to 20% in the presence of PVC showing that stability of PPy is reduced in the presence of PVC. Differntial scanning calorimetric analysis of the PPy/ PVC SIPN [14] showed that the glass transition temperature of SIPN was shifted to 113^{o}C from 120 ^{0}C of PPy. The lower Tg shift is due to the presence of PVC, which makes the PPy chains more flexible due to its plasticizing action.

In this chapter the effect of PPy and PPy coated short Nylon 6 fiber on the thermal degradation properties of NR and NBR based conductive elastomer composites is presented. The kinetics of thermal degradation is also discussed.

7.2 Results and discussion

7.2.1 Thermogravimetric analysis

7.2.1.1 *NR based CECs*

Formulation for the preparation of CECs is given in table 4.1(chapter 4). The thermal mass loss traces obtained from the TG analysis of composites of NP series are presented in Figure 7.1 (a). The TG curves of NPFp series are presented in figure 7.2(a). The TG curves of composites belonging to NFp series are given in figure 7.3(a). Thermal degradation of the NP series, NPFp series and NFp series are better visualized in the DTG curves which are given in figures 7.1(b), 7.2(b) and 7.3(b), respectively. The thermal degradation parameters of the composites are presented in Table 7.1. Pure NR (NP0) degrades in single major step between 332 ^{0}C and 480 ^{0}C with a peak

maximum at 390 ^{0}C. In the case of NR/ PPy composites, NP2 shows an additional degradation with a peak maximum at 158 ^{0}C. This degradation peak is also seen in all NR/PPy composites and the intensity increases with increase in PPy content. This may due to the evolution of moisture and dopant from PPy. This peak is visible in NPFp series also. However, such a peak is not apparent in NFp series of composites. This is because the PPy content of the coated fibers is very low. Similar observations in the case of NR-polyaniline composites have been reported by Chandran AS [15].

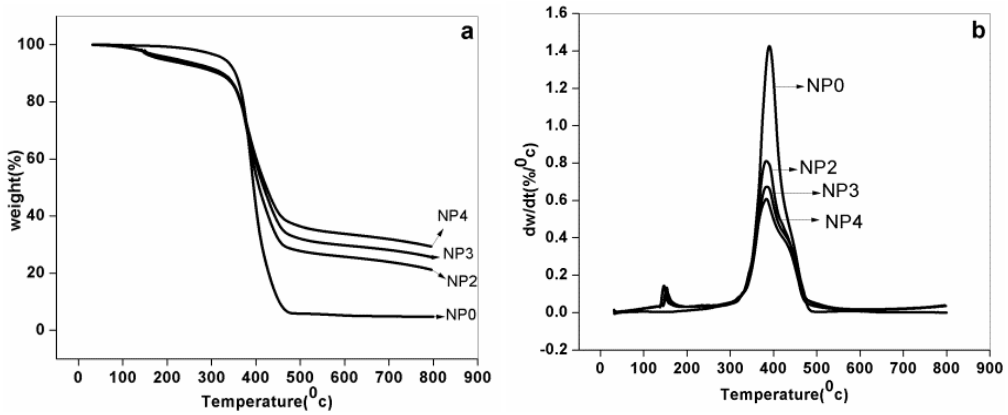

Fig. 7.1 (a) TG curves of NP series (b) DTG curves of NP series

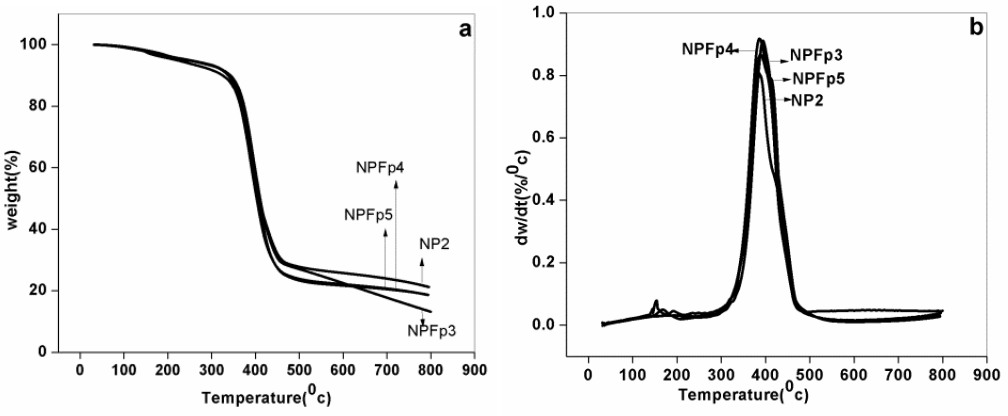

Fig. 7.2 (a) TG curves of NPFp series (b) DTG curves of NPFp series

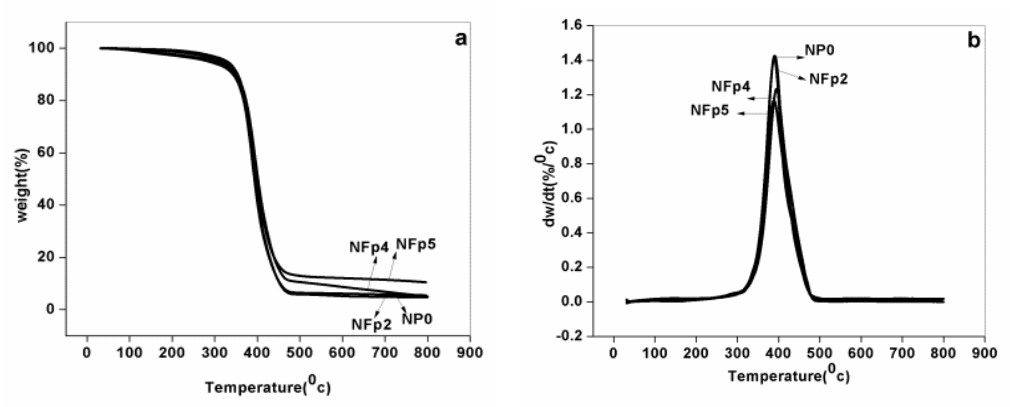

Fig. 7.3 (a) TG curves of NFp series (b) DTG curves of NFp series

It is found that PPy and F-PPy loadings do not alter the onset of degradation of NR except when the loading is very high . The temperature of maximum degradation remains almost the same. The peak degradation rate, i.e., the maximum rate of degradation recorded (at the peak degradation temperature) is less than that of NR gum compound for all the composites. Incorporation of PPy decreases the degradation rate significantly while F-PPy incorporation decreases the rate marginally. A lower rate of degradation indicates a better thermal stability.

The weight loss at peak degradation is reduced significantly in NR/PPy composites, compared to gum compound. Similar observation in the case of NR/polyaniline SIPN has been reported by John [14]. The temperature at which 50% weight loss occurs increases substantially in the presence of PPy. The effect of F-PPy is only marginal. The weight of residue at 300 ^{0}C decreases on adding 50 phr PPy to NR and this weight remains almost constant for other composites of NP series. This weight loss corresponds to PPy dopant evolution as discussed earlier. Addition of PPy coated fibers in the case of NPFp and NFp series does not cause significant fall in this weight as is

evident from the TG and DTG curves of these series. The residue weights at 600 ^{0}C and at 800 ^{0}C are more for NR/PPy systems compared to gum compound and NR/F-PPy systems. Aromatic compounds leave carbonaceous matter on charring. Hence, composites with higher PPy loadings gives rise to greater amounts of residue.

Table 7.1 Thermal characteristics of CECs based on NR

Thermal degradation parameters	Sample code									
	NP0	**NP2**	**NP3**	**NP4**	**NPFp3**	**NPFp4**	**NPFp5**	**NFp2**	**NFp4**	**NFp5**
Onset degradation temperature (^{0}C)	332	330	332	312	309	308	310	335	331	328
Peak degradation temperature (^{0}C)	390	387	385	389	390	392	393	392	394	393
Peak degradation rate (%/^{0}C)	1.42	0.81	0.67	0.60	0.92	0.91	0.86	1.40	1.22	1.16
Weight loss at peak degradation temperature (%)	90.9	63.0	57.9	53.9	63.0	68.5	68.8	90.1	83.3	78.6
Temperature at 50% weight loss (^{0}C)	394.9	410.8	419.2	428.1	407.3	408.8	411.7	396.3	397.4	401.2
Weight remaining at 300^{0}C (%)	96.8	91.9	91	91	93	93.5	93.5	96.2	95	94.5
Weight remaining at 600^{0}C (%)	5.1	25.8	29.8	33.6	22.3	22.2	21.7	5.8	8.6	12.0
Residue at 800^{0}C(%)	4.72	15.5	20.6	24.3	8.24	13.9	14.5	5.1	5.0	8.4

The kinetics of degradation reaction was studied by using Coats and Redfern method [16]. The Coats and Redfern method is correlative to the thermogravimetric function g(α). In the Coats and Redfern method activation energy is obtained from the equation:

$$\ln [1-(1-\alpha)^{1-n} / T^2(1-n)] = \ln [(AR/\beta E (1-2RT/E_a)] - E_a/2.303RT \quad \text{----(7.1)}$$

where 'α' is the decomposed fraction at any temperature, 'n' is the order of the reaction, 'T' is absolute temperature, 'A' is the Arrhenius constant, 'R' is the universal gas constant, 'E_a' is the activation energy and 'β' is the heating rate.

Equation (7.1) can be reduced to

$$\ln [g(\alpha)/T^2] = \ln [(AR/\beta E (1-2RT/E_a)] - E_a / 2.303RT \quad \text{----------(7.2)}$$

where, $g(\alpha) = [1-(1-\alpha)^{1-n} / (1-n)]$ ----------(7.3)

α, the decomposed fraction is given as:

$$\alpha = C_i - C/C_i - C_f \quad \text{----------(7.4)}$$

where 'C' is the weight at the temperature chosen, 'C_i' is the weight at initial temperature and 'C_f' is the weight at final temperature. Plots of $\ln [g(\alpha)/T^2]$ against the reciprocal of absolute temperature (1/T) can be drawn for different values of n. Order of the thermal decomposition reaction is the value of n that gives best linear fit to the kinetic curve: ie, one with maximum correlation coefficient. From the slope (–E/2.303RT) of the straight line drawn with this value of n, the activation energy can be calculated.

The Coats and Redfern equation (equation 7.2) for different values of n were applied for the CECs of NP, NPFp and NFp series. Best linear fit is

obtained for n=1. The plots of ln [g(α)/T^2] against 1/T taking n=1 are given in figs. 7.4, 7.5, 7.6 respectively for NP, NPFp and NFp series. The activation energies and correlation coefficients (R^2) obtained from the corresponding plots are presented in table 7.2. It may be concluded that the degradation reaction follows first order kinetics. The activation energies of the composites are found to be lower than that of NR gum vulcanizate.

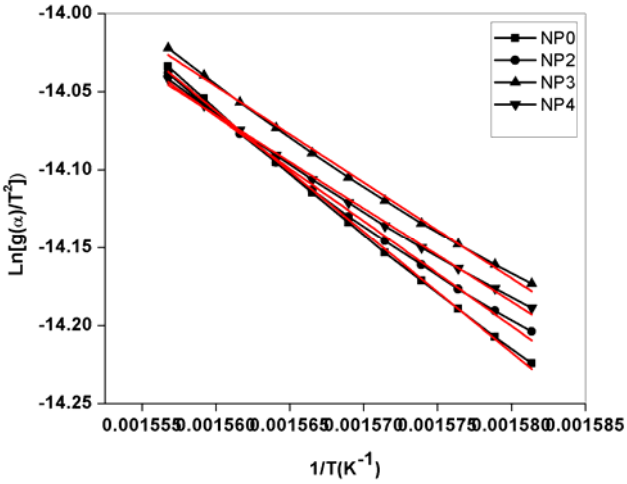

Fig. 7.4 Plots of Coats and Redfern equation for NP series

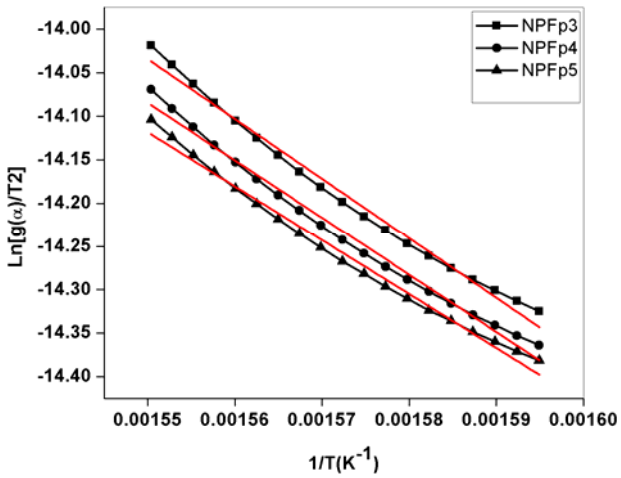

Fig. 7.5 Plots of Coats and Redfern equation for NPFp series

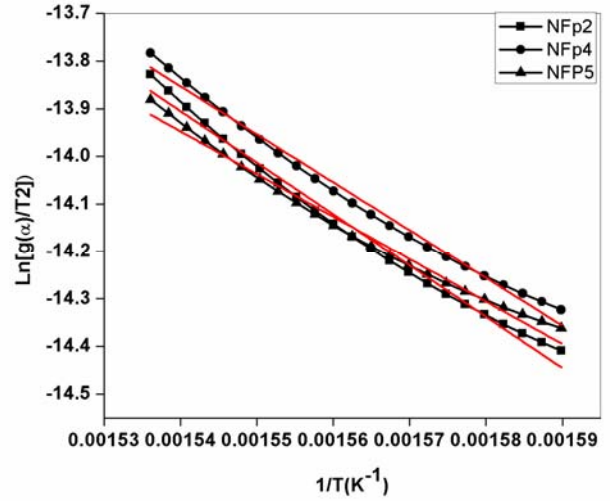

Fig. 7.6 Plots of Coats and Redfern equation for NFp series

Table 7.2 Thermal degradation kinetic parameters of CECs based on NR

Sample	R^2 (n=1)	E_a(kJ/mol)
NP0	0.998	64.3
NP2	0.996	55.9
NP3	0.997	51.1
NP4	0.997	49.7
NPFp3	0.989	57.1
NPFp4	0.989	54.9
NPFp5	0.989	51.7
NFp2	0.989	54.6
NFp4	0.989	54.8
NFP5	0.987	55.0

7.2.1.2 *NR based CECs prepared by in situ polymerization in NR latex*

Formulation of the mixes is given in table 5.1(chapter 5). The TG curves of the composites can be seen in Fig. 7.7(a) and 7.8(a) and the thermal characteristics are presented in Table 7.3. The onset of degradation shifts to higher temperatures on PPy addition for LNP series. In the case of LNPFp

series, the variation is not regular. The temperature of maximum degradation is more or less the same for the composites. The peak degradation rate (at the peak degradation temperature) is found to decrease with filler loading. The percentage weight loss at the peak degradation temperature decreases with filler loading. The temperature at which 50% weight lost is recorded increases for both series. The amount of material remaining at 300^0C is same for all the composites. The residue weight at 600^0C and at 800^0C increases with filler loading. Dependence of degradation of the composites on PPy loading and F-PPy loading is better visualized in the DTG curves (Fig. 7.7(b) and 7.8(b)).

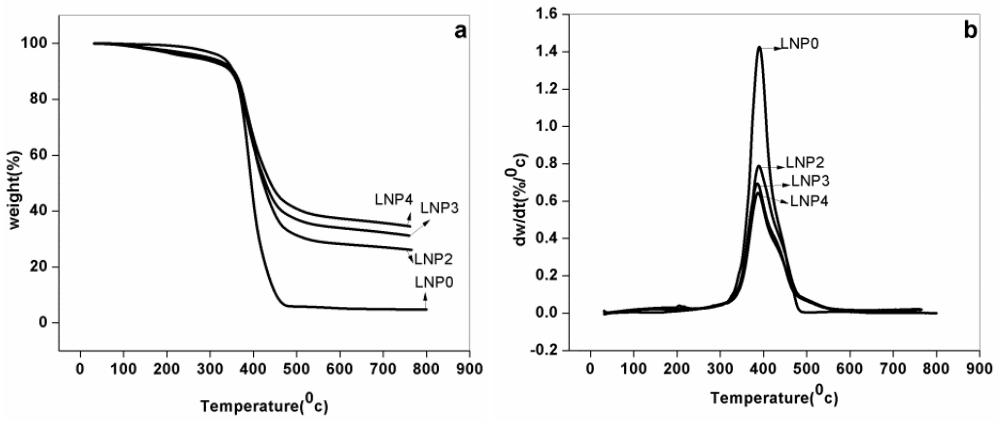

Fig. 7.7 (a) TG curves of LNP series (b) DTG curves of LNP series

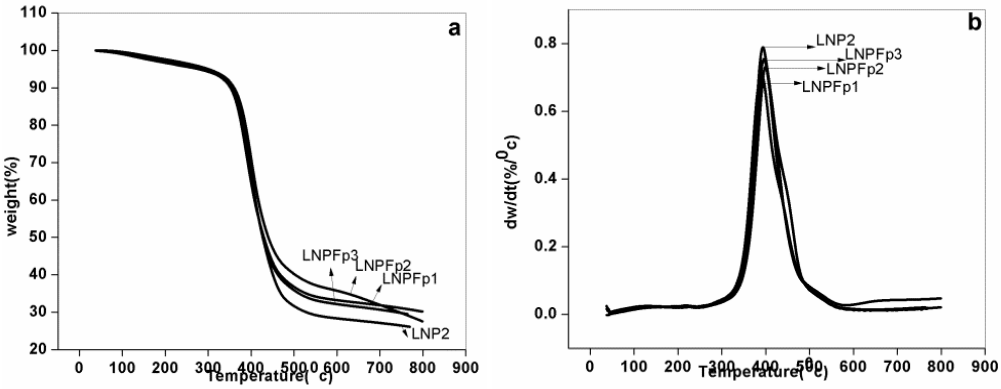

Fig. 7.8 (a) TG curves of LNPFp series (b) DTG curves of LNPFp series

Table 7.3 Thermal characteristics of the CECs prepared by in situ method

Thermal degradation parameters	Sample code						
	LNP0	**LNP2**	**LNP3**	**LNP4**	**LNPFp1**	**LNPFp2**	**LNPFp3**
Onset degradation temperature (^{0}C)	323	335	328	331	321	330	317
Peak degradation temperature (^{0}C)	390	387	388	389	389	391	393
Peak degradation rate of (%/^{0}C)	1.425	0.788	0.693	0.643	0.705	0.730	0.753
Weight loss at peak degradation temperature (%)	91	64	57	53	58	55	58
Temperature at 50% weight loss (^{0}C)	395	420	431	440	430	431	426
Weight remaining at 300^{0}C (%)	97	95	94	94	94	94	94
Weight remaining at 600^{0}C (%)	5	28	34	37	33	35	32
Residue at 800^{0}C(%)	5	26	30	34	30	27	29

The Coats and Redfern equation (equation 7.2) for different values of n were applied for the CECs of LNP and LNPFp series. Best linear fit is obtained for n=1. The plots of ln $[g(\alpha)/T^2]$ against 1/T taking n=1 are given in figs. 7.9 and 7.10 respectively for LNP and LNPFp series. The activation energies and correlation coefficients obtained from the corresponding plots are presented in table 7.4. The degradation reaction follows first order kinetics. The activation energies of the composites are found to be lower than that of the gum vulcanizate.

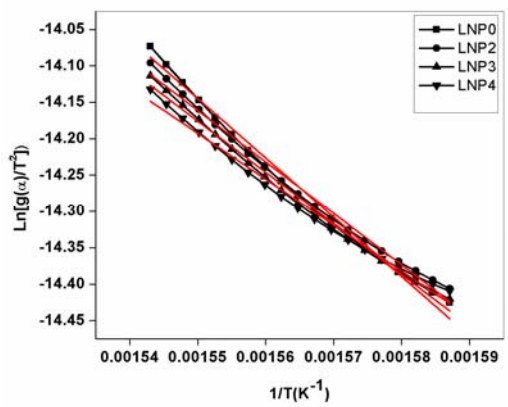

Fig. 7.9 Plots of Coats and Redfern equation for LNP series

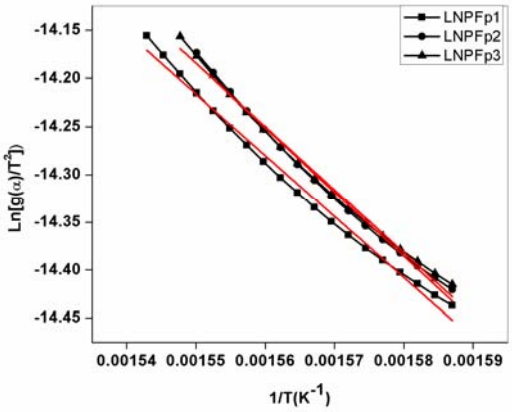

Fig. 7.10 Plots of Coats and Redfern equation for LNPFp series

Table 7.4 Thermal degradation kinetic parameters of CECs prepared by in situ method

Sample	R^2 (n=1)	E_a(kJ/mol)
LNP0	0.989	67.8
LNP2	0.990	58.7
LNP3	0.992	58.4
LNP4	0.988	52.4
LNPFp1	0.993	55.7
LNPFp2	0.993	54.8
LNPFp3	0.991	53.0

7.2.1.3 *NBR based CECs*

Formulation of the composites is given in table 6.1(chapter 6). The thermal mass loss traces obtained from the TG analysis of pure BP0, BP2 and BP3 are reported in figure 7.11 (a). The TG curves of BP0, BFp2 and BFp4 are presented in figure 7.12 (a). Dependence of degradation of the composites on PPy loading and F-PPy loading are better visualized in the DTG curves (figure 7.11 (b) and figure 7.12 (b)). The thermal characteristics of the composites are presented in Table 7.5.

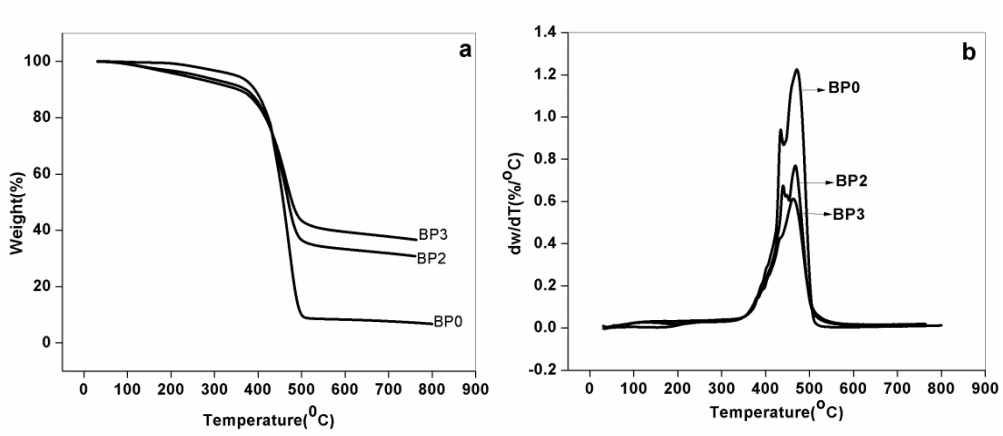

Fig. 7.11 (a) TG curves of BP series (b) DTG curves of BP series

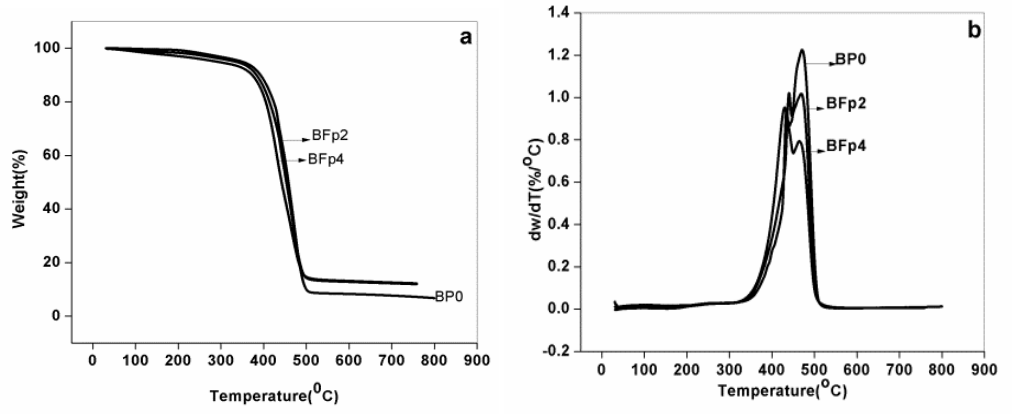

Fig. 7.12 (a) TG curves of BFp series (b) DTG curves of BFp series

Table 7.5 Thermal characteristics of CECs based on NBR

Thermal degradation parameters	Sample code				
	BP0	**BP2**	**BP3**	**BFp2**	**BFp4**
Onset degradation temperature (^{0}C)	337	351	348	336	339
Peak degradation temperature (^{0}C)	1st 434 2nd 476	1st 440 2nd 469	1st 430 2nd 464	1st 443 2nd 474	1st 434 2nd 470
Peak degradation rate of 2nd peak (%/^{0}C)	1.181	0.767	0.608	1.016	0.792
Weight loss at peak degradation temperature (%)	88.2	59.4	51.9	83.1	81.4
Temperature at 50% weight loss (^{0}C)	458	470	477	457	446
Weight remaining at 300^{0}C (%)	96.8	93.6	92.4	96.2	94.9
Weight remaining at 600^{0}C (%)	8.3	33.3	39.4	12.8	13.1
Residue at 800^{0}C(%)	6.8	30.8	36.6	11.9	12.2

TG analysis of composites shows that the onset of degradation shifts to higher temperatures on adding PPy to NBR. No such change is observed with the addition of F-PPy. First degradation occurs in the range 430 ^{0}C – 440 ^{0}C for all composites. The temperature at which the second degradation occurs decreases with loading for BP series while it remains almost constant in the case of BFp series. The peak degradation rate, i.e.,the maximum rate of degradation recorded (at the peak degradation temperature) decreases with filler loading for both series. This is better understood from the DTG plots. Table 7.5 shows that this decrease is more pronounced in the case of BP series, compared to BFp series. The same trend is observed for weight loss at peak degradation temperature. The sharp decrease in this weight loss on PPy loading compared to F-PPy loading is attributed to high thermal stability of PPy. The temperature corresponding to 50% weight loss increases for BP series while it remains almost same for BFp series. An increased weight loss is observed at 300 ^{0}C for BP series compared to BFp series. This is due to a weight loss occurring in pure

PPy between 67 ^{0}C and 140 ^{0}C (fig.3.5- chapter 3). Such a weight loss is not expected in the case of BFp series since PPy content, coated on fibers is very low. The weight remaining at 600 ^{0}C and 800 ^{0}C are much higher for PPy loaded samples. All these results ascertain that the thermal stability of the NBR based composites increases steadily with PPy and F-PPy loading. According to Gilman [17] improvement in thermal stability of polymers in presence of fillers is due to the hindered thermal motion of polymer molecular chain.

The Coats and Redfern equation (equation 7.2) for different values of n were applied for the CECs of BP and BFp series. Best linear fit is obtained when n=1. The plots of ln [$g(\alpha)/T^2$] against 1/T taking n=1 are given in figs. 7.13 and 7.14 respectively for BP and BFp series. The activation energies and correlation coefficients obtained from the corresponding plots are presented in table 7.6. It may be concluded that the degradation reaction follows first order kinetics. The activation energies of the composites are found to be lower than that of the gum compound.

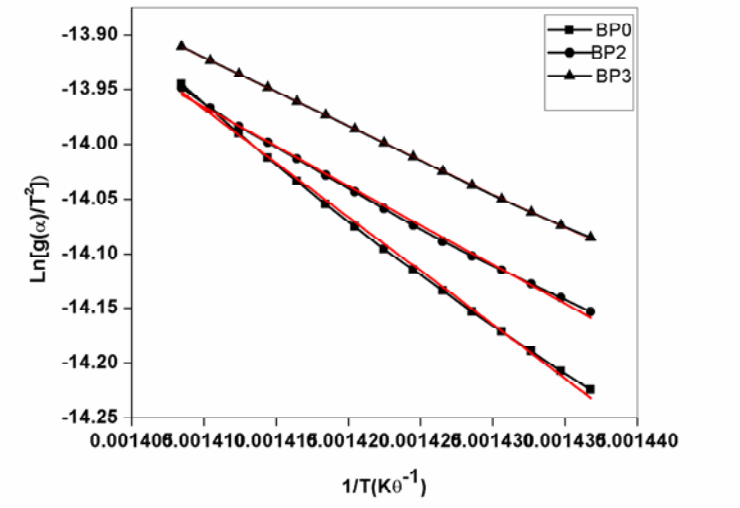

Fig. 7.13 Plots of Coats and Redfern equation for BP series

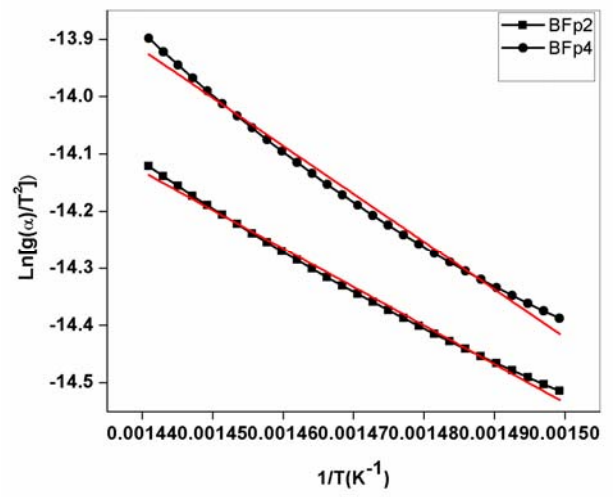

Fig. 7.14 Plots of Coats and Redfern equation for BFp series

Table 7.6 Thermal degradation kinetic parameters of CECs based on NBR

Sample	R^2 (n=1)	E_a(kJ/mol)
BP0	0.996	81.8
BP2	0.997	59.8
BP3	0.999	51.4
BFp2	0.995	56.0
BFp4	0.991	69.6

7.2.2 Differential scanning calorimetric analysis

DSC makes it possible to characterize the physical changes of states in the sample, in particular the glass transition. DSC thermograms of CECs of PPy and PPy coated short Nylon fibers based on NR prepared by dry rubber compounding and *in situ* polymerization in latex are given in figs. 7.15 and 7.16 respectively. Fig. 7.17 represents DSC curves of NBR/PPy and NBR/ PPy/F-PPy composites. The tables 7.7, 7.8 and 7.9 show that there isn't much variation in Tg of the elastomer by the incorporation of PPy or PPy coated fiber, which means that the PPy and F-PPy particles do not interact or only

weakly interact with the chain segments of the macromolecules in the elastomer matrix. This observation is supported by DSC studies of PPy-PMMA composites by Achour and co-workers [18].

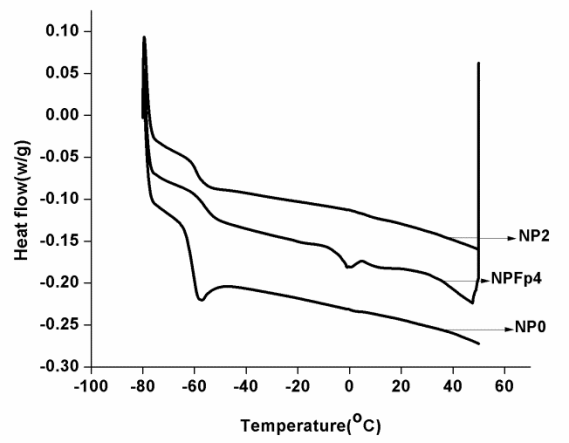

Fig. 7.15 DSC curves of CECs based on NR

Table 7.7 Tg values of CECs based on NR

Sample	Tg(^{0}C)
NP0	–60.9
NP2	–56.3
NPFp4	–59.6

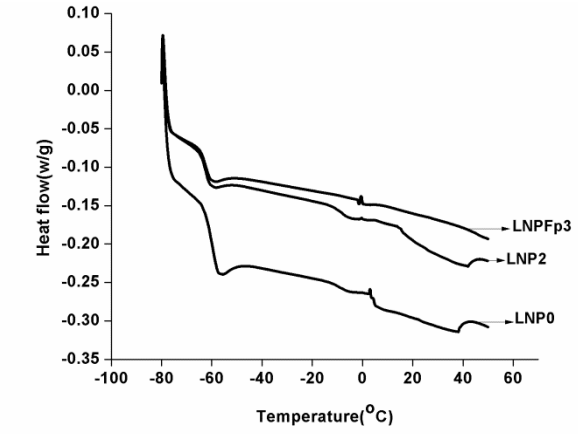

Fig. 7.16 DSC curves of NR based CECs prepared by in situ method

Table 7.8 Tg of NR based CECs prepared by in situ method

Sample	Tg(^{0}C)
LNP0	–59.6
LNP2	–62
LNPFp3	–63

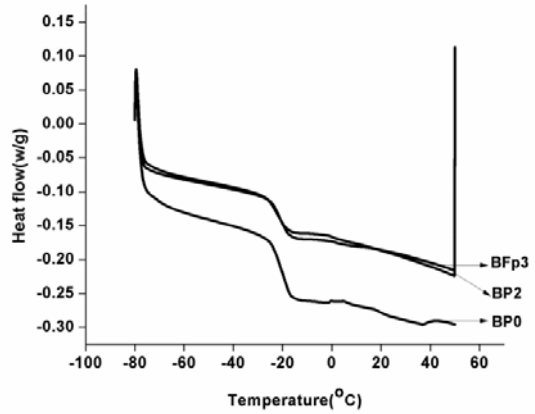

Fig. 7.17 DSC curves of CECs based on NBR

Table 7.9 Tg values of CECs based on NBR

Sample	Tg(^{0}C)
BP0	–19.4
BP2	–21.1
BFp3	–23.3

7.3 Conclusions

Thermal stabilities of the conducting elastomer composites based on NR and NBR prepared by conventional mixing and by *in situ* polymerization in NR latex were studied using thermogravimetric analysis. It is found that PPy and PPy coated fiber (F-PPy) do not alter the onset of degradation of NR at lower loadings when the composites are prepared by conventional mixing. In the case of NR/PPy systems prepared by in -situ polymerization in latex, the

degradation starts at higher temperature. Considering NBR based composites, the onset of degradation is delayed with the addition of PPy while no such change is observed with F-PPy. The peak degradation rate, i.e., the maximum rate of degradation decrease with filler loading for all the series of composites prepared. The thermal stability of elastomers is affected to a greater extent by PPy loading compared to fiber loading. PPy loading is found to improve the thermal stability of NBR more, compared to NR. The thermal degradation kinetics was studied by Coats and Redfern method. It is seen that the degradation reactions follow first order kinetics. The activation energies of thermal degradation reaction were estimated. Tg of the gum vulcanizates and the CECs were determined by DSC analysis. Incorporation of PPy and PPy coated fiber does not seem to affect the Tg of the elasomer considerably.

References

[1] Park S, Kim H. *J Polym Sci, Part B: Polym Phys*. **2001**, 39,121.

[2] Kutty SKN, Chaki TK, Nando GB. *Polym Degradation Stab.* **1992**, 38, 187.

[3] Younan AF, Ismail MN, Khalaf AI. *Polym Degradation Stab*. **1995**, 48, 103.

[4] Suhara F, Kutty SKN, Nando GB. *Polym Degradation Stab*. **1998**, 61, 9.

[5] Rajeev RS, De SK, Bhowmick AK, John B. *Polym Degradation Stab*. **2003**, 79, 449.

[6] Xiang XJ, Qian JW, yang WG, fang MH, Qian XQ. *J Appl Polym Sci*. **2006**, 100, 4333.

[7] Mahaling RN, Kumar S, Rath T, Das CK. *J Elastomers Plast*. **2007**, 39, 253.

[8] Reddy CS, Das CK. *Compos Interfaces*. **2005**, 11, 667.

[9] Mahaling RN, Das CK. *Compos Interfaces*. **2005**, 11, 701.

[10] Ran Q, Hua H, Tian Y, Wu S, Shan J. *Polym Compos*. **2008**, 14, 301.

[11] Zoppi RA, De Poli M. *Polymer*. **1996**, 37, 1999.

[12] Smirnov MA, Kuryndin IS, Nikitin LN, Sidorovich AV, Yu N, Sazanov OV, Kudasheva V, Bukosek AR, Khokhlov, Elyashevich GK. *Russ J Appl Chem*. **2005**, 78, 1993

[13] Gu Z, Zhang L, Li C. *J Macromol Sci, Part B*. 2009, 48,1093 .

[14] John H. *Ph. D. Thesis, Cochin University of Science and Technology, India,* **2003**.

[15] Chandran AS. *Ph. D Thesis, Cochin University of Science and Technology, India.* **2008**

[16] Coats AW, Redfern JP. *Nature*, **1964**, 201, 68.

[17] Gilman JW. *Applied Clay Science*. **1999**, 15, 31.

[18] Achour ME, Droussi A, Zoulef S, Gmati F, Fattoum A, Mohamed BA, Zangar H. *Spectrosc Lett*. **2008**, 41, 299.

Chapter

8

DIELECTRIC PROPERTIES OF THE CONDUCTING ELASTOMER COMPOSITES

Contents

Dielectric properties of PPy and its elastomer composites based on NR,NBR and that prepared by insitu polymerization in NR latex were studied in the frequency range 20Hz to 2 MHz using an impedance analyzer. Dielectric constant of the CECs decreased with increasing frequency owing to a decrease in interfacial polarization and increased with PPy and F-PPy loading due to an increase in interfacial polarization. Variation pattern of dielectric loss of composites with frequency suggested that both DC conductivity and interfacial polarization processes contributed towards dielectric loss. AC conductivity of PPy and its composites increased with frequency and the mechanism of conduction was mainly due to hopping of charge carriers. Frequency dependence of AC conductivity could be explained with the help of Maxwell–Wagner two-layer model. A maximum conductivity of 22.9 S/m at 1 MHz was recorded for the CEC, LNPFp3. Among all the CECs prepared those prepared by in situ polymerization in NR latex exhibied the best dielectric properties.

8.1 Introduction

Studying the dielectric properties (dielectric function, AC conductivity, and loss tangent) of a material may be useful in applications in the field of capacitor manufacture, besides it may lead to a better clarification of conduction or charge transport mechanism. Evaluation of magnetic and dielectric properties of the composites and correlation of results may help in tailoring composites for electronic and electrical applications such as electrostatic charge dissipation (ESD), touch control switches, electromagnetic interference (EMI) shielding, pressure sensor etc. [1-3]. Evaluation of A.C. electrical conductivity reveals a wealth of information on the usefulness of these materials for various applications. Moreover the study of A.C. electrical conductivity sheds light on the behaviour of charge carriers under an A.C. field, their mobility and the mechanism of conduction [4-6]. Synthesis of materials with high dielectric constant is very useful in integrated electronic circuits such as capacitor and for development of new generation dynamic random access memories and micro-electromechanical systems. Recent applications in the area of industrial microwave processing of food, rubber, plastic and ceramics have also been found to benefit from knowledge of dielectric properties. Accurate measurements of these properties will provide scientists and engineers with valuable information. This information when properly incorporated and correlated can pave way for intended applications or monitor a manufacturing process for improved quality control. A measurement of dielectric parameters can provide initial design parameters for many electronic applications. With this, one can relate the loss of a cable insulator, the impedance of a substrate or the frequency of a dielectric resonator with the dielectric properties. These properties are not constant; they can change with

the method of preparation, conductivity, molecular structure, particle size and crystal structure. They also depend on external factors such as frequency of the applied voltage, temperature, pressure and humidity [7].

The utmost dielectric property of importance to physicists and engineers is the permittivity. High dielectric constant materials with sufficient mechanical strength and ease of processing are required for development of electronic devices working at high operating frequencies such as fast computers, cellular phones etc. and for making embedded capacitors for integrated electronic devices. The unique combination of dielectric and mechanical properties is hard to achieve in a one component material. Pure polymers are easy to process into mechanically robust components but generally suffer from low dielectric constants [8]. On the other hand, typical high dielectric constant materials like ferroelectric ceramics, are brittle and requires high temperature processing, which is often not compatible with current circuits integration technologies [9]. The solution would be designing a high dielectric constant material that is mechanically robust and processable at ambient temperatures. This has led to development of hybrid materials such as polymer/ceramic composites. The high dielectric constant ceramics employed in these composites are niobates, titanates, zirconia, tantalum oxide, aluminium oxide, silicon carbide, simple ferrites like barium ferrite,mixed ferrites like nickel-zinc ferrite etc. The incorporation of hard ferrites into rubber matrices produces rubber ferrite composites (RFCs) [10] which are increasingly used as flexible permanent magnets, microwave absorbers and in other devices where flexibility and mouldability is an important criterion. Studies relating the dielectric properties of RFCs have extensively been carried

out [11-13]. The adhesion between these ceramics and polymer matrix is poor especially when ceramics loading is high [14].

Conducting polymer/ metal oxide and conducting polymer/polymer composites have been extensively investigated in the last decades in electronics industry. Tremendous efforts have been made to enhance the processibility and functionality of conducting polymers by making their composites or blends with inorganic materials, conducting and non-conducting polymers etc. in the last few years [15-17]. Among the conjugated polymers, polypyrrole (PPy) has emerged as one of the most promising conductive polymer because of its high electrical conductivity, good stability, ease of synthesis, good redox reversibility, and excellent microwave absorbing characteristics. Hence, it is being widely used as the package of electrical devices for the purpose of static charge dissipation [18-20]. Recently, appreciable enhancement in electrical conductivity, thermal stability and processibility have been reported in organic–inorganic hybrid nano composites of PPy with metal oxides like SiO2 [21], ZrO2 [22], Fe2O3 [23], Y2O3 [24], Al2O3 [25], TiO2 [26]etc. and with metal sulphides [27]. These composites act as potential cathode materials for rechargeable lithium batteries and in electrochromic displays. In addition, these conducting polymers are known to increase conductivity after polymerization in the presence of the commonly highly resistive oxide or sulfide and improve the redox capacity of the battery [28]. Studies on polypyrrole- lead titanate composites by Basavaraja *et al*. [29] indicated an increase in electrical properties compared to pure PPy which was attributed to increase in orderness. They report that this may be due to the occurrence of packing density and maximum space charge (Maxwell Wagner) polarization.

Saafan *et al*.[30] prepared polypyrrole samples by a chemical method using two different oxidizing agents, ferric chloride and potassium persulphate, in different concentrations and transformed to a dielectric state by heating. Then the frequency and temperature dependence of the dielectric constant, loss tangent and AC conductivity were investigated using a complex impedance technique. It had been found that the concentrations of the reactants used in the preparation have a noticeable effect on the dielectric properties. Sing et al. [31] had investigated the AC conduction in lightly doped polypyrrole films in the frequency range 100 Hz-10 MHz and in the temperature range 77-350 K. They observed that in high-temperature region the frequency dependence becomes weak at low frequencies but remains strongly frequency dependent at high frequencies. The weak frequency dependence was attributed to the contribution of DC conductivity to the measured AC conductivity. Harun *et al*.[32] synthesized poly(vinyl alcohol)/ polypyrrole composite films by chemical oxidative polymerization using $FeCl_3$ at different concentrations as dopant and oxidant and the dielectric properties were measured in the frequency range 20Hz to 1 MHz. The results showed that the dielectric properties varied with the concentration of $FeCl_3$ dopant. Polyurethane based polypyrrole composites with enhanced dielectric properties for smart textile applications were prepared by solvent casting from dimethyl formamide solutions of polyurethane-polypyrrole [33]. Dielectric study indicated that 20% weight pyrrole increases dielectric constant above 7000. Cetiner and co-workers[34] fabricated polypyrrole poly(acrylonitrile-co-vinyl acetate) composite film and the dielectric studies were carried out in a frequency range starting from 0.05 Hz to10 MHz. They found that the real and imaginary parts of the permittivity and AC conductivity of polypyrrole poly (acrylonitrile-co-vinyl acetate) composite film were considerably higher than PPy- polyacrylonitrile and poly (acrylonitrile-

co-vinyl acetate). The AC conductivity of polypyrrole- poly (methylmethacrylate) composites was studied in the frequency range of 600 Hz to 1 MHz and temperature interval 23°C to 110°C by Achour and co-workers [35]. The study highlighted three domains: at low frequencies the conductivity is independent of frequency; at intermediate frequencies, the AC conductivity followed a power law in frequency; and at high frequency the AC conductivity could be explained in terms of hopping process.

However, a survey of literature reveals that the dielectric studies on PPy incorporated elastomer composites are rather scarce. Elastomer composites are important in that they are suitable for devices where flexibility is an important parameter and these composites can be moulded into complex shapes. Dielectric spectroscopy has been found to be a valuable experimental tool for understanding the phenomenon of charge transport in conducting polymers. Low frequency conductivity and dielectric relaxation measurements especially have proven to be valuable in giving additional information on the conducting mechanism that DC conductivity measurement alone does not provide.

The aim of this part of the thesis is to analyze dielectric permittivity, dielectric loss and AC conductivity of the polypyrrole and its elastomer composites based on NR and NBR. These properties as mentioned earlier are very much dependent on the microstructure, nature of dopant used, type of matrix and the processing variables. Therefore the study of the dielectric properties of polypyrrole and its composites assume significance. A better understanding of the mechanism of conduction processes and other electrical properties may be very useful in improving the stability characteristics of these materials which are the key factors in the device performance.

8.2 Experimental

Dielectric constant or relative permittivity of a material is the ratio of the amount of electrical energy stored in a material by an applied voltage, relative to that stored in a vacuum. Similarly, it is also the ratio of the capacitance of a capacitor using that material as a dielectric, compared to a similar capacitor which has a vacuum as its dielectric.

$$\varepsilon_r = \varepsilon / \varepsilon_0 \quad \text{----------} \quad (8.1)$$

ε_r = relative permittivity

ε = complex frequency dependent absolute permittivity of material or permittivity of medium

ε_0 = electric constant or Permittivity of free space

$$\varepsilon = \varepsilon_r \varepsilon_0 \quad \text{----------} \quad (8.2)$$

An electrical conductor charged with a quantity of electricity 'q' at a potential 'V' is said to have a capacity C= q/ V. The capacity of a sample parallel plate capacitor is given by:

$$C = \varepsilon A / d \quad \text{----------} \quad (8.3)$$

'A' is the area of the parallel plates, 'd' is the separation between the plates Substituting eq.8.2 in eq. 8.3,

$$C = \varepsilon_r \varepsilon_0 A / d \quad \text{----------} \quad (8.4)$$

$$\varepsilon_r = Cd / \varepsilon_0 A \quad \text{----------} \quad (8.5)$$

Thus the relative permittivity (dielectric constant) of sample can be calculated if the capacitance , area and thickness of the samples are known.

When the sinusoidal electric field of frequency 'f' is applied to a dielectric, some of the bound charges will move with the applied field and contribute to permittivity, ε' while another set of bound charges will oscillate out of phase with the applied field with a phase shift angle 'δ' resulting in energy dissipation and contribute to the dielectric loss factor, ε".

Therefore absolute permittivity can be decomposed into in to real and imaginary parts

$$\varepsilon = \varepsilon' - i\,\varepsilon'' \quad \text{----------} \quad (8.6)$$

ε' is the real part of the permittivity, which is related to the stored energy within the medium.

ε" is the imaginary part of the permittivity, which is related to the dissipation (or loss) of energy within the medium(loss factor.)

The dielectric loss can also be expressed as tangent of phase shift angle, 'δ', where δ is called as the "loss angle" denoting the angle between the voltage and the charging current.

$$\tan\delta = \varepsilon''/\varepsilon' \quad \text{----------} \quad (8.7)$$

It is also known as dissipation factor and is a measure of the power dissipated.

The AC electrical conductivity can be calculated utilizing the dielectric parameters using the formula:

$$\sigma_{AC} = 2\pi f \tan\delta\, \varepsilon_r \varepsilon_0 \quad \text{----------} \quad (8.8)$$

The principle and theory underlying the evaluation of σ_{AC} from dielectric measurements is based on a treatment dealt by Goswamy [36].

The dielectric measurements were carried out at frequencies ranging from 20Hz to 2MHz using an Impedance analyzer, Agilent E 4980 A Precision LCR Meter (fig. 2.2). Disc shaped samples having diameter 12mm and thickness ≈ 2mm were used for the measurements. Dielectric constant (ε_r), Dielectric loss (ε'') and the AC conductivity (σ_{AC}) were obtained from the instrument. The results are directly read on the monitor and recorded on a computer data sheet file.

8.3 Results and discussion

8.3.1 Dielectric permittivity

8.3.1.1 *Frequency dependence of dielectric permittivity of pristine PPy and its CECs*

Dependence of dielectric constant as a function of frequency ranging from 20Hz to 1 MHz at room temperature for pure PPy is plotted in fig. 8.1. Dielectric constant of PPy shows a steep decrease from its initial higher values at low frequency and then it remains constant regardless of the applied frequency, especially above $\approx 10^3$ Hz. This is a normal behavior found in the case of PPy [37]. Maximum dielectric constant of 4.94×10^6 is shown at frequency 25Hz. Such large value of dielectric permittivity is not unusual and is related to effects of electrode polarization and space charge polarization [38].

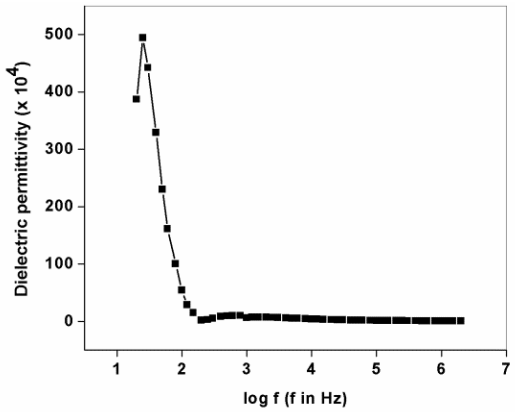

Fig. 8.1 Variation of dielectric permittivity of polypyrrole with frequency

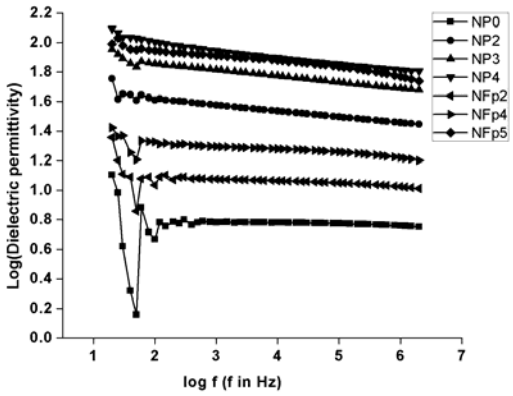

Fig. 8.2 Variation of dielectric permittivity of NR based CECs with frequency

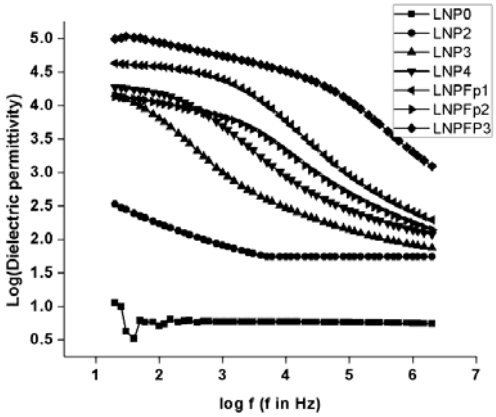

Fig. 8.3 Variation of dielectric permittivity of NR based CECs prepared by *in situ* polymerization with frequency

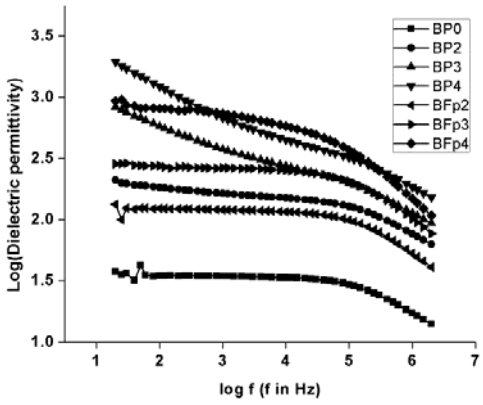

Fig. 8.4 Variation of dielectric permittivity of NBR based CECs with frequency

At 100 Hz the value decreases to 5.4×10^5 and becomes 5600 at 1MHz. At 100 Hz frequency, Vishnuvardhan*et al.*[37] have reported a dielectric constant of 25,900 for a polypyrrole sample prepared using $FeCl_3$ as oxidant. De *et al.* reports highest value of dielectric constant of ≈1000 for pure PPy [39]. The higher value obtained in the present case may be due to the difference in the microstructure and nature of dopant used as discussed in section 8.1. Studies of dielectric properties of PPy prepared using two different oxidizing agents by Saafan *et al*. [30] show that the nature and concentration of oxidant used highly influence the magnitude of dielectric permittivity of resulting PPy. PPy exhibits large value of **ε'** at lower frequencies while the value of **ε'** decreases at higher frequencies. As reported by other authors, the strong low frequency dispersion of permittivity is a characteristic of charged carrier systems [40]. It is known that dielectric response of solids is complex function of frequency, temperature and type of solids [41]. At low frequencies, all polarization mechanisms which include the interfacial (space charge), dipolar, ionic and electronic can follow the applied electric field. In this case, the highest value of **ε'** is obtained. These different polarization mechanisms have different relaxation frequencies. Dipolar and interfacial polarizations occurring at lower frequencies are especially important because they can greatly affect the capacitive and insulative properties [42]. At high frequencies, the electric field changes too fast for all the polarization effects to appear and they start dropping out. In this case, lowest value of **ε'** is obtained [43, 44]. Here, for PPy also the decrease in ε' at higher frequencies is attributed to the dropping out of dipolar and interfacial polarization components to ε' since it cannot follow the applied field. At lower frequencies, the dipole can respond rapidly to follow the field and dipole contribution has

its maximum value. At higher frequencies dipole polarizability will be minimum, as the field cannot induce the dipole moment, so dielectric permittivity values attains minimum. In addition to dipole contribution, space charge polarization also contributes to ε' of PPy at lower frequencies. This kind of behavior can be explained on the basis of Maxwell-wagner theory of interfacial polymerization. This interfacial polarization occurs in heterogeneous structures due to the accumulation of charges at the interfaces between various regions that differ from each other in its DC conductivity [42]. In heterogenous systems, the interfacial polarization is caused by the dispersion of islands of conductive regions in the polymer within an insulating matrix as previously stated by Rocha *et al*. [44]. It seems that PPy is a homogeneous dielectric material. The dielectric properties of PPy are influenced by various factors like method of preparation, chemical composition and grain size. Depending upon the synthesis conditions, it is possible for the formation of films of high resistivity over the constituent grains. Such materials in which the individual grains are separated either by air gaps or by low conducting layers behave as an inhomogeneous dielectric material. In this situation, the high values of ε' at low frequencies are due to interfacial polarization i.e., the building up of bound charges at interfaces within the bulk samples. Moreover, there is accumulation of bound charges at the interfaces between the sample and the electrodes that adds to the net polarization (electrode polarization). This space charge accumulation introduces an extra capacitive component into the system [45]. In addition to these factors, it is known that at low frequencies, the side groups or small units of main chains may be able to move and follow the variation of the field and therefore may contribute to the polarization, while on increasing frequencies, those side groups or small units of main chains lose gradually their ability to follow the field and consequently their contribution to the polarization ceases [42].

Figures 8.2, 8.3 and 8.4 represent the variation of dielectric permittivity with frequency of the conducting elastomer composites (CECs) based on NR prepared by dry rubber compounding, those prepared by *in situ* polymerization in NR latex and CECs based on NBR, respectively. It can be seen that ε' of composites is many orders of magnitude smaller than that of pristine PPy and it also depends upon the type of matrix, composition etc.

Here also, ε' for all samples exhibits a relatively high value at low frequency and decreases with increasing frequency, or remains nearly same for a certain frequency range, again depending upon the matrix forming the composite with PPy. At low frequencies, the dipole moments and charge carriers can freely move within the material under test and follow the varying electromagnetic field, while at higher frequencies dipole and charge carriers become unable to follow variations of the applied electric field resulting in a decrease in the dielectric constant. As our composite samples are heterogeneous consisting of conducting polymer in an insulating matrix, there is a difference in the dielectric constant and conductivity of filler and matrix which leads to the generation of some space charges at the heterogeneous interface leading to a field distortion. This distortion leads to interfacial polarization [46] which also contributes to ε'. Interfacial polarization has a lower relaxation frequency and therefore it decreases with increase of frequency and as a result, ε' also decreases with increase of frequency.

8.3.1.2 Loading dependence of dielectric permittivity of CECs of PPy

Variations of dielectric permittivity of conducting elastomer composites of PPy and PPy coated short Nylon fibers with NR and NBR with loading are shown in figs. 8.5 to 8.11. It is found that loading of elastomers with PPy (figs. 8.5, 8. 8

and 8.10) or PPy coated fiber (figs. 8.7 and 8.11) or with both PPy and coated fiber (figs. 8.6 and 8.9) increase the dielectric permittivity substantially compared to the gum vulcanizates. The increase is more pronounced at lower frequencies since there is a tendency for different polarization mechanisms to drop out with increasing frequencies as explained under section 8.3.1.1.

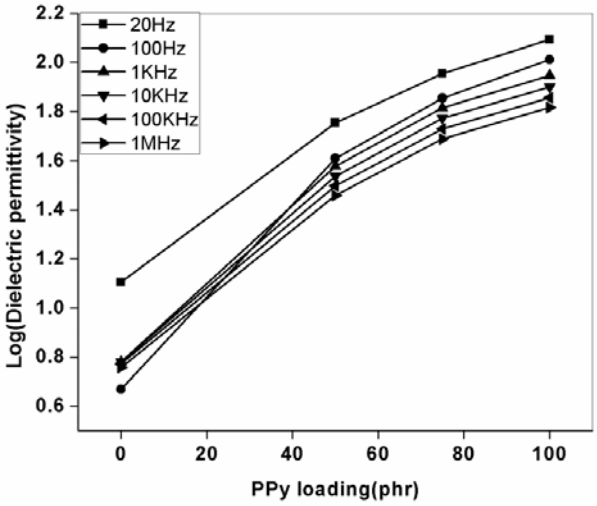

Fig. 8.5Variation of dielectric permittivity of NP series with loading

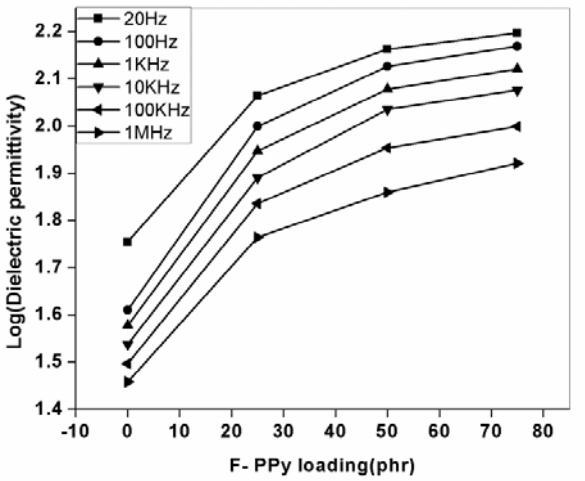

Fig. 8.6 Variation of dielectric permittivity of NPFp series with loading

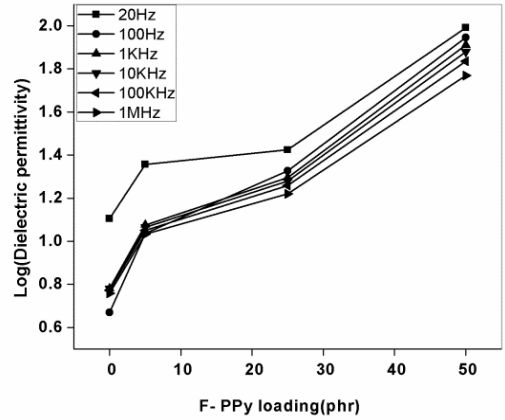

Fig. 8.7 Variation of dielectric permittivity of NFp series with loading

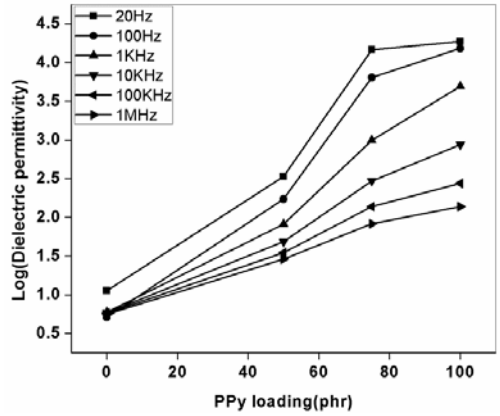

Fig. 8.8 Variation of dielectric permittivity of LNP series with loading

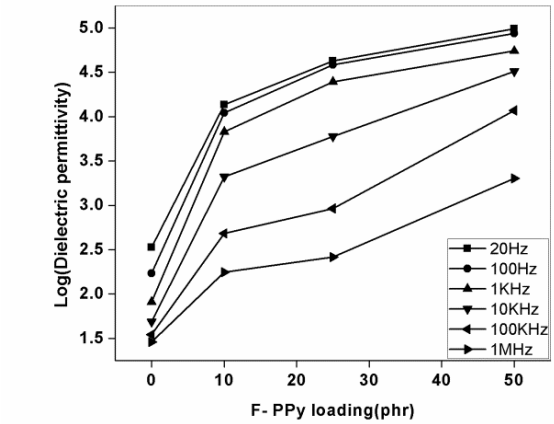

Fig. 8.9 Variation of dielectric permittivity of LNPFp series with loading

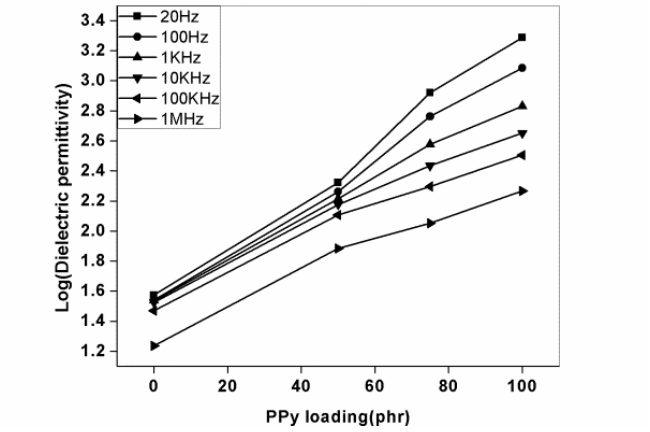

Fig. 8.10 Variation of dielectric permittivity of BP series with loading

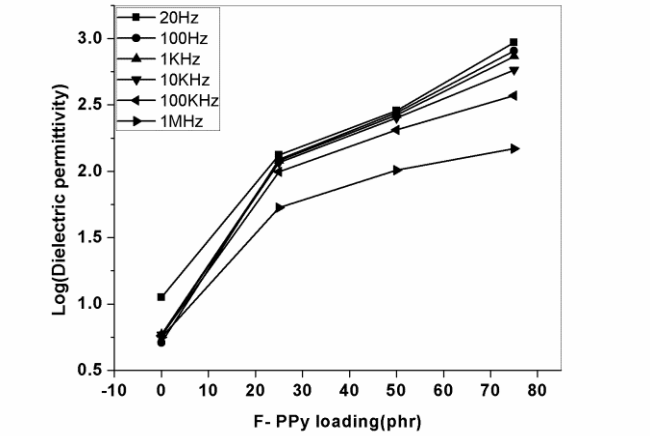

Fig. 8.11 Variation of dielectric permittivity of BFp series with loading

At any particular frequency, ε' increases with increase in loading. This is quite obvious as PPy is a polar material and increase in its concentration leads to increased dipole density or polarizability and hence dielectric constant. Another contribution to ε' with increased loading is increase in interfacial polarization (Maxwell-Wagner polarization). As polypyrrole content increases, packing density increases, interface between the PPy and matrix is more leading to maximum space charge polarization [47] contributing to highest dielectric behaviour. Large enhancement in ε' of composites in the low

frequency region occurs due to the Maxwell-Wagner polarization originating in the insulator-conductor interfaces [43,48,49]. Vishnuvardhan *et al*.[37] have described such a phenomenon in PPy/Y_2O_3 composites. Another reason for the increase in ε' of composite with addition of conductive particles, either PPy or F-PPy is the formation of mini-capacitor networks in the composites with increased filler loading [50].

Table 8.1 Dielectric constants of CECs of PPy

composite	Dielectric permittivity	
	at 20Hz	at 1MHz
NP0	12.7	5.7
NP2	56.8	28.7
NP3	90	48.8
NP4	124	65.5
NPFp3	115	58
NPFp4	145	72
NPFp5	157	83
NFp2	22.7	10.6
NFp4	26.5	16.6
NFp5	98	58.6
LNP0	11.2	5.6
LNP2	336	28.8
LNP3	1.4×10^4	82.9
LNP4	1.8×10^4	138
LNpFp1	1.3×10^4	261
LNPFp2	4.2×10^4	1700
LNPFp3	9.8×10^4	2000
BP0	37.4	17.2
BP2	209	76.5
BP3	832	112
BP4	1930	184
BFp2	132	53
BFp3	285	101
BFp4	933	148

The dielectric constants of NR and NBR gum vulcanizates and their CECs are presented in table 8.1. The dielectric constant of unvulcanized NR is reported to be in the range 2.6 to 3.04 [51] and a value of 4.3 (at 100kHz at 393K) is reported for NR gum vulcanizate [13]. A dielectric constant of 5.7 is obtained for NR gum vulcanizate at 1MHz frequency in the present study. It can be seen from table 8.1 that the ε' values of all the NR based composites exceed that of gum vulcanizate. Vulcanized NBR is reported to have a ε' value ≈ 15 at 1MHz frequency [52]. In the present case NBR gum vulcanizate is found to have ε' value 17.2 at 1MHz frequency. All the NBR based composites exhibit ε' value higher than this. Considering all the composites prepared, maximum dielectric permittivity is attained by LNPFp3(NR containing 50phr PPy and 50phr PPy coated fiber, prepared by *in situ* polymerization in NR latex). This sample has a permittivity value of 9.8×10^4 at 20Hz and 2000 at1MHz. This is quite remarkable compared to most of the polymers, conducting polymers, ceramics and their composites found in literature. Dielectric constants values ranging between 200-1000 have been reported for a PANI/polyvinyl alcohol composite by Dutta and co-workers [53] in the frequency range 1kHz - 5kHz. A dielectric constant of ≈ 1120 was obtained for a PANI/polyurethane blend which the authors [54] claim to have surpassed the highest value of ε' ever reported for the high dielectric constant polymer composites. Yanilmaz *et al*. [33] reported a dielectric constant of 7×10^4 at 10^{-2} Hz for a PPy/ polyurethane composite, which decreased to 10000 at 1Hz. PPy/ 50%Y_2O_3 composite [37] was found to exhibit a ε' value 28584 at 100Hz. Among NR based elastomeric composites, Soloman *et al* [13] reported that a 50 phr carbon black loaded NR/barium ferrite RFC showed a ε' value of 135 (at 100kHz at 393K). Chandran AS [55] prepared composites of PANI and

PANI coated short Nylon fiber with NR and chloroprene rubber (CR). The maximum ε' values obtained were 73 for NR/140phr PANI composite and 177 for CR/150phr PANI composite, both at 0.1MHz and 303K. The substantially high ε' values obtained in the present study makes the composites prepared applicable in capacitors, conductive paints, rechargeable batteries, sensors, actuators etc.

8.3.2 Dielectric Loss

8.3.2.1 Frequency dependence of dielectric loss of pristine PPy and its CECs

The variation of dielectric loss factor, ε", ie, the imaginary part of complex permittivity of pristine PPy with frequency is presented in fig. 8.12. It decreases steeply with frequency as in the case of dielectric permittivity (fig. 8.1) and reaches a constant value. Figs. 8.13 to 8.15 represent the variation of ε" with frequencies of the three types of conducting elastomer composites, viz. NR based prepared by dry rubber compounding, NR based prepared by *in situ* polymerization in NR latex and NBR based, respectively. Though the variation patterns are not exactly similar, a decreasing tendency for ε" with frequency is observed for the three systems.

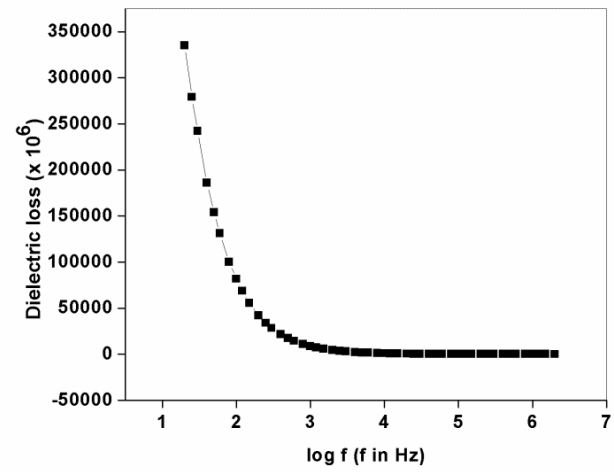

Fig. 8.12 Variation of dielectric loss of polypyrrole with frequency

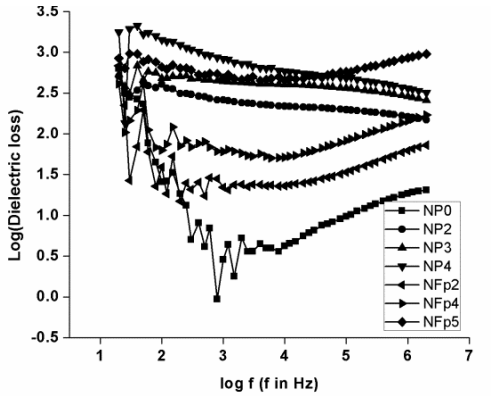

Fig. 8.13 Variation of dielectric loss of NR based CECs with frequency

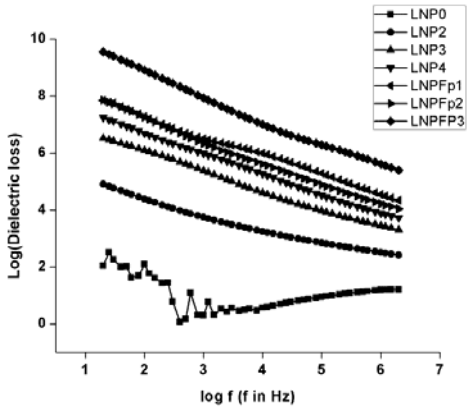

Fig. 8.14 Variation of dielectric loss of NR based CECs prepared by *in situ* polymerization with frequency

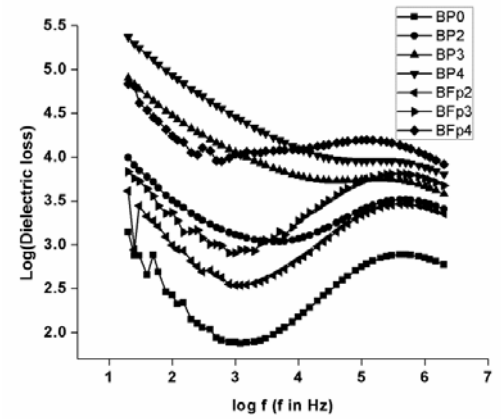

Fig. 8.15Variation of dielectric loss of NBR based CECs with frequency

ε" values of LNP and LNPFp series (fig. 8.14) show a regular decrease with increasing frequency. In fig. 8.13 some composites exhibit a gradual decrease while in some others ε" decrease first and then increases slowly. In the case of NBR based composites, the dielectric loss initially decreases then slowly increases and then remains almost constant. Such behaviour for NBR based composites has been reported [52]. As stated earlier the dielectric behavior of conducting composites depends upon the type of matrix, method of preparation, molecular structure, particle size and crystal structure. Dielectric loss arises due to the localized motion of the charge carriers. The highest dielectric loss observed for pure PPy is due to the free motion of the charge carriers. Decrease in ε" of PPy and its composites with frequency can be explained as follows: It is known that the doped PPy system contains two types of charged species, i.e. polaron/bipolaron system and bound charges (dipoles) [46]. The polaron/bipolaron system is mobile and free to move along the chain, while dipoles have only restricted mobility and account for strong polarization in the system. The decrease of ε"with frequency can be ascribed to the fact that at low frequencies, the value of ε" is due to the migration of ions in the material. At moderate frequencies, ε" is due to the contribution of ion jumps, conduction loss of ion's migration and ion's polarization loss. At high frequencies, the vibration of ions may be the only source of dielectric loss and so ε"has the minimum value [56].

Large values of ε" in lower frequency region may also be attributed to the interfacial polarization mechanism of the heterogeneous system. High values of ε"of the composites could be utilized for decoupling capacitor applications. The reduction in ε" with increase in frequency is also because of the induced charges gradually failing to follow the reversing field causing a

reduction in the electronic oscillations [43]. This phenomenon is a relaxation process due to Maxwell-Wagner interfacial polarization, which is revealed by a maximum of dielectric loss, but the maximum peaks of dielectric loss (relaxation peaks) are not observed in all the systems in the present study in the frequency range employed. It is believed that the ionic conduction in the low frequency region may mask any relaxation and these peaks are overlapped by DC conductivity contribution. A modulus representation of dielectric loss is usually used to clearly point out the loss peaks attributed to interfacial polarization relaxation process [57,40]. According Ravikiran *et al*. high dielectric loss at low frequency in all composites may also be attributed to DC conduction losses [58].

According to the dielectric physics theory, the dielectric loss represents the change of the energy which leads to the molecule relaxation polarization. When molecules are rubbed and impacted to each other by their re-orientation induced by an electric field, then relaxation appears. Dielectric loss must be the sum of the polarization loss and leak conductance loss when the leak conductance of the materials is considered:
The loss factor ε''_{obs} must be regarded as the sum of contributions of three distinct effects as [59]

$$\varepsilon''_{obs} = \varepsilon''_{DC} + \varepsilon''_{MW} + \varepsilon''_{D} \quad \text{---------- (8.9)}$$

where ε''_{DC} is due to DC conductance, ε''_{MW} is due to interfacial polarization and ε''_{D} is due to the the usual dipole orientation or Debye loss factor.

Different mathematical equations have been developed to distinguish between losses arising from different sources. These equations were developed

by considering the sample as parallel resistor-capacitor circuit [59-61]. The loss factor due to DC conductance is given by the equation [62]

$$\varepsilon''_{DC} = 1.8\times 10^{12}(G_{spe}) / f \quad \text{----------} (8.10)$$

where G_{spe} is the specific conductivity of the sample. The loss factor due to Maxwell Wagner interfacial polarization is given by [62]

$$\varepsilon''_{MW} = \varepsilon_{\infty} \ [1+K/1+\omega^2\tau^2] \quad \text{----------} (8.11)$$

where $\boldsymbol{\varepsilon}_{\infty}$ and K are calculated considering two different dielectric permittivity of the sample at the interfaces and τ is the relaxation time of the interfacial polarization, which is obtained by plotting the imaginary part of electric modulus (M") against log frequency. M" is given as [57]

$$M'' = \varepsilon''/(\varepsilon')^2+ (\varepsilon'')^2 \quad \text{----------} (8.12)$$

From this graph peak for angular frequency, ω_p is obtained and relaxation time is reciprocal of this value

$$\tau = 1/\omega_p \quad \text{----------} (8.13)$$

By expressing equations 8.10 and 8.11 in logarithm form and by plotting $\log\varepsilon''_{DC}$ and $\log \varepsilon''_{MW}$ vs. log frequency, two types of plots will be obtained. Log ε''_{DC} vs. log f will be a straight line and log ε''_{MW} vs. log f will be a sigmoidal curve.

Figures 8.12 to 8.15 representing variation of dielectric loss vs. log f can be analysed in the light of these findings. Linear decrease of ε''_{obs} with increase in frequency suggests that dielectric loss is due to DC conductivity

process, while interfacial polarization process is significant in the frequency range where a sigmoidal decrease in ε''_{obs} is observed.

8.3.2.2 Loading dependence of dielectric loss of CECs of PPy

Figures 8.16 to 8.22 show that dielectric loss increases with the addition of more and more PPy and PPy coated short Nylon fiber to NR and NBR matrix. This can be explained by considering the increase of mobility of charge carriers. Dielectric loss arises due to the localized motion of the charge carriers. Therefore increase in ε" with increased loading is due to increase of mobility of charge carriers. This increases DC conductivity and interfacial polarization, both of which contribute to increase in dielectric loss. A higher dielectric loss for a higher content of PPy and coated fiber can also be interpreted by an increase in crystallinity due to clustering of PPy particles in the polymer matrix [29]. This leads to increase in orderness and the increased interfacial interactions between PPy and the matrix resulting in maximum space charge polarization and increased loss. In the present study, maximum dielectric loss is exhibited by LNPFp3 (table 8.2) having a magnitude of 4.1×10^5 at 1MHz frequency. This is extremely high compared to the value corresponding to gum vulcanizate (15.26 at 1MHz). This sample is found to have high DC conductivity value compared to other CECs prepared (section 5.3.5). High values of ε" of the composites can be utilized for decoupling capacitor applications.

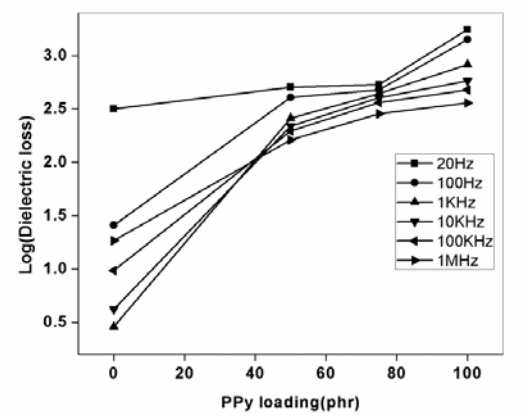

Fig. 8.16 Variation of dielectric loss of NP series with loading

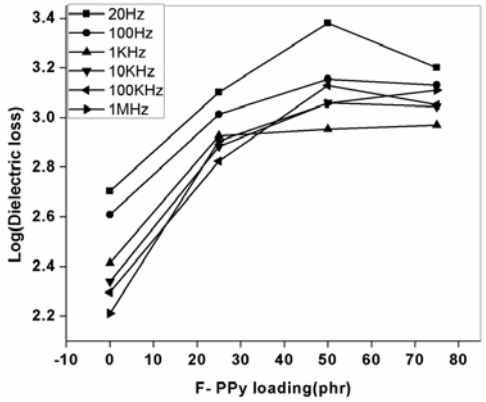

Fig. 8.17 Variation of dielectric loss of NPFp series with loading

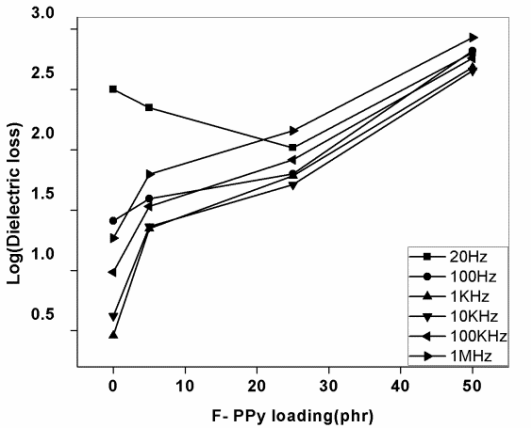

Fig. 8.18 Variation of dielectric loss of NFp series with loading

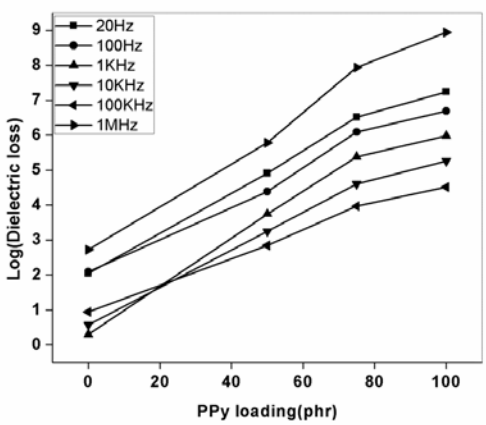

Fig. 8.19 Variation of dielectric loss of LNP series with loading

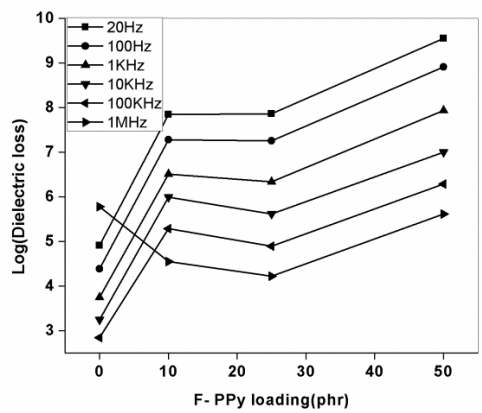

Fig. 8.20 Variation of dielectric loss of LNPFp series with loading

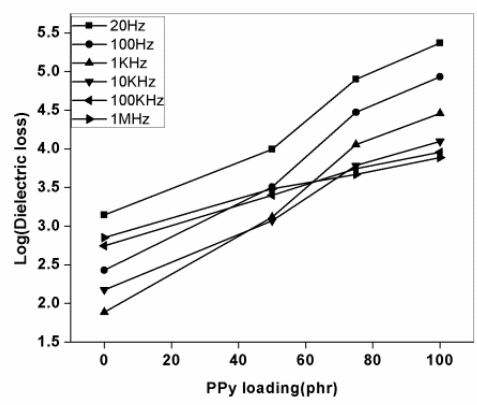

Fig. 8.21 Variation of dielectric loss of BP series with loading

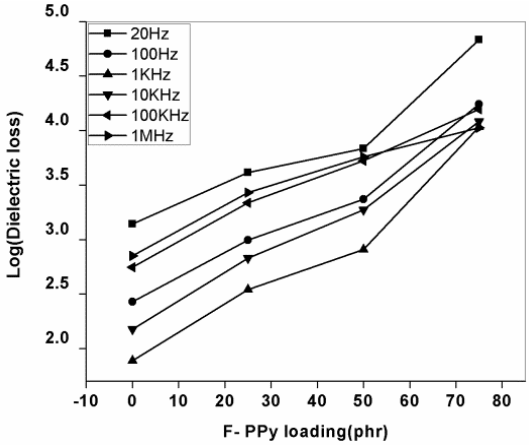

Fig. 8.22 Variation of dielectric loss of BFp series with loading

Table 8.2 Dielectric loss values of CECs of PPy

Composite	Dielectric loss	
	at 20Hz	at 1MHz
NP0	317	18.5
NP2	505	162
NP3	534	286
NP4	1758	359
NPFp3	1263	803
NPFp4	2399	1140
NPFp5	11588	1288
NFp2	223	62
NFp4	104	144
NFp5	638	852
LNP0	111	15
LNP2	80897	324
LNP3	3.2×10^{6}	2804
LNP4	1.7×10^{7}	7650
LNpFp1	6.9×10^{7}	35253
LNPFp2	7.2×10^{7}	16669
LNPFp3	3.5×10^{9}	4.1×10^{5}
BP0	1390	710
BP2	9870	3033
BP3	79483	4645
BP4	2.3×10^{5}	7694
BFp2	132	2700
BFp3	6827	5751
BFp4	68227	10617

8.3.3 AC Conductivity

8.3.3.1 Frequency dependence of AC conductivity of pristine PPy and its CECs

Fig. 8.23 represents the variation of AC conductivity of pristine PPy with frequency. The highest conductivity shown by PPy is 4.98×10^2 S/m. Here the conduction is due to the free motion and hopping of charge carriers (polaron and bipolaron). The low frequency behaviour (up to 10^3 Hz) looks like a straight line typical of hopping conduction [63]. AC conductivity of PPy is found to be increasing with frequency due to the increase in charge carriers and the increase in the hopping of these charge carriers. At very high frequencies this hopping frequency can not match the applied frequency and hence the variation of conductivity is found to be more or less frequency independent. This may also be due to random diffusion of the charge carriers via activated hopping, which is known to give rise to a frequency independent conductivity [64].

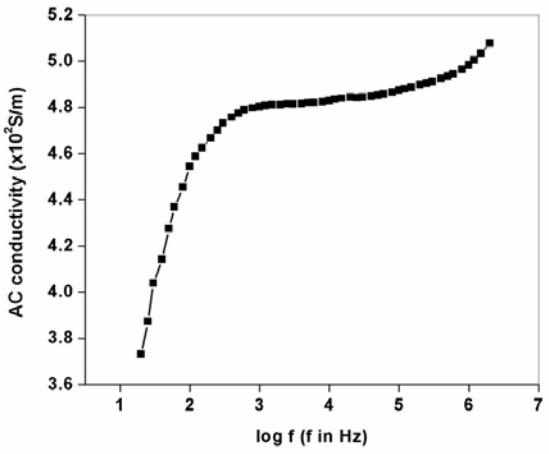

Fig. 8.23 Variation of AC conductivity of polypyrrole with frequency

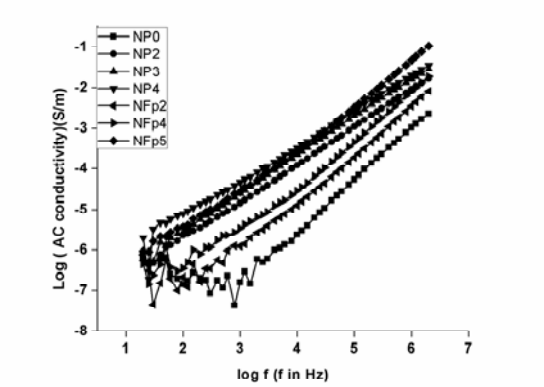

Fig. 8.24Variation of AC conductivity of NR based CECs with frequency

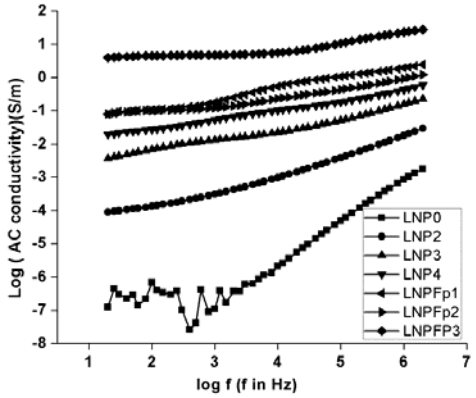

Fig. 8.25 Variation AC conductivity of NR based CECs prepared by *in situ* polymerization with frequency

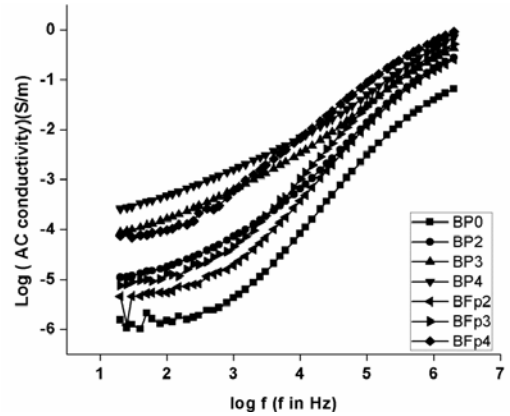

Fig. 8.26 Variation of AC conductivity of NBR based CECs with frequency

The total conductivity σ_{tot} (ω,T) at a given temperature over a wide range of frequency can be written as [62]

$$\sigma_{tot}(\omega,T) = \sigma_{DC}(T) + \sigma_{AC}(\omega,T) \quad \text{---------- (8.14)}$$

where σ_{DC} (T) is the DC conductivity and σ_{AC} (ω,T) the AC conductivity.
Here for PPy, At lower frequencies, there is an obvious increase in the total AC conductivity with increasing frequency and the sample seems to obey a well known universal law of the form [62]

$$\sigma_{AC}(\omega,T) \ \alpha \ \omega^{S} \text{ or } \sigma_{AC}(\omega,T) = A\omega^{S} \quad \text{----------(8.15)}$$

where 's' is power (frequency) exponent which depends on temperature($0 \leq S \leq 1$) and 'A' is temperature dependent constant.

The hopping AC conduction mechanism can be further analysed on the basis of variation of frequency exponent 's'with temperature [65]. The value of 's' at each temperature can be calculated from the slope of log (σ_{AC} (ω,T) - σ_{DC} (T)) versus log ω plot. Kumar *et al*. [26] have plotted such graphs for pure PPy and found that the frequency exponent 's' decreases with the increase of temperature. The AC conduction in this case can be estimated to follow correlated barrier hopping conduction model [66], which considers the hopping of the carriers between two sites over a barrier separating them.

Variation of AC conductivity with frequency of the CECs of PPy and PPy coated short Nylon fibers based on different matrices and that prepared under different conditions are presented in figs. 8.24 to 8.26. As in the case of pristine PPy, here also AC conductivity is found to be increasing with

frequency. At higher frequencies, either the conductivity tends to remain constant (fig. 8.25) or a small dip is observed (fig. 8.26). Frequency dependence of AC conductivity of the polycrystalline structure of ferrites [4] has been explained in the past with the help of Maxwell–Wagner (MW) – two-layer model or the heterogeneous model. According to MW theory two layers form a dielectric structure. The first layer consists of ferrite grains of fairly well conducting (ferrous ions), which is separated by a thin layer of poorly conducting substances, which forms the grain boundary. These grain boundaries are more active at lower frequencies and hence the hopping frequency of electron between Fe^{2+} and Fe^{3+} ion is less at lower frequencies. As the frequency of the applied field increased the conductive grains became more active by promoting the hopping of electron between $Fe^{2+}$and Fe^{3+} ions, thereby increasing the hopping frequency. They observed a gradual increase in conductivity with frequency but at higher frequencies the frequency of hopping between the ions could not follow the applied field frequency and it lagged behind it. This causes a dip in conductivity at higher frequencies [11].

The variation pattern of AC conductivity with frequency is not similar for all composite systems as is evident from a comparison of figs. 8.24, 8.25 and 8.26. This may be explained as follows: The total conductivity of the composite may depend on the microscopic and macroscopic conductivities. The microscopic conductivity depends upon the doping level, conjugation length or chain length etc., whereas the macroscopic conductivity depends on the inhomogeneities in the composites, compactness of pellets, orientation of micro particles etc. The CECs under study are inhomogeneous because of dispersion of conducting PPy particles

in the insulating elastomer matrices. The physical (macroscopic) properties viz. compactness and molecular orientations may significantly vary due to the variation in the weight percentage of PPy in the composites. Altogether, the macroscopic contribution towards total conductivity may vary in the composites under study. The three systems under study are: composites based on NR prepared by dry rubber compounding, composites based on NR prepared by *in situ* polymerization in NR latex and composites based on NBR prepared by dry rubber compounding. That means the matrix and synthesis conditions vary in the composite systems. This accounts for a difference in the contribution due to microscopic conductivity. It can naturally be expected that the variation of AC conductivity with frequency will be different for the three composite systems.

The plots representing variation of AC conductivity of NBR based CECs with frequency resemble those obtained by Achour *et al.* [35] for PPy-PMMA composites. As in the case of PPy-PMMA composites, here also the total frequency range can be divided into three domains. At low frequencies (domain 1), the conductivity does not almost depend on the frequency and is dominated by a percolative behaviour [67]: i.e., in this region, $\sigma_{DC}(T)$ contribution towards total conductivity is observed. At intermediate frequencies (domain 2), the AC conductivity increases following power law behavior [62], as discussed in the case of PPy. At high frequency (domain 3), a new contribution appears, which is related to the σ_{AC} contribution of intrinsic hopping conductivity in the composite material [63].

Two trends of AC electrical conductivity with frequency are observed in figs. 8.24 to 8.26. In some cases the conductivity changes slowly with frequency due to dominating DC conductivity component and in some

other cases the conductivity increases sharply with frequency showing a distinct change in slope. The former could be attributed to the free charges in the composite system, whereas the latter frequency dependent conductivity could be attributed to the release of trapped charges in the disordered system [26].

8.3.3.2 Loading dependence of AC conductivity of CECs of PPy

Effect of loading of PPy and F-PPy on AC conductivity of conducting elastomer composites are shown in figs. 8.27 to 8.33. An increment in AC conductivity with loading is found for all the series of composites studied at all frequencies. Compared to elastomer composites prepared by dry rubber compounding, a sharp increase in conductivity is observed for composites prepared by *in situ* polymerization in NR latex (figs. 8.30 and 8.31). The DC conductivity behaviour of these series (section 5.3.5 of this thesis) also supports this. At higher loadings AC conductivity values either remains constant or exhibits very low increment, indicating a percolation limit.

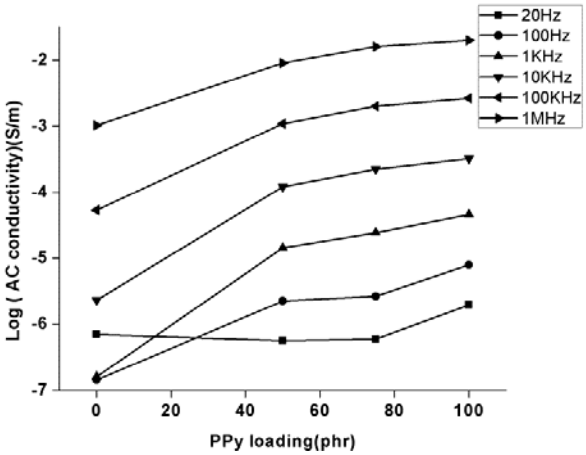

Fig. 8.27 Variation of AC conductivity of NP series with loading

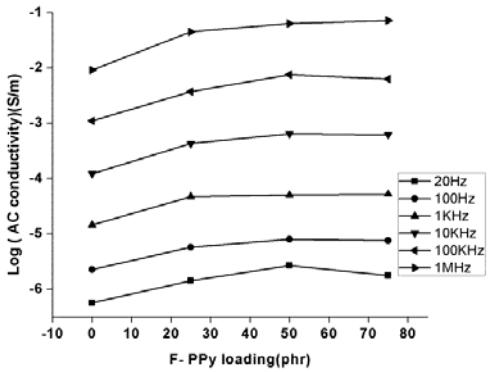

Fig. 8.28 Variation of AC conductivity of NPFp series with loading

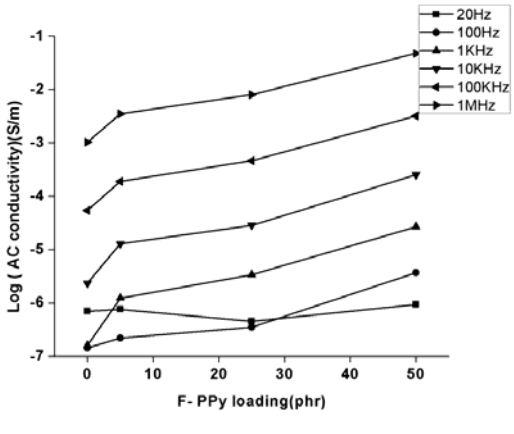

Fig. 8.29 Variation of AC conductivity of NFp series with loading

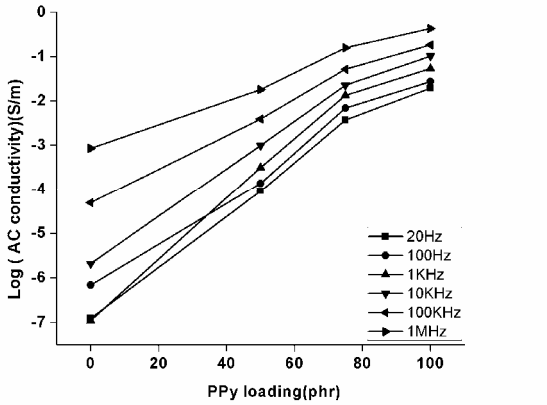

Fig. 8.30Variation of AC conductivity of LNP series with loading

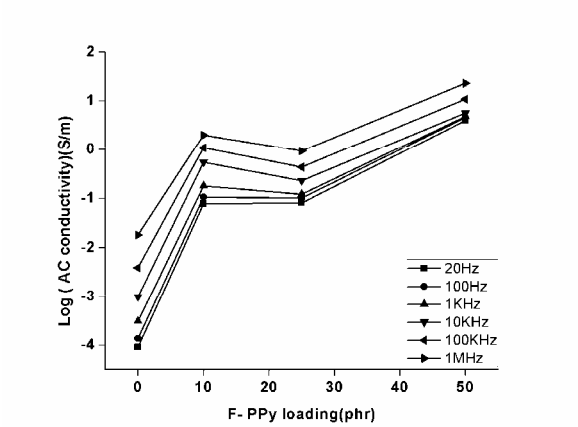

Fig. 8.31 Variation of AC conductivity of LNPFp series with loading

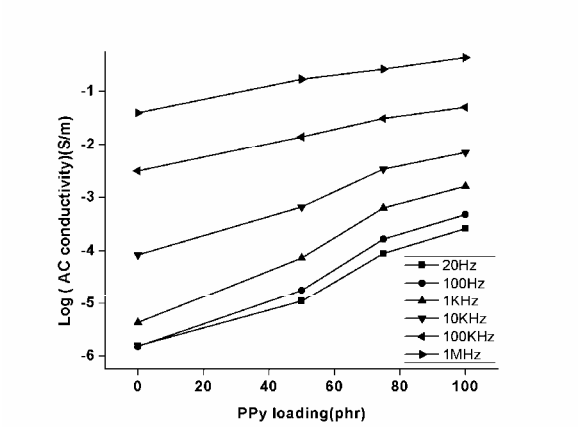

Fig. 8.32 Variation of AC conductivity of BP series with loading

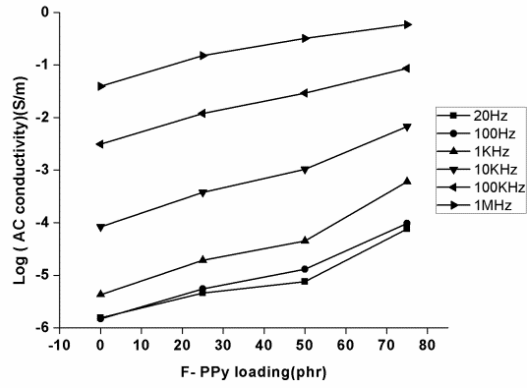

Fig. 8.33 Variation of AC conductivity of BFp series with loading

Table 8.3 AC conductivity values of CECs of PPy

Composite	AC conductivity	
	at 20Hz	at 1MHz
NP0	7×10^{-7}	1×10^{-5}
NP2	5.6×10^{-7}	9×10^{-3}
NP3	5.9×10^{-7}	1.5×10^{-2}
NP4	1.9×10^{-6}	1.9×10^{-2}
NPFp3	1.4×10^{-6}	4.4×10^{-5}
NPFp4	2.6×10^{-6}	6.3×10^{-2}
NPFp5	1.7×10^{-6}	7.1×10^{-2}
NFp2	7.6×10^{-7}	3.4×10^{-3}
NFp4	4.5×10^{-7}	8×10^{-3}
NFp5	9.3×10^{-7}	4.7×10^{-2}
LNP0	1.2×10^{-7}	8.4×10^{-4}
LNP2	9×10^{-5}	1.8×10^{-2}
LNP3	3.6×10^{-3}	1.5×10^{-1}
LNP4	1.9×10^{-2}	4.2×10^{-1}
LNpFp1	7.7×10^{-2}	1.96
LNPFp2	8×10^{-2}	9.2×10^{-2}
LNPFp3	3.9	22.9
BP0	1.5×10^{-6}	3.9×10^{-2}
BP2	1.1×10^{-5}	1.6×10^{-1}
BP3	8.8×10^{-5}	2.5×10^{-1}
BP4	2.6×10^{-4}	4.2×10^{-1}
BFp2	4.5×10^{-6}	1.5×10^{-1}
BFp3	7×10^{-6}	3.2×10^{-1}
BFp4	7.5×10^{-5}	5.9×10^{-1}

Extrinsically conducting polymer composites have conducting filler dispersed in polymer matrix in such a fashion that there is formation of some continuous conducting networks through aggregation of conducting filler particles in insulating matrix. This type of conducting network formation is possible only beyond the critical concentration of filler. Percolation limit depends on the filler characteristics like size, surface area and groups, aggregate structure and

matrix polymer characteristics like viscosity, presence of polar groups etc. [68,69]. Increase of AC conductivity with filler loading may be due to increased charge carrier concentration (polarons and bipolarons) with increased filler loading. Progressive increase in filler concentration also reduce the average inter- particle distance leading to a possibility of continuous conducting path formation through inter-particle contact. However it is not always required to have physical contact among particles to form continuous conducting network. If two particles are separated by a few nanometers then charge carriers can hop the gap thus making up the discontinuities existing between particle aggregates to form a continuous conducting path.

Another reason for increase in AC conductivity with increased loading may be attributed to increase in crystallinity leading to increase in orderness which results in maximum space charge polarization due to the interfacial interactions between PPy and the matrix [47].

The increase in conductivities observed by Bhattacharya *et al*. [22] for the case of ZrO_2 sol dispersed in the PPy matrix was accounted for the improved weak links between the grains, resulting in stronger coupling through the grain boundary. Vishnuvardhan and his group have reported that PPy–Y_2O_3 nano composites showed an increasing trend of AC conductivity with the increase in Y_2O_3 weight percentage in the nano composite due to increase in degree of crystallinity [37].This led to increase in orderness which resulted in maximum space charge polarization due to the interfacial interactions between PPy and the matrix [47].

Table 8.3 gives AC conductivity values of the prepared conducting elastomer composites at two frequencies, 20 Hz and 1 MHz. The maximum conductivity of 22.9 S/m at 1 MHz is recorded for the CEC, LNPFp3. This value is very

high compared to the AC conductivity values of conducting polymer composites [35,37, 56,57, 70] and ceramic/polymer composites [11] reported in literature.

8.4 Conclusions

The dielectric properties of PPy and the conducting elastomer composites were measured in the frequency range 20 Hz to 1 MHz. Dielectric constant of PPy shows a steep decrease from its initial higher values at low frequency and then remains constant regardless of the applied frequency. Maximum dielectric constant of 4.94×10^6 is shown at frequency 25Hz , while it decreases to 5600 at 1 MHz. Decrease in ε' at higher frequencies is attributed mainly to the dropping out of interfacial polarization components to ε' since it cannot follow the applied field. Dielectric constant of the CECs also decrease with increasing frequency owing to a decrease in interfacial polarization and increases with PPy and F-PPy loading due to an increase in interfacial polarization. A remarkably high value of permittivity, 9.8×10^4 at 20 Hz and 2000 at 1MHz is shown by the CEC, LNPFp3. At low frequencies dielectric loss of pristine PPy decreases linearly with increasing frequency suggesting that DC conductivity process is more significant than interfacial polarization process. In the case of composites, variation pattern of dielectric loss with frequency suggest that both DC conductivity and interfacial polarization processes contribute towards dielectric loss. Increase in dielectric loss of the composites on loading may be due to the increase in DC conductivity, increase in interfacial polarization and increase in crystallinity of the samples. AC conductivity of PPy and its composites increases with frequency and the mechanism of conduction is mainly due to hopping of charge carriers. Frequency dependence of AC conductivity can be explained with the help of

Maxwell–Wagner two-layer model. The variation pattern of AC conductivity with frequency is not similar for all the composite systems since the composites differ in microscopic as well as macroscopic conductivities. The study of AC conductivity dependence of frequency allowed to identify different mechanisms of the conduction in the elastomer composites. At low frequencies, the conductivity is dominated by a percolative behavior, and at intermediate frequencies it obeys the Jonscher power law. At high frequency, a new contribution appears which is related to the intrinsic hopping conductivity in the composite. All the composite systems exhibit increase of AC conductivity with filler loading which may be due to various reasons : (1) increased charge carrier concentration (polarons and bipolarons) with increased filler loading. (2) Progressive increase in filler concentration also reduce the average inter- particle distance leading to a possibility of continuous conducting path formation (3) Increase in crystallinity leading to increase in orderness which results in maximum space charge polarization due to the interfacial interactions between PPy and the matrix. A maximum conductivity of 22.9 S/m at 1 MHz is recorded for the CEC, LNPFp3. Among all the CECs prepared those prepared by *in situ* polymerization in NR latex exhibit the best dielectric properties.

References

[1] Soares BG, Amorim GS, Souza Jr FG, Oliveira MG, Silva JEP. *Synth Met*. **2006**, 156, 91.

[2] Faez R, Schuster RH, De Paoli M A. *Eur Polym J*. **2002**, 38, 2459.

[3] Moreira VX, Garcia FG, Soares BG. *J Appl Polym Sci*. **2006**, 100, 4059.

[4] Koops, C. G. *Phys. Rev*. **1951**, 83, 121.

[5] Brockman FG, Matteson KE. *J Am Ceram Soc*. **1971**, 54, 183.

[6] Jankowski S. *J Am Ceram Soc.* **1988**, 71, c-176

[7] Mateveeva ES, *Synth Met.* **1996**, 79, 127.

[8] Brandrup J, Immergut EH (editors) *Polymer Handbook. 2nd edition, New York: Wiley- Interscience*. **1974**. P. VIII-7

[9] Dimos D, Lockwood SJ, Schwarz RW, Rodgers MS. *IEEE Trans Comput Hybrid Manufact Technol***. 1994**, 18, 174.

[10] Anantharaman MR, Jagatheesan S, Sindhu S, Malini KA,Chinnasamy C N, Narayanasamy A, Kurian P and Vasudevan K. *Plas rubber compos Process appl.* **1998,** 27, 77.

[11] Sindhu S, Anantharaman M R, Thampi BP, Malini KA, Kurian P. *Bull Mater Sci*. **2002**, 25, 599.

[12] Malini KA, Kurian P, Anantharaman MR. *Mater Lett.* **2003**, 57, 3381

[13] Soloman MA, Kurian P, Anantharaman MR. *J Appl Polym Sci*. **2003**, 89, 769.

[14] Wong CP, Bollampally RS. *J Appl Polym Sci*. **1999**, 14, 3396.

[15] Khan AA, Khalid M. *J Appl Polym Sci*. **2010**, 117, 1601.

[16] Wang DW, Li F, Zhao J, Ren W, Chen ZG, Tan J, Wu ZS, Gentle I, Lu GQ, Cheng HM. *Am Chem Soc Nano* . **2009**, 3, 1745.

[17] Eftekhari A. *Nanostructured Conductive Polymers*, *Wiley, Chichester*, **2010**.

[18] LiY,Yi R, Yan A, Deng L, Zhou K, Liu X.*Solid State Sci*. **2009**, 11, 1319.

[19] Sahoo NG, Jung YC, So HH, Cho JW. *Synth Met*. **2007**, 157, 374.

[20] Li N, Shan D, Xue H. *EurPolym J*. **2007**, 43, 2532.

[21] Armes SP, Gottesfeld S, Beery JG, Garzon F, Agnew SF. *Polymer*.**1991,** 32, 2325.

[22] Bhattacharya A, Ganguli KM, De A, Sarkar S. *Mater Res Bull*. **1996**, l31, 527.

[23] Guo Z, Shin K, Karki AB, Young DP, Kaner RB, Hahn HT. *J Nanopart Res*. **2009**, 11, 1441.

[24] Cheng Q, Pavlinek V, Li C, Lengalova A, He Y, Saha P. *Appl Surf Sci*. **2006**, 253, 1736.

[25] Trung VQ, Tung DN, Huyen DN. *J Exp Nano Sci*. **2009**, 4, 213.

[26] Kumar A, SarmahS. *Phys Status Solidi A*. **2011**, 208, 2203.

[27] Girad F, Ye S, Laperriere G, Belanger D. *J ElectroanalChem.* **1992**, 334, 35.

[28] Gemeay AH, Nishiyama H, Kuwabata S, YoneyamaH. *J Electrochem Soc.* **1999**, *142*, 226.

[29] Basavaraja C, Choi YM, Park HT, Huh DS, Lee JW, Revanasiddappa M, Raghavendra SC, Khasim S, Vishnuvardhan TK. *Bull Korean Chem Soc*. **2007**, 28, 1104.

[30] Saafan SA, El-Nimr MK, El-Ghazzawy EH. *J Appl Polym Sci*. **2006**, 99, 3370.

[31] Singh RFL,Tandon P, Panwar VS, Chandra S. *J Appl Phys*. **1991**,69, 2504.

[32] Harun MH, Saion E, Kassim A, Mahmud E, Hussain MY, Mustafa IS. *J for the advancement of science and arts*.**2009**, 1,9.

[33] Yanilmaz M, Kalaoglu F, Karakas H, Sarac AS. *Tekstilve Konfeksiyon*. **2011**, 21, 1.

[34] Cetiner S, Kalaoglu F, Karakas H, Sarac IAS. *Polym Compos*. **2011**, 32, 546.

[35] Achour ME, Droussi A, Zoulef S, Gmati F, Fattoum A, Mohamed BA, Zangar H. *Spectrosc Lett*. **2008**, 41, 299.

[36] Goswamy A. *Thin film fundamentals. New age International Publishers Ltd., New Delhi.* **1996**.

[37] Vishnuvardhan TK, Kulkarni VR, Basavaraja C, Raghavendra SC. *Bull Mater Sci.* **2006**, 29, 77.

[38] Kim HM, Kim HM, Lee CY. Joo J, *Korean Phys Soc*. **2000**, 36, 371.

[39] Ashis D, Amitabha D, De SK. *J Phys Cond Mater*. **2005**, 17, 5895.

[40] Lee HT, Liao CS, Chen SA. *Macromol Chem*. **1993**, 194, 2443.

[41] Kittel C. *Introduction to solid state physics. Wiley eastern private limited, New Delhi. fourth edition*. **1974**.

[42] Zaky AA, Hawley R. *Dielectric Solids; Routledge& Kegan Paul Ltd. Great Britain*. **1970**.

[43] Panwar V, Sachdev VK, Mehra RM. *Eur Polym Mater*. **2007**, 43, 573.

[44] Rocha IS, Mattosa LHC, Malmonge LF, Gregorio RJ. *Polym Sci*. **1999**, 37B, 1219.

[45] Rellick GS, Runt JJ. *Polym Sci*. **1988**, 26A, 1425.

[46] Ku CC, Liepins R. *Electrical properties of polymers. Munich, Vienna, New York: Hanser Publishers*. **1987**, p 25.

[47] Maxwell JC. *A treatise on electricity and magnetism vol.1,Oxford University Press*. **1892.**

[48] Foulger SH. *J App Polym Sci*. **1999**, 72, 1573.

[49] Meakins RJ. *Progress in Dielectrics; Wiley: New York*. **1961**, p. 151.

[50] Panwar V, Mehra RM, Park JO, Park S. *J ApplPolym Sci*. **2012**, 125, E610.

[51] Malini KA. *Ph. D. Thesis, Cochin University of Science and Technology, Cochin, India*, **2001**.

[52] Bhadra S, Khastgir D. *Eur Polym J*. **2007**, 43, 4332.

[53] Dutta P, Biswas S, De SK. *Mater Res Bull*. **2002**, 37, 193

[54] Chwang CP, Liu CD, Huang SW, Chao DY, Lee SN. *Synth Met*. **2004**, 142, 275.

[55] Chandran AS. *Ph. D. Thesis, Cochin University of Science and Technology , India*, **2008.**

[56] Bhadra S, Singha NK, Khastgir D. *Curr Appl Phys*. **2009**, 9, 396.

[57] Ram MK, Annapoorni S,.Pandey SS, Malhotra BD. *Polymer*. **1998**, 39, 3399.

[58] Ravikiran YT,LagareMT, Sairam M, Mallikarjuna NN, Sreedhar B, ManoharS, MacDiarmid AG, Aminabhavi TM. *Synth Met*, **2006**, 156, 1139.

[59] Smyth CP. *Dielectric behavior and structure. New York: Mcgraw-Hill Book Company Inc*. **1955**, p. 191

[60] McCrum NG, Read BE, Williams G. *An elastic and dielectric effects in polymeric solids. New York: John Wiley & Sons.* **1967**, p. 211

[61] Riande E, Calleja RD. *Elecrical properties of polymers. Munich:Hanser Publishers*. **1987**, p.34

[62] Jonscher AK. *Dielectric relaxations in solids .Chelsa Dielectric Press, London*. **1983**

[63] Berner D, Travers J P, Rannou P. *SynthMet*. **1999**, 101**,** 836.

[64] Sidebottom DL, Rolling B, FunkeK. *Phys Rev*. **2000**, B63, 24301

[65] Elliott SR. *Adv Phys*. **1987**, 36,135.

[66] Ghosh A. *Phys Rev*. **1990**, B 42, 1388.

[67] Vanderputten D, Moonen JT, Brom HB, Brokkenzijp JCM, Michels MAJ. *Synth Met.***1993**, 57, 5057.

[68] Sau KP, Chaki TK, Khastigir D. *Polymer*. **1998**, 39, 6461.

[69] Sau KP, Chaki TK, Khastigir D. *Polym J Mater sci*. **1997**, 32, 5717.

[70] Murugendrappa MV, Myedkhasim, Ambika Prasad MVN. *Bull. Mater. Sci.* **2005,** 28, 565.

.....ൠ.....

Chapter

9

MICROWAVE PROPERTIES AND EMI SHIELDING EFFECTIVENESS OF THE CONDUCTING ELASTOMER COMPOSITES

Contents

The Dielectric properties at microwave frequencies of the conducting elastomer composites based on NR, NBR and that prepared by in situ polymerization in NR latex were measured in the S band (2-4 GHz) frequency using cavity perturbation technique. The absolute value of the dielectric permittivity, AC conductivity and absorption coefficient of the conducting composites prepared were found to be much greater than the gum vulcanizates. PPy and PPy coated fiber (F-PPy) were found to decrease the dielectric heating coefficient and skin depth significantly. Dielectric permittivities 35, 55.5 and 43 were obtained for the composites NPFp5, LNPFp3 and BP3 respectively. Maximum AC conductivity, 6.7 S/m was attained by the CEC, NPFp5 at a frequency 3.6 GHz. The electromagnetic interference shielding effectiveness of the CECs in the S band (2-4 GHz) and X band (7-13 GHz) frequencies were evaluated. The CECs were found to have appreciable shielding effect depending on loading of PPy and F-PPy and in turn the conductivity.

9.1 Introduction

Microwave properties of conductive polymers is crucial because of their wide areas of applications such as coating in reflector antennas, coating in electronic equipment, frequency selective surfaces, EMI materials,Camouflage nets and Radar Camouflage, satellite communication links, microchip antennas etc. [1-3].

Understanding the transport mechanism in conducting polymers and the potential use of it as EMI shielding and absorbing materials have encouraged the study of dielectric properties at high frequencies. Conducting polymers show some specific characteristics in microwave frequencies that make them far more interesting than traditional dielectric materials. Conducting polymers are excellent microwave absorbers and they show technological advantage when compared to inorganic electromagnetic absorbing materials, being light weight, easily processable, and the ability of changing the electromagnetic properties with nature and amount of dopants, synthesis conditions, etc. and can be used for making microwave absorbers in space applications [4]. The intrinsic conductivity of conjugated polymers leads, in the field of their microwave properties, to a dynamic conductivity leading to high levels of dielectric constant [5-8]. Many microwave absorbing materials based on conducting polymers have been developed [9,10]. Rimili and coworkers have developed polyaniline films of high conductivity (5000-6000 S/m) and permittivity of above 6000 over X and S bands [11]. This confirms the metallic character of PANI films and their efficient use in micro-electronic technology, such as microwave integrated circuits (MICs) and microwave devices. A number of studies on the electrical conductivity and dielectric properties of composites of a variety of conducting polymers also have been

carried out [12-16]. Electromagnetic wave absorbing materials used in gigahertz (GHz) range have attracted much attention with the development of GHz microwave communication, radar detection and other industrial applications in recent years. These absorbing materials can be manufactured by a number of magnetic and dielectric materials in powder form, loaded in various kinds of polymeric binders.

Important applications concerned with the microwave properties are EMI shielding and radar absorption. EMI is defined as spurious voltage and current induced in electronic circuitry by an external source. It is unwanted electrical and magnetic energy that causes a disturbance in a receiving device. EMI reduces the lifetime and efficiency of the instrument. An EMI shielding material is one that attenuates radiated electromagnetic energy. Light weight EMI shielding is needed to protect the workspace and environment from radiation emanating from computers and telecommunication equipments as well as for protection of sensitive circuits. Radiation shielding materials are essential for high operational reliability and long life of electronic equipment since they reduce or suppress the electromagnetic noise [17,1]. Conducting polymers being excellent microwave absorbing materials [18], are well known for shielding electromagnetic waves in both near and far fields [19,20]. Conducting polymers and composites are excellent candidates as shielding materials [21,22]. The EMI shielding efficiency of a composite material depends on many factors, including the filler's intrinsic conductivity, dielectric constant and aspect ratio [23,24]. Since the shielding effectiveness at a particular frequency depends upon the electrical conductivity of the shielding material and its ability to attenuate electrical and magnetic fields at the specific wavelength, there exists the possibility of selective filtering shielding. In this

field conducting rubber composites have inspired much interest because of their light weight, hard corrosion, good processability and easy control of conductivity. Several research groups have reported electromagnetic shielding behavior of conducting polymer composites. Polyaniline powder is the most commonly reported filler in matrices like thermoplastics and thermoplastic-elastomeric matrices [25,26-30]. Polypyrrole powders have been incorporated in thermoplastics [31], silicon based plastics [32] and fluroplastics [33]. Fibers and textiles coated with PPy are reported to yield high shielding effectiveness [34,35]. The EMI shielding properties of polypyrrole/polyester composites in the 1-18 GHz frequency range were investigated by Hakansson *et al*. [36]. Compared to conventional metal– based EMI shielding materials, electrically conducting polymer composites have gained popularity recently because of their light weight, resistance to corrosion, flexibility and processing advantages [37-44]. The incorporation of conducting polymer powders in non conducting matrices gives a SE value consisting of both reflection and absorption components. The ability to absorb part of the radiation is an attribute of these particle filled composites [36].

This chapter is divided into two parts. Part-I describes the microwave properties of the conducting elastomer composites. All dielectric materials are characterized by their dielectric parameters such as dielectric constant, conductivity and dielectric loss factor. These parameters differ with frequency, temperature, pressure etc. Part-II deals with electromagnetic interference shielding effectiveness of the CECs. The target value of the EMI shielding effectiveness needed for commercial applications is around 20dB (i. e., equal to or less than 1% transmission of the electromagnetic wave) [45].

Part-I

9.2 Microwave characteristics

9.2.1 Experimental

Microwave properties of materials can be evaluated with coaxial probe, transmission line, free space, parallel plate and resonant cavity method. In cavity method there are different types of cavities and methods. The most widely used one is Cavity Perturbation Technique [46,47]. In cavity Perturbation Technique, generally rectangular or cylindrical wave-guide resonators are used. When a dielectric material is introduced into a cavity resonator at the position of maximum electric field, the resonant frequencies of the cavity are perturbed. The contribution of magnetic field for the perturbation is minimum at this position. So from the measurement of perturbation due to sample, the dielectric parameters can be determined.

The microwave characteristics of the prepared conducting elastomer composites (CECs) were studied using ZVB20 vector network analyzer. The schematic design of the network analyzer is shown in fig. 2.3. The measurements were done in S (2-4 GHz) band frequency at room temperature. The cavity resonators are constructed from brass or copper wave-guides. The inner walls of each cavity are silvered to reduce the wall losses. Both the resonators are of transmission type. The dimensions of the S band rectangular wave-guide resonator used in the measurements are 34.5cm× 7.2cm× 3.4cm.

When a dielectric material is introduced in a cavity resonator at the position of maximum electric field, the contribution of magnetic field for the perturbation was minimum. The field perturbation is given by Kupfer *et al*. [48]

$$-(d\Omega/\Omega) \approx [(\varepsilon^{*}-1) \int_{Vs} E.E_0^{*} dV]/ 2 \int_{Vc} |E_0|^2 dV \quad \text{---------- (9.1)}$$

where $d\Omega$ is the complex frequency shift, Vc and Vs are the volumes of the cavity and the sample, respectively. E and E_0 are the perturbed and unperturbed fields in the cavity, respectively; and ε^{*} is the relative complex permittivity of the sample material. $\varepsilon^{*} = \varepsilon' - j\varepsilon''$ where, ε' is the real part of the complex permittivity and ε'' is the imaginary part of the complex permittivity. Complex frequency shift is related to the quality factor, Q as:

$$(d\Omega/\Omega) \approx (d\omega / \omega) + j/2 [(1/Qs) - (1/Q_0)] \quad \text{----------(9.2)}$$

Qs and Q_o are the quality factors of the cavity with and without sample. Quality factor, Q is given by $Q = f/\Delta f$ where f is the resonant frequency and Δf is the corresponding 3dB bandwidth. For small samples, we assume that E = E_0 and for the dominant TE_{10p} mode in a rectangular wave guide,

$$E_0 = E_{omax} \sin (\Pi x/a) \sin (\Pi pz /d), \; p = 1, 2 , 3 \text{ etc} \quad \text{----------(9.3)}$$

E_{omax} is the peak value of E_0, a is the broader dimension and d is the length of the wave guide cavity resonator. From equations (1) to (3), the real and imaginary parts of the relative complex permittivity are given by

$$\varepsilon' = 1+(f_0 - f_s)/2f_s .(V_c/V_s) \quad \text{----------(9.4)}$$

$$\varepsilon'' = (V_c/4V_s) [(Q_o - Q_s)/ Q_o Q_s] \quad \text{----------(9.5)}$$

The real part of the complex permittivity, ε', is generally known as the dielectric constant/dielectric permittivity and the imaginary part, ε'', is related to the dielectric loss of the material. The dielectric constant represents the amount of dipole alignment, both induced and permanent and the dielectric loss represents the energy required to align dipoles or move ions. The

dielectric loss can also be expressed as tangent of phase shift angle, δ, where δ is called as the "loss angle" denoting the angle between the voltage and the charging current.

The loss tangent (tan δ) is given by:

$$\tan \delta = (\sigma + \omega\varepsilon'')/ \omega \varepsilon' \quad \text{----------(9.6)}$$

where$(\sigma+\omega\varepsilon'')$ is the effective conductivity of the medium. When the conductivity σ due to free charge is negligibly small (good dielectric), the effective conductivity is due to electric polarization and is reduced to:

$$\sigma_e = \omega \varepsilon'' = 2\Pi f \varepsilon_0 \varepsilon'' \quad \text{----------(9.7)}$$

The efficiency of heating is usually compared by means of a heating coefficient, J, which is defined as [49,50]

$$J = 1/\varepsilon^* \tan \delta \quad \text{----------(9.8)}$$

The absorption of electromagnetic waves when it passes through the medium is given by the absorption coefficient (α_f), which is defined as [51].

$$\alpha_f = \varepsilon'' f_s /nc \quad \text{----------(9.9)}$$

where $n = \varepsilon^*$ and 'c' is the velocity of light.

Penetration depth, also called skin depth, is basically the effective distance of penetration of an electromagnetic wave into the material, given as [52]:

$$\delta_f = 1/ \alpha_f \quad \text{----------(9.10)}$$

The quality factor; Q_0 of the cavity and resonance frequency, f_0, in the unperturbed conditions were measured. The samples in the form of thin rectangular roads, the length of which equals the height of the cavity, so that both

the ends of the specimen are in contact with the cavity walls, were used. The samples were inserted into the cavity through a slot and positioned at the maximum electric field. The resonance frequency, $f_{s,}$ and loaded quality factor, $Q_{s,}$ of the samples were measured. Knowing the volume of cavity, Vc and volume of sample, $V_{s,}$ dielectric permittivity, dielectric loss, AC conductivity, dielectric heating coefficient, absorption coefficient and skin depth were calculated using the equations 9.4, 9.5, 9.7, 9.8, 9.9 and 9.10 respectively.

9.2.2 Results and discussion

9.2.2.1 NR based CECs

9.2.2.1.1 Dielectric permittivity

The variation of dielectric permittivity (ε') of the three series of CECs in S band frequency are shown in fig. 9.1. Higher the polarizability of the material, the greater is the dielectric constant. The frequency dependence of dielectric permittivity of these composites can be explained as follows: Below frequencies of 10^{10} Hz all polarization mechanisms – electronic, ionic and dipolar – contribute to dielectric permittivity. Further, the prepared composites are a heterogeneous mixture of conducting polypyrrole separated by highly resistive rubber matrix. The dielectric permittivity of such heterogeneous, conducting composites arises mainly due to interfacial polarization along with some contributions from intrinsic electric dipole polarization [53]. Doped polypyrrole possesses permanent electric dipoles. Therefore orientation or dipolar polarization is expected to contribute to the dielectric permittivity. Of these polarization mechanisms, dipolar and interfacial (space charge) are more frequency-dependent. It has been shown that ε' is almost constant regardless of applied frequency for NP series. Therefore in these, the polarization mechanisms contributing to ε'may be electronic and ionic. When it comes to

NPFp and NFp series, PPy coated fibers contribute more conducting regions in the system, leading to increase in space charge polarization which depend more on the frequency of applied field. The observed decrease in ε' with increasing frequency in the case of these two series may be attributed to the decrease in space charge polarization with increasing frequency [54,55]. This behaviour is in accordance with Maxwell-Wagner interfacial polarization. As the frequency of applied field increases, interfacial polarization decreases and hence dielectric permittivity decreases. As the frequency is increased, the time required for the interfacial charges to be polarized or for the dipoles to be arranged is delayed, thus the dielectric permittivity decreases with frequency.

There is a substantial increase in ε' with PPy loading and F-PPy loading. The increase in ε' with increasing PPy content may be due to increase of conducting regions. According to Koops, the dielectric permittivity is inversely proportional to the square root of resistivity [56]. The DC conductivity of NR based composites increases with loading (section 4.3.5). A dielectric permittivity of 35 is obtained for NPFp5 at 2.9 GHz frequency. For a PANI/NR semi interpenetrating network from NR latex, John *et al.* [57] have reported a permittivity of 20 at a NR:PANI proportion of 2:1. For a PANI/NR composite, Chandran AS [58] has reported a dielectric permittivity of 35 for 140 phr PANI loaded sample at 4 GHz frequency. Fig.9.2 (a) shows an abrupt increase in ε' at higher concentrations of PPy. This is because at higher concentrations, the tendency of conductivity chain formation increases through the aggregation of the PPy particles network, whereas at lower concentration, the particles of PPy are widely dispersed through the polymeric matrix [59]. Thus it is clear that dielectric permittivity of NR matrix gets highly modified by addition of PPy and F-PPy and the required dielectric constant can be achieved by varying their concentrations.

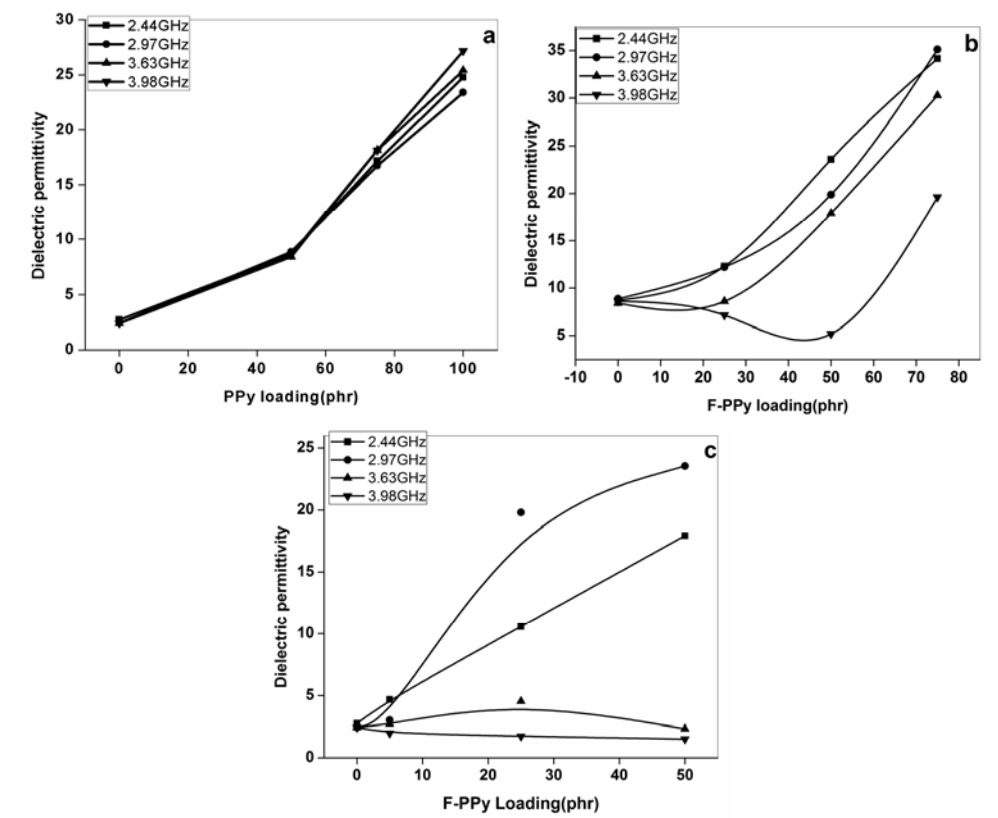

Fig.9.1 Variation of dielectric permittivity with loading of (a)NP, (b)NPFp and (c)NFp series

9.2.2.1.2 Dielectric loss

Dielectric loss is utilised to heat food in a microwave oven: the frequency of the microwaves used is close to the relaxation frequency of the orientational polarisation mechanism in water, meaning that any water present absorbs a lot of energy that is then dissipated as heat. At dielectric relaxation region, the polarization acquires a component out of phase with the field and the displacement current in phase with the field, resulting in thermal dissipation of energy. The dielectric loss (ε") is a measure of energy dissipated in the dielectric in unit time when an electric field acts on it. The increased mobility of charge

carriers results in an increase in the dielectric loss [53]. While the conducting polymers increase the conductivity of a composite and thereby the dielectric permittivity, they can also impart high dielectric loss. Therefore ε" tends to be higher in materials with high ε' value. In heterogeneous dielectrics, the accumulation of virtual charges at the interface of two media having different dielectric constant, ε'_1 and ε'_2, and conductivities σ_1 and σ_2, respectively, lead to interfacial polarization [60]. In the case of NP, NPFp and NFp series of composites, which consists of more than one phase, a charge build up can occur at the macroscopic interface as a result of the differences in conductivity and dielectric permittivity of the components. This accumulation of charge then leads to field distortions and dielectric loss. This interfacial loss depends on the quantity of the weakly polar material present, as well as on the geometrical shape of its dispersion[61]. Here NR as a second phase, with a different dielectric permittivity and conductivity, contributes to the interfacial polarization and thereby a high dielectric loss is observed for the prepared conducting polymer composites. Loading-dependence of ε" of PPy filled and F-PPy filled NR composites in S band frequencies are depicted in fig.9.2. Dielectric loss is found to increase with PPy loading and F-PPy loading due to increased mobility of charge carriers. Increase in frequency also increases dielectric loss. The values of ε" in the low frequency range is due to contribution of both interfacial polarization and conductivity while the increase in ε" at higher content of conducting polymer is mainly due to the increase in the electrical conductivity [62]. Dielectric loss at S band is due to the free charge motion within the material [63,64]. The variation of dielectric loss with frequency is a function of relaxation process and its origin is due to the local motion of polar groups. At lower frequencies, the dipoles synchronize their orientation with the field. As the frequency is increased, the

inertia of the molecule and the binding forces become dominant and this is the basis for high dielectric loss at higher frequencies. The NR gum compound offers a very low dielectric loss (0.02) while dielectric loss as high as 33 is achieved by NPFp5 at a frequency 3.6GHz. It is generally known that high shielding effectiveness in a radio frequency band is related to increased dielectric loss of composite due to presence of a high quantity of polarizable dipoles dispersed in a non- conducting polymer matrix [65].

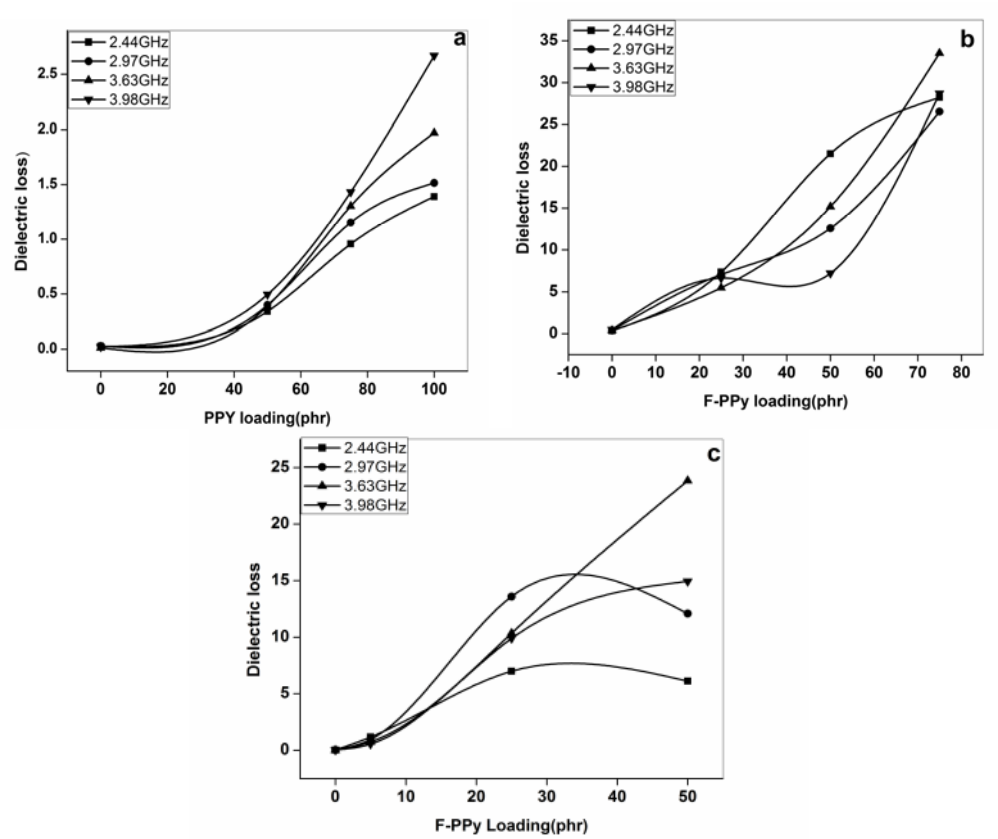

Fig. 9.2 Variation of dielectric loss with loading of (a)NP, (b)NPFp and (c)NFp series

9.2.2.1.3 AC conductivity

The microwave conductivity is a direct function of dielectric loss and hence the fig.9.3, showing the variation of the AC conductivity (S/m) of composites

with PPy and F-PPy loading at different frequencies, has the same nature as that of the dielectric loss factor. Conductivity of the matrix at lowest loading of filler is affected by three parameters, viz. the intrinsic conductivity of the filler, the shape of the filler and also the surface tension of the matrix and the filler [66]. It was expected that fibrous fillers will yield a percolation threshold at lower loadings compared with irregularly shaped particles, since the former will afford many more inter particle contacts. This may be the reason for lower threshold and higher AC conductivity of fiber filled composites. Maximum conductivity 6.7 S/m is obtained for NPFp5 at a frequency 3.6 GHz.

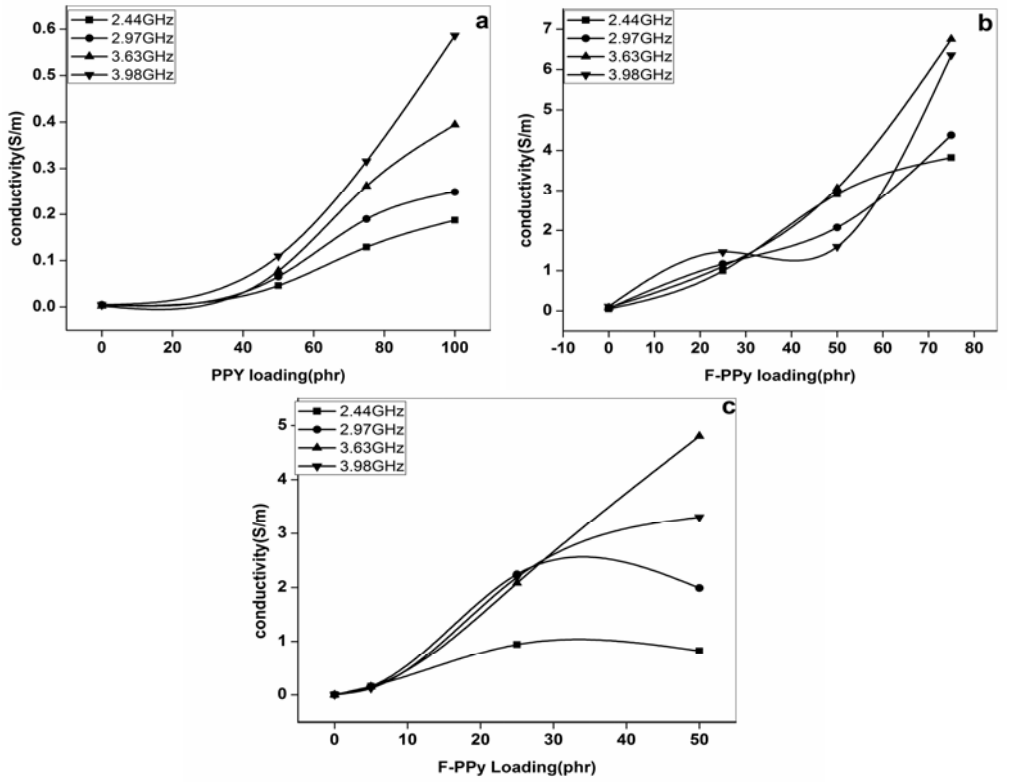

Fig. 9.3 Variation of A. C. conductivity with loading of (a)NP, (b)NPFp and (c)NFp series

9.2.2.1.4 Absorption coefficient

As the absorption coefficient is derived from the complex permittivity and is a measure of propagation and absorption of electromagnetic waves when it passes through the medium, the dielectric materials can be classified in terms of this parameter indicating transparency of waves passing through it [51]. The microwave conductivity and absorption coefficient are direct functions of dielectric loss. The variation of absorption coefficient with frequency and filler loading is same as that for AC conductivity as is evident from fig.9.4. It is clear that the absorption coefficient increases with increase in frequency and also with filler loading and maximum absorption coefficient value is obtained for NPFp5 at 3.6 GHz frequency.

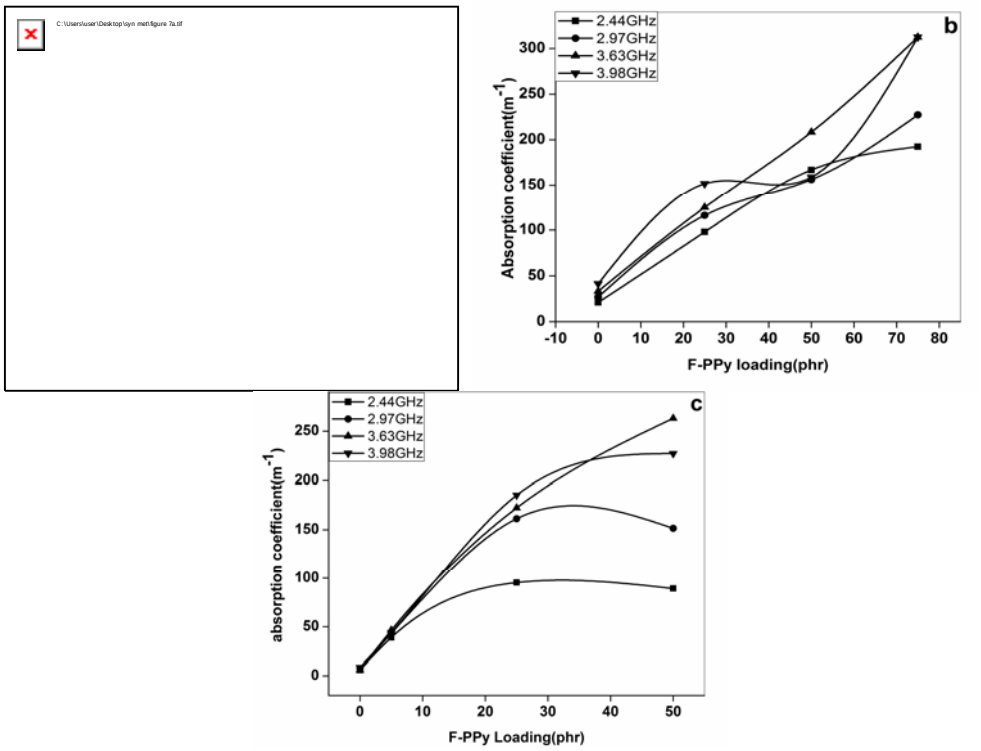

Fig.9.4 Variation of absorption coefficient with loading of (a)NP, (b)NPFp and (c)NFp series

9.2.2.1.5 Skin depth

As the skin depth also called the penetration depth, is basically the effective distance of penetration of an electromagnetic wave into the material [52], it can be applied to a conductor carrying high frequency signals. The self-inductance of the conductor effectively limits the conduction of the signal to its outer shell and the shells thickness is the skin depth which decreases with increase in frequency. From fig.9.5, it is clear that skin depth of the composites decreases with filler loading and the lowest value of skin depth is for the CPC, NPFp5 at 3.6GHz frequency.

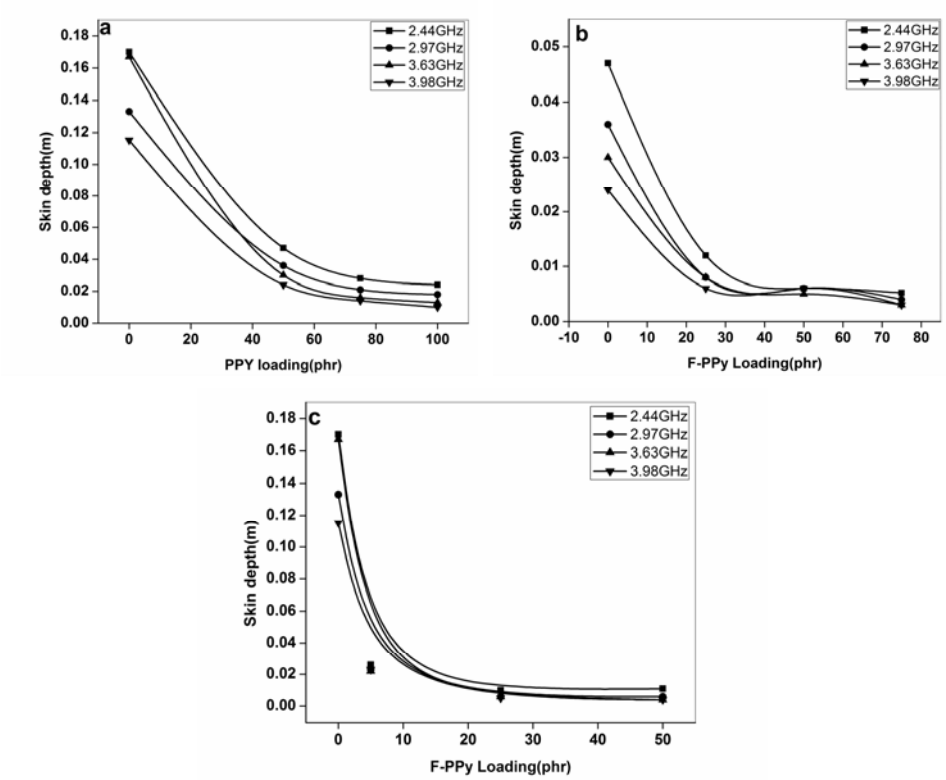

Fig.9. 5Variation of skin depth with loading of (a)NP, (b)NPFp and (c)NFp series

9.2.2.1.6 Dielectric heating coefficient

Fig. 9.6 shows the variation of dielectric heating coefficient (J) with frequency and with loading. It is observed that the heating coefficient decreases with frequency and also with filler loading. The J value of microwave absorbing materials can be calculated using the equation 9.8. The heat developed is proportional to both frequency and the product of ε and tan δ. Higher the J value poorer will be the polymer for dielectric heating purpose. The heat generated in the material comes from the tangent loss, but that loss may not come entirely from the relaxation loss. Rather, conductivity of the material may also contribute to tan δ [49]. In the present study J value is found to be the lowest for NPFp5 at 3.6GHz frequency. At 3.6GH the heating coefficient of NR gum vulcanizate is 80.6 while the CPC, NPFp5 gives a value as low as 0.03.

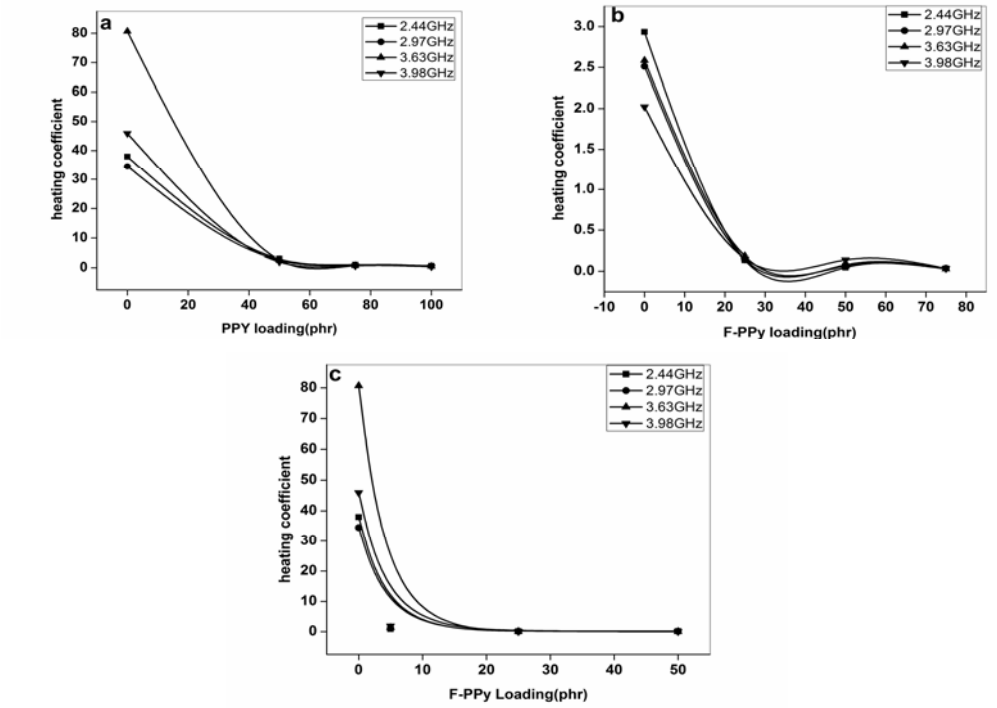

Fig. 9.6 Variation of heating coefficient loading of (a)NP, (b)NPFp and (c)NFp series

9.2.2.2 NR based CECs prepared by in situ polymerization in NR latex

9.2.2.2.1 Dielectric permittivity

The variations of dielectric permittivity (ε') of the LNP and LNPFp series of CECs in S band frequency are shown in Fig. 9.7. ε' is almost constant regardless of applied frequency for LNP series. When it comes to LNPFp series, PPy coated fibers contribute more conducting regions in the system, leading to increase in space charge polarization which depends more on the frequency of applied field. The observed decrease in ε' with increasing frequency in the case of LNPFp series may be attributed to the decrease in space charge polarization with increasing frequency [54,55]. This behavior is in accordance with Maxwell-Wagner interfacial polarization.

There is a substantial increase in ε' with PPy loading and F-PPyloading . The increase in ε' with increasing PPy content may be due to increase of conducting regions. A dielectric permittivity of 55.5 is obtained for LNP4 at 3.98 GHz frequency. This value is high compared to maximum of 35 obtained for NPFp5(section *9.2.2.1.1)*. This result is in accordance with DC conductivity values. The DC conductivity of NR based composites prepared by in situ polymerization method is very high compared to composites prepared by dry rubber compounding (section 4.3.5 and section 5.3.5).

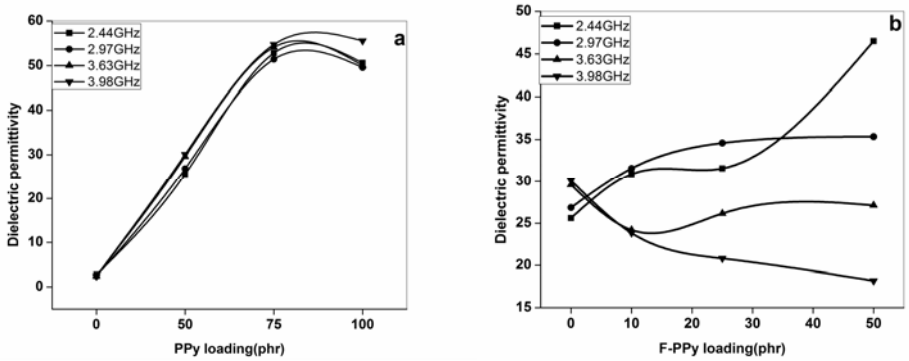

Fig. 9.7 Variation of dielectric permittivity with loading of (a)LNP, (b)LNPFp series

9.2.2.2.2 Dielectric loss

Loading-dependence of ε" of PPy filled and F-PPy filled composites in S band frequencies is depicted in Fig. 9.8. The behaviour is same as that of NP and NPFp series. Dielectric loss is found to increase with PPy loading and F-PPy loading due to increased mobility of charge carriers. Increase in frequency also increases dielectric loss, in the case of LNP series. The gum compound LNP0 offers a very low dielectric loss (0.02) while dielectric loss as high as 27 is achieved by LNPFp3.

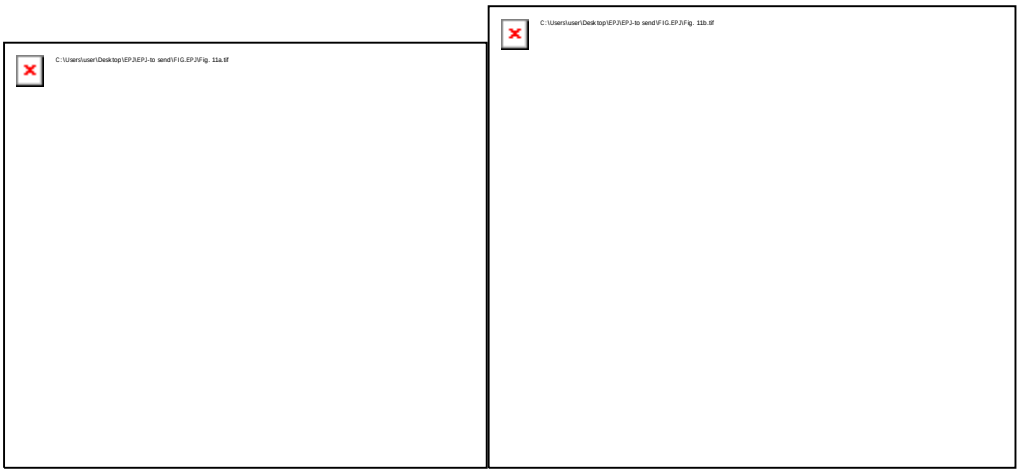

Fig.9. 8 Variation of dielectric loss with loading of (a)LNP, (b)LNPFp series

9.2.2.2.3 AC conductivity

The microwave conductivity is a direct function of dielectric loss and hence the Fig. 9.9, showing the variation of the AC conductivity (S/m) of composites with PPy and F-PPy loading at different frequencies, have the same nature as that of the dielectric loss factor. Lower threshold and higher AC conductivity are exhibited by fiber filled composites. Maximum conductivity 3.4 S/m is obtained for LNPFp3 at a frequency 3.98 GHz.

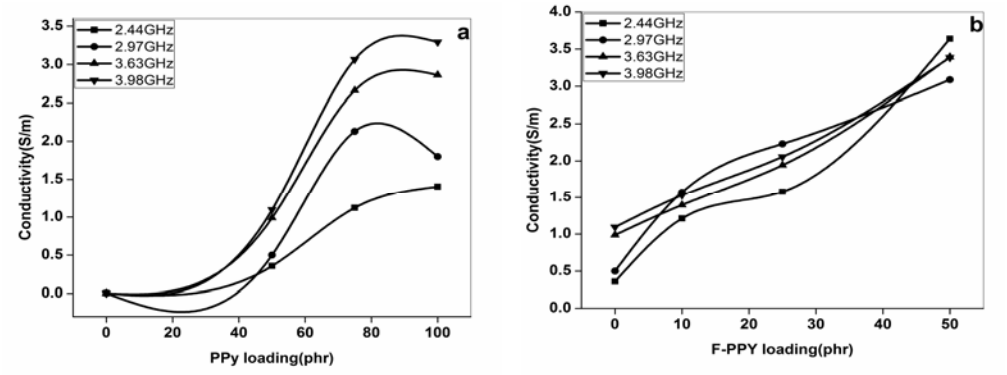

Fig. 9.9 Variation of conductivity with loading of (a)LNP, (b)LNPFp series

9.2.2.2.4 Absorption coefficient

The variation of absorption coefficient with frequency and filler loading is same as that for AC conductivity as is evident from fig. 9.10. It is clear that the absorption coefficient increases with increase in frequency and also with filler loading and maximum absorption coefficient value is obtained for LNPFp3 at 3.98 GHz frequency.

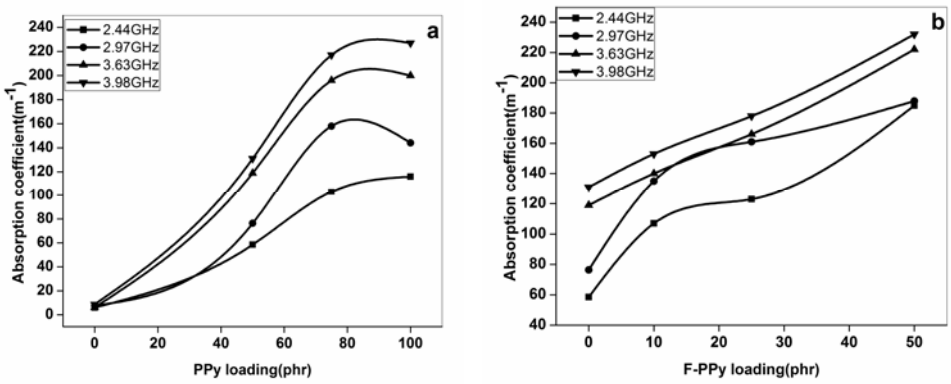

Fig. 9.10 Variation of absorption coefficient with loading of (a)LNP, (b)LNPFp series

9.2.2.2.5 Skin depth

From fig.9.11 it is clear that increased frequency and increased loading decreases the skin depth and the lowest value of skin depth is for the CEC, LNPFp3 at 3.98GHz frequency.

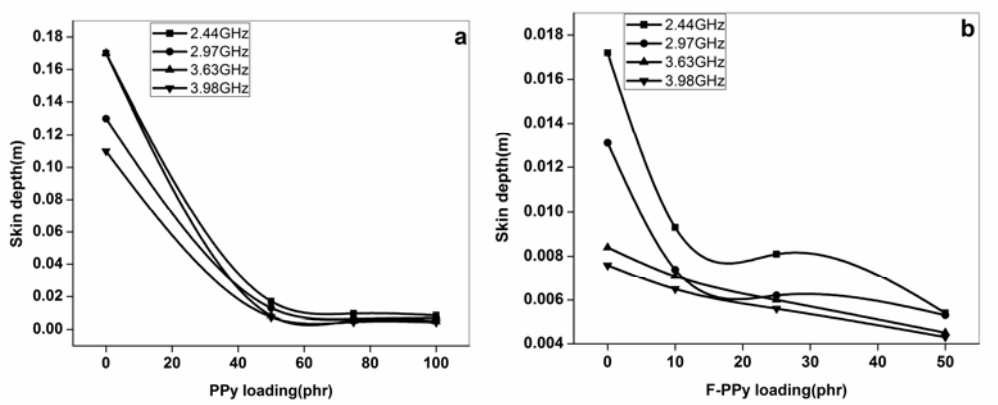

Fig.9. 11 Variation of skin depth with loading of (a)LNP, (b)LNPFp series

9.2.2.2.6 Dielectric heating coefficient

Fig.9.12 shows the variation of dielectric heating coefficient (J) with frequency and with loading. It is observed that the heating coefficient decreases with frequency and also with filler loading. J value is found to be the lowest for LNPFp3 at 3.98GHz frequency. At 3.98GH the heating coefficient of gum vulcanizate is 46 while the CEC, LNPFp3 gives a value as low as 0.06.

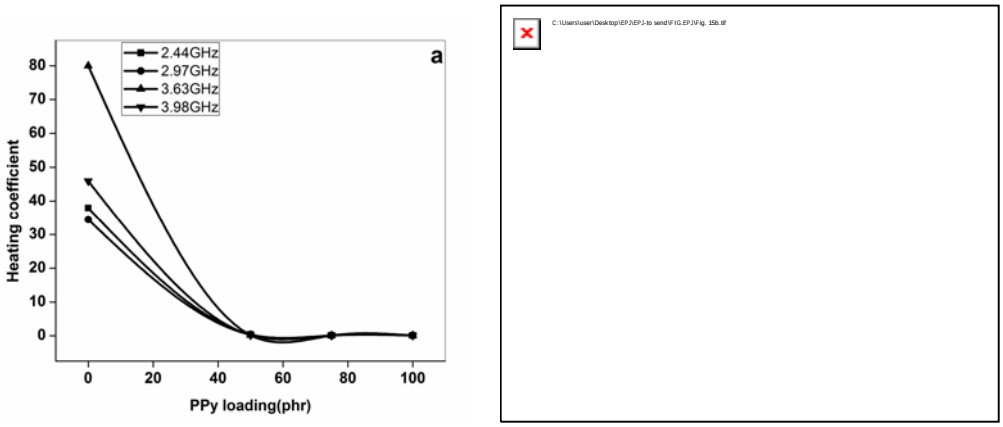

Fig. 9.12 Variation of heating coefficient with loading of (a) LNP, (b)LNPFp series

9.2.2.3 NBR based CECs

9.2.2.3.1 Dielectric permittivity

The variations of dielectric permittivity (ε') of NBR with PPy loading and F-PPy loading in S band frequency are shown in Figures 9.13(a) and 9.13(b) respectively. It has been shown that ε' is almost constant regardless of applied frequency for BP series especially BPO and BP2. Therefore in these the polarization mechanisms contributing to ε' may be electronic and ionic. For BP3 and BP4 there is a slight increase in ε' with frequency which can be attributed to the contribution due to increased dipolar polarization arising from increased PPy content. When it comes to BFp series, PPy coated fibers contribute more conducting regions in the system, leading to increase in space charge polarization which depend more on the frequency of applied field. The observed decrease in ε' with increasing frequency in the case of BFp series may be attributed to the decrease in space charge polarization with increasing frequency. This behavior is in accordance with Maxwell-Wagner interfacial polarization as explained under section *9.2.2.1.1.*

ε' increases substantially with PPy loading due to increase in DC conductivity of NBR based composites with loading (section 6.3.5). A dielectric permittivity of 43 is obtained for 75 phr PPy loaded composite (BP3) at 3.98 GHz frequency. Incorporation of F-PPy causes an increase in ε', reaches maximum at 50phr loading and then decreases. This is in accordance with DC conductivity values. At 50phr F-PPy loading maximum conductivity is attained. Further loading does not bring about any increase in conducting regions and therefore in space charge polarizability.

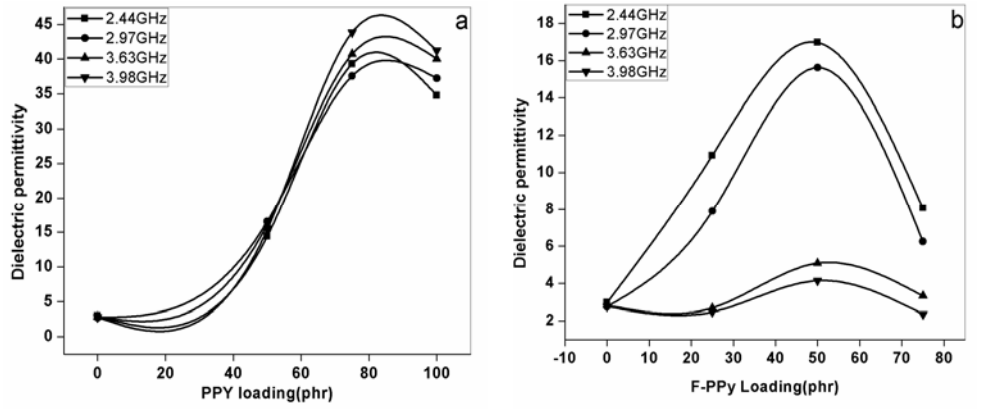

Fig. 9.13 Variation of dielectric permittivity with loading of (a)BP, (b)BFp series

9.2.2.3.2 Dielectric loss

Loading dependence of ε" of PPy filled and F-PPy filled NBR composites in S band frequencies is depicted in Fig. 9.14. Dielectric loss is found to increase with PPy loading due to increased mobility of charge carriers while frequency has little effect on ε" except at higher loading. In the case of BFp series, dielectric loss increases with loading, reaches a maximum at 50phr loading and then decreases.

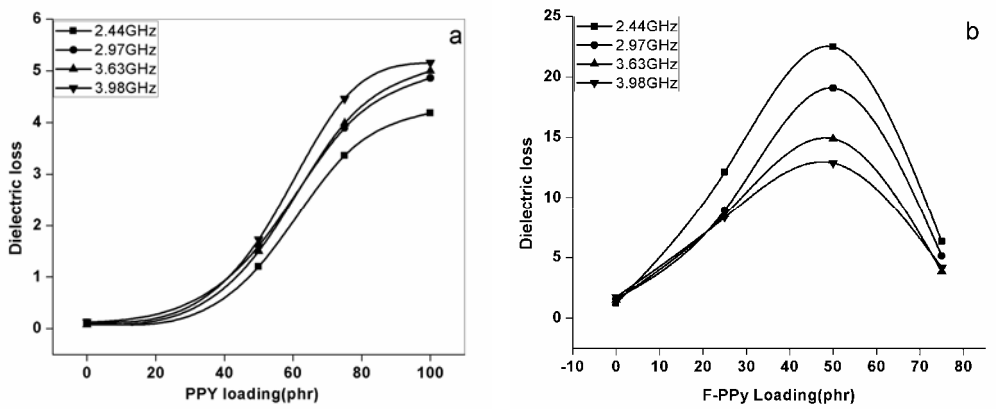

Fig. 9.14 Variation of dielectric loss with loading of(a)BP, (b)BFp series

9.2.2.3.3 AC conductivity

Fig. 9.15 showing the variation of the AC conductivity (S/m) of composites with PPy and F-PPy loading at different frequencies, have the same nature as that of the dielectric loss factor. The reason for lower threshold and higher AC conductivity of fiber filled composites compared to PPy filled composites is as given in section *9.2.2.1.3***.** Maximum conductivity 3.1S/m is obtained at 50phr F-PPy loaded sample at a frequency 2.97GHz.

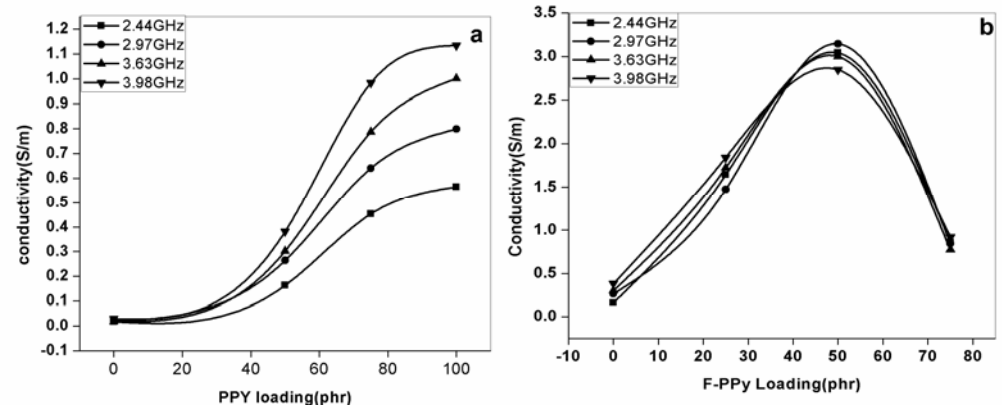

Fig.9. 15 Variation of conductivity with loading of(a)BP, (b)BFp series

9.2.2.3.4 Absorption Coefficient

Since microwave conductivity and absorption coefficient are direct functions of dielectric loss, the variation of absorption coefficient with frequency and filler loading is same as that for AC conductivity as is evident from Fig. 9.16. It is clear that the absorption coefficient increases with increase in frequency and also with filler loading and maximum absorption coefficient value is obtained for 50 phr F-PPy loaded composite.

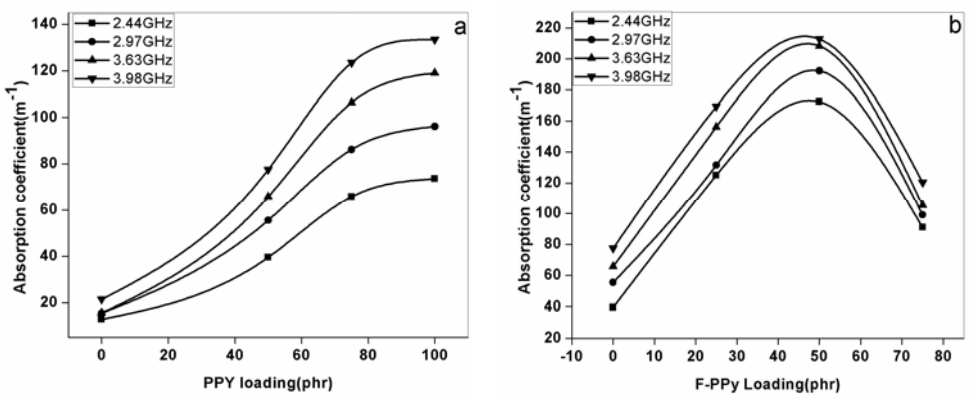

Fig. 9.16 Variation of absorption coefficient with loading of(a) BP, (b)BFp series

9.2.2.3.5 Skin depth

Variation of skin depth of BP and BFp series with frequency and with loading are depicted in fig. 9.17. It is clear that the skin depth decreases with frequency and with loading and lowest value of skin depth is for the 50 phr F-PPy loaded NBR.

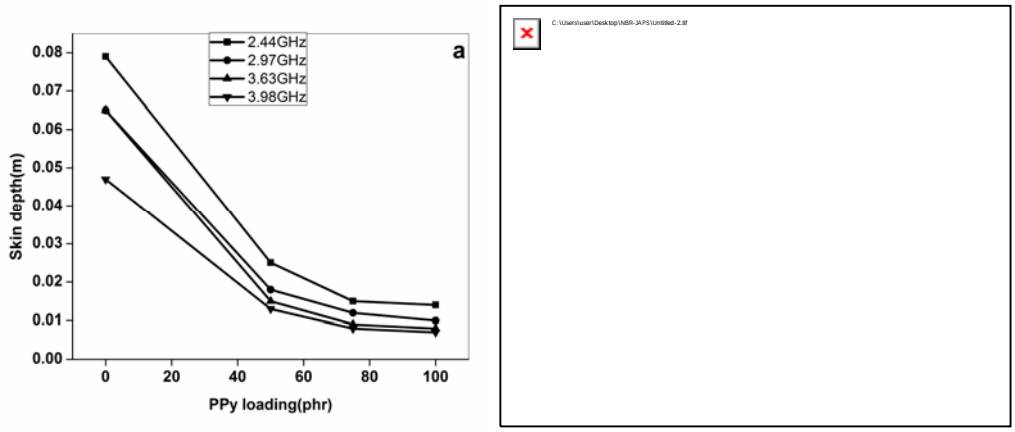

Fig. 9.17 Variation of Skin depth with loading of (a)BP, (b)BFp series

9.2.2.3.6 Dielectric heating coefficient

From fig. 9.18 it is observed that the heating coefficient decreases with frequency and also with filler loading. The heat developed is proportional to both frequency and the product of ε and tan δ. Higher the J value poorer will be the polymer for dielectric heating purpose. In the present study J value is found to be the lowest for 50phr F-PPy loaded sample.

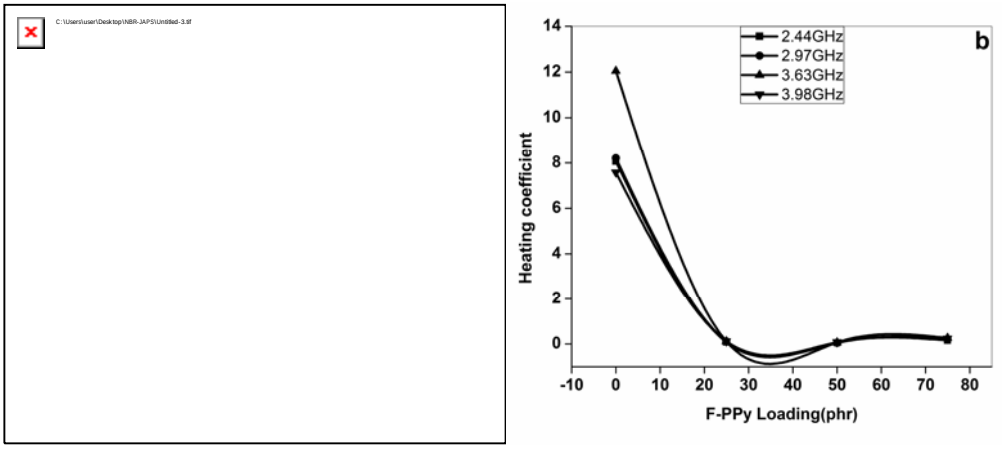

Fig.9.18 Variation of heating coefficient with loading of(a)BP,(b)BFp series

Part-II

9.3 Electromagnetic interference shielding effect

9.3.1 Experimental

The shielding effect (SE) is a number that quantifies the amount of attenuation typical of a particular material [66]. It is measured as the ratio of the output energy to the input energy across the shielding material, expressed in decibels (dB), and is calculated according to [67,68]

$$SE=10 \log_{10}(P_{trans}/P_{inc}) \quad \text{---------- (9.11)}$$

Where P_{inc} is the incident power density at a measuring point before shield is in place and P_{trans} is the transmitted power density at the same measuring point after shield is in place. If, P_{ref} is the reflected power density at the same measuring point, then reflection loss, RL which is a measure of the amount of electromagnetic wave reflected is given as

$$RL= 10 \log_{10}(P_{ref}/P_{inc}) \quad \text{---------- (9.12)}$$

SE is related to RL. Lower the reflection loss, better is the shielding effectiveness, since a lesser amount of incident wave is reflected [69]. From equation 9.11 an attenuation of the incident beam by a factor of 100 (i.e.,1% transmission) is equivalent to 20 dB of SE. When electromagnetic radiation is incident on a slab of material, the absoptivity (A), reflectivity (R) and transmissivity (T) must sum to the value one.

$$\text{i.e., } T+R+A=1. \quad \text{---------- (9.13)}$$

The total EMI shielding effectiveness (SE_{total}) is the sum of contributions from absorption (SE_A), reflection (SE_R) and multiple reflection (SE_M)[25,68,70, 71]

$$SE_{total}=SE_A+SE_R+SE_M \quad \text{---------- (9.14)}$$

The absorption loss is due to the energy dissipation while the electromagnetic wave interacts with the material. It is caused by the heat loss under the action between electric dipole and magnetic dipole in the shielding material and the electromagnetic field. Reflection loss arises due to the impedance mismatch between air and the sample at the frequency of interest. It is the result of interaction between conducting particles in the conducting material and the electromagnetic field. Larger the conductivity and smaller the magnetic permeability, larger the reflection loss will be. This mechanism plays a major role in producing loss in EMI SE mechanisms. Multiple reflection loss arises due to the inhomogeneity within the material. It occurs due to re-reflection from the shield. This loss is very low and is the correction term for the reflection loss [72]. It is usually assumed that $SE_{total} \approx SE_A+SE_R$ (i.e.,SE_M is neglible).

EMI shielding measurements were carried out in S (2-4 GHz) band and X(8-12 GHz) band frequencies using wave-guides coupled to a ZVB20 vector network analyzer (fig.2.3). The wave-guides were of dimensions 2.3cm× 1cm× 13.5cm for X band and 7.2cm × 3.4cm× 35.2 cm for S band. The two test port cables of the network analyzer were connected via two wave-guide to coaxial adapters. The photographs of the X and S band waveguides are shown in figs. 2.4(a) and 2.4(b) respectively. The sample was placed between the two sections of the waveguide and the output recorded. The output from the vector network analyzer is in terms of scattering parameters, S_{xy}. The first number in the suffix refers to what port the output is measured at and the second number refers to where the signal originate from. Hence S_{11} is the reflected signal and S_{21} is the transmitted signal. Shielding efficiency of the sample can be calculated from

S_{21}. Knowing reflectivity(R) and transmissivity(T), absorptivity(A) can be calculated using the relation, A=1−T−R.

9.3.2 Results and discussion

Figs. 9.19(a) and (b) represent variation of shielding efficiency with S band frequency of NP and NFp series. For NP series there is only a nominal increase in SE on addition of 50phr PPy(NP2). On increasing the PPy loading to 75 phr(NP3) there is a sudden increase in SE. A maximum of 12.5 is obtained for 100phr PPy loaded CEC, NP4. Increase in SE with increased loading of PPy is due to increase in DC conductivity. In the case of NFp series, increase in shielding effect is observed at very low loading, 5phr PPy coated fiber. Further additions do not have much effect on SE. These observations are similar to the trend seen in variation of DC conductivity of NFp series(Fig. 4.9). For NP series in X band (Fig. 9.20(a)), at 50phr PPy loading, there is substantial increase in SE from 7.8dB to 16.2dB. There is not much increase on further additions, and the maximum value attained is 19.8 for NP4. For NFp series in X band a gradual increase is observed with a maximum of 15.4 dB at 50phr F-PPy loading(Fig. 9.20(b)).

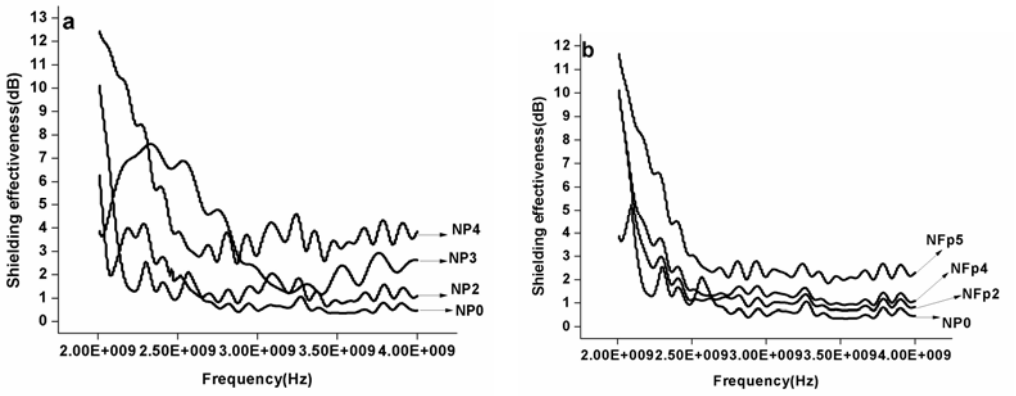

Fig. 9.19 Variation of shielding effectiveness with frequency(S band) of (a)NP, (b)NFp series

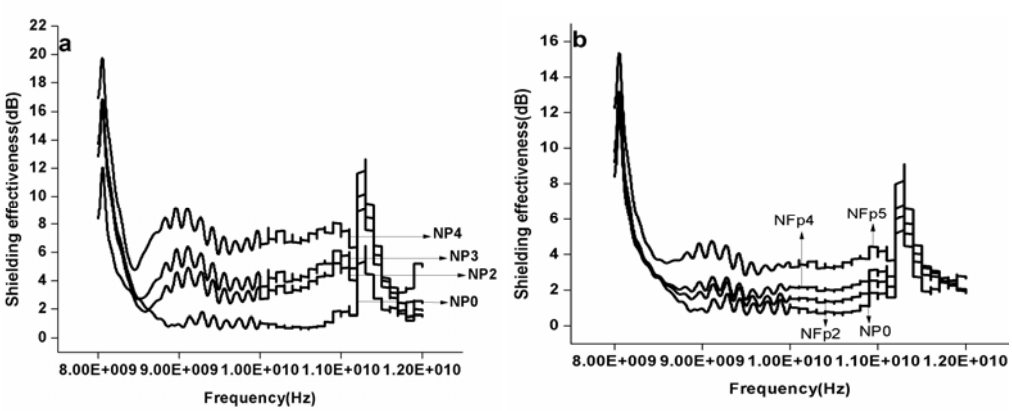

Fig. 9.20 Variation of shielding effectiveness with frequency (X band) of (a)NP, (b)NFp series

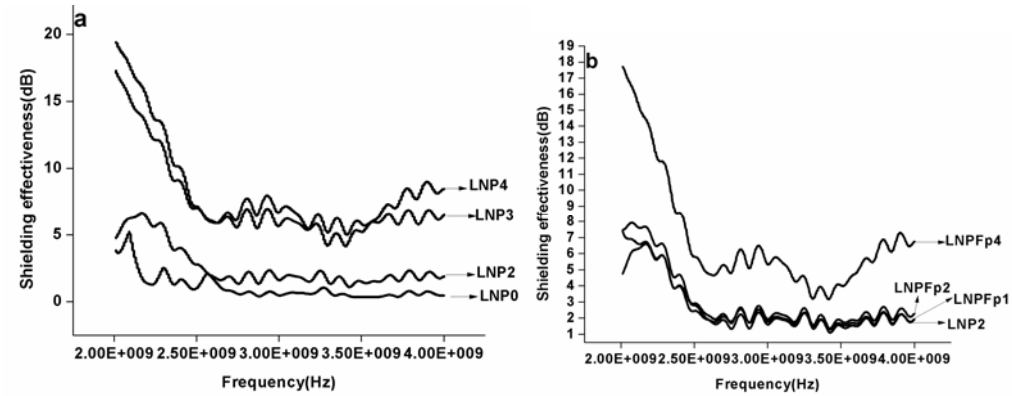

Fig. 9.21 Variation of shielding effectiveness with frequency(S band) of (a)LNP, (b)LNPFp series

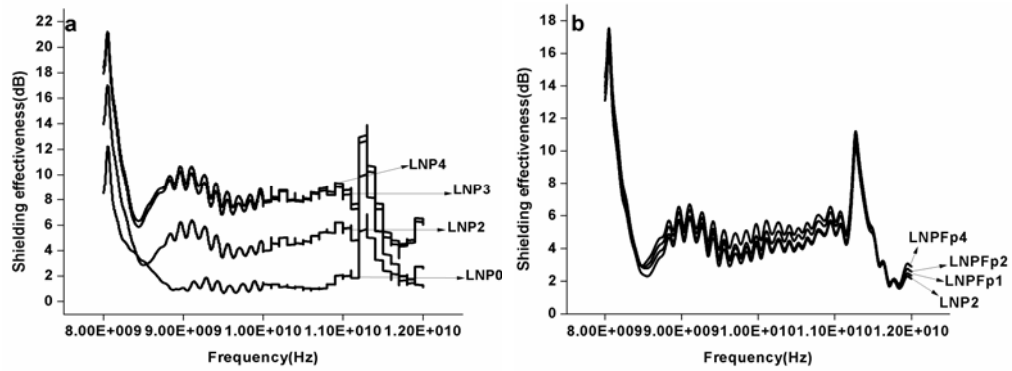

Fig. 9.22 Variation of shielding effectiveness with frequency(X band) of (a)LNP, (b)LNPFp series

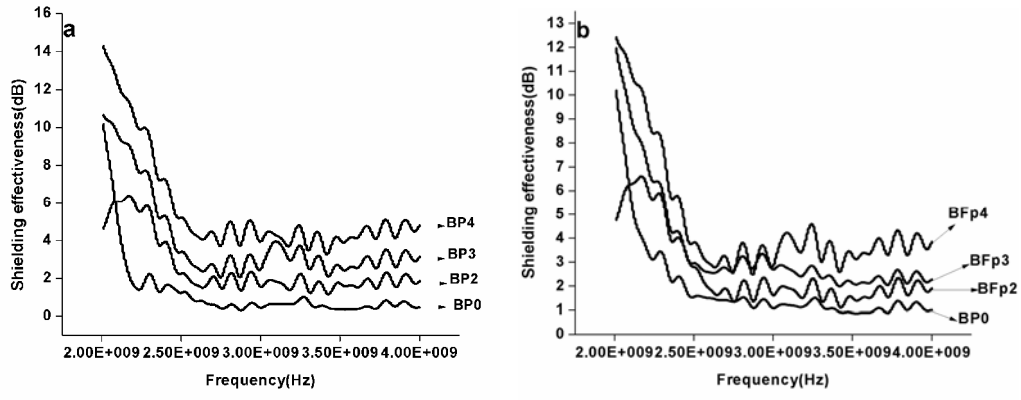

Fig. 9.23 Variation of shielding effectiveness with frequency (S band)of (a)BP, (b)BFp series

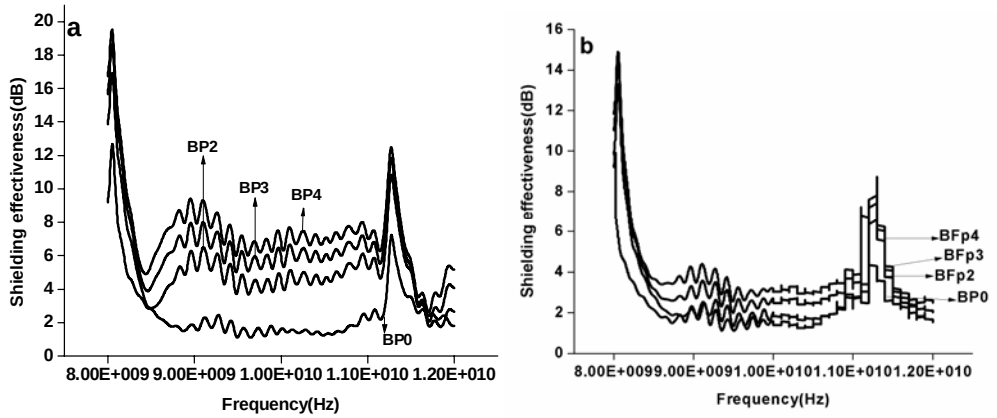

Fig. 9.24 Variation of shielding effectiveness with frequency(X band) of (a)BP, (b)BFp series.

The EMI shielding effectiveness of NR/PPy and NR/PPY/F-PPy composites prepared by *in situ* polymerization in latex, in the frequency range 2-4GHz is shown in figs.9 21(a) and (b) and in the frequency range 4-8GHz is shown in figs. 9 22(a) and (b). The variations are similar to that of NR based composites prepared by dry rubber compounding except that the SE values are higher when the composites are prepared by *in situ* polymerization method. This may be attributed to the enhanced DC conductivity of composites

prepared by *in situ* method. Among LNP and LNPFp series, the maximum SE is observed for LNP4, 19.5dB in S band and 21.2dB in X band. The Highest shielding effectiveness among LNP and LNPFp series in S band are recorded by LNP4 (19.5 dB) and LNPFp4(17.7 dB) respectively at 2 GHz. In X band frequencies also the same composites exhibit maximum SE, the values being 21.2 dB and 17.7 dB respectively at 8 GHz.

The shielding efficiency of NBR/PPy composites increases with PPy loading in S and X band frequencies (Figs. 9.23(a) and 9.24(a)). There is appreciable increase in SE of the gum NBR on 50 phr PPy incorporation(BF2) in X band: i.e, from 9.5dB to17dB. Among BP series the maximum SE attained is 19.6 dB for the 100phr PPy loaded sample, BP4 in X band. The SE of NBR /F-PPy systems vs frequency is presented in figs. 9.23(b) and 9.24(b). In this case 25phr F-PPy loaded sample has a sudden increase in SE in both S and X band frequencies, after which there is only a nominal increase. PPy loaded and F-PPy loaded NBR show increase in DC conductivity(section6.3.5) which enhances their shielding effectiveness. Among BP series, BP4 gives maximum SE of 13.7dB, at 2 GHz in S band and 19.6 dB at 8 GHz in X band. BFp4 exhibits maximum SE among BFp series and has a value 12dB in S band and 14.9dB in X band.

Comparing figures 9.19 to 9.24 with figures representing variation of DC conductivity with loading (Figs. 4.3.5, 5.3.5 and 6.3.5), the direct relationship between the conductivity and SE can be followed. With increased loading and hence conductivity, SE increases. This can be explained as follows [73]: when a conductive filler is incorporated into an insulating matrix, initially conductive filler agglomerates are isolated by insulating polymer matrix, so the conductivity of the composites is nearly equal to that of the base

polymer. With increasing filler loading, the fillers more easily touch each other or are close enough to allow the electrons to hop across gaps between the fillers and a drastic change occurs in the electrical conductivity or a breakdown in its resistivity that is the threshold percolation concentration is reached. At this concentration, the conductive filler forms a continuous conductive network through which electrons are moved. When the conductive network structure of the conductive filler is formed, the electromagnetic wave can be shielded better than the composites having many discontinuity points at which the filler aggregates. This observation is in good agreement with other published results on EMI SE of PPy coated fabrics and composites. Avloni J *et al*.[74]have discussed attenuation of electromagnetic waves with PPy coated polyester fabrics. They found that as the electrical DC resistance increases, reflectivity decreases and SE decreases. SE up to 37 was obtained for a surface resistance 3Ω cm, while it became 16dB when the resistance was 40Ω cm. They concluded that increase of EMI SE with electrical conductivity results from the increase in shielding by reflection, due to decrease in surface resistivity. A high reflection coefficient is due to a shallower skin depth of the composites with high electrical conductivity. For the composites prepared here, as loading and thus conductivity increases, skin depth decreases as is evident from sections 9.2.2.1.5, 9.2.2.2.5, 9.2.2.3.5. As skin depth decrease, reflection coefficient increases leading to an increase in shielding effectiveness. Kim *et al*. [75] have reported variation of SE with specific volume resistivity of PPy/PET woven fabric. The specific volume resistivity of composites prepared by them was extremely low as 0.2Ω cm and SE was about 36dB over a wide frequency range upto 1.5GHz. EMI SE gradually increased from 13 to 26dB with decrease of specific volume resistivity in the region from 2.85 to 0.75Ω cm

and then more steeply increased to 36dB below 0.75Ω cm, which is due to increase of the conductivity towards a metallic conductivity. The results also agrees with relationship between SE and electrical conductivity of PPy composites [76] and for other conducting systems such as polyaniline films [18] and polyaniline/polymer composites [77].

The SE depends not only on the conductivity, but also on the reflection and absorption coefficient of the dispersed filler. To evaluate the role of reflection and absorption in the shielding effectiveness of the prepared composites, the reflectivity, absorptivity and transmittivity of the composites were calculated as described in section 9.3.1. and as an illustration, the shielding contributions from reflection and absorption in S band frequencies are plotted against loading for NP, LNP and BP series (figs. 9.25, 9.26, 9.27).

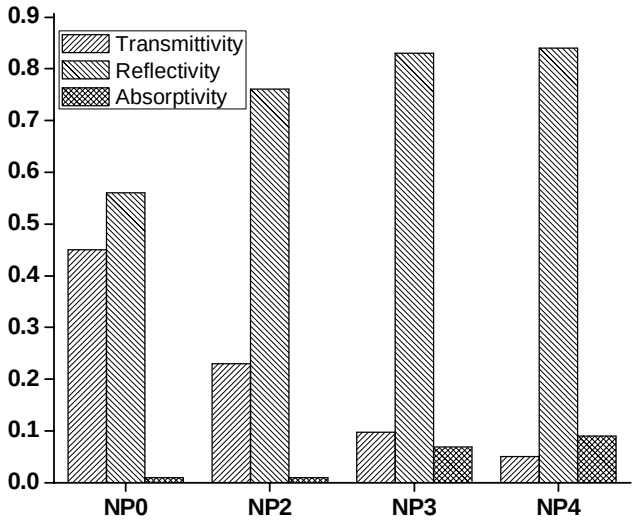

Fig. 9.25 Transmittivity, Reflectivity and Absorptivity of NP series at 2GHz frequency

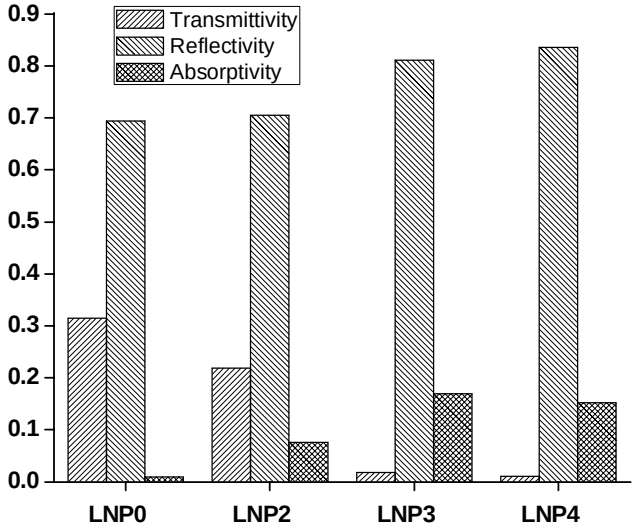

Fig. 9.26 Transmittivity, Reflectivity and Absorptivity of LNP series at 2GHz frequency

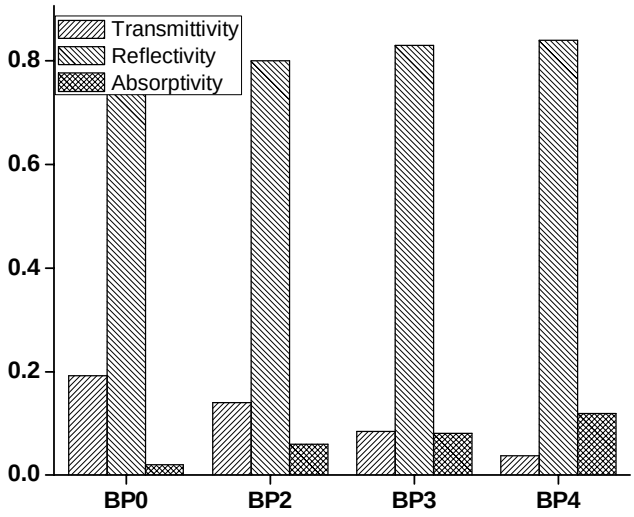

Fig. 9.27 Transmittivity, Reflectivity and Absorptivity of BP series at 2GHz frequency

The figures show that there is substantial decrease in transmittivity while increase in reflectivity and absorptivity of the conducting elastomer composites compared to gum compound. Kim *et al.* [35] found that PET fabric/polypyrrole

composite shielded EMI by absorption as well as by reflection and that EMI shielding through reflection increased with the electrical conductivity. When electromagnetic radiation encounters a material interface, some of the radiation is reflected and some is transmitted. Radiation entering the material may be absorbed if the material properties allow. An insulating material will generally transmit almost all the radiation not reflected from the surface, and a very highly conductive material (eg. metal) reflects almost all radiation [35]. In medium level conductivity materials a large part of radiation is absorbed in the material and lost as heat. The conducting polymer composites investigated in this work both reflect and absorb radiation and they can act as efficient shields of electromagnetic radiation. Even though the composites with lower SE cannot be used for shielding of electromagnetic waves, studies have shown that such composites can be used for the static charge dissipation [28,30]. Hence the CECs with lower SE may be used for the dissipation of static charge.

9.4 Conclusions

Microwave properties of the conducting elastomer composites based on NR,NBR and that prepared by *in situ* polymerization in NR latex were studied in S band (2-4 GHz) frequency using cavity perturbation technique. The absolute value of the dielectric permittivity, AC conductivity and absorption coefficient of the conducting composites prepared are much greater than the gum vulcanizates. PPy and F-PPy reduce the dielectric heating coefficient and skin depth significantly. Dielectric permittivities 35, 55.5 and 43 are obtained for the composites NPFp5, LNPFp3 and BP3 respectively. The electromagnetic interference shielding effectiveness of the CECs in the S band (2-4 GHz) and X band (7-13 GHz) frequencies were evaluated. The CECs have appreciable shielding effect depending on loading of PPy and F-PPy and in turn the conductivity.

References

[1] Dhawan SK, Singh N, Venkitachalam S. *Synth Met*. **2002**, 129, 261.

[2] Das NC, Yamazaki S, Hikosaka M, Chaki TK, Khastigir D, ChakrabortyA. *Polym Int*. **2005**, 54, 256.

[3] Baibarac M, Romero G, Pedro. *J of Nanoscience and Nanotechnology*.**2006**, 6,2,289.

[4] John H, Joseph R, Mathew KT. *J Appl Polym Sci*. **2007**, 103, 2682.

[5] Nalwa HS, *Handbook of organic conductive molecules and polymers, vol.3, (Ed.), John Wiley and sons*. **1997**.

[6] Saville P. *Review of radar absorbing materials. DRDC Atlantic TM 2005-003, DRDC Atlantic*.**2005**.

[7] Unsworth J, Conn C, Jin Z, Kaynak A, Ediriweera R, Innis PC, Booth N.*J Intell Mater Syst Struct*. **1994**, 5, 595.

[8] Rupich MW, Liu YP, Kon AB. *Mater Res Soc Symp Proc*. **1993**, 293, 163.

[9] Faez R, Martin IM, De Paoli M, Rezende MC. *J Appl Polym Sci*. **2001**, 83, 1568.

[10] Duan Y, Liu S, Wen B, Guan H Wang G. *J Compos Mater*. **2006**,40, 1841.

[11] Rmili H, Miane JL, Zangar H, Olinga TE. *Eur Phys J Appl Phys*. **2005**,29, 65.

[12] Gangopadhyay R, De A, Ghosh G. *Synth Met*. **2001,** 123, 529.

[13] Murugesan R, Subramanian E, *Bull Mater Sci.* **2003,** 26, 529.

[14] Tanwar A, Gupta K K, Singh P J, Vijay Y K. *Bull Mater Sci.* **2006,** 29, 181.

[15] Yang J, Hou J, Zhu W, Xu M, Wan M. *Synth Met*.**1996**, 80, 283.

[16] Yoon CO, Reghu M, Moses D, Cao Y, Heeger AJ. *Synth Met*. **1995,** 69, 255.

[17] Maeda T, Sugimoto S, Kagotani T, Tezuka N, Inomata K. *J Magn Magn Mater*. **2004**, 281,195.

[18] Chanderasekhar P, Naishadhan K. *Synth Met*. **1999,** 105, 115.

[19] Olmedo L, Hourquebie P, Jousse F. *Adv Mater*. **1993**, 5, 373.

[20] Joo J, Epstein AJ. *Appl Phys Lett*. **1996**, 68, 894.

[21] Dhawan SK, Trivedi DC. *J Electromagnet Compat*. **1991**, 1, 1.

[22] Barnes A, Despotakis A, Wright PV, Wong TCP, Chambers B, Anderson AP. *Electron Lett*. **1996**, 32, 358.

[23] Joo J, Lee CY. *J Appl Phys*. **2000**, 88, 513.

[24] Chung DDL. *Carbon*. **2001**, 39, 279.

[25] Colaneri NF, Shacklette LW. *IEEE Trans Instrum Meas*.**1992**, 41, 291.

[26] Wojkiewicz JL, Fauveaux S, Redon N, Miane JL. *Int J Appl Electrom*. **2004**, 19, 203.

[27] Wojkiewicz JL, Fauveaux S, Miane JL. *IEEE Seventh International Conference on Solid Dielectrics, Eindhoven, Netherlands*. **2001**, p. 46.

[28] Dhawan SK, Singh N, Rodrigues D, *Sci Technol Adv Mater*. **2003**, 4, 105.

[29] Koul S, Chandra R, *Antec 2004 Plastics; Annual Technical Conference*, **2004**, 3, 3039.

[30] Koul S, Chandra R, Dhawan SK, *Polymer*, **2000**, 41, 9305.

[31] Costa LC, Henry F,Valente MA, Mendiratta SK, Sombra AS, *Eur Polym J*. **2002,** 38, 1495.

[32] Williams N, Varadan VK, Ghodgaonkar DK, Varadan VV. *IEEE Trans Electromagn Compat.* **1990**, 32 , 236.

[33] Lafosse X. *Synth Met*. **1995,** 68, 227.

[34] Hakansson E, Amiet A,Nahavandi S, Kayanak A. *Eur Polym. J*. **2007**, 43, 205.

[35] Kim HK, Kim MS, Chun SY, Park YH, Jeon BS, Lee JY.*Mol Cryst Liq Crys*. **2003**, 405, 161.

[36] Hakansson E, Amiet A, Kayanak A. *Synth Met*. **2006**, 156, 917.

[37] JiaW, Tchondakov K, Segal E, Joseph R, Narkis M, Siegmann A. *Synth Met*. **2003**, 132, 269.

[38] Chan HSO, Hopok H, Khor E, Tan MM, *Synth Met*. **1995**, 31, 95.

[39] Mc Crum NG, Read BE, Williams G, *Anelastic and Dielectric Effects in Polymeric Solids*, *Dover: New York*. **1967.**

[40] Avakian P, StarkweatherJr HW, Kampert WG. *Dielectric analysis of polymers. In: Hand book of Thermal Analysis and Calorimetry*. **2002**, 3, 147.

[41] Nagai KL, Tendell RW, Skotheim TA, Eds., *Handbook of Conducting Polymers*, *Marcel Dekker: New York*. **1986.**

[42] Feldblum A, Park YW, Heeger AJ, MacDiarmid AG, Wnek G, Karasz F, Chien, J.C.W. *J Polym Sci Polym Phys Edn*. **1981**, 19, 173.

[43] Phillips G, Suresh R, Waldman J, Kumar J, Chen JI, Tripathy S, Huang JC. *J Appl Phys* .**1991**, 69, 899.

[44] Unsworth J, Kaynak A, Lunn BA, Beard GE. *J Mater Sci*. **1993**, 28, 3307.

[45] Li N, Huang Y, Du F, He X, Lin X, Gao H, Ma Y, Li F, Chen Y, Eklund P C. *Nano Lett.* **2006**, 6, 1141.

[46] Nakamura E, Furuichi J. *J Phys Soc Japan*. **1960**, 15, 1955.

[47] Champlin KS, Krongard RR. *IRE Trans Microwave Theory Tech*. **1961**, MTT9, 545.

[48] Kupfer K, Kraszewski A, Knooche lR. *In Sensors Update*, *Wiley-VCH: Weinheim,* **2000**, 7, 186.

[49] Ku CC, Liepins R. *Electrical properties of polymers: Chemical principles*, *Hansen Publishers, Munich*. **1987**, 92.

[50] Ezquerra TA, Kremmer F, Wegner G. *Dielectric properties of heterogeneous materials*: *Progress in electromagnetic research*. *Vol.6, Elsevier, New York*. **1992**.

[51] Bradford LS, Carpentier MH. *The Microwave Engineering Hand Book, Chapman& Hall, London.* **1993**.

[52] Stephen CW, Frederic HL. *Microwaves made simple: Principles and applications. United States Book crafters, Chelsea*. **1985**.

[53] Abbas SM, Chandra M, Verma R, Chatterjee R, Goel TC. *Composites Part A*. **2006**, 37, 2148.

[54] Dunia KM, Al-Nasrawy. *J Electron Devices*. **2011**, 9, 409.

[55] Soloman MA, Kurian P, Anantharaman MR, Joy PA. *J Appl Polym Sci*. **2003**, 89, 769.

[56] Koops, CG. *Phys. Rev*. **1951**,83, 121.

[57] John H. *Ph. D Thesis, Cochin University of Science and Technology, India*. **2003**

[58] Chandran AS. *Ph. D Thesis, Cochin University of Science and Technology, India.***2008**

[59] Bishay IK, Abd-El-Messieh SL, Mansour SH. *Meter Des*. **2011**, 32, ,62.

[60] Maxwell JC. *A treatise on electricity and magnetism vol.1,Oxford University Press*. **1892.**

[61] Sillars RW. *IEEE J*. **1937**, 80, 371.

[62] Reffaee ASA, Nashar DEL, Abd-El-Messieh SL, Nour KNA, *Mater Des*. **2009,** 30, 3760.

[63] Mac Callum RJ, Vincent CA. *Polymer electrolyte reviews II, Elsevier Applied Science Publishers Ltd, London and New York, chapter 2.* **1987**.

[64] Kyritsis A, Pissis P, Grammatikakis J. *J Polym Sci Part B*. **1995**, 33, 1737.

[65] Moucka R, Mravcakova M, Vilcakova J, Omastova M, Saha P. *Mater Des*. **2011**, 32, 2006.

[66] Donald RJ White, Michel Mardiguian. *Electromagnetic Compatibility Handbook*. V-3, *Don White Consultants, Inc.* **1981**.

[67] Ott HW. *Noise reduction techniques in electronic systems*, *Wiley, New York. 2nd ed*. **1988**.

[68] Hund E. *Microwave communications Components and circuits. McGraw Hill, New York*.**1989**.

[69] Barba AA, Lamberti G, Matteod'Amore, Domenico Acierno. *Polym Bull*. **2006,** 57, 587.

[70] Joo J, Epstein AJ. *Appl Phys Lett*. **1994**, 65, 2278.

[71] Schulz RB. *IEEE Trans Elec comp.***1968**, EMC-10, 95.

[72] Kayanak A. *Mater Res Bull*. **1996**, 31, 845.

[73] Das NC, Khastgir D, Chaki TK, Chakraborty A. *J Elast Plast.* **2002**, 34, 199.

[74] Avloni J, Florio L, Henn AR, Lau R, Ouyang M, Sparavigna A. *PACS numbers: 72. 80.Le, 73.25.+i*

[75] Kim MS, Kim HK, Byun SW, Jeong SH, Hong YK, Joo JS, Song KT, Kim JK, Lee CJ, Lee JY. *Synth Met.* **2002**, 126, 233.

[76] Kuhn HH, Child AD, Kimbrell WC. *Synth Met.* **1995**, 71, 2139.

[77] Wessling B, *Synth Met.* **1998**, 93, 143.

.....ooo.....

Chapter

10

SUMMARY AND CONCLUSIONS

The intrinsically conducting organic polymers that possess the electronic, magnetic, electrical and optical properties of a metal have been attracting the attention of countless of group of researchers all over the world because of their potential applications in modern technology. Amongst conducting polymers, polypyrrole (PPy) is one of the most studied one because of its high electrical conductivity, environmental stability and ease of synthesis. However, the principal problems with the practical utilization of polypyrrole include its undesirable mechanical properties like high brittleness and low processability. To overcome PPy's drawbacks of poor mechanical properties and processability, incorporating PPy within an electrically insulating polymer appears to be a promising method, and this has triggered the development of conducting polymer blends or composites. Natural and synthetic rubbers, polyolefins, polystyrene, polycaprolactone, polyethylene glycol, polyvinyl acetate etc. are some among the polymers forming composite materials with PPy.

Conductive elastomer composites (CECs) of polypyrrole are important in that they are composite materials suitable for devices where flexibility is an important parameter. Moreover these composites can be moulded into

complex shapes. Electrically conductive vulcanized rubber finds application in fuel hoses, spark plug cables and high voltage cable insulations. A survey of literature reveals that the studies on PPy incorporated elastomer composites are rather scarce. In the works reported, it can be seen that even though the processability and mechanical properties of polypyrrole are enhanced, the composites never attained the strength of the host polymer matrix as there was deterioration of properties of polymer by the incorporation of PPy. If PPy is adhered to a strong substrate and then used as a filler in polymer matrix, improvement in mechanical properties is expected.

In the present work the incorporation of Nylon-6 fiber as filler for improving the mechanical properties of conducting elastomer composites based on PPy is explored. Since the introduction of Nylon fiber, an insulating material, tends to affect the conductivity of the composite, PPy coated Nylon fiber was used. The use of PPy coated fiber was expected to improve the mechanical properties of the elastomer composites of PPy, at the same time increasing the DC conductivity.

Pyrrole was polymerized in the presence of anhydrous ferric chloride as oxidant and p-toluene sulphonic acid as dopant. PPy coated short Nylon fibers were prepared by polymerizing pyrrole in the presence of short Nylon fibers of 6mm length. The coating conditions were optimized to get a uniform coating of PPy on Nylon. Scanning electron microscopic studies revealed a dense uniform coating of PPy on Nylon fiber. The prepared PPy coated fiber found application as a strain sensor.

PPy and PPy coated short Nylon fiber (F-PPy) were used to prepare rubber composites based on natural rubber (NR) and acrylonitrile butadiene

rubber (NBR) by proper compounding on a two roll mill followed by moulding. NR/PPy/F-PPy composites were also prepared by *in situ* polymerization of pyrrole in NR latex, containing short Nylon fibers of 6mm length, using anhydrous ferric chloride as oxidising agent, *p*- toluene sulphonic acid as dopant and vulcastab VL as stabilizer. The products were coagulated, dried and then compounded on a two roll mill followed by moulding.

Compared to PPy, F-PPy was effective in increasing the cure rate. This was supported by cure kinetic studies. The cure reaction followed first order kinetics. PPy and F-PPy got well dispersed in NR and NBR matrix at lower loadings as was evident from filler dispersion studies. At higher loadings, agglomeration occured. The DC conductivity of the composites was found to be better for the F-PPy system compared to PPy-filled elastomer composites. Maximum conductivities 3.6×10^{-5}S/cm, 5×10^{-5}S/cm and 6.25×10^{-2}S/cm respectively were obtained for the CECs based on NR, NBR and those prepared by *in situ* polymerization in NR latex. The mechanical properties of NR were reduced by PPy loading which was compensated by the addition of F-PPy. Both PPy and F-PPy were very effective in improving the mechanical properties of NBR. The percentage swelling index and swelling coefficient of the composites were found to decrease with increase in PPy loading and F-PPy loading. The solvent sorption mechanism in the conducting composites was found to deviate from Fickian mode.

The thermal stability of conducting elastomer composites of PPy and F-PPy were investigated and compared with virgin matrices.The results showed that thermal stabilities of the elastomers were not seriously affected by PPy or

fiber loading. The thermal degradation kinetics was studied by Coats and Redfern method. The degradation reactions followed first order kinetics.

Dielectric spectroscopy has been found to be a valuable experimental tool for understanding the phenomenon of charge transport in conducting polymers. Evaluation of AC electrical conductivity reveals a wealth of information regarding the usefulness of these materials for various applications. Since the properties of PPy and its elastomer composites are very much dependent on the microstructure, nature of dopant used, type of matrix and the processing variables, study of dielectric properties of these materials assume significance. Dielectric properties of PPy and its elastomer composites were measured in the frequency range 20 Hz to 2 MHz. Dielectric constant of the CECs decreased with increasing frequency owing to a decrease in interfacial polarization and increased with PPy and PPy coated fiber loading due to an increase in interfacial polarization. A remarkably high value of permittivity, 9.8×10^4 at 20 Hz and 2000 at 1MHz was shown by the NR based composite containing 50phr PPy and 50phr coated fiber, prepared by *in situ* polymerization in latex. Variation pattern of dielectric loss with frequency suggested that both DC conductivity and interfacial polarization processes contribute towards dielectric loss. Increase in dielectric loss of the composites on loading may be due to the increase in DC conductivity, increase in interfacial polarization and increase in crystallinity of the samples. AC conductivity of PPy and its composites increased with frequency and the mechanism of conduction was mainly due to hopping of charge carriers. Frequency dependence of AC conductivity could be explained with the help of Maxwell–Wagner two-layer model. All the composite systems exhibited increase of AC conductivity with filler loading mainly due to increased charge

carrier concentration (polarons and bipolarons) with increased filler loading. A maximum conductivity of 22.9 S/m at 1 MHz was recorded for the elastomer composite, containing 50phr PPy and 50phr coated fiber, prepared by in situ method in NR latex. Among all the CECs prepared those prepared by *in situ* polymerization in NR latex exhibited the best dielectric properties.

It is also very important to investigate the response of a conducting composite to microwave radiations as there are many areas of applications such as coating in reflector antennas, camouflage, satellite communication links etc. for these composites. Inherently conducting polymers are excellent microwave absorbers and make ideal materials for effecting welding of plastics. Two important applications concerned with the use of microwave properties are electromagnetic interference (EMI) shielding and radar absorbing materials. The microwave properties of the composites were studied in the S band (2-4 GHz) frequencies. The absolute value of the dielectric permittivity, AC conductivity and absorption coefficient of the conducting composites prepared were found to be much greater than the gum vulcanizates. PPy and PPy coated fiber were found to decrease the dielectric heating coefficient and skin depth significantly. Maximum dielectric permittivities of 35, 55.5 and 43 were obtained respectively for NR based composites prepared by dry rubber compounding, NR based composites prepared by *in situ* polymerization in latex and for NBR based composites. The electromagnetic interference shielding effectiveness of the conducting elastomeric composites in the S band (2-4 GHz) and X band (7-13 GHz) frequencies were also evaluated. The CECs were found to have appreciable shielding effect depending on loading of PPy and coated fiber and in turn the conductivity.

Thus polypyrrole coated Nylon fiber was found to be very effective in improving mechanical properties and DC conductivity of all the three elastomeric composite systems. Latex stage polymerization gave composites having the highest DC conductivity and dielectric properties.

.....ꕥ.....

τ	Relaxation time
ω_p	Anglular frequency
^0C	Degree Celsius
A	Arrhenius constant/Area /Absorptivity
AC	Alternating current
APS	Ammonium persulphate
AQSA	Antraquinone-2-sulphonic acid
ASTM	American soceity for testing and materials
BIS	Bureau of Indian standard
c	Velocity of light
C	Capacitance
CEC	Conducting elastomer composite
CPE	Chlorinated polyethylene
CR	Chloroprene rubber
CRI	Cure rate index
dB	decibel
DBSA	Dodecylbenzene sulphonic acid
DC	Direct current
dNm	deci Newton metre
DRC	Dry rubber content
DSC	Differential scanning calorimetry
DTG	Differential thermogravimetry
$d\Omega$	Complex frequency shift
E_a	Activation energy
EMI	Electromagnetic interference
EPDM	Ethylene-propylene-diene rubber
Er	Relative moduli
f	Frequency
$FeCl_3$	Ferric chloride

F-PPy	Polypyrrole-coated Nylon fiber
FTIR	Fourier transform infrared
Fv	virgin Nylon fiber
GHz	Giga Hertz
h	hour
I	Current
ICP	Intrinsically conducting polymer
J	Heating coefficient
k	Rate constant
keV	kilo electron Volt
kN	Kilo Newton
l	length
MBTS	Dibenzthiazyl disulphide
M_H	Maximum torque
Min	Minutes
M_L	Minimum torque
MPa	Mega Pascal
n	Order of reaction
NBR	Acrylonitrile butadiene rubber
NDS	Naphthalene disulphonic acid
Nm	Newton metre
NR	Natural rubber
NSA	Naphthalene sulphonic acid
PANI	Polyaniline
PET	Poly(ethylene terephthalate)
phr	Parts per hundred rubber
PMMA	Poly(methyl methacrylate)
PPy	Polypyrrole
PVCEE	Poly(vinyl carboxy ethyl ether)
Q_t	Mol % uptake of the solvent
R	Universal gas constant / Reflectivity

R^2	Correlation coefficient
RADAR	RAdio Detection And Ranging
RAM	Radar absorbing material
RCS	Radar Cross Section
RFC	Rubber ferrite composite
RPA	Rubber Process Analyzer
SE	Shielding effect
SEM	Scanning electron microscopy
SIPN	Semi interpenetrating network
T	Absolute temperature / Transmissivity
T_{10}	Scorch time
T_{90}	Cure time
T_g	Glass transition temperature
TGA	Thermogrvavimetric analysis
TMTD	Tetra methyl thiuram disulphide
V	Voltage
XRD	X-ray diffraction
α	Decomposed fraction at any temperature
α_f	Absorption coefficient / Filler specific constant
β	Heating rate
δ	Loss angle
$\boldsymbol{\delta_f}$	Skin depth
ε^*	Relative complex permittivity
ε'	Dielectric permittivity
ε''	Dielectric loss
ε_0	Permittivity of free space
η_r	Relative viscosity
σ	Electrical conductivity

.....ജാര.....

Publications and Presentations

[1] Synthesis and Characterization of Conducting Composites of Polypyrrole/ Polypyrrole-Coated Short Nylon Fiber and Natural Rubber. Pramila Devi D. S., Jabin Thekkedath , Sunil K. Narayanan Kutty. *Polymer-Plastics Technology and Engineering*. 2012, 51, 823-831.

[2] Mechanical, Thermal, and Microwave Properties of Conducting Composites of Polypyrrole/ Polypyrrole-Coated Short Nylon Fibers with Acrylonitrile Butadiene Rubber. D. S. Pramila Devi, Ajalesh. B. Nair, T. Jabin, Sunil K. N. Kutty. *Journal of Applied Polymer Science.* 2012, 126, 1965-1976.

[3] Enhanced electrical conductivity of polypyrrole/ polypyrrole coated short nylon fiber/ natural rubber composites prepared by *in situ* polymerisation in latex. Pramila Devi D.S. , Bipinbal P. K. , Jabin T., Sunil K. N. Kutty. *Materials and Design.* 2013, 43, 337-347.

[4] Dielectric properties of polypyrrole/ polypyrrole coated Nylon fiber/ natural rubber composites prepared by in situ polymerisation in latex D. S. Pramila Devi, Paulbert Thomas, Sunil K. Narayanan Kutty. *Journal of Elastomers and Plastics* (communicated)

[5] Thermal and Microwave properties of Polypyrrole/ Polypyrrole Coated Nylon fiber/ Natural Rubber Composites. D. S. Pramila devi, Paulbert Thomas, Sunil K. Narayanan Kutty *Polymer-Plastics Technology and Engineering* (communicated)

[6] Synthesis and Characterization of Conducting Polypyrrole-Coated Nylon Fiber -Natural Rubber Composites D. S. Pramila Devi, T. Jabin, Sunil K. Narayanan Kutty *International Conference on Advancements in Polymeric Materials*, APM 2011, March 25-27, 2011, CIPET, Chennai.

[7] Enhanced Electrical Conductivity of composites of Polypyrrole/ polypyrrole coated short Nylon fibers and Natural rubber prepared by Latex Masterbatching. D. S. Pramila Devi, T. Jabin, Sunil K. Narayanan Kutty 5th *National Conference on Plastic and Rubber Technology*, POLYCON-2011, April 25-26, 2011, SJCE, Mysore.

[8] Enhanced Electrical Conductivity of Composites of Polypyrrole/Polypyrrole-Coated Short Nylon Fiber and Natural Rubber prepared by *in situ* Polymerization in Latex. D. S. Pramila Devi, T. Jabin, Sunil K. Narayanan Kutty. *Recent Trends and the Sequels in Chemistry*, RTSC 2011, December 7-8, 2011, Department of Chemistry, Sacred Heart College, Thevera, Kochi.

.....ഠോര.....

Response to comments of the Examiner in respect of Mrs.D. S. Pramila Devi, Research Scholar, Dept. of Polymer Science and Rubber Technology, CUSAT.

Chapter 2, pag45 and chapter 3, pages 65-67: It has not become clear to me how thePolypyrrole –modified **short fibers** were produced. Such 6mm fibers are commonly made by cutting continuous cords, before or after modification. Page 45 speaks about Nylon-6 **fiber**: were these chopped already or were they continuous cords containing a multitude of individual yarns /fibers? On page 65 the candidate speaks about Nylon-6 **fibers**, chopped to 6mm length, …subjected to *in situ* polymerization of pyrrole. However on page 66 the candidate speaks about measuring the mechanical properties of the **fibers** with a tensile testing machine with a load capacity of 10kN. I presume this was done on cords, because I don"t see how you can measure the strength of individual 6mm fibers with a load capacity of 10kN, nor how you would hold the 6mm fibers. Also Fig. 32 on page 67 apparently shows continuous **cords,** hower these don"tagree with the preparation methods described on page 65.

Page 45: Continuous cords of Nylon-6 fiber was obtained from SRF Ltd., Chennai. Page 65-section 3.2.3, F-PPy prepared as in this section were used to incorporate with dry NR and NBR for preparing elastomeric composites(chapers 4 and 6). Chopped uncoated fibers were used for preparing elastomeric composites by latex stage preparation(chapter 5). For optimization of coating conditions and for evaluating mechanical properties and DC conductivity(chapter 3) continuous cords of Nylon-6,were used

Page46 It is worth-while to mention the specific grade of ZnO, in particular the crystal particle size, as this influences the vulcanization behavior of the compounds wherein it is used.

Commercial grade ZnO of particle size approximately 15 microns and surface area 4-6 m^2/g was used.

I found chapters 4,5 and 6 rather empirical of nature and would have liked a bit more in depth critical analysis of the results obtained. Examples

Page 97, Fig 4.2: Why the sudden jump in torque vs time curve for NFp5 compared to the little difference for NP0 till NFp4?

From NP0 to NFp4 there is only gradual increase in filler concentration as 3, 5, 15 and 25phr, while from NFp4 to NFp5, there is a sudden jump in filler concentration, from 25 to 50phr. This causes a sudden jump in torque value also.

Page104 : a lamellar structure of NR is visible in fig 4.8(a). Are these real lamellae indeed, or is this an artifact due to the preparation method: tensile fracture? And lines 6-8: is this really NR particles covered by spherical PPy or the other way around: how can that be confirmed?

Such a lamellar structure for NR is found in many works. It is also seen that lamellar structure is lost at very high filler concentration. If it is due to tensile fracture, it should be visible in loaded samples also.Lines 6-8:It is NR particles covered by spherical PPy. This can be confirmed by two factors: (1)Comparison with SEM image of PPy(fig. 3.7) (2) This is why increased PPy concentration increases the conductivity.

Page108, at the bottom: has the candidate considered the possibility of loss of strain crystallization by NR due to the introduction of the large amounts of PPy? Compare then results in Fig. 4.10 for example with fig. 6.10 for NBR, where the effect of varying amounts of PPy is totally different and less dramatic: NBR does not strain crystallize. That the addition of short fibers has a strong reinforcing effect on strength or modulus at short strains is a well-known effect.

Page 108, after line 21

Another reason for the decrease in tensile strength of NR with PPy loading may be loss of strain crystallization of NR due the introduction of large amounts of PPy.

Page 153, after line 5

The effect of varying amounts of PPy is totally different from that of NR(sections 4.3.6 and 5.3.6)This may be due to the fact that NBR does not strain crystallize and the deterioration of tensile strength in NR with PPy loading due to loss of strain crystallization of NR is not applicable here.

Page108-112: Has the candidate considered the option to simulate the finding with theoretical calculations based on eg; the Halpin-Tsai model? I don't think that this would not have been successful, however it would have added to the scientific value of this work.

Not done. This was not done particularly because the current composite is not amenable to the conditions assumed by Halpin-Tsai model.

Page114, table 4.4: the swelling parameters for the NP series, in particular n and k jump up and down. Similar in table 5.4 for the LNP series and in table 6.4 for the BP series. Is this due to limited accuracy or reproducibility of the swelling test, or other?

Diameter after solvent sorption, Swelling index and swelling coefficient values decrease without any ups and downs for NP, LNP and BP series. In the case of n, it is

true that the n does not give a very specific trend. The values vary between a range indicative of a Fikian mode. The k values, though do not show a regular variation, are lower than that of gum compound indicating less interaction between composite and solvent.

Page127, Figure 5.2: the data series LNPFp looks rather scattered: no logical order:WHY? And where are the results of LNP1?

There is a regular variation among LNPFp series except LNPFp1 which came above LNPFp2. This may be an experimental scatter of data. Fig. 5.2 is meant only to prove that cure reactions proceed according to first order kinetics. Results of LNP1 included in graph. The modified graph is incorporated in the thesis.

Page 132: The "better adhesion" of PPy and PPy coated fiber to NR via the latex route: is this assumption or is there other (mechanical) proof for that?

From the increased conductivity found in this case compared to dry rubber compounding(sections 4.3.5 and 6.3.5), it is assumed that since polymerization of pyrrole and coating of Nylon fiber are carried out in latex, rubber particles were coated more with PPy and there is better adhesion.

Pages 136-137: Apart from the explanations given for the reduced swelling in Figures 5.14 and 5.16, there is also the effect of "dilution" of the NR by the introduction of large amounts of PPy. PPy of PPy- coated fibers do not contribute to the swelling. In particular, the reduction with a factor 1.5 in swelling in Fig. 5.16 going from LNP2 to LNPFP3 corresponds with the same factor 1.5 of increased filler loading.

Reduced swelling due to increased dilution of NR when loaded with PPy is understood. The aim of swelling study was to show that PPy or PPy coated fiber in no way enhance solvent swelling property, which may add to the application of elastomeric composites prepared.

Page 145 Fig. 6.2: Why the sudden jump in torque vs time curve for BP3 vs BP2?

The sudden increase may be attributed to the fact that the percolation limit is reached at 75 Phr, ie.,beyond 50 phr. Beyond the percolation limit, the filler – filler interaction becomes prominent and hence the matrix becomes more restraint. This is manifested as higher torque for BP3.

Page 147: WHY does the CRI for the BP series decrease first and then increase substantially? Is there any mechanistic explanation?

First decrease in CRI is due to the presence of acidic dopant in PPy. (page 146, lines 4, 5.). At very high loading, the mixing time and hence the heat generated are higher

leading to some extent of premature curing during mixing. Thisresults in shorter time requirementsie higher CRI for completion of cure duringmoulding of these samples.

Page 155 Fig.6.15 **and page 156**, Fig. 6.17. The decrease in swelling for these NBR based systems are much more, than observed for the corresponding NR based systems. Is there an explanation for that, eg:- an increased interaction between filler and matrix(page157, lines 8 and 9)? Any proof?

Compared to NR based systems(sections 4.3.7 and 5.3.7), decrease in swelling for NBR based systems are much more. This is due to the fact that filler-matrix interaction in NBR based systems is more (both polar) compared to that in NR based systems, where matrix is non polar.

Page 169 Table 7.2: Is the change in Ea not simply a dilution effect by the PPy or fibers, making the blends more thermally stable, as the PPY can stand much higher temperatures?

Yes, the change in Ea is only a dilution effect.

Page 240 Fig. 9.6(a) **and page 244**, Fig. 9.12(a): WHY the illogical order in heating coefficients for the 0-phr PPy loading data as a function of frequency?

As mentioned on page 240, line 4 the heat developed is proportional to both frequency and the product of ε and tan δ. This accounts for an irregular variation of heating coefficient with frequency.